FACULDADE DE ENGENHARIA DA UNIVERSIDADE DO PORTO

Gait Analysis and Rehabilitation using Inertial Sensors

Patrícia Loureiro Rodrigues

Mestrado Integrado em Bioengenharia

Supervisor at DEI & FEUP: Rui Camacho

Supervisor at SWORD Health: André Gomes

June 30, 2017

Gait Analysis and Rehabilitation using Inertial Sensors

Patrícia Loureiro Rodrigues

Mestrado Integrado em Bioengenharia

Approved in public examination by the Jury:

President: Prof. Doutor Artur Agostinho dos Santos Capelo Cardoso

Opponent: Prof. Doutor Paulo José Cerqueira Gomes da Costa - FEUP/DEEC

Referee: Prof. Doutor Rui Carlos Camacho de Sousa Ferreira da Silva - FEUP/DEI

Referee: Eng. André Branquinho Gomes - SWORD Health

June 30, 2017

Resumo

Caminhar é uma função essencial que facilita praticamente todas as atividades do dia a dia, como ir para o trabalho, ir às compras, fazer o jantar, entre outras. Com a ocorrência de certas doenças, como por exemplo neurológicas e musculoesqueléticas, esta função fica degradada, diminuindo a confiança da pessoa ao caminhar. Isto faz com que haja um risco de queda maior, aumentando também a dependência de outros para realizar as atividades do dia a dia.

A reabilitação da marcha é uma forma de restabelecer esta função. Consiste na repetição continuada das diversas fases do ciclo da marcha. Feita corretamente, permite que o paciente restabeleça a sua independência, diminuindo o risco de queda e aumentando, no geral, a sua mobilidade. No entanto, sendo uma atividade complexa, avaliar a marcha torna-se uma tarefa complicada e dependente da experiência do terapeuta.

O objetivo deste trabalho centrou-se no desenvolvimento de um algoritmo para reabilitação de marcha. Este deve permitir aceder a parâmetros de marcha adequados para a avaliação do paciente e oferecer *feedback* em tempo real enquanto realiza os exercícios de reabilitação.

Para realização do trabalho foi necessário obte reventos de marcha que permitissem determinar parâmetros temporais. Após compreensão do sinal, foram usados detetores de picos como *peakdetect* e algoritmo de *Trahanias*, para detetar quando o pé é retirado do chão. Para encontrar o instante em que ocorre o pé é colocado no chão e se dá a absorção de choque foram usadas *wavelets*. Para detetar o início e fim de marcha, foi usada a cross-correlation

Com o conjunto dos métodos apresentado foi possível obter uma precisão de 99% e uma sensibilidade de 100% para deteção do instante em que o pé sai do chão com um erro de cerca de $0,04$ segundos. Para deteção do instante em que o pé é colocado no chão obteve-se uma precisão de 100% e uma sensibilidade de $73,7\%$ com um erro de aproximadamente $0,06$ segundos, com comparação com sistema *gold standard*. Também foram implementados parâmetros de marcha b temporais derivados destes dois instantes. Por fim, o sistema foi adaptado para funcionar em tempo real, e dar informação a cada novo passo.

Abstract

Walking is an essential function that facilitates practically every day-to-day activity, such as going to work, going shopping, making dinner, among others. With the occurrence of certain diseases, such as neurological and musculoskeletal, this function becomes impaired, reducing the person's confidence in walking. The person starts to have a higher falling risk, also increasing dependence on others to carry out the activities of the daily living.

Gait rehabilitation is a way of restoring this function. It consists of the continuous repetition of the various phases along the gait cycle. When performed in a correct way, it allows the patient to re-establish his independence, reducing the falling risk and increasing his mobility in general. However, being a complex activity, evaluating gait becomes a elaborated task and dependent on the therapist's experience.

The goal of this work was the development of an algorithm for gait event detection in the context of rehabilitation rehabilitation. It should allow access to appropriate gait parameters for patient evaluation and provide feedback in real time to the patient while performing the rehabilitation exercises.

In order to carry out the work, it was necessary to obtain gait events to determine temporal parameters. Peak detectors such as peakdetect and Trahanias algorithm were used to detect when the foot lifts from the ground. To find the instant when the foot is placed on the floor, the Wavelets Transform was used. To detect start and end of gait, cross-correlation was used.

With the set of methods presented it was possible to obtain a precision of 99 % and a recall of 100 % for detection of the moment when the foot leaves the ground with an error of about 0.04 seconds. For detection of the instant the foot is placed on the ground, a precision of 100 % and a recall of 73.7% with an error of approximately 0.06 seconds were obtained, comparing with a gold standard system. Temporal gait parameters derived from these two events were also implemented. Finally, the system was adapted to operate in real time, to give information to each new step.

Agradecimentos

A realização desta dissertação, que marca o fim do meu percurso académico, teve um apoio e incentivo sem os quais não se tornaria realidade e pelos quais estou muito grata.

Em primeiro lugar aos meus pais, por todo o esforço que tiveram com a minha educação e formação. Sempre me incentivaram a ir mais longe dando-me o apoio que podiam e que não podiam. O que sou hoje é o fruto do vosso esforço. Estou-vos eternamente grata.

Ao Professor Dr. Rui Camacho, por ter aceite a minha aventura nesta tese, por toda a disponibilidade, apoio, pelos conhecimentos que me transmitiu, pelas críticas que me fez e me ajudaram a compreender melhor o problema e por me incentivar.

Ao Engenheiro André Branquinho e à Engenheira Clara Matos, por me apoiarem, perderem o seu tempo a discutir comigo a fazer *brainstorming*, pelas ideias que me deram e por tudo o que me ensinaram. Aprendi imenso convosco.

Aos meus amigos de curso, por me desafiarem, apoiarem, distraírem e fazerem ver que a vida não é só trabalho. À Diana e ao João, os meus dicionários de Oxford, por nunca me deixarem ir abaixo, por me ajudarem e acreditarem sempre em mim. E acima de tudo, pela vossa amizade.

Por último, mas não em importância, ao Mário. Desde aturar as minhas frustrações ao stress de curso, sempre esteve ao meu lado acreditando sempre em mim. Com uma disponibilidade infindável e sempre com vontade de ajudar. Obrigada pelo teu apoio e carinho.

Patrícia Rodrigues

"If your ship doesn't come in, swim out to meet it."

JONATHAN WINTERS
Grammy Award-winning comedian, actor, writer and artist.

Contents

List of Figures

List of Tables

Symbols and Abbreviations

ADL	Activities of the daily living
BESS	Balance Error Scoring System
BSS	Berg Balance Scale
CA	Composite Acceleration
CoP	Center of Pressure
CoV	Coefficient of Variation
CTSIB	Clinical Tests of Sensory Organization and Balance
DLS	Double Limb Support
DWT	Discrete Wavelet Transform
ECG	Electrocardiogram
EMG	Electromyography
FN	False Negatives
FNN	Feed-forward Neural Network
FP	False Positives
FTSTS	Five Times Sit To Stand
GC	Gait Cycle
GRF	Ground Reaction Force
HMM	Hidden Markov Models
HS	Hybrid Systems
IC	Initial Contact
IDLS	Initial Double Limb Stance
IMU	Inertial Measurement Unit
LR	Loading Response
mBESS	Modified Balance Error Scoring System
mCTSIB	Modified Clinical Tests of Sensory Organization and Balance
MS	Multiple Sclerosis
MSE	Mean Squared Error
mTBI	mild Traumatic Brain Injury
NWS	Non-Wearable Sensors
PCA	Principal Component Analysis
PD	Parkinson's Disease
PS	Pre-Swing
ROM	Range Of Motion
SD	Standard Deviation
SLS	Single Limb Stance
TDLS	Terminal Double Limb Stance
TP	True Positives
TUG	Timed Up and Go

WS	Wearable Sensors
ZC	Zero Crossing

Chapter 1

Introduction

Walking is one of the most natural, common and essential physical activities of the human life, which allows the body to move from one location to another [Perry and Burnfield, 1992] [Aminian et al., 2002]. Cooking, going to work, running, going to see a movie, are activities dependent on walking. However, sometimes there are certain neurological, muscular or other diseases that cause changes in gait, causing gait impairments. The injured person begins to have higher dependence on walking, having difficulties in carrying out the normal activities of the daily living (ADL), losing the confidence in walking and increasing the risk of falling.

The development of science and technology has led to an increase in the average life expectancy, resulting in a rise in the aging population. In most developed countries, this is already a social problem. According to [United Nations and Affairs, 2009], it is expected that by 2050 there will be about 3.5 working-age individuals for every old person. It is estimated that more people will have fewer children, having less support in old age. On the other hand, with the relative decrease of younger people compared to older people who need care, there is already a lack of rooms for people over 65 years old in healthcare centers [Zhang et al., 2012]. Compared to this fact, rehabilitation centers are becoming crowded with patients, and with fewer human resources to respond to all needs. One way to increase mobility in the elderly is to promote physical rehabilitation. With it, they remain active and dependent until later ages, and recover from neurological or musculoskeletal diseases that may have occurred.

1.1 Problem and Motivation

In the presence of certain diseases that cause walking problems, rehabilitation comes as a solution to restore the whole function to walk properly and increase mobility. Most rehabilitation studies indicate that programs should begin as early as possible, be intense, and prolonged as possible for effective function recovery, preferably near the patient's home [Zampolini et al., 2007]. Gait rehabilitation involves repetitive training. Gait relearning should be done soon after the patient is ready for rehabilitation, without having to wait weeks.

Not all patients have access to rehabilitation, for several reasons. Some patients live in more isolated places far from rehabilitation centers, or are in wheelchairs, having higher difficulty in being transported, or even do not have a vacancy in the rehabilitation center. For them, the cost of transportation, resources and medical staff becomes high, and they begin to reduce their time in rehabilitation.

Rehabilitation is traditionally done by human resources and hence associate with low accuracy and/or precision. Even the most experienced physiotherapists can fail in the joints' angles estimation [Perry and Burnfield, 1992]. In addition, they do not have access to complete and accurate information on gait metrics used, such as temporal, spatial, and/or kinematics parameters, which may cause deviations in the rehabilitation program and thus, impair the patient instead of rehabilitating. Patients who make mistakes in rehabilitation, due to their weakened state, can suffer serious consequences. In this way, the rehabilitation program must be followed completely.

Exercise programs are individually prescribed for each patient to address specific patient's therapeutic goals, pathology, and limitations as well as additional impairments. The exercises must be individually tailored by a clinician who has several patients every day, with different exercise programs. The written instructions are typically hard to follow, and in most cases, patients do not receive feedback on the quality of the exercises during its performance [Zhao et al., 2014]. The lack of monitoring and feedback during exercises is a serious problem. Patients become discouraged due to the loss of interest and knowledge of their performance, and can wrongly perform exercises and harm themselves [Zhao et al., 2014].

Several technological systems have provided solutions to the problems mentioned above, such as camera-based motion capture systems, or walkways with force platforms. These systems already allow a better monitoring of patient movement, and acquisition of more precise parameters. They also allow the data to be stored and thus observe the evolution of the patient through the rehabilitation sessions. However, these methods are generally costly, a walking laboratory is required, the physiotherapist needs to have computer skills, perform time-consuming calibrations, and most of them do not provide real-time feedback [Tao et al., 2012]. In this way, they are mainly used for research or clinical diagnosis [Aminian et al., 2002] [Baker, 2006]. With this, the problem of lack of access remains [Zampolini et al., 2007], as well as the lack of real-time feedback, and the simplicity and accessible cost for a use in clinics and by patients. Due to these systems that perform gait analysis at a specific walkway, the evaluation is far from the patient's normal activity, being more controlled and with a shorter distance. Several studies prove that the ground surface and distance traveled greatly affect performance of the gait function [Najafi et al., 2009].

In the last decades, the use of wearable sensors began to emerge, such as Inertial Measurement Units (IMUs), which allow the acquisition of human movement outside a walking laboratory [Roetenberg et al., 2009]. With the acquired information, it is possible to develop systems that can accurately measure gait parameters, provide real-time feedback (while the patient does rehabilitation), allow the results storage for an observation of the patient's evolution over time, and outside a gait laboratory, such as at the patient's home.

With a system with these characteristics, it is possible to prescribe specific gait exercises for

the patient so that he can restore his autonomous life [Najafi et al., 2009] [Zampolini et al., 2007]. Gait function can be fully recovered, the patient can regain his confidence in walking, reducing the risk of falling, and increasing his independence on his ADLs, in order to need less help in old age.

1.2 Goals

The main goal of this thesis was the development of an automatic system to evaluate the gait quality for rehabilitation purposes, with feedback in real time, using IMUs. In order to develop the mentioned system, it was crucial to do the following topics.

Study the human gait analysis and rehabilitation state-of-the-art. This included anatomical, physiological and biomechanical information of the gait and pathologies that cause an abnormal gait; gait cycle with the focus on the human gait phases; analysis methods for human gait (based on wearable sensors); and study of the spatial and temporal gait parameters.

Analysis of the gait parameters aiming the selection of a set of the most important ones.

Development of an algorithm for the acquisition, and detection, of gait events, using inertial sensors in real time. Implementation of temporal parameters from the detected gait events to quantify and evaluate gait quality.

1.3 Research Proposal

It was proposed the development of a Python[1] application that allowed gait evaluation under conditions of rehabilitation allowing real-time feedback. In this way, it was proposed the use of inertial sensors IMUs to acquire the person's gait pattern. A method capable of obtaining temporal gait parameters for the gait assessment under rehabilitation conditions was suggested. It was required a simple setup to be used by patients in need of rehabilitation.

1.4 Contributions

The main contributions of this project were focused on the effective detection of temporal events with only two sensors, one in each foot.

No innovative methods were used per se, however, methods were implemented that, underway and in these conditions, no reference was found to its use. Among them, use of the Trahanias algorithm applied to the gait signal for detection of gait events. And also the use of cross-correlation for gait start and end detection. Another contribution was the acquisition of gait data with events annotations obtained by golds standard systems.

[1] Python. `https://www.python.org/` (visited on 02/02/2017)

1.5 Document Structure

This document is structured in seven chapters. In this chapter (Chapter 1) the general problem regarding the theme of this dissertation is addressed. The goals, work proposal, the contributions and the present structure of the document are also presented. Chapter 2 addresses the background of the gait analysis. In Chapter 3 the materials that will be used throughout the practical work of this dissertation and also the state-of-the-art methods concerning the theme are presented in more detail. Chapter 4 presents the data collected, the way the problem was addressed, the methods used and the validation strategy that was implemented. In Chapter 5 the results obtained from the detection of IC and PS events are discussed. In Chapter 6 the temporal parameters obtained from the events detected in the previous two chapters, the real-time implementation, and simulation in pathology are addressed. Finally, the conclusions and suggested future work is presented in Chapter 7.

Chapter 2

Gait Analysis

Gait function recovery after a disability or injury, or re-learning how to walk, can be assisted by gait analysis. Some disabilities are the result of the relationship between motor control and brain function, and result in instabilities in gait function and other activities. Gait analysis is a powerful tool to understand this relationship and make a connection between them and the patient's condition [Kraan et al., 2016]. Gait analysis can determine the timing in gait, rhythm, gait variability and other parameters, and identify an unstable gait. Can also be applied in a rehabilitation process, where gait analysis, especially with feedback in real-time, is crucial to present results to the patient and help him achieve a more correct and safe gait.

Gait and movement analysis has been studied for many years. The first reference to gait and locomotion was made by Aristotle in the publication (translated to English as) "*On the Movement of Animals*" [Young, 2010]. Since then, in 1860 by Giovanni Borelli, and in the 1890s, Braun and Fischer published a set of papers about the kinematics of human gait, that started an emerging gait research. In the 1940s the development of several methods to assist gait analysis, started in response to the lack of human eye perception when continuous gait was performed by the patient. Technology evolved in a way that allowed its use in gait analysis, for example with the use of video cameras [Whittle, 1996] [Al-Zahrani et al., 2008] [Baker, 2007]. With them, it was possible to acquire gait data, during the patient's exercise, and analyze it in more detail after the session. This process was done manually, but with a higher precision, especially in the acquisition of the joint's angles in the video frames. Soon these processes became automatic and other types of systems to measure angles, forces, momentum, and muscular activity emerged. However, these processes were complicated to install, to set up, to perform, to process and analyze the acquired data [Sutherland, 2002] [Baker, 2007]. They require specialized laboratories and most of them expensive equipment. As a result, they have been used only for research and diagnostic purposes. Until recently, most of the gait rehabilitation has been performed without technological assistance, leading to a lack of patient sessions' information, and their evolution over time, among others [Tao et al., 2012].

In the following sections the background of gait from the fundamentals to the application of gait analysis is presented. Pathologies associated and gait parameters that allow the evaluation of gait are also shown. Concepts of gait rehabilitation and movement test to access the capacity of the patients' movement and also systems currently used for gait data acquisition are presented.

2.1 Lower Limbs Overview

In this section, concepts will be introduced about the lower limbs and their physiology that are crucial to understand the gait, gait events, and the motion sequences while walking, that are discussed thought the extent of this work.

2.1.1 Lower Limbs Human Skeleton System

We can move due to the presence of bones and joints that give to our body a rigid configuration suitable for the locomotion. As it will be shown in the following sections, in walking activity, the most important body parts are the lower limbs and the pelvis, while the superior part (head, trunk, and arms), act like a whole part. With this, the bone structure of the lower body part is presented (Figure 2.1).

In Figure 2.1, the pelvis part joins the two lower limbs. The lower limbs are composed by the femur in the superior part, and by tibia and fibula in the lower part. The *hip joint* is the structure that exists between the pelvis and the femur. The femur and the tibia (and fibula) are separated by the patella (knee cap) and in this location exists the *knee joint*. The calcaneus is the bone of the heel and it is adjacent to the *ankle joint*.

2.1.2 Terms Of Motion

The human movement can be described by anatomical terms that are used by the physiotherapy and medical community, so that there is an understanding and consensus in the movements performed at the level of each joint of the human body. This nomenclature of movement is crucial to identify human motion, especially in each event that occurs while walking.

While walking, the movements that occur are knee and hip flexion and extension and dorsiflexion and plantar flexion of the ankle. In the presence of some pathologies, hip adductions and abductions of the hip can be verified. In this way, the terms previously mentioned (flexion, extension, abduction, and so on) will be introduced.

Flexion and Extension

Flexion and Extension describe the angle of a joint while moving that occurs in the sagittal plane (Figure 2.2b and 2.2c).

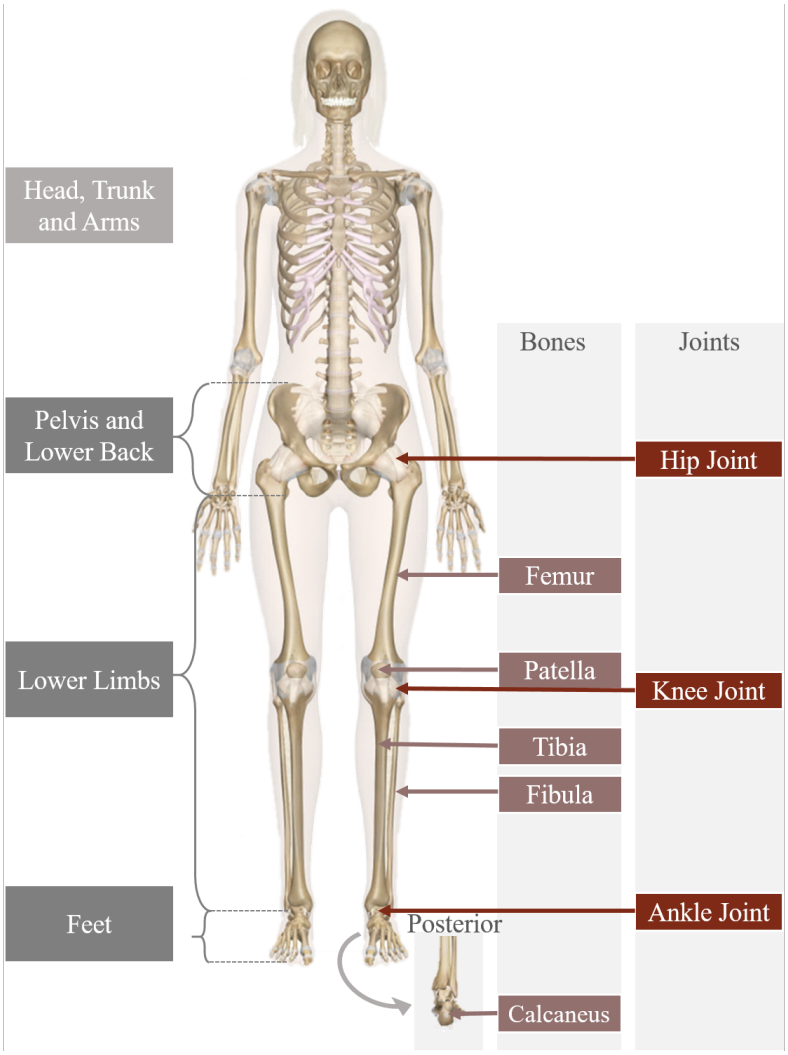

Figure 2.1: Human skeleton. This figure evidences the lower part of the human body, especially the pelvis, lower limbs and feet. The locations of the major joints that are involved in gait activity are highlighted: hip, knee and ankle joints[2].

Flexion: Occurs when the angle of the joint decreases. In other words, is the movement that decreases the angle between two connected body parts. For example, the knee flexion occurs when the ankle moves closer to the posterior part of the hip joint[1].

Extension: Occurs when the angle of the joint increases. For example, the extension of the knee straightens lower limb[1].

Abduction and Adduction

Abduction and Adduction describe movements of the joints that move its structure in relation to the midline of the body (Figure 2.2e).

[2]InnerBody. `http://www.innerbody.com/image/skelfov.html` (visited on 15/12/2016)

[1]TechMeAnatomy.`http://teachmeanatomy.info/the-basics/anatomical-terminology/terms-of-movement/` (visited on 19/12/2016)

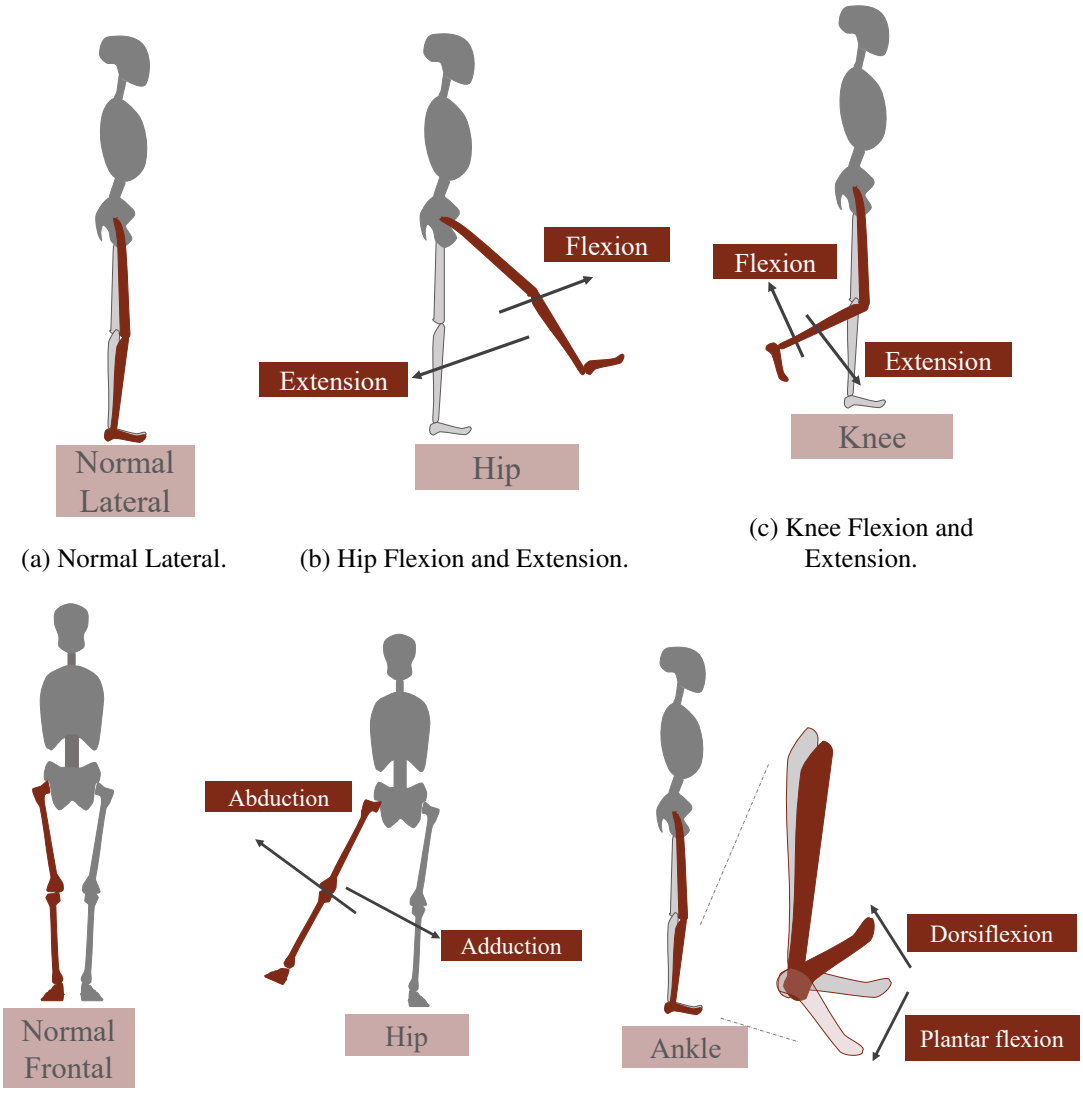

(a) Normal Lateral.

(b) Hip Flexion and Extension.

(c) Knee Flexion and Extension.

(d) Normal Frontal.

(e) Hip Abduction and Adduction.

(f) Ankle Dorsiflexion and Plantar Flexion.

Figure 2.2: Terms of Motion. While walking, there are several joint movements that occur. The subfigures (a) and (d) are related to the lateral and frontal views, respectively. The movements that are made by the hip are flexion and extension (b), abduction and adduction (e), by the knee are flexion and extension (c), and by the ankle are dorsiflexion and plantar flexion (f) (adapted from [1]).

Abduction: Occurs when the body structure is moved away from the midline (sagittal plane) of the body. For example, abduction of the hip is the movement of the lower limb away from the midline of the body[1].

Adduction: Occurs when the body structure is moved toward the midline (sagittal plane) of the body. For example, the adduction of the hip squeezes the lower limbs together[1].

Dorsiflextion and Plantar Flexion

Dorsiflexion and plantar flexion are motion terms related to the movements performed by the ankle. The ankle has two surfaces: dorsum (superior) and plantar (sole), giving the origin to dorsiflexion and plantar flexion to the orientation of each ankle flexion (Figure 2.2f).

Dorsiflexion: Occurs when the toes are brought closer to the tibia so that the foot points up[1].

Plantar flexion: Occurs when the angle between the toes and the anterior part of the tibia is increased, so that the foot points down[1].

2.2 Human Gait Fundamentals

Walking involves a set of lower limb sequential movements that allows the body to move forward while maintaining body stability. These sequential movements involve a set of interaction between the two lower limbs in tune and the body total mass. In this sense, is crucial to identify gait events, and it is necessary to observe gait in different points of views.

2.2.1 Basic Functions

While walking, our body behaves as two main units: locomotor unit and passenger unit. Understanding this distinction is important to know what to analyze in more detail during a gait analysis.

Passenger Unit: The passenger unit is composed of the head, neck, upper limbs and trunk. Their main function is to ensure its posture integrity, and because of this, is mainly a passive unit. Its muscular activity, including that of the upper limbs, it is to maintain a neutral vertebral alignment, with less variance as possible, during gait.

Locomotor Unit: The locomotor unit is responsible for the locomotion activity. It is composed by the two lower limbs and pelvis and it is a multisegmented unit, as each lower limb assumes the body weight alternatively, with the goal to move it forward or doing locomotion.

The locomotor unit has four functions that have to be completed to successfully accomplish gait: it has to generate a propulsive force, in order to do the advancement of the lower limb swing; the stability of the passenger unit has to be accomplished, even when the body is moving forward and has a continuous posture change; the shock in the beginning of each stance has to be minimized, in order to avoid injuries; and the total energy has to be conserved in all these functions, to minimize the muscular effort in the overall walking activity [Perry and Burnfield, 1992]. This terminology is important for analyzing the human body according to the parts in which it can be divided while walking. Understanding the two great unitary parts of the human body and its functions in relation to the gait, will be important when analyzing the existing gait analysis methods.

2.2.2 Gait Cycle

When we walk, we move one lower limb forward in relation to the other, and our body is transferred forward. This causes a sequential body weight transferring from one lower limb to the other. A single sequence of these events, referring only one limb, is a Gait Cycle (GC), and was firstly introduced by [Murray et al., 1964] [3]. One CG is followed smoothly by the following GC, and there is not precisely an initial and final point. Conventionally, the contact of the heel with the ground is defined as the initial point of the GC.

A GC begins when the heel is placed on the ground (with both feet on the ground), then there is a forward posture advancement of the body that causes the body weight to be transferred to the foot that has just been placed on the floor. Then, the opposite foot lifts up and makes a push to set it forward, meanwhile, the foot under analysis stands alone on the ground supporting all the weight of the body. The body posture is continuously balanced forward until the opposite foot begins its cycle (with its heel placed on the ground), and at this moment both feet are on the ground. The weight passes to the opposite foot and the foot under analysis begins to lift (leaving the floor). It makes an impulse to move forward, passes through the opposite leg (in the coronal plane), and arrives at the ground, with the heel. An illustration of this description can be seen in the Figure 2.3.

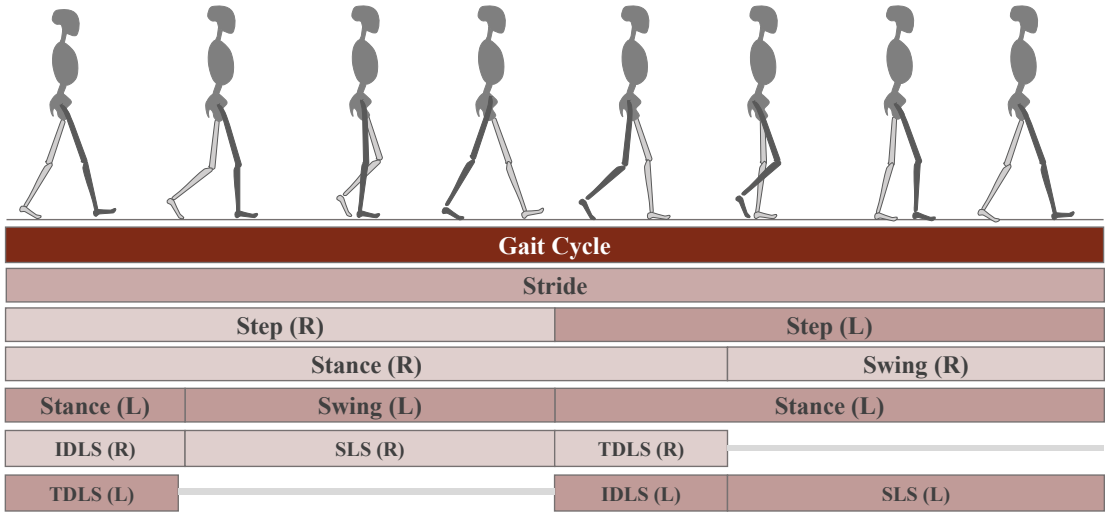

Figure 2.3: Relationship between the step, stance and swing of the right (R) and left (L) leg, during one GC. Some of the terms will then be introduced in the following subsections: IDLS - initial double limb support; SLS - single limb support; TDLS - terminal double limb support. (adapted from [Perry and Burnfield, 1992])

The Figure 2.3 shows a GC with reference to the periods that occur in each lower limb (right and left). The terms in this figure will be explained in the following subsection. It can be observed that there is a relationship between swing and stance of the right and left lower limbs in sequence along the gait. It should be noted that when the stance occurs at the same time in both lower

[3]This reference was extracted trough the book [Perry and Burnfield, 1992].

limbs, double limb support occurs, and when swing occurs, the opposite limb is in the single limb support.

2.2.3 Gait Phases

One GC can be split into two main periods (stance and swing), which are defined according to the touch of the foot with the ground (Figure 2.4).

In Figure 2.4, a complete GC is defined as a complete cycle of one lower limb (with color), in this case, related to the right lower limb. GC can be also called stride and is composed of two steps, right and left.

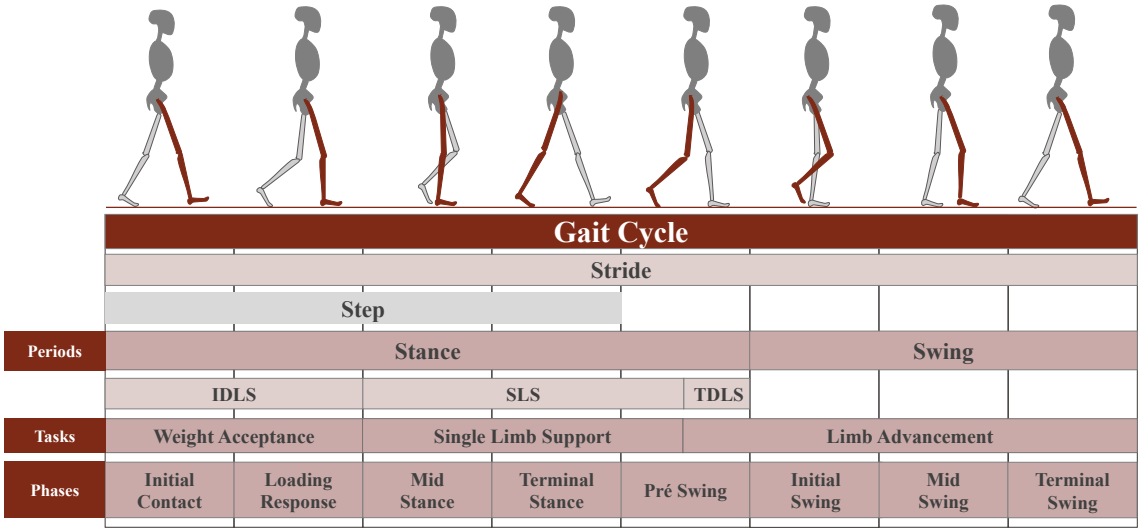

Figure 2.4: Gait Cycle, Periods, Tasks and Phases. Gait Cycle is also called stride and is composed of two steps, right and left. The definitions presented are related to the shaded lower limb (right). The beginning of the GC starts with the stance period (the limb's foot is in contact with the ground). This can be split into three other periods: Initial Double Limb Stance (IDLS), Single Limb Stance (SLS), and Terminal Double Limb Stance (TDLS). In Initial Double Limb Stance, the task of Weight Acceptance occurs and the weight is transferred from one limb to the other. In Single Limb Stance, all the body weight is in one limb (on the right), that is the only limb in stance period - when the Single Limb Support task occurs. In Terminal Limb Stance, both limbs are in contact with the ground. After the stance period, the swing occurs - when the foot is in the air, and doing the Limb Advancement Task. Gait Cycle can also be divided into eight different phases: and each one has different functions and segment and joint positions (adapted from [Perry and Burnfield, 1992])

Stance: is the period when the foot is on the ground. It Is about 60% of the GC and starts when the heel first touches the ground until it leaves the floor. During this period, the opposite lower limb runs through its stance (end and beginning of the next CG stance), and swing, causing an occurrence of three main sub-periods (inside the stance of the foot under analysis) The examples will consider the stance of the right limb:

1. *Initial Double Limb Stance (IDLS):* Occurs when the left limb is also on the ground, and the body is supported by the two limbs. In this period, the left limb will start to swing.
2. *Single Limb Stance (SLS):* Occurs when the left limb starts to swing and continue, leaving the body with only one support - the right limb.
3. *Terminal Double Limb Stance (TDLS):* Occurs when the left limb has finished its swing, and starts its stance period. The body is again supported by the two limbs (right and left). At this stage both limbs are in stance: the right is finishing its stance, and the left is starting its stance and is in its IDLS (left) period.

Swing: is the period when the foot is in the air, to move forward in relation to the other foot. It is about 40% of the GC and the body advances forward. During this period, the opposite foot is in its sub-period of single limb support.

The combination of the two periods of double limb stance - IDLS and TDLS, corresponds to the *Double Limb Support (DLS)*. If there is no DLS present in all GC, it means that the person is running [Perry and Burnfield, 1992].

While walking three tasks occur, and are crucial to moving the body forward. They are presented as (Figure 2.4):

1. *Weight Acceptance:* is the most challenging task in the GC. It is composed by initial contact and loading response phases. The body weight is transferred from one limb to the one that has just finished its swing and is still in an unstable alignment. In Figure 2.4, the right limb (shaded), is starting its stance and has just finished its swing. When the heel touches the ground, a shock absorption occurs, and the failure of this task can provoke a fall.

2. *Single Limb Support:* is composed by mid stance and terminal stance phases. Following the example in the Figure 2.4, in this task, the right limb is in the stance, and the left limb has just started its swing (it is in the air doing the body forward progression). All the body weight is on the right limb, and the stance lower limb has to maintain the body stability, while progression. The SLS duration is the best index of the limb support capability. This task ends when the opposite limb (in this case, the left limb), ends its swing and starts its stance (beginning of the TDLS).

3. *Limb Advancement:* is composed by the pre-swing, initial swing, mid swing and terminal swing phases. In the beginning of this task, the right limb does an impulse forward and then passes through three positions while is moving forward (described in the Table 2.1). It is responsible for the movement of the body forward while walking.

In Figure 2.4, the functional phases in gait are presented. They correspond to different alignments and foot positioning. According to the patient's pathologies, all the eight gait phases may not occur. Gait analysis by phases directly identifies the functional meaning of the different movements that occur in each joint. In Table 2.1, the specifications for each gait phase are presented .

The percentage of time in a GC is displayed first, and then, the main functional activities of each phase. The most significant joint events that occur in each gait phase are also presented.

Table 2.1: Gait Phases Definitions. This table presents the different phases of the gait cycle, and the goals and main functions of each one. Based on [Perry and Burnfield, 1992].

Phase	Duration in GC	Main Goals and Function	Joints Events
		Stance Period	
Initial Contact (IC) (heel strike)	0% – 2% GC	The limb is positioned to start the stance, with the heel in the ground direction. The IC starts when the foot touches the ground (typically with the heel). The joint's posture determines the limb's loading response pattern.	Hip flexion, knee extension, and the ankle is dorsiflexed to neutral.
Loading Response (LR)	0% – 10% GC	When the whole foot is on the ground, the shock absorption occurs and the weight of the body shifts from the opposite lower limb to the present limb. Stability is maintained and the weight is supported by the limb. It also occurs the preservation of progression, done by the opposite foot.	Knee and ankle (plantar) flexion.
Mid Stance (midfoot strike)	10% – 30% GC	Progression over the stationary foot while the trunk and limb are stable. Starts with the elevation of the opposite lower limb (mid swing), and ends when the limb is almost in vertical position.	Ankle dorsiflexion, knee and hip extension
Terminal Stance (heel-off)	30% – 50% GC	Progression of the body beyond the supporting foot. Begins when the heel rises and ends when the heel of the opposite foot touches the ground.	Knee extension (increases till maximum), and then starts to flex. Increased hip extension.
Pre-Swing (PS) (toe-off)	50% – 60% GC	The limb is positioned to start the swing. Starts when the IC of the opposite limb occurs, and ends with the toe-off of the current foot. There is a weight transfer from one foot to the opposite one (LR of the opposite foot).	Increased ankle plantar flexion, greater knee flexion, and loss of hip extension (start of the hip flexion).
		Swing Period	
Initial Swing	60% – 73% GC	The foot leaves the ground. The limb advances in relation to the point where it leaves the ground. Ends when the swing limb passes through the coronal plane of the stance limb (medium support).	Hip flexion and increased knee flexion. Partially ankle dorsiflexion.
Mid Swing	73% – 87% GC	The limb is moving forward by balance. Begins when the swing limb passes beyond the stance limb. Ends when the swing limb is in the front and the tibia is in the vertical direction.	Hip flexion. The knee extends and ankle continues dorsiflexing to neutral.

Phase	Duration in GC	Main Goals and Function	Joints Events
Terminal Swing	87% – 100% GC	Completes the advancement of the swing limb. Prepares the limb for the next stance (next GC). This phase begins with the tibia in vertical position and ends when the foot reaches the floor (beginning of the new GC).	Knee extension. Hip maintains its earlier flexion, the ankle remains dorsiflexed to neutral.

2.2.4 Main Applications

Gait analysis has several applications, the main ones are focused in three areas: Sports, Rehabilitation, and Clinical Diagnosis. In the following subsections some interesting applications of gait analysis are presented that encouraged its development over the last years.

Sports

In high competition sport, athletes are taken to their physical extreme, and sometimes have injuries. Some sports, especially those related to walking and running, can provoke injuries that can be associated with the foot positioning on the ground (the heel) at the IC phase. By informing the athlete that he has to correct this exercise, the injury risk at this location decreases.[4] Ground reaction forces (GRF) can also be analyzed along the gait cycle in order to determine the athlete's physical state. Gait analysis in sports is used during the athletes' train with the goal to prevent injuries at the same time that the athletes' performance is pushed to the limit [Tao et al., 2012].

Rehabilitation

Gait analysis is present in two points of gait rehabilitation: in the analysis of the patient and in the rehabilitation itself. In the analysis of the patient, it is important to understand the state in which he is and the gait impairment level (the intensity of movements and amplitude of the joint's angles). In rehabilitation, the patient performs the prescribed exercises, with the aid of a physician or a system in order to identify if he is performing them correctly.

Gait analysis in rehabilitation can be used with automatic systems. Gait is a complex and repetitive movement. For a proper analysis, accurate and complex measures are necessary to estimate. These would be difficult to extract without resorting to instruments, such as step length, joints' angles, among others.

Throughout rehabilitation exercises patients need to have access to relevant information about the quality of their performance. Without access to the gait parameters, this process can be complex. In addition, many patients today find it difficult to go to rehabilitation centers to perform the

[4] Labiomep.`http://www.labiomep.up.pt/services/clinical-gait-analysis/` (visited on 06/01/2017)

exercises, due to lack of access and/or mobility. The use of automatic systems facilitates the acquisition of gait information, indication of patient performance as the patient performs the exercise and portability so that it is possible to perform the rehabilitation in their home.

As mentioned in Section 1, the intensity of rehabilitation is important for a complete recovery of the patient. Walking is an activity that requires great coordination between the neurological and motor systems, and it is also a cyclical and repetitive task. In this way, the intensity of the gait training is even more necessary for a complete gait recovery. Gait analysis in rehabilitation becomes an essential point and base of all the gait rehabilitation [Tao et al., 2012].

Clinical Diagnosis and Healthcare Monitoring

Gait analysis in the clinical diagnosis and healthcare monitoring has many applications. Those include the detection of certain diseases and their severity, pre-operative planning, especially for patients with cerebral palsy, and surgical decision making. It can also give information about gait after and before surgical interventions, and reduce the number of medical appointments needed to correct some aspects that were not found at the beginning. The number of subsequent surgical interventions (that used to be necessary to correct aspects not fully solved in the first surgical intervention) are minored, thus reducing the cost of care.

Gait analysis can also be useful to determine if the prescribed treatment is appropriate for the patient [Tao et al., 2012], or even if a prosthesis is correctly placed. It can also assist in the determination of gait abnormalities and occurrence of diseases such as Parkinson; an indicator of neurodegenerative diseases progression or other adverse health problems. It can be employed as a fall detector, by detecting fall itself, or by determining the most unstable gait phase, by analyzing qualitatively the GC [Tao et al., 2012].

2.2.5 Pathologies Associated with Gait Impairments

The walking activity involves interaction between the action of bones, muscles, and the nervous system. The gait pattern depends on the level of integration that exists between these three systems. When there is a defect in any of these parts, gait impairment occurs [Ren et al., 2016]. Pathologies that cause changes in the relationship between motor and brain functionalities can be neurological, cardiovascular, motor, musculoskeletal, sensory and even psychological.

The neurological diseases with high prevalence that cause greater influence in gait are Parkinson' disease (PD) [Ren et al., 2016] [Uchitomi et al., 2016], Stroke [Chen et al., 2016] [Eng and Tang, 2007], Multiple Sclerosis (MS) [Comber et al., 2016], cerebral dysfunctions, traumas (mild Traumatic Brain Injury (mTBI)), among others. These require a high care in both the cure of the disease itself and in the gait relearning process.

Cardiovascular diseases are characterized by arrhythmias, thromboses (especially in the lower limbs) and heart attack.

In motor and musculoskeletal fields, there are patients who have suffered from injuries in the ligaments (for example the internal ligaments of the knee), bone fractures, muscle injuries, hip and

knee replacement, and others. Patients with these conditions have a simpler rehabilitation process because the cognitive function is in a healthy state.

The loss of some sensations such as vision and hearing cause a reduction of the awareness around the patient, where they sometimes cause crashes with obstacles leading to a fall (for example, falling from the stairs due to lack of sensitivity in seeing the steps) [Salzman, 2010].

Psychological conditions also cause changes in gait, such as fear of falling, sleep disorders and abuse of toxic substances [Salzman, 2010].

All of these conditions get aggravated with age. Below there is some data about the prevalence of diseases that are inserted in the groups mentioned above, with the aging.

In the neurological field, according to [Bots et al., 1996], the stroke prevalence increases with age in men and women. In Portugal, it can achieve 14% in men between 65 to 74 years old. Portugal is the country with the higher number of stroke death cases in Europe [Sousa-Uva and Dias, 2014]. According to [Gordon R. Kelley, 2015], the prevalence of Parkinson disease also increases with age, especially from the age of 50 with the highest incidence from 60 years old forward. Multiple sclerosis, although it affects younger people (30 to 50 years old [Baum and Rothschild, 1981]), the movement difficulties associated with the disease also increases with age. The main problem is the falling risk that can result in serious injuries, such as broken bones, broken ligaments, head injuries or even death.

In the musculoskeletal field, osteoarthritis' prevalence, according to [Felson et al., 2000], increases 2 to 10 fold from 30 to 65 years of age and increases further thereafter. Osteoporosis prevalence, with special attention to the spine, knee and hip cases, increases significantly with age in men and in women [Cummings and Melton, 2002].

Each of the diseases presented get worse with age, and even in the absence of them, age can cause loss of senses and agility resulting in changes in gait pattern. In all these cases, rehabilitation of gait helps to maintain confidence in walking, to keep the patient focused on the repetition of the steps while walking, and to reduce the risk of falling, which is one of the main factors causing disability in the elderly.

2.3 Gait Parameters

As presented in Section 2.2, gait can be divided in: periods, tasks, and phases. In order to do a quantitative gait analysis, it is important to have metrics that allow a comparative evaluation. Gait can be evaluated regarding spatial, temporal, kinematic and kinetic parameters. Spatial and temporal parameters consist of the time and space dimensions. They give information about the distance between each step, or between the two feet, or stride velocity, etc. A kinematic analysis is focused on the joints' angles while walking. The intensity and direction of the forces made by the feet during gait are also analysed: these are kinetic parameters. More details about the previous mentioned type of parameters are described in the following subsections. The analysis presented is related to the use of the mentioned parameters and also has an annotation about in

which pathologies they are evaluated and used. The gait parameters are described in the Tables 2.2, 2.3, 2.4, and 2.6.

2.3.1 Spatio-Temporal Parameters

Spatial and temporal gait parameters are extracted from gait, while walking, and are related to the time and space dimensions. The spatial parameters are presented and defined in Table 2.2, the temporal parameters are presented in Table 2.3. In Table 2.4 the parameters that join spatial and temporal information are summarized.

Table 2.2: Spatial Gait Parameters and their definition.

Parameter	Definition	Requirements	Applications
GC Length (Stride length) [Muro-de-la Herran et al., 2014], [Najafi et al., 2011], [Aminian et al., 2002],[Kraan et al., 2016], [Alfuth, 2017]	Linear distance in anterior-posterior direction, between two successive placements on the ground by the same foot. It is the difference between the position of the following IC and the previous IC, of the same foot (i.e., two steps).	Space or velocity information, and IC identification.	MS, PD, and general evaluations.
Step Length [Muro-de-la Herran et al., 2014], [Simoes, 2011], [Spain et al., 2012],[Kraan et al., 2016], [Alfuth, 2017]	Linear distance in anterior-posterior direction, between the placement of both feet. It is the difference between the position of the IC of one foot and the IC of the opposite foot (i.e.,one step).	Space or velocity information, and initial contact identification.	mTBI, MS, PD, musculoskeletal, and general evaluations.
Step width [Muro-de-la Herran et al., 2014], [Kraan et al., 2016], [Alfuth, 2017]	Linear distance in medio-lateral direction, between two equivalent points of both feet (also known as base of support).	Space or distance information, and angles of the body (lower limbs) segments.	MS and general evaluations.

In Table 2.2, the most used spatial parameters in the evaluation of gait are the GC length, step length, and step width (Figure 2.5). Even in healthcare centers, these three parameters are widely used by physiotherapists in gait rehabilitation. Even without a sophisticated system, they can be determined by simply painting the patient's feet and having him walk on a paper walker.

Figure 2.5: Spatial Parameters: GC length (stride length), step length and step width.

Temporal parameters also have important information about patient's gait, helping physiotherapist on the gait rehabilitation process and patient's performance evaluation. In Table 2.3 are presented and defined temporal parameters related to gait rehabilitation.

Table 2.3: Temporal Gait Parameters and their definition.

Parameter	Definition	Requirements	Applications
Swing Time [Muro-de-la Herran et al., 2014], [Kraan et al., 2016], [Alfuth, 2017]	Time interval between the foot leaving the floor and touching it again (for each foot).	Identification of the PS and IC times.	MS, PD, musculoskeletal, and general evaluations.
Stance Time [Muro-de-la Herran et al., 2014], [Najafi et al., 2011], [Alfuth, 2017]	Amount of time the foot is on the floor. Is the time difference between the PS and IC of the same foot. Also known as Support Time.	IC and PS times identification.	MS, PD, and general evaluations.
GC Time (Stride Time) [Najafi et al., 2011], [Kraan et al., 2016], [Alfuth, 2017]	Duration of each GC. Time interval between two successive contacts of the same foot with the ground (i.e., two steps).	IC identification.	MS, PD, musculoskeletal.
Step Time [Kraan et al., 2016], [Alfuth, 2017]	Duration of one step. Time interval between two successive contacts of opposite feet with the ground (i.e., one step).	IC identification.	General evaluations.
Initial Double Support Time [Aminian et al., 2002]	Time between the IC of one foot and the PS of the opposite foot. Also known as Double Thrust Support.	Identification of the IC and PS times.	MS, PD.
Terminal Double Support Time [Aminian et al., 2002]	Time between the IC of the opposite foot and the PS of the foot being analyzed.	Identification of the IC and PS times.	MS, PD.
Double Support Time [Spain et al., 2012], [Aminian et al., 2002], [Kraan et al., 2016], [Alfuth, 2017]	Time interval where there is support of both feet. Is the sum of the initial double support time and terminal double support time.	Information about IC and PS of both feet.	MS, PD.
Single Support Time [Kraan et al., 2016], [Alfuth, 2017]	Time interval of the stance of one foot, when it is the only foot on the ground (in SLS period). Is equivalent to the swing time of the opposite foot: is the time interval between the IC of the opposite foot and the PS of the opposite foot.	Identification of the IC and PS times.	MS, PD.

After an evaluation and search through clinical practices, it is possible to ensure that, of the overall temporal parameters presented and defined in Table 2.3, the most used parameters are the swing time, stance time, CG time and double support time (Figure 2.6). Although, these

parameters are the most common, but the remaining parameters can provide other interesting information about gait. For example, when a subject presents a small single support time, it can mean that he has pain in the corresponding lower limb, or does not have endurance in that limb, or other aspects, that may not be noticed by the most used parameters.

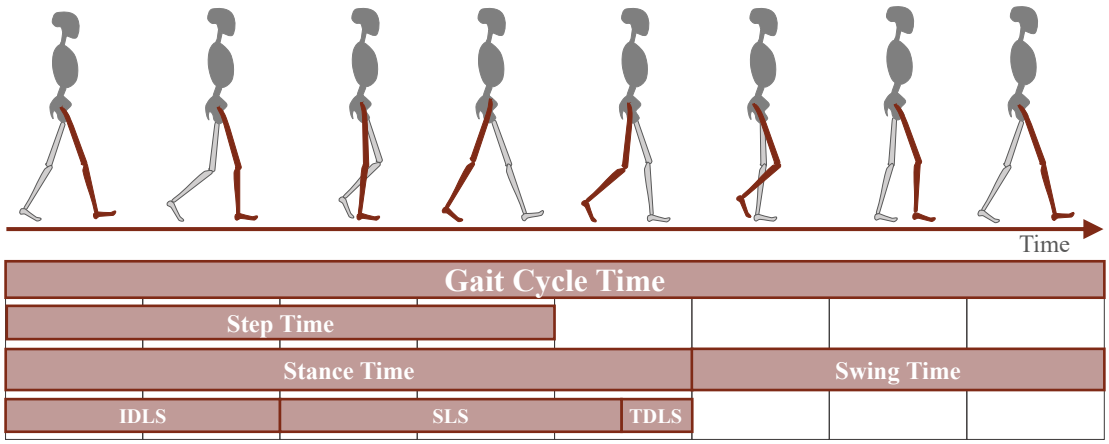

Figure 2.6: Temporal Parameters: gait cycle, step, stance, swing, initial double limb support, single limb support and terminal double limb support times.

In Table 2.4 are described parameters that are the result of joining the dimension of space and time.

Table 2.4: Spatio-Temporal Gait Parameters and their definition.

Parameter	Definition	Requirements	Applications
Velocity [Muro-de-la Herran et al., 2014], [Kraan et al., 2016], [Alfuth, 2017]	Distance walked per time.	Distance walked (or step length), and time.	MS, PD, Stroke, musculoskeletal and general evaluation.
Stride Velocity [Najafi et al., 2011]	Distance walked per stride (of each foot) per time.	Distance walked and time information, and IC identification.	General evaluation.
Cadence or Rhythm [Murray et al., 1964], [Simoes, 2011], [Spain et al., 2012], [Kraan et al., 2016], [Alfuth, 2017]	Number of steps per time unit (usually in minute). It is also defined as stepping frequency.	Step (or IC of each foot) identification.	mTBI, MS, PD, musculoskeletal, and general evaluation.
Gait Autonomy (Walking Distance) [Muro-de-la Herran et al., 2014], [Alfuth, 2017], [Eng and Tang, 2007]	The maximum time a person can walk, taking into account the number, duration, and length of the steps.	Information of time and distance walked. It can be used also the number of steps (IC).	PD, stroke.

Parameter	Definition	Requirements	Applications
Tremors presence or Freezing of Gait [Muro-de-la Herran et al., 2014], [Horak and Mancini, 2013]	Presence of tremors in the lower limbs segments.	Frequency behaviour of the segments and time.	PD.
Balance [Horak and Mancini, 2013]	Control of the body center of mass during daily activities.	Information about the trunk movements and time.	PD and general evaluation.
Postural Transitions [Horak and Mancini, 2013]	Body center of mass control during the weight acceptance task.	Balance, IC and PS identification.	PD, stroke, musculoskeletal, and general evaluation.
Gait Variability [Najafi et al., 2011], [Kraan et al., 2016], [Alfuth, 2017]	It is generally the calculated coefficient of variation (CoV) or standard deviation (SD) of one spatiotemporal parameters mentioned in Tables 2.2 and 2.3. It is often determined upon stride length, step length, stride time, step time, step width, stance time, stride time and double support time.	Two spatiotemporal parameters of the same foot, and the CoV or SD between them.	PD, stroke, musculoskeletal and general evaluation.
Gait Asymmetry [Kraan et al., 2016], [Yang et al., 2013], [Casamassima et al., 2014]	It is the relation (CoV or SD) between one of the spatialtemporal parameters mentioned in Tables 2.2 and 2.3, of left and right lower limb, during gait.	Two spatiotemporal parameters of both feet, and the CoV or SD between them.	PD, stroke, musculoskeletal and general evaluations.

In Table 2.4 the most used spatial-temporal parameters are the velocity, cadence or rhythm (Figure 2.7), variability (Figure 2.8a, and asymmetry (Figure 2.8b). But, depending on the patient's condition, it can be also crucial to analyze the presence of tremors, among others.

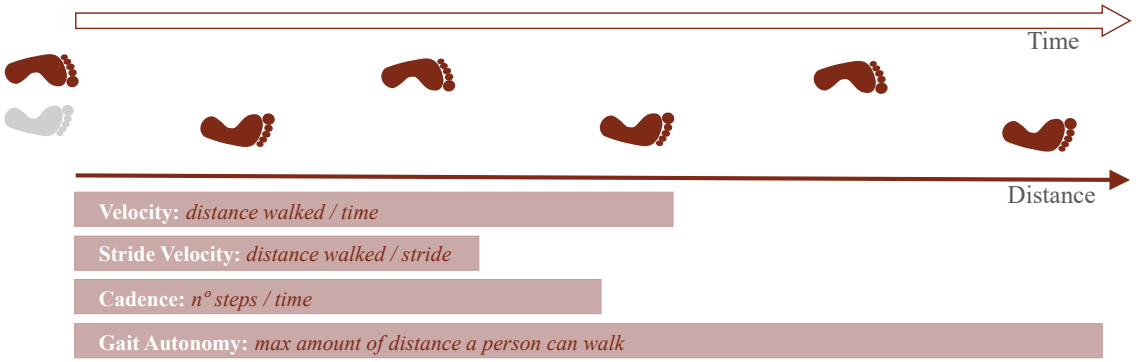

Figure 2.7: Spatio-temporal Parameters: velocity, stride velocity, cadence and gait autonomy.

The balance and postural transitions are crucial parameters in walking because while walking, there is a constantly body-weight change from one leg to the other, constantly having a balance

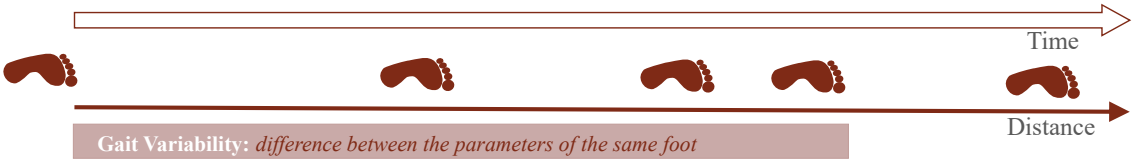

(a) Gait Variability.

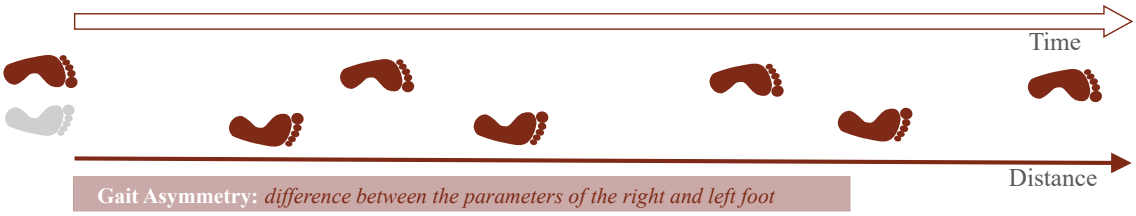

(b) Gait Asymmetry.

Figure 2.8: Spatio-temporal Parameters: gait variability and asymmetry. While the variability compares parameters of the same lower limb, the asymmetry, compares parameters of the two lower limbs.

in the forward direction. The result of the posture is different from the one that exists when in standing position.

2.3.2 Kinematic Parameters

Kinematics aims to evaluate the motion of segments without considering its mass. Thus, a kinematic analysis in gait is made upon the angles and Range of Motion (ROM). In Table 2.1, it was shown a set of different motion events that occur and define each gait phase. As mentioned in the Subsection 2.1.2, these motion events are flexion, extension, abduction, adduction, dorsiflexion and plantar flexion. The relation between them can be characteristic of each phase of gait. With a kinematic analysis, it is possible to determine these events and assist the gait analysis.

Table 2.5: Gait kinematic parameters and their definition.

Parameter	Definition	Requirements	Applications
Steps' angle [Muro-de-la Herran et al., 2014]	Direction of the foot during the step (in relation to the trunk).	Orientation of the foot.	General evaluation.
Direction of the lower limb segments [Muro-de-la Herran et al., 2014]	Direction of each leg while walking.	Orientation of the foot, knee and leg segments during the walk, in relation to the trunk.	General evaluation.
Joints' angles [Muro-de-la Herran et al., 2014], [Alfuth, 2017],	ROM of the hip, knee and ankle joints.	Relation between the orientation of the lower limb segments (specially at heel strike and toe-off).	MS, stroke, musculoskeletal, and general evaluation.

Parameter	Definition	Requirements	Applications
Torso rate of rotation [Simoes, 2011]	Rate of the rotation of the torso, around the vertical axis.	Definition of the vertical axis, and torso orientation.	mTBI.
Head rate of rotation [Simoes, 2011]	Rate of the rotation of the head, around the vertical axis.	Definition of the vertical axis, and head orientation.	mTBI.

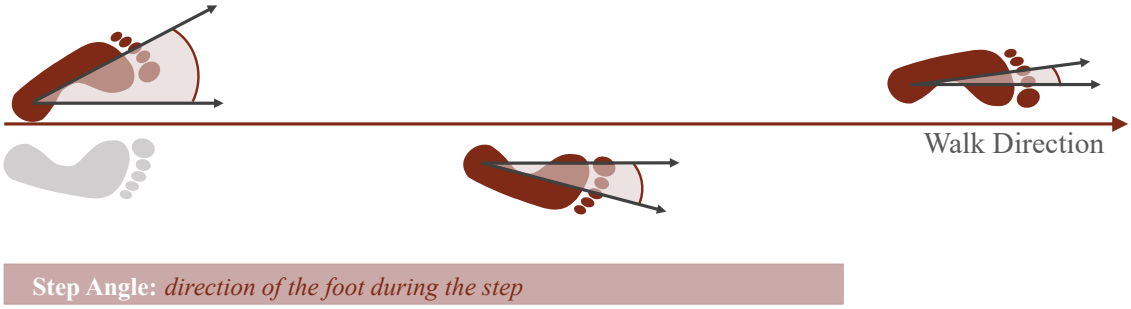

Figure 2.9: Kinematic Parameters: step angle.

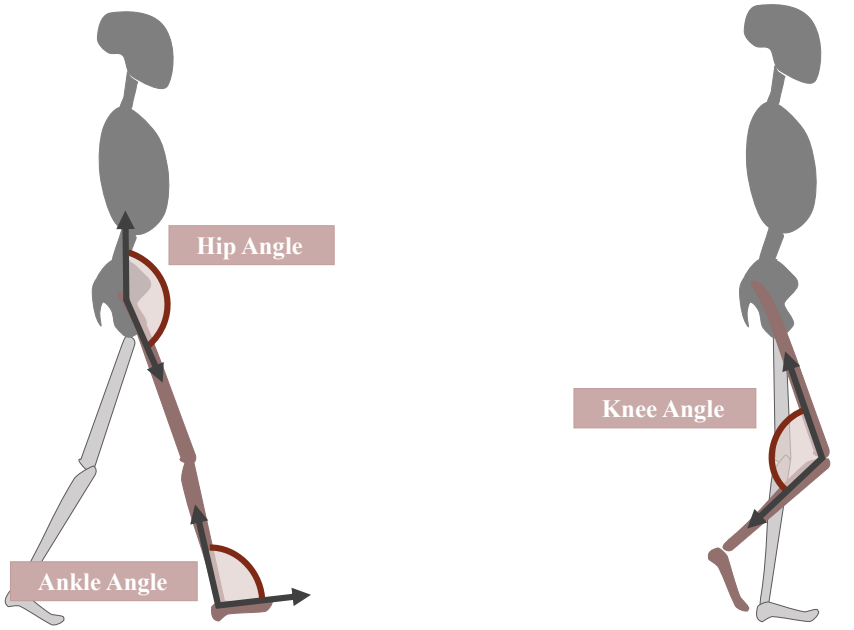

(a) Hip and ankle joint's angles.

(b) Knee joint's angle.

Figure 2.10: Kinematic Parameters - joint's angles (in the sagittal plane).

Most of these parameters (Figure 2.9 and 2.10) require sophisticated instrumental systems, in order to do the measurements. For example, the joints' angles (Figure 2.10) are important to know if the patient is doing a proper gait pattern. Patients with stroke tend to avoid the knee flexion (by compensating with the lifting of the hip to raise the foot) on the injured side while moving the lower limb forward [van Meulen et al., 2016]. By identifying this joint's angle, it is possible to

determine if the patient is doing a proper gait pattern, and inform him to do the flexion of the knee in that specific moment.

2.3.3 Kinetic Parameters

Kinetics is the branch of mechanics that deals with forces, their effect on bodies at rest and in motion (static and dynamic, respectively) [Zatsiorsky, 2002]. Thus, the gait kinetic parameters are related to the forces and moments made by the body parts while walking.

Table 2.6: Gait kinetic parameter: ground reaction forces.

Parameter	Definition	Requirements	Applications
Ground Reaction Forces (GRF) [Alfuth, 2017]	During stance times, is the direction and intensity of the forces produced in the ground by a set of different parts of the foot.	Forces and momentum of the foot in the ground, while walking.	MS, musculoskeletal, and general evaluation.

During the walking activity, we place the feet on the ground, one at a time, and automatically transfer the body weight from one foot to the other. Analysing in detail (Figure 2.11), the resulting force changes since the moment when the foot first touches the ground (IC) untill it lifts it. Then, tends to be higher in the IC (shock absorption), reduces to the equivalent of the body weight in the mid-stance (in the SLS), and increases again when the foot initializes the impulse to begin its swing and move the leg forward. The GRF can be interesting to analyze patients with an orthopedic prosthesis, and estimate the stress between the prosthesis and the patient's bone.

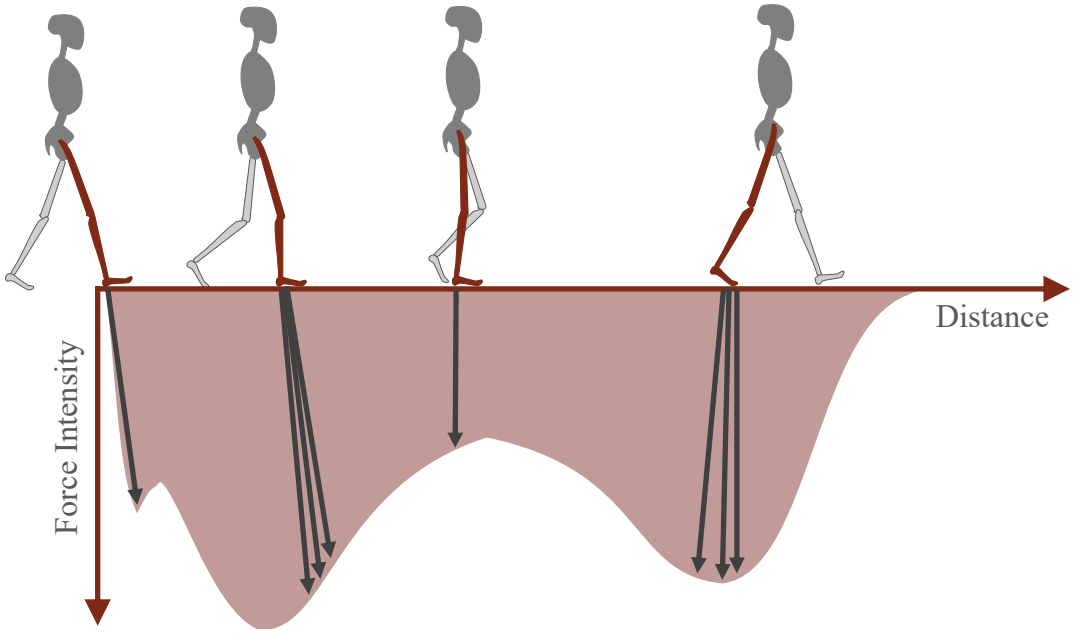

Figure 2.11: Kinetic Parameters: ground reaction forces (in the sagittal plane) (adapted from [Pohl and Mehrholz, 2006]).

Concluding this section, the parameters of gait measured are key metrics in gait analysis. If an automatic data acquisition is made (through a technological system), these parameters can determine leading to a more accurate and precise analysis. In this way, applied to rehabilitation, they can allow a higher care and accuracy. The patient is evaluated correctly as well as being encouraged to make the gait exercises according to their capacity (evaluated previously), according to the movement that he is doing, and with feedback and movement correction in real time.

2.4 Gait Rehabilitation

Rehabilitation in health refers to specialized treatments and healthcare programs, designed to facilitate the recovery process of patients after an injury, illness, disease or surgery. It aims to improve, maintain or restore physical strength, cognition, and mobility, in a way as close as possible to a normal condition.[5] There are different types of rehabilitation: drug, physical, vision, speech, occupational, vocational and others. In general, the rehabilitation aims to help people gain a higher independence after an injury or surgery. After an event that compromises the physical activity, rehabilitation is prescribed in order to help people to achieve higher functional levels and quality of life so that they are able to do their ADLs freely. It has to be noted that rehabilitation does not reverse the patient's damage, caused by disease or trauma, but helps to restore some features in order to increase the health quality. Each rehabilitation program is individually prescribed to a specific patient's needs, and can include more than one type of exercises.[2]

Gait rehabilitation is the type of physical rehabilitation that focus on the walking activity. The main goals of the gait rehabilitation are, in a short-term, lower the falling risk by increasing the lower limbs' strength, dynamic balance and posture.[6] The long-term goal is to recover a safe and confident walk in a way that can bring a complete independence to the patient. To achieve these two goals, the gait rehabilitation is divided into two types of training: strength training and task-specific training.

Strength Training: Is composed of exercises that have the purpose of increasing the strength of specific muscles. The exercises are repetitive aiming the patient to remember this repetition, through the mechanisms of neural plasticity, and thus improving confidence in walking. Some strength training exercises consist of just moving the body weight from one leg to the other, standing on one leg, calf raises, and others.[7]

Task-specific Training: Is composed of exercises involving walking. There are two types of training: with and without body-weight support. With weight support are exercises that consist of alternating the body weight from one lower limb to the other (without walking), and without

[5] TheFreeDictionary. `http://medical-dictionary.thefreedictionary.com/rehabilitation` (visited on 21/12/2016)

[6] HealthLine.`http://www.healthline.com/health/gait-training` (visited on 22/12/2016)

[7] Flint Rehabilitation Devices. `https://www.flintrehab.com/2015/what-is-gait-training/` (visited on 22/12/2016)

weight support, are exercises (with the use of body weight supports) in which the patient performs the movements characteristic of the gait.

Through all the gait rehabilitation exercises, the patient has to be able to develop the following aspects:[6]

Muscles and joints with higher strength: With the repetition of the exercises, the patient has to develop the muscles responsible for each gait phase. With this, he can increase the joints' and muscles' strength.

Improve dynamic balance and increase posture stability: Two of the most important aspects while walking, are the balance and posture. While we walk forward, we are constantly changing our posture forward. Controlling the posture is a key aspect in order to prevent falls, and thus improve patient's confidence in walking.

Build/increase endurance: Endurance while walking is a key area, since we have to support all of the body weight, and also ensure a considerable distance for walking without feeling neither pain or fatigue.

Develop muscle memory: After an intervention or disease, muscles can lose the natural memory in doing some activities. In walking, there are several muscles that are activated in group with a specific coordination. Repetition of the gait exercise, with real-time guidance, helps to regain a proper muscle memory.

Increase control during transitional movements: While we walk, one of the tasks made by the lower body part is ensuring that the body weight passes from one lower limb to the other, safely. Exercises are prescribed so the patient will train the support of the body in each of the lower limbs.

Retrain the legs for repetitive motion: The walking activity is composed by the repetition of several GC, and the lower limbs have to be prepared in strength and endurance for this.

Lower the fall risk, while increasing the mobility: The greatest consequence of an abnormal gait is the falling event. Thus, gait rehabilitation plays an important role in preventing falls.

Depending on the patient's condition, the rehabilitation may occur at different levels, and the patient has also different responses while walking. In a general way, the gait rehabilitation theme can be divided into the two most important disease areas: neurological diseases and musculoskeletal traumas.

When the patient has neurological conditions, their rehabilitation can be planned in two senses: *top down* and *bottom up*. *Top down* is based on what the patient knows, what he is capable of doing, and his abilities. Begins with exercises that the patient can do, with the support of a clinician who corrects him when he can not do the exercise properly. *Bottom-up* exercises are based on the brain plasticity of learning. The patient has to do certain exercises with the sense of learning to do them,

often resorting to a physician or system. Each patient that suffers from neurological diseases is almost always unique, being necessary to have a well-attended and specialized treatment. For each patient may be more adequate to have top down or bottom up approaches [Ren et al., 2016], according to his condition.

When it comes to rehabilitation of musculoskeletal conditions, the patient has complete awareness and cognitive ability only suffered trauma in the most distal parts of the body. In this case, rehabilitation can insist in force, and as already mentioned, in repetition, so that when tissue regenerates (or adaptates to the prosthesis, depending on the trauma), it is adapted to its gait functionality.

2.4.1 Clinical Tests Applied to Gait Analysis

Clinical tests applied to gait analysis aims to determine, in a simple way, the falling probability, especially in the elderly. The main goal of these methods is to evaluate the patient's balance and posture while walking and moving. They consist in simple methods that evaluate the patient's stability, by measuring the time of the exercise, posture and stability, while the patient is doing a specific exercise.

These tests do not directly evaluate gait, they are used to collect information about the patients' mobility status, and in the clinical setting to perform the evaluation of the state of the patient's movement.

Timed Up and Go (TUG)

TUG is a gait analysis method that consists in having the patient to sit on a chair, get up, walk 3 meters, then turn around, go back to the chair, turn around again, and sit down. The TUG value is obtained from several trials, in order to obtain an average of the time that the patient takes to go through the described route [Simoes, 2011].

In order to evaluate the patients, there are four scales presented in Table 2.7. The table relates the state of the patient's movement and also the risk of falling with the time that the patient takes to do the task.

Table 2.7: Relation between the time the patients have in performing the TUG test and its movement condition (adapted from [Simoes, 2011])

Time required to complete the task	**Description of the patient's movement**	**Falling Risk**
10 seconds	Generally freely mobile	*Low*
10-20 seconds	Mostly independent	*Low*
20-29 seconds	Variable mobility	*Moderate*
more than 29 seconds	Mobility impaired	*High*

Berg Balance Scale (BBS)

The BBS is a scale whose utility is grading the different patient's balance ability in order to obtain a functional balance over time. This scale is commonly used between treatments since it is a good tool to evaluate the patient's responses to the respective treatment. The BBS can also be applied while the patient is performing different tasks. The total range of the scale is from 0 to 56, where a lower score is related to a lower walking function and balance capacity, that leads to a higher falling risk [van Meulen et al., 2016].

Walk

Walking is the most common and simple way to obtain a qualitative knowledge about the gait pattern. There are several ways to assess the patient's gait: through asymmetry, variability, and ability to rotate with respect to the lower limbs, upper limbs, and trunk. Depending on the method used, the arms may or may not be considered, since they belong to the passenger unit that acts as a whole along the gait (as seen in Subsection 2.2.1).

Postural Sway or Center of Pressure (CoP)

CoP is a method used to measure the balance while the patient is standing. It is often called the center of pressure, and, by comparison, associated with the center of mass (CoM), being characterized by the ground reaction force vector.

In many CoP exercises, the patient is instructed to perform changes of posture with the feet fixed on the ground, both in the sagittal and coronal planes. Thus, a set of parameters such as angle reached without loss of posture control is evaluated in both planes [Yamamoto et al., 2015].

Clinical Test of Sensory and Balance (CTSIB) and Modified CTSIB (mCTSIB)

CTSIB is a method designed to access the ability of a person to control their balance with the use of the senses. According to [Wrisley and Whitney, 2004], there are six conditions :

1. Standing on a flat, firm surface with eyes opened,
2. Standing on a flat, firm surface with eyes closed,
3. Standing with a visual obstacle on a firm surface,
4. Standing on a compliant surface with eyes opened,
5. Standing on a compliant surface with eyes closed,
6. Standing with a visual obstacle on a compliant surface.

This process is quite complex, thus a modified version of it is usually used. It is defined as the modified CTSIB and contains only conditions 1, 2, 4, and 5 [Wrisley and Whitney, 2004].

Balance Error Scoring System (BESS) and Modified BESS (mBESS)

BESS is a method commonly used by clinicians and researchers to evaluate patient's balance. Contains three stances:

1. Double-leg stance (hand on the hips and feet together),
2. Single-leg stance (standing on the non-dominant lower limb with hands on hips),
3. Tandem stance (non-dominant foot behind the dominant foot).

These tasks are performed on a firm surface and on a foam surface, with eyes closed, with error counts every 20 seconds. An error is defined as: opening the eyes, moving the hands off the hips, stepping, stumbling or falling out of position, lifting forefoot or heel, doing hip abduction more than 30 degrees, or falling and taking more than 5 seconds to get back to the test position [Bell et al., 2011].

360º Turn Test

The turn test is a test used to measure the balance. The patient is required to perform a turn on 360º himself. In this way, the dynamic balance is evaluated according to the number of steps that the patient needs, and the time taken to complete the task. The patient can also make the turn in both directions[8].

Five times sit-to-stand test (FTSTS)

Sit to stand is a physical exercise that is highly influenced by muscle strength, especially the lower limbs muscles. Older people or those with gait problems tend to have less strength in the lower limbs. In this way, the evaluation of this activity is a good metric to predict the physical state of that person's lower limbs. Since there is a change in posture from sitting to lifting, this activity is also a good way to assess the balance. The score associated with this test is the time the patient takes to do it, and the larger the score, the greater the likelihood of the patient falling [Duncan et al., 2011].

2.5 Automatic Systems in Gait Analysis

To date, there is a large set of automatic systems and there are researchers studying more possibilities to better analyze the gait giving more accurate, crucial, and representative data to the gait specialists. As presented in Subsection 2.2.4, the analysis of gait has several applications. Depending on the application, different systems can be implemented to respond to each need.

In the following subsections different approaches are presented for an automatic motion analysis. Those devices can be classified into [Muro-de-la Herran et al., 2014]:

[8]Rehab Measures. `http://www.rehabmeasures.org/Lists/RehabMeasures/DispForm.aspx?ID=1123` (visited on 11/01/2017) (Author: Janson Raad)

Non-wearable sensors (NWS): These systems are mostly non-portable. Adequate rooms or laboratories are needed to capture gait data while an individual walks on a defined walkway.

Wearable sensors (WS): Allows its use outside the gait laboratory. In this way, it is possible to analyze the patients' gait during their ADLs.

Hybrid Systems (HS): are systems with markers placed on the body segments whose location is captured by cameras.

The following sections serve as a brief overview of these systems, with the main application in gait analysis.

2.5.1 Non-Wearable Systems

NWS can also be classified into two subgroups [Muro-de-la Herran et al., 2014]:

Image processing: Systems based on this technology consist of image capture. There are several conformations for data acquisition: a 2D camera, a 3D camera or several cameras scattered in a room (3D). There are other optical sensors such as laser range scanners, infrared sensors and Time-of Flight.

Floor Sensors: Systems based on pressure sensors (force platforms), which capture the force exerted on its surface. These systems, unlike the previous ones, allow to measure kinetic parameters (like GRF).

Image Processing

As already mentioned, image processing motion capture systems may consist of 2D, 3D camera capture or even multiple cameras in one room. A very basic method of image processing usually used by these systems consists of threshold filtering that removes the background of the image leaving only the silhouette of the patient's body, which will then be evaluated to extract the gait parameters. The evaluation setup usually consists of the patient walk on a specific walkway and then joints' angles and the number of steps, given a known-size walkway, can be measured. Temporal and even spatial parameters can also be determined, allowing its use in gait rehabilitation applications. There are rehabilitation systems based on image analysis, such as NeuroAtHome[9] (Figure 2.12), Reflexion Health[10], Virtualware[11], among others.

Systems based on motion image analysis are able to capture gait data neither touching the patient nor placing markers or sensors. However, these systems are not very portable because they require a room or laboratory with the cameras installed in order to acquire the movement. The movement captured is restricted to a specific path, not being close to the patients' ADLs. The algorithms that compose them are in general complex, because they need to segment the silhouette

[9] NeuroAtHome. `http://www.neuroathome.com/en/` (visited on 30/01/2017)
[10] Reflexion Health. `http://reflexionhealth.com/for-patients/` (visited on 30/01/2017)
[11] Virtualware. `http://virtualwaregroup.com/en/products/virtualrehab` (visited on 30/01/2017)

Figure 2.12: Example of a gait rehabilitation exercise with a image-based system (NeuroAtHome[9]).

of the patient's human body, they must be able to distinguish the patient from the background, even with the presence of other people.

Floor Sensors

Some of the structures with lateral supports, used in clinics for evaluation of gait, contain pressure sensors. These systems are the most basic and general of all systems used in gait analysis and are also the most used in rehabilitation facilities. There are two types of pressure sensors associated with these systems: force platforms and pressure measurement systems.

The force platforms allow the identification of the places where a pressure has been applied (the footprints). In this way, it is possible to locate the pressure center and, with space and time references, it is also possible to obtain spatial and temporal parameters.

Pressure measurement systems, in addition to the pressure platforms features, are also capable of quantifying the pressure (direction and intensity). However, it is only in the vertical direction, they do not allow to obtain horizontal force components or shear [Muro-de-la Herran et al., 2014].

There are several commercialized systems such as GAITRite[12] (Figure 2.13), AMTI force and motion[13], Kistler (force and gait analysis products)[14], among others. These systems are among the few ones to measure the GRF. Its use consists of placing the patient to walk on the treadmill where the sensors are (an example is demonstrated in Figure 2.13). These systems continue to require expensive, non-portable equipment and are poorly suited to patients' home use. In this way, the path is limited to the space of the treadmill, and also decreases its portability. In addition, as the information captured is only when the foot is on the ground, little information about the swing phase is obtained. It is also not possible to estimate the kinematic parameters.

[12]GAITRite `http://www.gaitrite.com/` (visited on 30/01/2017)

[13]AMTI. `http://amti.biz/` (visited on 30/01/2017)

[14]Kistler. `https://www.kistler.com/lv/en/products/products-by-applications/motion-gait-analysis-products/#large__force__plate_for__research_and__sports_9287_c` (visited on 30/01/2017)

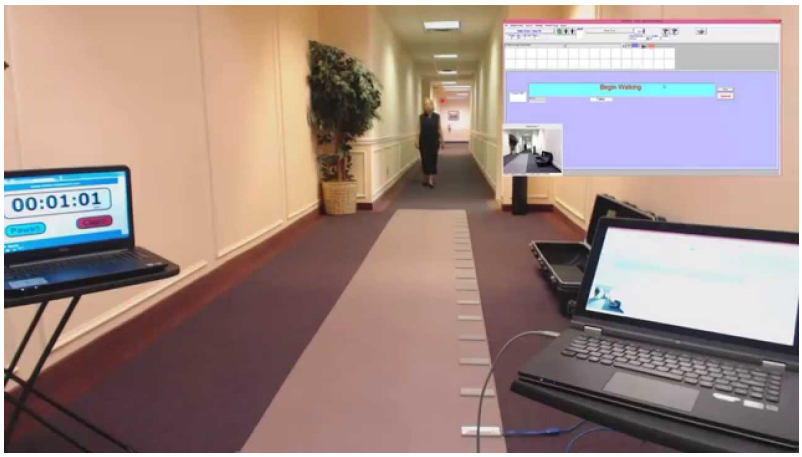

Figure 2.13: Example of a gait rehabilitation exercise with a floor sensor system (GAITRite[12]).

2.5.2 Wearable Systems

WS can be used on various parts of the body such as feet, knees, thighs, shank or waist, to measure different gait parameters. Sensors that can capture gait data, include accelerometers, gyroscopes, magnetometers, force sensors, extensometers, goniometers, active markers, electromyography sensors, among others [Muro-de-la Herran et al., 2014]. Not all of these are portable and easy to use at home.

Force Sensors

Pressure sensors on insoles (under each foot) are similar to force platforms and pressure measurement systems. They allow the measure of the GRF of each foot while walking (Figure 2.14).

Piezoelectric, resistive, capacitive, piezoresistive are different types of sensors that can be used in insoles and are chosen according to the pressure range to be exposed, and the linearity and sensitivity in that range [Muro-de-la Herran et al., 2014].

Force sensors placed inside shoes are used in gait analysis systems, such as the Insole X (Smart Insoles' product) [15] (Figure 2.14a). There are also some models that are able to observe the difference in pressure along the foot area (from the heel to the toes), allowing to do a mapping of the pressure exerted on the sole of the foot [Tao et al., 2012], such as the Moticon's Insole[16] (Figure 2.14b).

These systems, being used in insoles, allow the evaluation of gait analysis anywhere along the patient's ADLs, and are easy to use. However, they do not allow the acquisition of data on the swing phase joint's angles and balance, containing incomplete information for a gait analysis in rehabilitation.

[15] Smart Insoles - Insole X. `http://sennostore.com/` (visited on 02/02/2017)
[16] Moticon - Insole. `http://www.moticon.de/products/science-research` (visited on 02/02/2017)

(a) Insoles with force sensors that capture gait data (Smart Insoles[15]).

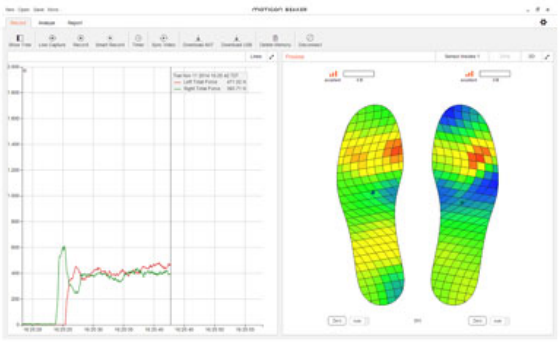

(b) Insoles with force sensors that mapp the foot area while walking (Moticon[16]).

Figure 2.14: Example of a gait analysis system with a force sensors in insoles. In (a) are insoles systems that perform gait analysis. In (b) are insoles that are able to mapp all the foot area.

Inertial Sensors

Inertial sensors are devices that contain accelerometers and gyroscopes and often magnetometers, allowing to measure the angular velocity of an object, its acceleration, and/or orientation. IMUs are devices inserted in this type. Depending on its position in the segments of the human body, temporal parameters and angles of the segments can be acquired. The spatial parameters can be obtained with trigonometry models with the measurement of the respective body segment [Tao et al., 2012].

There are wireless IMUs, allowing for greater usability during rehabilitation sessions, such as LEGSys[17] (Figure 2.15a), and G-Walk[18] (Figure 2.15b).

Recently, we have witnessed the increase in the accuracy of these systems being now about 2 degrees in marketable inertial sensors, such as (MTw from Xsens[xse, 2015b], InertiaCube 3 from Intersense[19], Inertia-Link from Micro-strain[20], among others). Those are portable and easy to attach to the body. In this way, they can be used anywhere, with close proximity to the ADLs of

[17]Biosensics - LEGSys. `http://www.biosensics.com/products/legsys/` (visited on 02/02/2017)

[18]G-Walk. `fhttp://www.btsbioengineering.com/products/kinematics/bts-g-walk/` (visited on 02/02/2017)

[19]Intersense - InertiaCube3. `http://www.intersense.com/pages/67/59/` (visited on 24/01/2017)

[20]Micro-strain - Inertia-Link. `https://www.microstrain.com/content/inertia-link%C2%AE-product-no-longer-stocked-%E2%80%93-limited-availability` (visited on 24/01/2017)

(a) IMU system that perform gait analysis (LEGSys[17]).

(b) IMU system that perform gait analysis (G-Walk[18]).

Figure 2.15: Example of a gait analysis system based on IMUs. In (a) is one approach based in several IMUs placed at the lower limb. In (b) is another approach based in one IMU placed at the lower back.

the patient. However, there is still a strong problem associated with magnetic interference and drift due to continued use of the sensors. These interferences reduce the accuracy of the information provided by the sensors. In this sense, complex algorithms are needed to solve this problem.

Electromyography (EMG)

EMG measures the electrical activity of muscles. When a muscle contracts, there is an electrical activity associated, which can be acquired by an electrode. The electrodes may be non-invasive or invasive (needle type), depending on the specificity of data that is required.

The use of these systems in gait analysis is in a different approach, than the other systems. These systems allow the detection of muscles spasticity, loss of motor selectivity in antagonistic muscles, among other properties that can be inferred from muscle activity [Muro-de-la Herran et al., 2014]. To accomplish this analysis the electrode is placed on muscles specifically related to these activities. [Tao et al., 2012]. This level of detail is often difficult to acquire with the previously mentioned systems.

The placement of the electrodes is the first step of this system, being quite meticulous. It has to be adjacent to certain muscles that go into action along the gait. In addition, it is very sensitive to interferences that may occur near the sensors (such as other electrical signals from the body resulting from other activities such as heartbeat), which are also felt on the skin (where the electrodes are). There are EMG systems that require the electrodes to be placed in the muscle (invasive), that suffer less noise interference. These systems are highly complicated to be used both in clinics and at home for rehabilitation practice, being mostly used for medical diagnosis and sports.

These systems allow access to lower limbs muscle activity, which provides more detailed information on the patient's physical state in more anatomical terms [Tao et al., 2012]. However,

do not allow direct measurement of gait parameters indicated in Section 2.3, being not suitable for use in gait analysis for rehabilitation.

2.5.3 Hybrid Systems

HS are systems that require the installation of components in a room, such as cameras, and the placement of markers along the body. These systems are also called vision-based tracking with markers.

The basic technique of these system consists in the acquisition of movements of the human body from the capture of the location of markers (which are placed along the body segments being analyzed) by optical sensors [Zhou and Hu, 2004]. The setup is similar to the one shown in Figure 2.16, where it can be seen by cameras in the upper corners of the room and markers placed along specific locations at the people's body segments.

Marketable systems using this type of technology are for example the VICON[21] (Figure 2.16), and Qualisys[22].

Figure 2.16: Example of the gait analysis performed by a camara based system with markers (HS) (VICON gait analysis[22]).

These are the systems with higher accuracy, being considered the gold standard. They are used in many researches as the method of comparison to provide the ground truth. These are even used in cinematography, in the acquisition of movement for animation of films. Of all the systems previously described, they are the ones that present the best performance and results. However, they are quite expensive, its installation is time-consuming, it takes a long time in calibration processes, making it practically impossible to use in clinics with a large amount of patients and at patients' home.

In order to summarize all the advantages and disadvantages of the presented systems, the Table 2.8 was constructed. This table has information already mentioned previously, as well as other small details taking into account the application in rehabilitation.

[21] VICON. `https://www.vicon.com/` (visited on 30/01/2017)
[22] Qualisys. `http://www.qualisys.com/` (visited on 30/01/2017)

Table 2.8: Overview of the advantages, disadvantages, general accuracy and price of several automatic systems for the human gait capture.

System	Advantages	Disadvantages
NWS: Image based and **NWS:** Floor Sensors	- It is not restricted to battery consumption, - It does not require sensor placement, - It is not invasive, - Better repeatability.	- Requires complex algorithms, - Sensitive to image interference similar to the human body, - Expensive equipment, - Impossible to monitor movements outside the observation region, - Impossible to monitor in conditions close to the ADL of the patient (with obstacles, distances and floor surfaces he faces daily).
WS: Force Sensors	- Easy to setup, - It allows the evaluation of gait in any environment (clinics, home or even in the street), - Moderately expensive (compared to camera, markers and floor sensors), - It allows the evaluation of the gait in environments closer to the patients' ADL.	- They do not provide enough data to evaluate kinetic parameters, - They do not provide information about the swing phase, - The battery is limited,
WS: Inertial Sensors	- Relatively easy to place, - It allows the evaluation of gait in any environment (clinics, home or on even in the street), - Cheaper systems (compared to camera, markers and floor sensors), - It allows the evaluation of the gait in environments closer to the patients' ADL, - They allow to evaluate a large amount of gait parameters, except the kinetic parameters.	- The battery life is limited, - Some patients may have difficulty placing the sensors properly, requiring the help of a family member, - In general, complex algorithms are required to solve magnetic's and calibration's problems.
WS: Electromyography	- Detail more directly the muscular activity, - Can detect more locally the problems that cause gait impairments (to detect the muscles or problematic sections).	- Placement of sensors is complex (requires a specialist), - Complicated to analyze certain gait parameters from the EMG data, - Indicated to an clinical analysis - not for rehabilitation.
HS: Markers	- High precision and accuracy in the determination of the gait parameters,	- Very expensive system, compared to systems based on cameras (only) or on inertial sensors. - The setup is very complex, both the placement of the sensors in the segments of the human body and the strategic placement of the cameras. - Requires highly specialized technical personnel.

Depending on their applicability some systems may be more suitable than others. For example, the HS are more suited to the use in cinematography applications and in clinical research due to its high accuracy and performance. However, for rehabilitation purposes, the most indicated in terms of setup, portability, and usability, are the inertial sensors and the camara based systems. These characteristics are crucial for a rehabilitation system, because: portability ensures that multiple patients can use similar systems at the same time in the same space and also that patients can do home-based rehabilitation exercises; and usability is crucial in order to ensure that the system performs its movement acquisition functions in an adequate way to evaluate rehabilitation exercises while being simple for the therapists' and patients' use, offering an adequate user experience with effectiveness, efficiency and satisfaction.

Hereafter, a review of the (generic) gait parameters that can be measured by the different systems, is presented. In order to organize the gait parameters that can be measured by the different systems, the Table 2.9 was constructed.

Table 2.9: Overview of the parameters that can be acquired from the automatic systems. Y means that the gait parameters set can be measured, N means that they can not be measured.

System	Spatial	Temporal	Kinematic	Kinetic
NWS: Image based	Y (with dimension reference)	Y	Y	N
NWS: Floor Sensors	Y	Y	N	Y
WS: Force Sensors	Y	Y	N	Y
WS: Inertial Sensors	Y (with patient height)	Y	Y	N
WS: Electromyography	N	N	N	N
HS: Markers	Y	Y	Y	N

As can be seen from Table 2.9, there is no single unique system, capable of measuring all the parameters mentioned in Section 2.3.

As previously mentioned, of all the systems presented, those that consist of EMGs are the ones that are less able to measure the presented gait parameters. Of the remaining systems, there are, in one side, those based on pressure at ground level (which allow to measure the GRFs), and, in the other side, those based on image and inertial sensors (that, although they can not measure the GRF, allow the acquisition of kinematic parameters).

Some image-based systems and inertial sensors require spatial references in order to acquire spatial parameters (such as rugs with specific dimensions in the case of imaging, and measurement of the dimension of the patient's lower limbs in the case of inertial sensors). The only parameters that can not be measured directly by inertial sensors are the kinetic parameters.

Combining all the advantages and disadvantages of the different methods presented, it can be concluded that, although the inertial sensors have not all the advantages for acquiring movement (for example, are not capable to measure GRFs), they are comparable to the others, taking advantage of the ease setup, portability, usability and possible parameters to be measured.

2.6 Summary

Each GC is divided into several phases in which different anatomical movements (flexions and extensions of the hip, knee and ankle joints) occur. Knowledge of these gait details allows for a more careful, gait-focused analysis.

There are several pathologies that cause impairments to walking patterns and, in many cases, increase the falling risk, such as neurological, musculoskeletal, and other diseases. One way to improve these conditions is to perform controlled rehabilitation so that a correct walking pattern is performed by the patient and thus restore the walking function properly.

In order to evaluate an exercise, it is necessary to take into account metrics that are easily interpreted by specialists in the rehabilitation field. These metrics, in gait rehabilitation, are the gait parameters, such as stride length, step length, step time, joint angles, asymmetry, cadence, among others. It is also verified that most of the spatial parameters can be obtained after the detection of IC and PS of the GC. The kinematic parameters require more information about the orientation of the lower limb segments and are also better suited to help to give feedback to the patient while performing the exercise (for example, instructing the patient to flex the knee for the advancement of the leg). Kinetic parameters (such as GRF) are important to realize the load placed on each lower limb, helping therapists to better understand the load capacity of each lower limb (especially in the LR phase). This is especially important for the evaluation of patients with prostheses. However, these metrics are complex to measure without instruments.

One way to access patients' ability to move in clinics is through testing such as TUG and CTSIB. They allow an analysis of the patient's stability of the gait and balance. However, the assessment is very dependent on specialists' experience.

In order to evaluate with more accuracy and to obtain more gait parameters, automatic systems are used, such as cameras, force platforms, and inertial sensors, among others. After a brief review of these systems, it can be concluded that pressure-based sensors are the only ones able to measure kinetic parameters, however they lack the estimation of kinematic parameters, important for rehabilitation. The market-camara-based systems, such as the golf standard VICON, are the most accurate automated motion capture systems. However they are very expensive, requiring calibrations and time-consuming installations, a specific gait laboratory is required, where cameras are installed, making them unfeasible for clinics' and patients' use. Cameras based systems are also used in rehabilitation, however they are limited to a fixed space where the cameras are. Finally, there are the inertial sensors that, although they do not allow kinetic parameters to be measured, and contain some problems related to calibrations and magnetic field interferences, can be used anywhere, adjustable for use in rehabilitation clinics, and patients' homes. They also contain the accuracy and battery-life enough to be implemented in rehabilitation exercises.

Chapter 3

Gait Analysis with Inertial Measurement Units

The purpose of this thesis is the development of a gait analysis system for rehabilitation with inertial sensors. IMUs were chosen due to their ease of integration into a portable system, they are convenient for the usage outside the healthcare center, or even at the patient's home.

The following sections present details about the materials that will be used throughout the thesis work, as well as some methods that belong to the state-of-the-art related to these devices (IMUs) and the analysis of gait.

3.1 Inertial Measurement Units

In general, IMUs are systems composed of three sets of accelerometers and gyroscopes, and sometimes can have a triad of magnetometers. These sensors allows measuring linear and angular movements. The main advantages of systems that use IMUs are their simplicity, they are unobtrusive, portable, wireless, self-contained, relatively low-cost, have a compact size, are lightweight, appropriate for real-time applications and allow unconstrained motion monitoring [Bergamini et al., 2014]. Due to these characteristics, they are a very interesting device to use with high repeatability in rehabilitation environments.

Most common IMUs provide angular velocity information and sensor acceleration. Other systems already provide integrated signal processing filters, that output other signals, derived from the integration of the information given by its devices' sensors.

3.1.1 Introduction to IMUs

As already mentioned, inertial sensors contain gyroscopes, accelerometers, and magnetometers. The following sub-subsections are intended to introduce these systems. In addition, in order to take advantage of the data acquired by these three sensors, a combination of their values is made to obtain the orientation of the tracker in relation to an Earth frame. This is accomplish with fusion

sensor algorithms, and the following sub-subsections will also present a brief introduction to this topic.

Accelerometers

Accelerometers are devices that measure acceleration. The ones that make up the IMUs are accelerometers with three acceleration axes: X, Y, and Z. In this way they feel the acceleration in the three directions, allowing to detect the gravitational acceleration [Su et al., 2014], which is important for understanding the vertical orientation towards the Earth. The base application of this sensor is to detect static and dynamic motion activities.

The acceleration vector contains information of: dynamic acceleration ($\vec{a}$) (which is the acceleration of any movement (on any acceleration axis)), static acceleration relative to gravitational acceleration ($\vec{g}$) (acceleration of gravity), accelerometer offset ($\vec{O}_A$), and measured noise ($\vec{n}_A$). This results in Equation 3.1. The matrix S_A provides normalization of the differing scaling factors [Young, 2010].

$$\vec{A} = S_A(\vec{g} + \vec{a} + \vec{O}_A + \vec{n}_A) \tag{3.1}$$

Gyroscopes

The gyroscope is a device that measures the rotation rate. The rotation that it senses is along with the X, Y, and Z device's axes, respectively. It can be considered that the gyroscope vector $\vec{G}$ is composed of the rotation rate ($\vec{\omega}$) (gyro rotation rate), the gyroscope bias offset ($\vec{O}_G$) and the measured noise ($\vec{n}_G$). In this case, S_G is the scaling factor normalization (Equation 3.2) [Young, 2010].

$$\vec{G} = S_G(\vec{\omega} + \vec{O}_G + \vec{n}_G) \tag{3.2}$$

In motion recognition applications, the gyroscope allows the detection of the orientation of the tracker, thus having a great application in human movement analysis [Su et al., 2014]. However, with temperature and motion, over time, the gyroscope accumulates errors that lead to a bias drift [Madgwick, 2010]. This event is the major cause of error detected when the gyroscope is operating, causing loss of accuracy [Bergamini et al., 2014]. One way to overcome this problem is to implement fusion algorithms, especially based on the *Kalman filter* (discussed later in Subsubsection 3.1.2).

Magnetometers

The magnetometer is a device that measures the magnetic field, in the X, Y and Z axes. Traditionally it detects the direction in which the magnetic north pole is, but can also be used to detect the presence of other sources of magnetic fields [Su et al., 2014]. The magnetic vector $\vec{M}$ is composed of the magnetic field ($\vec{m}$) (corresponding to the magnetic north of the Earth), the magnetometer

offset ($\vec{O}_M$), and the measured noise ($\vec{n}_M$) (corresponding to magnetic interferences such as soft and hard magnetic effects). In this case, the matrix S_M also provides the scaling factor normalization (Equation 3.3) [Young, 2010].

$$\vec{M} = S_M(\vec{m} + \vec{O}_M + \vec{n}_M) \tag{3.3}$$

It is the property of detecting any magnetic field that causes sources of errors in the magnetometer. Ferromagnetic elements are able to distort the Earth magnetic field where they are located. But there are other sources that cause changes in the magnetic field, such as electrical components and cables, furniture with metal components (for example, chairs), and metal structures that exist in the buildings construction [Madgwick, 2010]. Even the device associated with the system can cause deviations to the magnetic north of the sensor. By distorting the surrounding magnetic field, the presence of ferromagnetic materials in the vicinity of the device can cause a severe loss of accuracy.

Interference sources that are attached to the sensor's coordinate axis can be removed by calibration. However, variable interference sources (on the Earth's coordinate frame) cause errors in measuring the direction of the Earth's magnetic field (which is the case of soft iron effects). Deviations from the horizontal plane relative to Earth's surface can not be corrected without additional references and heading orientation. If the deviation is due to inclinations with vertical components relative to the Earth's surface, they can be corrected or compensated with additional information of the accelerometer (sensor's attitude) [Madgwick, 2010].

3.1.2 Sensor Fusion Algorithm

To evaluate movement during gait, trackers (sensors) are used to acquire information. To measure these movements it will be necessary to place a set of trackers along the lower limbs of the body so that the orientation of these can be correlated to the orientation of the body segments where they are located. In relation to the trackers, it is necessary to understand their orientation in order to achieve the orientation of the body segment. In this sense, an accurate and precise system is required to determine the three-dimensional (3D) orientation of each body segment. This orientation is relative to a Earth-fixed reference frame [Bergamini et al., 2014], and can be extracted from the sensor data, previously mentioned (Subsubsections 3.1.1, 3.1.1, and 3.1.1).

The accelerometer, gyroscope and magnetometer values, when used separately, present drift errors (in particular, from the gyroscope data), reducing the precision in movement detection. Using fusion algorithms, which integrate the values of the three sensors, it is possible to limit these errors and thus increase the accuracy, robustness, and consistency of the data acquired [Bergamini et al., 2014] (see Figure 3.1).

There are several fusion sensor algorithms. One of the most used algorithm is the *Kalman Filter* [Kalman, 1960], which is also the basis for the implementation of many other sensor fusion algorithms. According to [Madgwick, 2010], the *Kalman Filter* is the basic data fusion algorithm

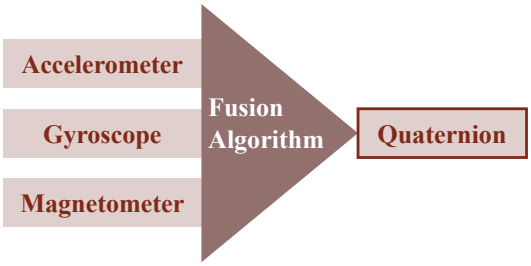

Figure 3.1: Diagram representing the inputs and outputs of a generic sensor fusion algorithm. It takes the individual values of the sensors (accelerometer, gyroscope and magnetometer) as inputs and returns a quaternion (explained later).

used in xsens[1], micro-strain[2], VectorNav[3], Intersense[4] and PNI[5] sensors. Since the *Kalman Filter* is very important in the inertial sensors field, a brief description of this algorithm is presented below.

Kalman Filter

The *Kalman filter* is a statistical mathematical method used to filter signals containing amounts of statistical and systematic noise. In a generic and simple way, the Kalman filter fuses measured data in successive discrete time intervals, forming an estimated maximum likelihood of the measured parameters. It removes noise from the sensor signals to produce fused data to estimate smoothed values of position, velocity, and acceleration of a series of points in a path [Elmenreich, 2002].

According to [Elmenreich, 2002], the Kalman filter is divided into two linear components: the first is related to the dynamic conditions of the system and the second describes the noisy observations of the system. It takes into account past values to compute a likelihood. With the introduction of new noisy data, and joining the previously determined likelihood, the resulting signal is more in accordance with the one that really happened. In this way, nonsense or noisy values, concerning the continuous human movement, are discarded.

This algorithm (generically presented) works only for linear conditions. However, there are several applications that have non-feasible behaviors, and before that, algorithms have been created in order to meet the new requirements of non-linearity. Among them are the algorithms Extended Kalman Filter (EKF) [Elmenreich, 2002].

3.1.3 Commercial Sensors: Brief Overview

There are several commercially available inertial sensors (some already mentioned in Subsection 3.1.2). A brief analysis of them is presented below. The Vectornav[3] products are not wireless and

[1]Xsens. `https://www.xsens.com/` (visited on 19/01/2017)
[2]Micro-stain. `https://www.microstrain.com/` (visited on 19/01/2017)
[3]Vectornav. `http://www.vectornav.com/` (visited on 19/01/2017)
[4]Intersense. `http://www.intersense.com/` (visited on 19/01/2017)
[5]PNI. `https://www.pnicorp.com/` (visited on 19/01/2017)

thus are not suitable for use as wearables in rehabilitation. For the remaining products, a short survey was carried out with the public available information and shown in Table 3.1.

Table 3.1: Brief review of marketable inertial sensor specifications with bluetooth connection, according to information publicly available. In this table the root mean square is defined as RMS.

Property	**MTw** *(Xsens)* [xse, 2015b]	**InertiaCube 3** *(Intersense)*[6]	**InertiaCube BT** *(Intersense)*[7]	**Inertia-Link** *Micro-strain* [8]	**SENtral** *(PNI)*[9] [PNI,]
Wireless	Yes	Yes	Yes	Yes	Yes
Update Rate (Hz)	50 (internal 240)	180 (2 devices) 120 (4 devices)	180	1000	200
		Static Accuracy			
Heading (deg RMS)	1	1	1	0,5	2
Roll & Pitch (deg RMS)	0,5	0,25	0,5	0,5	-
		Dynamic Accuracy			
Heading (deg RMS)	1,5	-	-	2	-
Roll & Pitch (deg RMS)	0,75	-	-	-	-
		Physical Specifications			
Weight (grams)	16	20	67	39	-
Dimensions (mm)	47 x 30 x 13	31,1 x 43,2 x 14,8	60 x 54 x 32	41 x 63 x 24	1,6 x 1,6 x 0,5

The Intersense[4] product *InertiaCube BT* has large dimensions (60 x 54 x 32 mm) and is considerably heavy (67 grams). Thus, is not very comfortable to be used in the foot or ankle, and by patients with lower physical capacities. One of the smallest and suitable wearable products for human movement monitoring of the PNI [5] company is the *SENtral*, with a 2 degree heading accuracy. The remaining sensors have similar characteristics and have simillar accuracy.

Many of Xsens[1] sensors are not wireless, however, as will be described later, a version similar to *MTw* was built to meet the requirements of the SWORD Health company: with roll, pitch and yaw accuracy less than 1,5 degree (in dynamic conditions), wireless communication via Bluetooth, small dimensions (47 x 30 x 13 mm), and lighter (16 grams weight) [xse, 2015b]. In addition, it is a product designed specifically for monitoring human movement.

In spite of the relatively close characteristics between the different sensors, the ones that will be used throughout the thesis work will be the *MTw* (Xsens), which, despite being the ones with better characteristics (presented in the Table 3.1), are also provided by SWORD Health. A brief description about the *MTw* (Xsens) will be made in the following Subsection 3.1.4.

[6]Intersense - InertiaCube3. `http://www.intersense.com/pages/67/59/` (visited on 24/01/2017)

[7]Intersense - InertiaCube BT. `http://www.intersense.com/pages/69/60` (visited on 19/01/2017)

[8]Micro-strain - Inertia-Link. `https://www.microstrain.com/content/inertia-link%C2%AE-product-no-longer-stocked-%E2%80%93-limited-availability` (visited on 24/01/2017)

[9]PNI: SENtral. `https://www.pnicorp.com/sentral/` (visited on 19/01/2017)

3.1.4 Sensors Specifications

The *MTw* (Figure 3.2) is a wireless tracker, therefore requiring an internal battery that allows free use in the segments of the human body [xse, 2015a]. It is an accurate, small and lightweight 3D human wireless motion tracker [xse, 2015b].

Figure 3.2: IMU MTw, Xsens's product.

MTw is a very convenient tracker to be used to measure the orientation of segments of the human body by its ease of placement (with straps with Velcro® that are in the back of the tracker). In this way, the angles of human joints can be determined. The *MTw* tracker also has a battery life that lasts long enough for therapy sessions [xse, 2015a].

Table 3.2: *MTw* Sensor Specifications, adapted from [xse, 2015b]

Description	**Specification**
Tracker placement	Easy fastening with Velcro straps
Internal update rate	240 Hz
Update rate	50 Hz
Batery life	8 Hours
Charging	USB 2.0 Micro
Dimensions Tracker	$47 \times 30 \times 13$ mm ($1.85 \times 1.18 \times 0.51$ in)
Weight	16 g (0.56 oz.)
Operating temperature range	$0^0C - 50^0C$
Communication	
Range open space	Up to 20 m (65 f.)
Range office space	Up to 10 m (33 f.)
Wireless protocol	Bluetooth 4.0
Orientation	
Static Accuracy (Roll/Pitch)	0.5 deg RMS
Static Accuracy (Heading)	1 deg RMS
Dynamic Accuracy (Roll/Pitch)	0.75 deg RMS
Dynamic Accuracy (Heading)	1.5 deg RMS
Tracker Components	
3 axes Angular velocity (Full scale)	$\pm$2000 deg/s
3 axes Acceleration (Full scale)	$\pm 160\ m/s^2$
3 axes Magnetic field (Full scale)	$\pm$1.9 Gauss

As already mentioned, these trackers are small and light. In addition, they present a high dynamic accuracy (comparing to experienced physiotherapists that perform errors close to 5 degrees [Perry and Burnfield, 1992]), (1.5 deg root mean square (RMS)), being suitable for use in health applications.

The specifications of the tracker that will be used in the thesis work are presented in Table 3.2. This table is based on the specification's sheet for the defined sensors: *MTw* [xse, 2015b].

It is crucial to mention the orientation specifications. In Table 3.2 the orientation accuracy under optimum conditions of the *MTw* trackers can be seen. Optimal conditions can be defined as conditions without magnetic field variations (for example, the presence of heavy magnetic distortions or hard and soft iron effects). The accuracy of these sensors is in the order of one degree in almost all the components (roll, pitch, and yaw). Roll, Pitch and Heading are introduced in the following subsections.

Orientation Integration System

The *MTw*, *Xsens*'s product, already comes with a 3D drift-free orientation integration software system, which combines information from the three sensors, and returns the orientation of the sensor's frame relative to a local Earth's frame. The algorithm used by Xsens, in the *MTw* trackers, is called *XKF3*, according to the technical report [Fai, 2015]. The *XKF3* is an algorithm that processes 3D inertial information with 3D magnetometer data to estimate 3D orientation and is based on the *Kalman filter*, as mentioned in Subsection 3.1.2.

In a simple way, the data obtained by the accelerometer and the magnetometer is used to collect information on the static position of the tracker. In Figure 3.3, it can be seen that the z axis of the tracker is determined symmetrically in relation to the orientation of the gravitational force, and the y axis of the tracker is defined using the direction of the Earth's magnetic field (magnetic North).

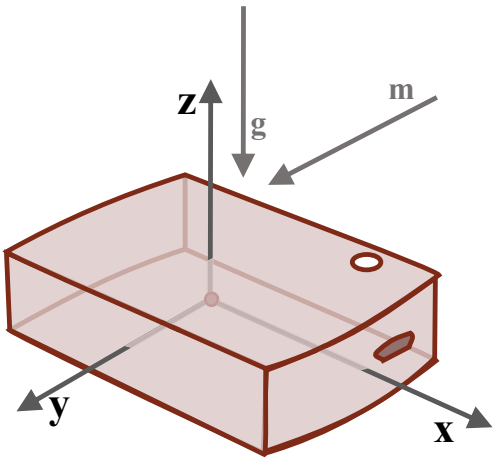

Figure 3.3: Coordinates of the tracker frame in relation to the Earth frame. The z axis is in relation to the opposite direction of the gravity (g) and the y axis is in relation to the Earth's magnetic field (North) (m). The tracker is represented by the object, and the frame is positioned in the center of the object (note in the LED in the left corner of the tracker), (adapted from [Fai, 2015]).

All signals provided by the tracker sensors are complementary to each other. Following these concepts, the accelerometer and the magnetometer provide important information to define the

static orientation of the sensor. Gravitational and magnetic sensing provide stabilization information over a long period of time. The gyroscope is introduced to, along with the previous ones, be able to capture the rotation (dynamic) of the tracker during its use. According to [Fai, 2015], continuous integration of sensors signals allows the detection of the short-term accurate, high-bandwidth, and high-resolution tracker movements. However, after a prolonged use of the gyroscope, an inherent integration drift of the object's frame in relation to its real axis, grows.

This algorithm is also able to do a continuous auto calibration, allowing the use of the trackers for longer periods of time without deviations. The main causes of these deviations are diverse, for example, temperature differences, mechanical stress, soft iron effects, vibrations, trackers' aging, the magnetization of the device itself, the environment around the trackers and so on. This algorithm allows an automatic calibration without the interruption of the user's tasks. Since it is being commercialized with the sensors, more detailed information about it is confidential.

The *XKF3* algorithm returns a normalized unit quaternion that expresses the orientation of the sensor in relation to local (Earth) coordinates. The form of this quaternion can be expressed by the Equation 3.4, where W is the real component and X, Y, and Z are the imaginary components [Fai, 2015].

$$q = [WXYZ]; \tag{3.4}$$

The following subsection is presented to understand the concepts related to quaternions.

3.1.5 Theoretical Background

An object can be considered as an axis itself. In this way, any rotation that occurs in the object in relation to an external frame can be represented by a combination of the Roll, Pitch and Yaw rotations (shown in the Figure 3.4). In this sense, the roll (or bank) is defined as a rotation of the object around the X axis, the pitch is defined as the rotation of the object around its Y axis, and the yaw (or heading), is defined as the rotation of the object around its Z axis.

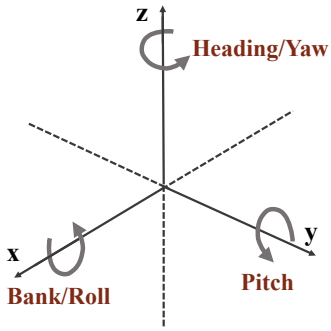

Figure 3.4: The inertial frame. Rotations roll, pitch and yaw in a frame, (adapted from [10]).

[10]CHRobotics. http://www.chrobotics.com/library/understanding-euler-angles (visited on 10/01/2017)

These rotations refer to orientations using the Euler angles. Those are simple and intuitive with respect to the interpretation of the physical movement that occurs, based on the combination of the three previously defined rotations. However, they are limited to rotations less than 90 degrees, so that the *Gimbal Lock* phenomenon can be avoided [Dam et al., 1998]. This phenomenon occurs when two of the three axes are superimposed after a sequence of rotations. After two or more axes are superimposed, their separation is very complex, being almost impossible to differentiate the axes involved. One way to avoid this phenomenon is to use quaternions, instead of the Euler angles, to acquire object rotation.

Quaternions

Based on the previous subsections, it is possible to conclude that the extraction of information that the *MTw* trackers provide are related to sensor orientation information with respect to a local (Earth) coordinate frame (in the form of a quaternion). With this, it can be understood that, if the IMU device is placed in an object, each quaternion value acquired through the tracker provides information about the orientation of the object, relative to a fixed coordinate axis on Earth.

Along the practical work of this dissertation, sensors will be used in body segments in order to find the orientations while walking and to determine parameters that are determinant for gait analysis and rehabilitation. In this way, it is necessary to understand concepts related to the quaternions, in order to find gait patterns. Thus, in this subsection, a brief explanation about the theoretical background concepts related to quaternions, and rotation is presented.

Rotation in 3D can be defined in different ways. According to [Dam et al., 1998], the definition given by Euler's theorem is described as:

> "Let O, O' in $\mathbb{R}^3$ be two orientations. There exists an axis $l \in \mathbb{R}^3$ and an angle of rotation $\theta \in [-\pi, \pi]$ such that O yields O' when rotated θ about l."

In other perspective, the orientation of a frame B relative to a frame A can be obtained by rotating a θ angle around an axis ${}^A\hat{r}$ defined in frame A. An illustration of this example is shown in Figure 3.5 [Madgwick, 2010].

It is important to mention that an *orientation* of an object in $\mathbb{R}^3$ can be defined by a normal vector, while a *rotation* can be defined by an axis and an angle of rotation. Using Euler's theorem, the rotation can be represented by two forms: *transformation matrices* or *quaternions*. According to the information provided by the sensors (quaternions), some aspects related to them will be introduced.

A unit quaternion is defined according to $\mathbf{i}^2 = \mathbf{j}^2 = \mathbf{k}^2 = \mathbf{ijk} = -1$. Being thus a four-dimensional complex number, that represents the orientation of a rigid object in a three-dimensional space.

In accordance with this, a quaternion is usually written as $[s, \mathbf{v}]$, where $s \in \mathbb{R}$ and $\mathbf{v} \in \mathbb{R}^3$. In this notation, s is defined as a *scalar part* of the quaternion, and the $\mathbf{v}$ the *vector part*, and is defined as $\mathbf{v} = (x, y, z)$

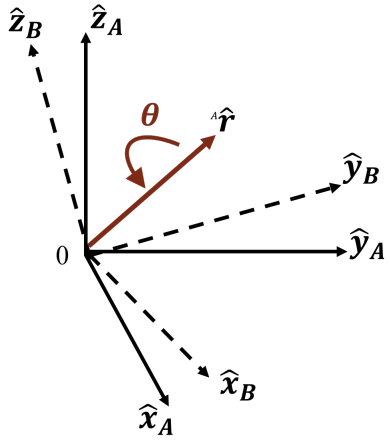

Figure 3.5: Orientation of a frame B relative to a frame A. The axes $\hat{x}_A$, $\hat{y}_A$ and $\hat{z}_A$ represent frame A and axes $\hat{x}_B$, $\hat{y}_B$ and $\hat{z}_B$ represent frame B. the vector ${}^A\hat{r}$ has components r_x, r_y and r_z relative to frame A. The angle of rotation is made on the vector ${}^A\hat{r}$ and is presented by θ (adapted from [Madgwick, 2010]).

In this sense, and according to [Dam et al., 1998], *quaternions* can be defined as is Equation 3.5:

$$\begin{aligned} q &= [s, \mathbf{v}] && ,s \in \mathbb{R}, \mathbf{v} \in \mathbb{R}^3 \\ &= [s, (x, y, z)] && ,s, x, y, z \in \mathbb{R} \\ &= s + \mathbf{i}x + \mathbf{j}y + \mathbf{k}z && ,s, x, y, z \in \mathbb{R} \end{aligned} \tag{3.5}$$

Taking into account the example in Figure 3.5, the quaternion describing the orientation of the frame B in relation to a frame A is defined by the Equation 3.6 and considers the components of the axis of rotation (unit vector ${}^A\hat{r}$), and the rotation angle θ [Madgwick, 2010].

$$\begin{aligned} {}^A_B\hat{q} &= [q_1 \;\; q_2 \;\; q_3 \;\; q_4] \\ &= [cos\frac{\theta}{2} \;\; -r_x sin\frac{\theta}{2} \;\; -r_y sin\frac{\theta}{2} \;\; -r_z sin\frac{\theta}{2}] \end{aligned} \tag{3.6}$$

A 3D rotation of an object can be achieved by a unit quaternion. Having a vector p, a unitary quaternion q, treating p as a quaternion $p = (0, p)$, the rotation of p by q is (Equation 3.7) [Williams et al., 2015]:

$$p' = qpq^{-1} \tag{3.7}$$

Considering this equation, it will be necessary to process the multiplication between quaternions, and the inverse of the quaternion.

The *multiplication* between quaternions is defined in Equation 3.8:

$$\begin{aligned} qq' &= [s,\mathbf{v}][s',\mathbf{v}'] \\ &= [s,(x,y,z)][s',(x',y',z')] \\ &= (s+\mathbf{i}x+\mathbf{j}y+\mathbf{k}z)(s'+\mathbf{i}x'+\mathbf{j}y'+\mathbf{k}z') \\ &= [ss'-\mathbf{v}\cdot\mathbf{v}',\mathbf{v}\times\mathbf{v}'+s\mathbf{v}'+s'\mathbf{v}] \end{aligned} \tag{3.8}$$

where $\cdot$ and $\times$ define the scalar and vector product in $\mathbb{R}^3$, respectively [Dam et al., 1998].

The product of quaternions is useful for defining compound orientations, which result, for example, from two successive orientations [Madgwick, 2010]. And also to specify the combined rotation (multiplication between two quaternions) [Young, 2010]. It has to be noted that if $\mathbf{ij}=\mathbf{k}$, and $\mathbf{ji}=-\mathbf{k}$, the multiplication between quaternions cannot be commutative ($qq' \neq q'q$).

The conjugate becomes useful for changing the frames that describe the orientation. The *conjugate* of a quaternion ($q*$) (Equation 3.9):

$$\begin{aligned} q* &= [s,\mathbf{v}]* \\ &= [s,-\mathbf{v}] \\ &= [q_1 \quad -q_2 \quad -q_3 \quad -q_4] \\ &= {}^{A}_{B}\hat{q}* = {}^{B}_{A}\hat{q} \\ &= q^{-1} \quad (if \;\; q \;\; is \;\; unit \;\; quaternion) \end{aligned} \tag{3.9}$$

For example, in the previous Equation (3.9), ${}^{B}_{A}\hat{q}$ is the ${}^{A}_{B}\hat{q}$ conjugate and describes the orientation of frame A relative to the frame B (unlike what was assumed in Equation 3.6 [Madgwick, 2010]). The *inverse* rotation is given by the quaternion conjugate [Young, 2010].

Normalization is important to ensure that the quaternions used are unitary. The *norm* of a quaternion is defined as (Equation 3.10):

$$\begin{aligned} ||q|| &= \sqrt{s^2+\mathbf{v}\cdot\mathbf{v}} \\ &= \sqrt{s^2+x^2+y^2+z^2} \end{aligned} \tag{3.10}$$

The norm of the conjugated quaternion is equal to the norm of the quaternion itself (Equation 3.11):

$$||q*|| = ||q|| \tag{3.11}$$

The norm of the the multiplication of two quaternions is defined as (Equation 3.12):

$$||qq'|| = ||q||||q'|| \tag{3.12}$$

It is possible to normalize according to the following Equation 3.13 [Young, 2010].

$$norm(q) = \frac{q}{|q|} \tag{3.13}$$

3.2 Gait and Balance Training and Analysis

As already mentioned in previous sections, the technological solutions of movement capture are able to acquire parameters from complex movements with high accuracy. With the emergence of these technologies that are lighter, smaller, wearable and wireless, and more autonomous, portable and accurate; there is the possibility of making software systems with the aim of assisting rehabilitation. It is important that these systems are able to provide objective metrics and clinically validated reports to physiotherapists and also inform the patient how well he is performing the exercise in a way that he is able to improve it (in real-time) [Horak et al., 2015].

In gait and balance, there are several metrics capable of giving this information objectively either to the physiotherapist or physician or to the patient when performing the exercise. These metrics must be able to characterize the gait and balance impairments. They must also be able to answer questions such as "how" is occurring and "why" is occurring specific impairments throughout the functional performance. In the concept of physical therapy, it is important that these systems have high quality, efficiency and efficacy in obtaining gait and balance metrics, high applicability, usability, accessibility, replicability, portability, safety, among others. These features are the major advantages of having an automatic, portable, lightweight, motion monitoring system in rehabilitation, which can be done at a distance [Horak et al., 2015].

Human gait is a complex movement, due to the set of unit movements that are controlled by distinct neuronal structures (both in the balance and in gait itself), and also certain adaptive mechanisms to maintain mobility and balance in gait, which occur with the incidence of certain diseases. It becomes easier to evaluate these complexities with a portable monitoring system that is capable to detect small characteristics of the movement that are unnoticed to the human eye. In addition, many methods used in clinics (such as some mentioned in the Subsection 2.4.1) are evaluated subjectively, being necessary a specialist with high experience and also, results often vary from expert to expert.

In order to be used clinically and also at home, these systems should be easy to use, quick to install and calibrate, provide relevant information (for example, in addition to the parameters, the risk of fall and/or severity of a condition or illness), and reports the sessions with information easy and quick to interpret [Horak et al., 2015].

Regarding gait and balance, it is important to evaluate the risk of falling in each patient and, in order to reduce this risk, practically all specialists recommend gait training. However, not all patients have access to physiotherapy and gait training centers in order to do it correctly. In the case of an incorrect gait training, more serious injuries can occur, causing an opposite effect.

There are already companies with gait analysis products, such as McRoberts[11], SwayStar[12], Kinematix[13] and Xsens[14], where the application is focused more on sport, but are neither focused for people with gait impairments nor rehabilitation applications.

3.3 Related State-of-the-art Methods

There are two main areas of motion acquisition from inertial sensors: activity monitoring and motion monitoring.

Activity monitoring is concerned with the acquisition of movement information to classify it in daily activities, such as detecting whether the person is walking, sitting, standing still, sleeping, running, or other activities. Many of them even estimate the amount of calories they expend during these activities. Others contain features that allow counting the number of steps, hours of sleep, and amount of time spent in certain postures, as a way of measuring the sedentary lifestyle. In these cases, only one tracker is typically worn on the wrist or waist. They usually have long-lasting batteries and are not very expensive. However, they do not provide information about gait quality and balance. Information on gait movement patterns, kinematic quality or motor impairment are also not shown to the therapists. These systems are not adequate nor provide relevant information on running quality (nor running damage). These products were not designed to be used in clinical practice, have not been tested or validated in patients with lower motor and cognitive abilities. These devices use mostly accelerometers (either uniaxial or triaxial) and detect the number of acceleration peaks associated with body movement.

On the other hand, motion monitoring trackers generally contain 3 motion axes of 3 or more types of inertial sensors. Generally consist of more than 1 tracker, being necessary a care in the synchronization of data and interpretation of the human model in movement. This is to be able to accurately measure parameters that provide more qualitative movement monitoring to be implemented in clinics. These include kinematics of joints, spatial and temporal gait parameters, and other gait balance aspects.

3.3.1 Commercial Solutions

Systems marketed in the area of gait analysis and rehabilitation are already available. These systems can be divided into those using one tracker, two trackers, and more than three trackers.

Using only one tracker, there are products that allow the measurement of posture, and some gait characteristics such as cadence, trunk stability and a number of steps. This is the case with McRoberts[15], SwayStar[16] and BTS[17].

[11] McRoberts. `http://www.mcroberts.nl/` (visited on 26/01/2017)
[12] SwayStar. `http://www.b2i.info/web/index.htm` (visited on 26/01/2017)
[13] Kinematix. `https://www.kinematix.pt/` (visited on 26/01/2017)
[14] Xsens. `https://www.xsens.com/` (visited on 26/01/2017)
[15] McRoberts. `http://www.mcroberts.nl/` (visited on 27/01/2017)
[16] SwayStar. `http://www.b2i.info/web/index.htm` (visited on 27/01/2017)
[17] BTS Bioengineering. `http://www.btsbioengineering.com/` (visited on 27/01/2017)

There are other companies that have products that use two sensors, especially one in each shank or foot, they can measure a higher number of gait parameters, and, like this, they are more suitable for clinics than the previous ones. It is the case of Hasomed Gmbh[18], and one of BioSensics (LEGSys)[19]. However, these products are not able to offer parameters that assess the patient's posture and balance. This is due to the fact that they do not have the tracker in the lumbar part.

There are other products that include more modules, such as YouRehab (YouKicker)[20], Bio Sensics (LEGSys +)[21], APDM[22], XSens (MVN Biomech)[23] and (Gait Up[24]). These contain three or more sensors, with one in the lumbar part indicated to get balance metrics. They allow a higher characterization of spatial and temporal parameters of movement during the gait.

3.3.2 Methods

The methods currently in use, related to gait analysis and detection, are very diverse, using sensors with different specifications, different sensor settings, access to different signals (angular velocity, linear acceleration or quaternions), and parameters.

In an overview of several methods analyzed, it is observed that there are two groups: those that analyze values of linear acceleration and angular velocity, and those that analyze orientations obtained by sensor fusion algorithms (quaternion-based systems).

In addition to this division, it is also observed that within angular velocity and linear acceleration articles, there are some methods that start detecting peaks at angular acceleration values (in a general way) to determine the IC and the PS (described in Table 2.1), and others started determining the joints' angles involved in gait to determine gait phases (based on information similar to that of Table 2.1). These two approaches generally also present a number of different trackers. For the first one, it is observed that normally two to three trackers are used, whereas in the second more trackers are needed, between four to seven. However, even within these groups there are variability which will be more detailed.

The quaternion-based systems focus on obtaining the angles of the joints and, in a similar way as previously described, reach the gait cycle's phase in which the patient is at that moment. In these types of systems also generally more than three sensors are used to acquire the angles of the knee, hip and ankle joints. However, there are also studies that use the quaternions to get peaks at the angular velocity and thus determine the IC and the PS (for example, [Aminian et al., 2002], [Aminian et al., 2004], [Sabatini, 2005], [Najafi et al., 2011], [Chen, 2011], [Jasiewicz et al., 2006], [Najafi et al., 2009], among others).

In this chapter, a separate analysis is made for these two groups of methods, as well as the number and placement of the sensors addressed by each one.

[18] Hasomed Gmbh - RehabGait. `https://www.hasomed.de/de/rehagait/startseite.html` (visited on 27/01/2017)

[19] BioSensics - LEGSys. `http://www.biosensics.com/products/legsys/`(visited on 27/01/2017)

[20] YouRehab - YouKicker. `http://yourehab.com/our-products/youkicker/` (visited on 27/01/2017)

[21] Bio Sensics - LEGSys + . `http://www.biosensics.com/products/legsys/`(visited on 27/01/2017)

[22] APDM - Gait & Balance. `http://www.apdm.com/mobility/` (visited on 27/01/2017)

[23] Xsens - MVN Biomech. `https://www.xsens.com/products/mvn-biomech/` (visited on 27/01/2017)

[24] Gait Up. `https://www.gaitup.com/` (visited on 27/01/2017)

The method presented by [Aminian et al., 2002], was used by many other authors, such as [Aminian et al., 2004], [Sabatini, 2005], [Najafi et al., 2011], and [Chen, 2011]). The method consists of detecting the IC and PS phases in the gyroscope signal. Aminian uses Wavelet Transform to detect the negative peaks of medium and high frequencies of the sensors located in the shank, which are characteristics of the moments when the foot is placed on the floor and lifted off the ground. After detecting the moments in which IC and PS occur, it is possible to determine temporal parameters, such as CG time, stance time, swing time, SLS time, DLS time, and so on. To determine spatial parameters, Aminian measured the patient's size (for example, thighs and shanks). He used double pendulum and inverse double pendulum models, to, along with the dimensions of the patient and using trigonometry, determine the spatial parameters, like stride length, and stride velocity. In this method, an accuracy of about 99% was obtained for the detection of the PS instant and 95% for the IC. These results were compared with the time of placing foot on the floor (pressure sensor at the heel), and the foot leaves the floor (pressure sensor on the big toe of both feet). This method served as inspiration for many other investigations.

Najafi's method [Najafi et al., 2009] (inspired by the [Aminian et al., 2002] method), consists in determining the moment at which IC and PS occur from the location of the local minimum peak of gyroscopes located in each shank. Using biomechanical models (such as the dimension of segments of the lower limb of the patient), spatial parameters are estimated (similarly to the Aminian's method). This method was tested at different gait speeds. The parameters evaluated were stride velocity, gait cycle, and inter-stride variability. The inter-stride variability had worse results, with an agreement (with results obtained with a GAITRite system) being about 4.6% for normal speed, 1.5% for low speed, and 9.1% for high speed. For the GC time and for the stride velocity, better results were obtained, with a random difference $< 6.8\%$ for the stride velocity and $< 4.4\%$ for the gait cycle time in the set of all velocities.

The gait analysis system presented by [Chen, 2011] consists in the use of five inertial sensors to obtain gait parameters (one in the back, one in each thigh and one in each shank). This paper is the basis of the LEGSys[12] product. The parameters collected by this method are divided into three sections: temporal, spatial and center of body mass parameters. The temporal parameters are obtained by the method described by [Aminian et al., 2002], and [Aminian et al., 2004], and consists of obtaining the times in which the IC and PS occur. From these instants, parameters are derived for each stride, such as GC time, stance time and swing time. In order to obtain the spatial parameters, it is necessary to know the height of the patient, using the method described by [Aminian et al., 2002] (two-link inverse pendulum model), and integrating the angular rate of thigh and shank rotation, it is possible to obtain the stride length and the stride velocity. Lastly, the center of mass is obtained during the gait by analyzing the sensor that is in the lower back.

These works consisted of detecting moments in which the IC and the PS occurred. Throughout the research on the current literature of this theme, it is possible to conclude that there are many similar works. They usually start from the detection of peaks in angular acceleration or zero crossing, to detect the moments when the heel is placed on the ground and when the foot leaves the ground to swing. More methods related to those presented above are shown in Table 3.3, and

are the majority of related articles found. However, these methods lack information about the swing phase, in which the foot is advancing in the air.

The method presented by [Yuwono et al., 2014], focuses on a different approach because uses unsupervised nonparametric methods and takes into account the sequence of the gait phases detected. Although centered in the determination of IC and PS, it uses unsupervised nonparametric methods. Yowono initiates the method by determining the cadence of each episode using Hidden Markov Models (HMM), then uses the discrete wavelet transform to detect peak characteristics of the data of the accelerometers and the gyroscope. It reduces the dimensionality of these features using a principal component analysis (PCA) and uses Rapid Centroid Estimation to classify the peaks into three classes: right IC, left IC and artifacts. Finally, it applies a Bayes filter that takes into account the prior detections and models the following predictions. This work was presented using two accelerometers and gyroscopes in both feet and obtained accuracies on the order of 90%.

On the other hand, there are methods which rely first on the detection of angles to form a determination of gait phases, according to the state of flexion or extension (among others) of the joints. Some examples of work related to this point of view are presented in Table 3.4. The method presented by [Liu et al., 2009] is based exactly on the determination of the angles of each joint and, therefore, the movement performed at each moment by each joint determines the phase state in which the subject is. Liu determines the angles of each joint from the data of the gyroscope (feet, shanks and thighs). From the interpretation of sequences of anatomical movements, estimates the gait phase. The Root Mean Square Error (RMSE) was less than 10^{o}, in most joint angles, being larger for the ankle joint.

A different perspective was presented by [Evans and Arvind, 2014], which starts with the values of the gyroscope as input to a feed-forward neural network (FNN). This network allows the classification of five different gait phases. Then, Evans adds a HMM that aims to assess the sequentially of these phases (see if they make sense in the concept of human gait behavior). This method uses accelerometers and gyroscopes placed in the trunk, both thighs, both shanks and both feet. It presents an error lower than 23 milliseconds for determination of each phase, being evaluated against a gait analysis VICON system.

Most of the presented methods contain drift correction steps, mainly caused by the use of the gyroscope, as well as several calibration sequences. Other set of methods, that are presented in Table 3.5, use quaternions as the tracker's output signal. The quaternions are output of a sensor fusion algorithm that has calibration methods and reduces the drift effects (mentioned in Subsection 3.1.2). Thus, the use of quaternions as output of a tracker, has lower sensor drift, improving signal quality, accuracy, and robustness. However, few studies have been found linking gait analysis with the use of quaternions as the main signal. It is estimated that it is due to the fact that there are commercial interests related to this kind of sensors and rehabilitation products already commertialized, with little public information about its genesis method. In the following paragraphs some works that were found that use quaternions acquisition to determine gait parameters are presented. In Table 3.5 a small overview about studies that involved quaternion processing to

obtain gait parameters is shown.

Within the methods that use quaternions, it is also observed that they are similar among them. All of them start from the estimation of the angles of the joints and from there they extract gait parameters. However, the major focus of these works is more on obtaining the joints' angles than analyzing the gait patterns.

[Cloete and Scheffer, 2008] presents a model that is based on obtaining the angles of each joint, calculating the relationship between the orientation of the distal segment and the proximal segment. However, it did not achieve good results for the ankle joint. In the following work [Cloete and Scheffer, 2010], attempts to study the repeatability of the method, achieving results with RMS greater than 90%. In these two studies, Cloete used the MOVEN system of Xsens containing 16 IMUs, but only analysed the trackers placed in the lower limb.

The method proposed by [Ahmadi et al., 2015] is a real-time method that starts from the processing of the quaternions and applies a descending gradient algorithm to obtain the 3D orientations of each segment. Using the foot sensor, it determines the stance phases of the gait cycle that allow the detection of the times in which IC occurs. He sets the foot sensor as the root node and determines the 3D orientation and position of the other 2 segments and the angles of the knee and ankle joints. Finally, Ahmadi applies a biomechanical model to verify that the movements acquired are consistent with a natural human behavior during gait. The Ahmadi model uses IMUs on the thighs, skanks, and feet.

Table 3.3: Methods related to analysis of movement with angular velocity and linear acceleration to determine IC and PS instants.

Year & Author	Sensor	Method	Parameters	Dataset	Results
[Aminian et al., 2002]	Gyroscopes (both shanks).	IC PS instants detection, using wavelet transform (for temporal parameters). Dimensions of the patient's legs were measured (to estimate spatial parameters).	Swing, stance, SLS and DLS times, and stride length and velocity.	9 Young and 11 elderly.	95% confidence interval for IC was [7 ms, 13 ms], for PS was [-5 ms, 4 ms] .
[Jasiewicz et al., 2006] Algorithm 1	Gyroscope and accelerometer (both feet and mid-shank).	PS detection by searching for peak in x-directed foot acceleration, and IC detection by searching for peak in z-directed foot acceleration. Spatial parameters: double integration of the horizontal accelerations between PS and IC.	Stride and Step length, gait velocity, single and double support time.	26 Healthy and 15 injured.	Mean error (std): IC: -11 (23) ms; EC: 19 (34) ms.
[Jasiewicz et al., 2006] Algorithm 2	Gyroscope and accelerometer (both feet and mid-shank).	PS detection by searching for the first maximum in the angular velocity, and IC detection by searching for the velocity zero crossing point (peak foot dorsiflexion). Spatial parameters: double integration of the horizontal accelerations between PS and IC.	Stride and Step length, gait velocity, single and double support time.	26 Healthy and 15 injured.	Mean error (std): IC: -12 (22) ms; EC: 15 (26) ms.
[Jasiewicz et al., 2006] Algorithm 3	Gyroscope and accelerometer (both feet and mid-shank).	Decomposition of the shank sagittal angular velocity with wavelet transform, searching for rapid changes in timing characteristics and selecting the two minimum on either side of a peak in velocity (1^{st} minimum associated with PS and the 2^{nd} minimum with IC). Spatial parameters: double integration of the horizontal accelerations between pS and IC.	Stride and Step length, gait velocity, single and double support time.	26 Healthy and 15 injured people.	Mean error (std): IC: -14 (23) ms; EC: 23 (28) ms.
[Najafi et al., 2009]	Gyroscopes, attached to each thigh shank.	Local minimal peak detection (IC and PS moments detection). Biomechanical model, with patients' lower limbs height, for integrate the angular rate of rotation of the thigh and shank: spatial parameters.	Stride Velocity, GC time and inter-stride variability	22 Elderly.	Inter-stride variability (4.6%; 1.5%; 9,1% for normal, low and fast speed) of agreement. Stride velocity and CG time (< 6,8%; < 4,4%) (all velocities) of random difference.

Year & Author	Sensor	Method	Parameters	Dataset	Results
[González et al., 2010]	Accelerometers (foot and knee).	Zero Crossing (ZC) occurrence from positive to negative of an 11th order FIR filter output (applied to incoming antero-posterior acceleration (ZC point)). In each ZC found, the area enclosed by positive values of the filtered signal, preceding the detected ZC is determined. If the area is below a defined threshold, the ZC is discarded, if not, is associated with the occurrence of an initial contact event.	Walking velocities.	11 Healthy.	Initial contact timing error (mean:13 ± 35 ms) and Final contact timing error (mean:$9 \pm$ 54 ms).
[Kotiadis et al., 2010] Single accelerometer algorithm)	Accelerometers (shank)	Translation of state conditions. Evaluation of the A_x acceleration: in heel off - A_x negative; in PS - A_x positive; IC negative until heel strike that causes a negative spike.	Temporal parameters.	1 Stroke survivor.	68/69 true and 1/2 false stride detections (in flat surface).
[Kotiadis et al., 2010] Two accelerometer algorithm	Accelerometers (shank)	Evaluation of the A_x and $A_y$acceleration: in heel off - A_x negatively increase and A_y maintains; in PS - A_x is positive and A_y negative; in IC - A_x negative and A_y becomes positive.	Temporal parameters.	1 Stroke survivor.	68/69 true and 1/2 false stride detections (in flat surface).
[Kotiadis et al., 2010] Single gyroscope algorithm	Gyroscope (shank)	Evaluation angular velocity around the G_z axis: in heel off - angular velocity negatively increase; in PS - angular velocity positively increase; in IC - angular velocity is negative.	Temporal parameters.	1 Stroke survivor.	68/69 true and 0/2 false stride detections (in flat surface).
[Kotiadis et al., 2010] Two accelerometers and one gyroscope algorithm	Accelerometers and gyroscope(shank)	Combination of the 3 previous algorithms.	Temporal parameters.	1 Stroke survivor.	68/69 true and 1/2 false stride detections (in flat surface).
[Mariani et al., 2012]	Inertial sensor (feet)	The foot, heel and toe orientation and trajectory are estimated, and the heel and toe times are determined.	Foot clearance parameters.	12 Healthy.	Max error was $47,6 \pm 25.6mm$

Year & Author	Sensor	Method	Parameters	Dataset	Results
[Yang et al., 2012]	Accelerometer (along the back)	Manual input (Sample rate, distance and a threshold). Detect heel contacts by peaks preceding the sign change of acceleration. After a low pass and a 4^{th} order zero lag Butterworth, a threshold is performed with a input value.	Number of steps, walking time, and walking velocity.	15 Healthy.	For step regularity: control (0.86 ± 0.07) proposed system: (0.55 ± 0.21)
[Rueterbories et al., 2014]	Accelerometer (fore-foot)	Based on a state machine, with transitions determined by 5 reference signals: composite acceleration (CA), 1^{st} derivative of CA, 2^{nd} derivative of CA, CA low pass filtered (w. 200 samples), and CA low pass filtered (w. 50 samples).	Swing, LR, mid-stance, PS.	10 Healthy and 10 hemiparetic.	For healty: sensitivity [0.96 - 1.00] and specificity [0.91 - 1.00].
[Seel et al., 2013]	IMU (foot and shank)	Determine the ankle joint angle from the angular rates measured from the foot. A strap-down is restarted at the end of each foot-flat phase. With the shank angular velocity, is determined the dorsiflexion angle.	IC and PS estimation.	Healthy subjects	Achieves "small tracking errors".
[Casamassima et al., 2014]	IMU (feet)	Estimate IC and PS events by processing the angular velocity signals along the foot medio-lateral axis. All positive peaks - mid-swing events, and the first negative peak is the IC and the second is the PS.	Cadence, step length, gait speed, gait asymmetry, trunk flexion, clearance.	5 PD patients.	Mean error close to zero with SD for stride duration and stride length of 3% and 2%.
[Tereso et al., 2014]	Accelerometers (ankle and trunk)	Detection of the time peak on IC and PS events. The data of each axis was transformed to produce a signal vector machine, that was filtered and was reconstructed a third least-square polynomial derivative approximation filter. For each gait cycle two peaks in the polynomium exist and are related to the IC and PS.	7 Elderly with knee osteoarthritis and with knee anthroplasty.	Gait events and fall risk evaluation.	Comparative results between the patients with crutches, standard walkers and forearms supports.

Year & Author	Sensor	Method	Parameters	Dataset	Results
[Yuwono et al., 2014]	Accelerometer and gyroscope (feet)	Cadence episode is detected by HMM. Discrete wavelet transforms are applied to extract peak features from accelerometers and gyroscopes. The feature dimensionality is reduced using PCA. Rapid centroid estimation is used to cluster the peaks in three classes: left IC, right IC and artifacts. Bayes filter is used to mode predictors, with prior detections.	15 Healthy.	IC.	Accuracy ($86.1 \pm 9.9\%$ and $93.4 \pm 2.4\%$) with gyroscope features.

Table 3.4: Methods related to analysis of movement with angular velocity and linear acceleration to determine joint angles.

Year & Author	Sensor	Method	Parameters	Dataset	Results
[Liu et al., 2009]	Gyroscopes and accelerometer (foot, shank and thigh)	The angles of each joint are determined, and according to the state of each join, the 8 gait phases are estimated.	8 gait phases.	10 Healthy.	The RMSE was less than 10^{o}.
[Hamdi et al., 2014]	IMU (feet, shank, thigh and trunk)	Lower limb joints and segments inclination are estimated in the sagittal plane (integrating the difference of the connected segments angular velocities around the joint axis).	knee, ankle and hip joint angles.	6 Healthy	RMS between 0.00 and 0.83 (p-value).
[Tadano et al., 2016]	Inertial sensors (pelvis, thighs, shanks and feet)	3D kinematic parameters of patients during walk were estimated based on acceleration and angular velocity data.	Hip, knee and ankle joint angles.	Healthy and osteoarthritis patients.	Comparative analysis between Healthy and osteoarthritis patients.
[Evans and Arvind, 2014]	3-axis accelerometer, gyroscope and magnetometer sensors.	FNN to estimate gait phases embedded in a HMM that ensures the phases sequence.	5 gait phases	5 Healhty	Methods accurate within 23 milliseconds

Table 3.5: Methods related to analysis of movement with quaternions to determine gait parameters.

Year & Author	Sensor	Method	Parameters	Dataset	Results
[Cloete and Scheffer, 2008]	16 IMUs (MOVEN inertial motion capture system)	Lower body joint angles were found by calculating the joint orientation of the distal segment with respect to the proximal segment (thought a quaternion multiplication).	Hip, Knee and ankle angles	8 Healthy.	Correlation averages: hip (0.94), knee (0.89) and ankle (0.08)
[Cloete and Scheffer, 2010]	16 IMU (MOVEN inertial motion capture system)	Lower limb joint angles were found by calculating the joint orientation of the distal segment with respect to the proximal segment. Without the Lycra suit to avoid relative movements (between trackers and body segments).	Hip, knee and ankle angles - repeatability study.	30 Healthy.	Mean and SD for all joints higher than 0.90 for right and left.
[Meng et al., 2013a]	4 IMU (shank and thight)	Adaptative threshold and searching intervals. Uses the [Meng et al., 2013b] method: from the orientation of each segment and the displacement of each foot - given the length of the bone segments, the human model while walking is constructed.	LR, mid-stance, terminal stance, PS, initial swing, mid-swing and terminal-swing.	5 Healthy, 2 elderly and 2 severe dementia.	Comparative analysis between each group of subjects.
[Qiu et al., 2014]	IMU (shank)	Converts the body frame to the ground frame by filtering (with Kalman filter) the acceleration and angular velocity extracted from the quaternions.	Walking distance and knee angle	Healthy.	Average percentage error 4.96%.
[Martori et al., 2013]	6 Opal IMU (chest, shank and thigh)	In each gait cycle, the local maximum and minimum peaks were identified.	Knee and hip joint angles.	10 Healthy.	Average error - overall - 4.17 and 5.15 degrees (right and left).
[Ahmadi et al., 2015]	IMU (foot, tibia and thigh)	Gradient Descent algorithm to obtain 3D orientation of the 3 segments. With foot sensor, detect the stance phase, then the 3D orientation of the 2 segments and joint angles were determined. Customised kinematic model to adjust the output as a coherent behaviour.	Segments orientation, foot position, 3D reconstruction.	(without dataset)	(without results)
[Williams et al., 2015]	IMU (foot, shank and thigh)	Consists in determine the joint angles with a similar method described by [Cloete and Scheffer, 2008]. The subject's leg is measured to determine spatial parameters with trigonometric equations.	Knee and ankle angles.	1 Healthy.	RMSE of 3.03^{o}.

3.4 Final Considerations

IMUs are devices capable of monitoring movement of the human body, being easy to use, with sufficient autonomy for rehabilitation exercises, and (with adequate signal fusion algorithms) accurate, precise and robust enough to be used in rehabilitation environments.

The rehabilitation of the gait should be prescribed individually for each patient. The system should be able to report crucial and relevant information for the patient and for the therapist. In this sense, metrics are needed, which are obtained by the calculation of gait parameters.

Few published methods are related to the development of a gait analysis system concerning a rehabilitation application. Even within these, there are few that use sensors with specifications close to those that will be used in the practical work of this thesis. However, it is observed that many authors begin by determining the IC and PS moments, and from them, estimate all other gait parameters. In general, the results of the methods have different formats and many of them reported only information of gait patterns between two populations of different subjects (healthy and unhealthy), not providing information against a gold standard of movement acquisition. Those that provided show accuracies between 80% and 95%.

Chapter 4

Temporal Events

After collecting all the information as described in the previous chapters, the assessment part of the work used a simple setup, with two trackers. The process started with the extraction of the Initial Contact (IC) and Pre Swing (PS). With these two events, it was possible to determine a large set of the temporal parameters used for gait analysis, evaluation and rehabilitation, as mentioned in Section 2.3.

The work begun by acquiring the data from the sensors that were placed on each foot. The orientation of each sensor was obtained and then IC and PS events are extracted. Information concerning the detection of the IC and PS events and their instants was used to calculate the temporal parameters, such as stance time, swing time, gait cycle time and step time. The work flow is shown in Figure 4.1.

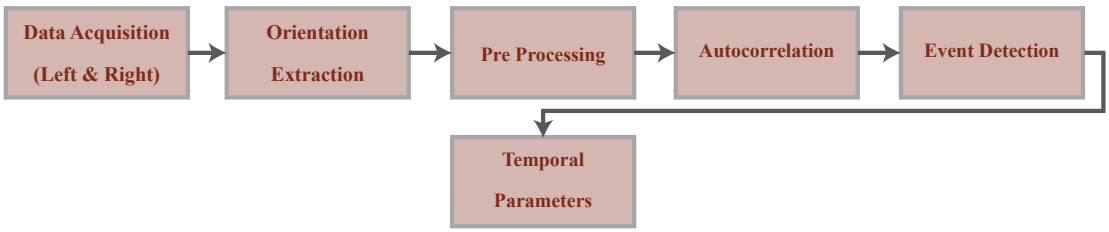

Figure 4.1: Block diagram for the first development phase.

In this chapter are presented: the data acquisition protocol and the definition of the dataset; the interpretation of the extracted signal; the detection methods of peaks and valleys (to be explained hereinafter); and the and detection of disturbances (higher frequency components). The chapter also includes information concerning the used validation approach.

4.1 Overview and Parameter Selection

After collecting all the information presented in Chapters 2 and 3, the following summarization can be made:

- Temporal parameters are important for gait analysis, evaluation, and rehabilitation (Subection 2.3.1).
- Temporal parameters also allow finding differences between groups of people with different diseases, namely people with Parkinson's and stroke from healthy people (Subsection 2.3.1).
- Most temporal parameters are determined from the instant the foot touches the floor (IC) and the instant when the foot leaves the floor (PS) (Section 2.3).

Throughout this chapter, it is shown that it was possible to determine the IC and PS events with only two trackers (one in each foot) and calculate temporal parameters with these two events. Using information presented in Subsection 2.3.1, the temporal parameters that only depend on IC and PS are:

- Gait Cycle Time (stride time),
- Stance Time,
- Swing Time,
- Step Time,

4.2 Data Acquisition

The data was initially collected to undestand the problem and then to elaborate of the algorithm outlined in Figure 4.1. The following considerations had to be made regarding data acquisition, due to different types of shoes. People, namely the volunteers, wear different types of shoes. They had different conformations, and in order to reduce the variability of the obtained signals, a protocol that describes the placement of the sensors, was elaborated for the data acquisition.

With the goal of comparing and interpreting data, this acquisition was performed in parallel with video recording. After the synchronization of both signals (quaternions and video), it was possible to perceive the signals characteristics to which the different events belong, in other words, the signal behavior while in the IC and PS events occur.

4.2.1 First Dataset

The volunteers who participated in the first data acquisition were healthy people, aged between 22 and 23 years, and with a healthy gait. The goal of this phase was to find signal characteristics that correspond to healthy gait events, in order to build an algorithm capable of detecting these events in healthy people. Table 4.1 presents basic features of these volunteers.

Table 4.1: General information about the volunteers of the first data set. In this table is information about the gender, age, height, weight, health condition and type of walk.

Subject	Gender	Age (years)	Height (cm)	Weight (Kg)	Type of walk	Condition
no. 1	Female	22	160	56	Free normal style	Healthy
no. 2	Female	23	168	72	Free normal style	Healthy
no. 3	Female	22	170	58	Free normal style	Healthy
no. 4	Male	22	180	75	Free normal style	Healthy

The data collected using these subjects was used to elaborate and perform the first evaluation of the algorithm. This development phase was not yet in real time, so it was decided to collect data from fewer people to be more proficient in evaluating all the videos recorded during the acquisition. The protocol used for sensor placement and signal acquisition is described bellow.

First Protocol Setup

In order to reduce the variability of the placement of the sensors (IMU *MTw*, Xsen's product), in particular due to different shoes, as mentioned before, it was decided to use a barefoot setup, containing only socks. Two straps of feet were placed, one on each foot, with the thinnest part of the strap immediately posterior to the bone known as a *bunion*, and with the Velcro® rectangle positioned in line with the big toe and the heel, in a way to be located in a flat area of the foot . The sensor was placed with the led and the power input facing the back, as shown in Figure 4.2. Following the order of sensor colors chosen by the company, the setup chosen was the green sensor placed on the right foot and the blue sensor on the left foot.

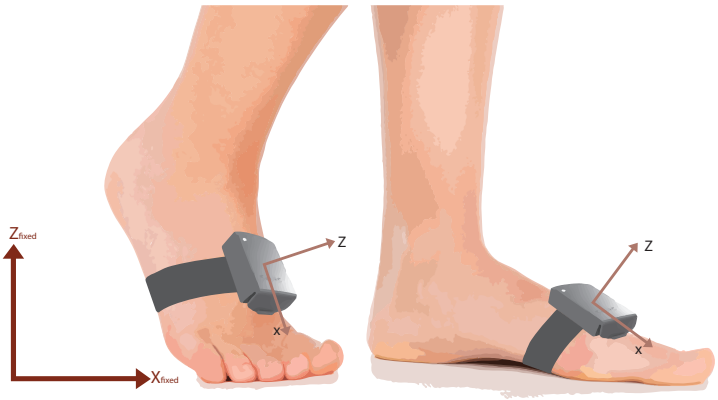

Figure 4.2: Sensor Placement - First Setup.

After placing the sensors a GoPro HERO5 Session[1] video camera, whose characteristics are presented in Table 4.2, was positioned with visibility to cover the whole area of the room where the volunteers made the march. The synchronization was done with a quick touch on the two sensors so as to be visible from the video camera and detected in the signal. This moment could be seen

[1]GoPro HERO5 Session. `https://www.cnet.com/products/gopro-hero5-session/specs/` (visited on 28.03.2017)

in the video (Figure 4.3a) with Kinovea [2] platform, and in the signal (Figure 4.3b) as exemplified in Figure 4.3.

Table 4.2: Technical Specifications of the GoPro video Camera[1] .

General	**Information**
Max Video Resolution	3840 x 2160
Widescreen Video Capture	Yes
Sampling Frequency	50 Hz to 100 Hz
Lens System	**Information**
Focus Adjustment	focus free
Memory / Storage	**Information**
Memory Card Slot	microSD card

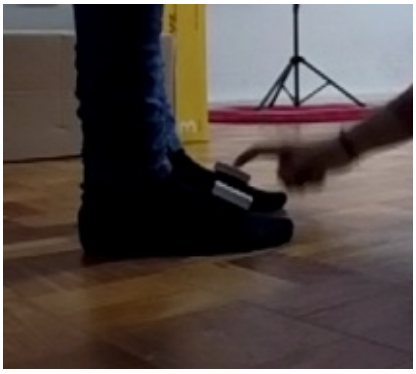

(a) Synchronization - in the video side (using Kinovea[2] software).

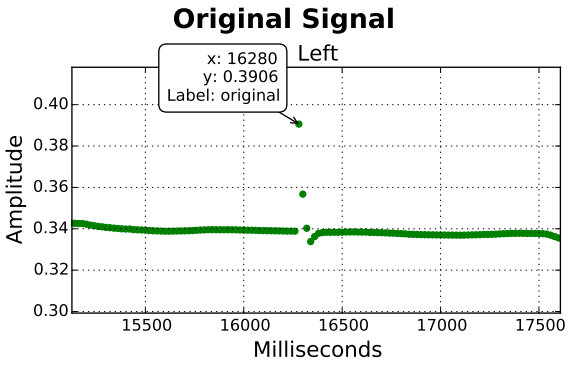

(b) Synchronization - in the signal side.

Figure 4.3: Procedure for synchronizing the video with the signal.

The synchronization was done within the visibility of the camera, giving a strong and fast touch in the tracker, as shown in Figure 4.3a. On the signal side, it was possible to see about three to five points that were destabilized beyond the resting line for a short period of time (example in Figure 4.3b). This corresponds to the moment when a strong, quick touch struck the sensor. By relating the moments of touch on the video side (Figure 4.3a) and the rapid destabilization of points (Figure 4.3b) in the sensor, it was possible to synchronize the two systems.

The volunteers were asked to walk freely back and forth so that the signal could be collected by the sensors and visible through the video camera, as shown in Figure 4.4.

From the Kinovea[2] platform, it was possible to view the videos collected frame by frame (which is equivalent to 20 milliseconds intervals in a video acquired at 50 Hz). However, some problems were found in viewing the video, namely this frame-to-frame visualization and transition. According to the sampling frequency specified in the camera (100Hz), it was not possible to observe all video frames even with several video editors, including Adobe Premiere, VLC, Movie

[2]Kinovea. `https://www.kinovea.org/` (Used in February and March 2017)

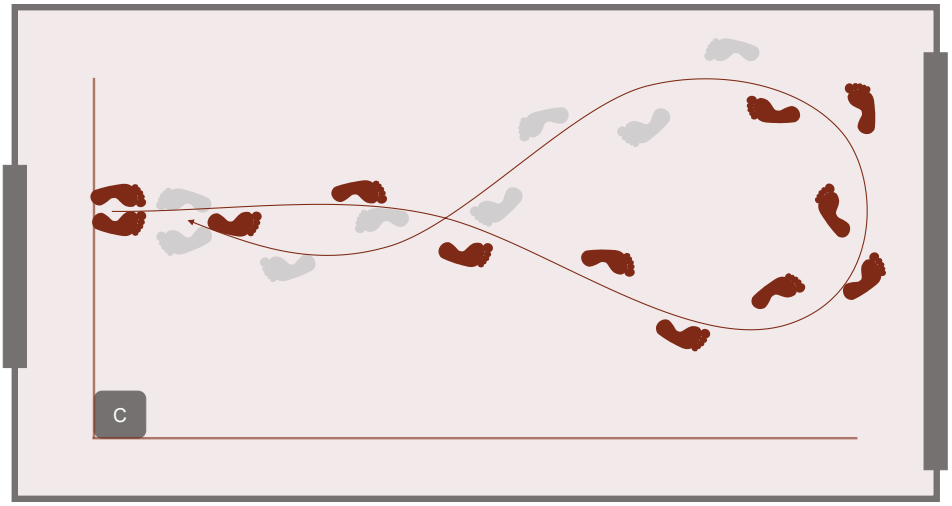

Figure 4.4: Setup of the room where the fist data set was acquired. In this sketch, the gray rectangles are doors and windows, the video camera is represented by a rectangle with the letter C. The volunteer walks around the region inside region of visibility of the video camera.

Maker (Windows), among others. This may be because of the format in which the video was recorded (MP4) which automatically reduces the quality of the video. This causes loss of frames resulting in frequency decrease. This problem will be addressed latter on.

The working setup of this project consists of the sensors tablet and computer. The connection between the sensors and the tablet is Bluetooth. This tablet is connected by USB to the computer where the program under study is located. The output of the sensors are quaternions, which are emitted every 20 ms. Quaternions are the inputs of the program.

4.3 Orientation Extraction

After obtaining the signals from the sensors, the information was extracted. In Figure 4.5 it is possible to observe the imaginary part of the signals resulting from the quaternion multiplication with the X and Z fixed frames ($[1,0,0]$ and $[0,0,1]$, respectively). It can be observed that the Z components of each resulting vector had higher periodicity. For the vectors obtained by the multiplication of the fixed Y frame ($[0,1,0]$), it is also possible to see some periodicity. However it has became highly sensitive to the gait orientation that the person was taking. This means, it depends on the direction the volunteer' walking. Since, for this analysis, the values of the sensors multiplied by the Y fixed frame ($[0,1,0]$) were not necessary, they were not considered as input for the algorithm.

Following the visualization of the data, it is also possible to observe that there was a good relation between the Z components (X_Z and Z_Z) of the quaternions after multiplication by $[1,0,0]$ and by $[0,0,1]$[3]. In some cases, a small saturation occurs in these signals, due to a large slope value of the foot when walking. However, it did not occur at the same time in both X_Z and Z_Z.

[3] from now designated by X_Z and Z_Z, respectively

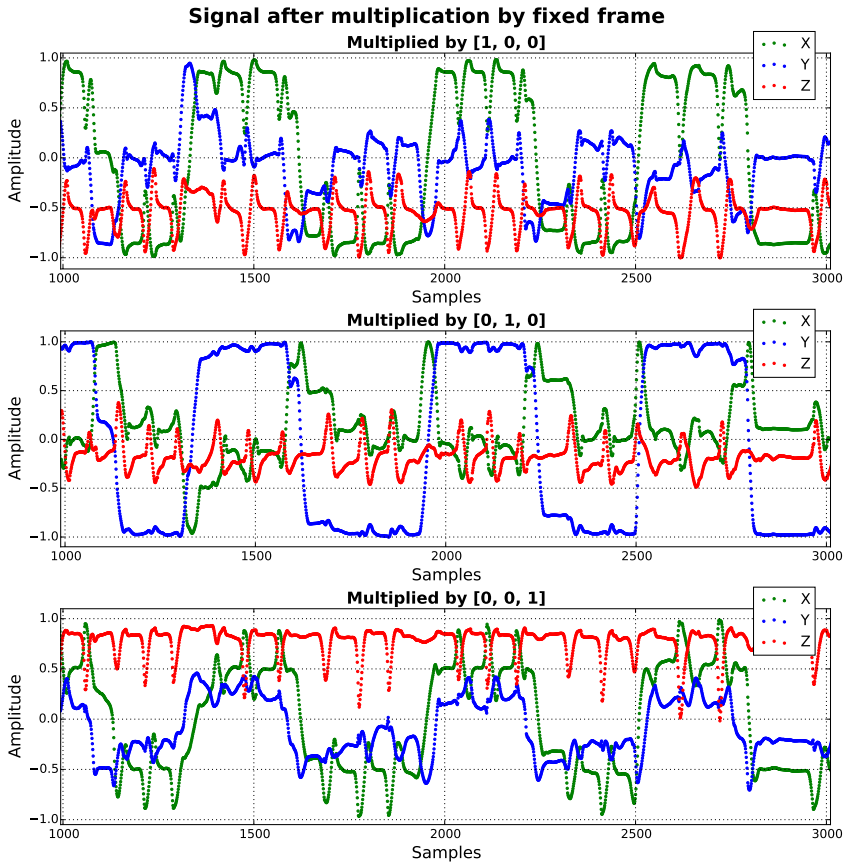

Figure 4.5: Orientation of the quaternions when multiplied by a fixed frame. Only the signals obtained from the left foot are presented. On the top is the multiplication of each quaternion of the signal acquired by the vector $[1,0,0]$. The different colors represent the corresponding part of the resulting vector (green is the component x of the result of the multiplication of each quaternion by the fixed vector $[1,0,0]$. The same procedure was repeated for the remaining examples.

Figure 4.6 shows the result of the sum of the z components ($X_Z + Z_Z$). It can be seen that there was a good periodicity of the signal and there was a similarity between the values of the signal and the annotations made in the video. It can be observed that there was a good agreement between the peaks and the valleys of the signal with the events of placing the foot on the ground (IC) and taking the foot off the ground (PS) on the video.

Figure 4.6 contains a portion of the signal in which five Gait Cycles (GC) of the left foot can be observed. The vertical lines represent the video annotations (after synchronization) in which the solid blue lines represent the events of PS and the dashed red lines represent the IC events. According to the video annotations, all the PS events were closer to the signal valleys and all the IC events were closer to the positive peaks of the signal. These events were visualized for all data from all volunteers and the conclusion was the same: signal negative peaks correspond to PS events and signal positive peaks correspond to IC events. This conclusion can also be supported with information already presented in Subection 2.2.3 in Figure 2.4 and in the Table 2.1. With this information, it was possible to begin to interpret, in a more detailed way, the macro phases of the

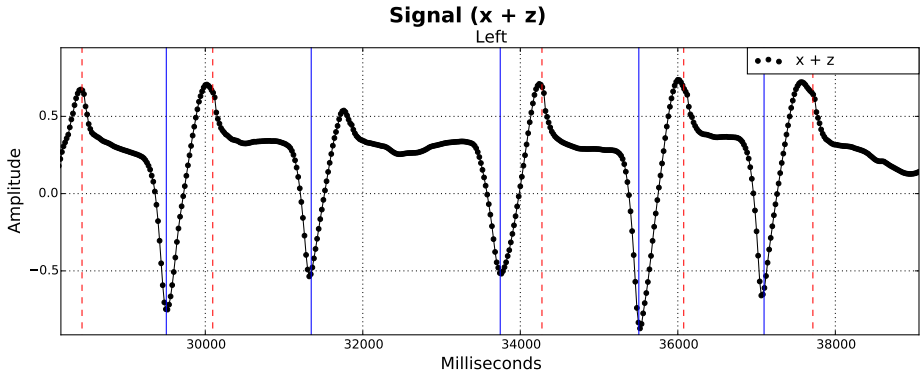

Figure 4.6: Part of the signal acquired from the sensor placed on the left foot with video annotations obtained at the same time as the acquisition. The vertical red dashed lines corresponds to IC events (in the video) and the vertical blue continuous lines corresponds to the PS events (in the video), after synchronization between the video and the signal. The label $X+Y$ refers to the sum of the resulting Z components of the multiplication of the signal with the X and Z fixed frame: $X_Z + Z_Z$.

signal as the stance and the swing, which will be described in the following sections.

4.3.1 Direct Interpretation

As already mentioned, in Figure 4.6 the continuous blue vertical lines represent events of lift the foot from the ground (PS) and the red dashed lines represent events of putting the foot on the ground (IC), annotated by the observation of the videos collected at the same time of the acquisition of the signal.

Video Annotations

However, before analyzing these points in more detail, it was necessary to mention the conditions for collecting the video annotations. As already mentioned, the videos were analyzed frame by frame (with a frequency of acquisition of $100Hz$) by a tool of visualization of videos - Kinovea. After adjusting the display settings, for example, to see the time in milliseconds to be possible to compare with the signals, it was observed that not always the video frame advanced for each 10 millisecond (1000 milliseconds in each second/ $100Hz$). The reason may have been related to how the video file was saved by the camera GOPRO, i.e. in MP4 format. There was a reduction in video quality, also related to the loss of frames.

During the analysis of the video, it was possible to see the problem mentioned before. There were frame advance every 20 or 30 milliseconds, which represents a loss of between 50 and 67 Hz of acquisition frequency (determined with Equation 4.1 and Equation 4.2). In this way, the frequency obtained became to be around 50 to $33Hz$, smaller than the frequency of the sensors (Equation 4.1). This way, there was an associated error, due to the impossibility of viewing frames in about 30 milliseconds. As the time displacement between each sample acquired by the tracker

had a distance of 20 milliseconds, the error of the video became slightly above and may not be feasible. This problem had to be considered when validating the results of the algorithm considering the video annotations.

$$Time\_between\_frames = \frac{1000 \quad (ms)}{Frequency} \tag{4.1}$$

$$Desired\_frequency - \frac{1000 \quad (ms)}{Time\_between\_frames} = Loss\_of\_frequency \tag{4.2}$$

Another problem associated with video annotation was the occlusions. Occlusions, in this context, are defined as events of PS and IC in the video that are not clearly visualized, such as the examples shown in Figure 4.7. These cases occurred due to the overlapping of the two feet in the video, the foot of interest (the one that was doing IC or PS), behind the foot in stance, making it impossible to know the exact moment when the event occurred.

(a) Occlusion of the PS event of the right foot. (b) Occlusion of IS event of the left foot.

Figure 4.7: Examples of occlusions that occur along the videos. This turned unfeasible the precise determination of moment in which the events of CI and PS occurred. In this case, occlusion occurerd by one foot standing in front of the other.

During the video analysis, there were several cases similar to those shown in Figure 4.7. To avoid having a higher error associated with the difficulty of knowing the exact moment when the foot left the ground (Figure 4.7b), and the placement of the foot on the floor (Figure 4.7a), these cases were ignored. An example of this is shown in Figure 4.6, where the third peak presented would correspond to an IC event, however, there were no annotations in the video, because at that moment an occlusion occurred.

Leave the Ground - Pre Swing

Despite these problems described above, it was possible to directly realize that the lift of the foot from the ground was related to the maximum negative slope of the foot (i.e. - the signal valley).

This was concluded due to information presented in Subsection 2.2.3, the high correspondence between these events in different subjects, and the different displacements (about 30 ms) between the annotation and the signal (forward and backwards in time for the same synchronization). In all observed signals, the events noted as PS correspond to the negative peaks. In this sense, one way to find PS moments would be to find these negative peaks.

The placement of the tracker on the foot was with the VELCRO part facing down and the LED facing the tibia. This had to be in a relatively flat area of the foot, as explained in Subsection 4.2.1. According to this configuration, by analyzing the Z_Z vectors (nominated in Subsection 4.3), when plantar flexion is performed (or tip toe down), the value of this component decreases, approaching 0 (Figure 4.8e). Now, considering the X_Z vectors, when the same motion is performed, its values approaches -1 (Figure 4.8e).

When the foot is in the rest position on the ground, the Z_Z value becomes close to 1, since the Z axis of the tracker is very close to the Z reference's axis (Figure 4.8c). Considering the X_Z value, when the foot is at rest on the ground, the value of this vector is close to -0.5. This is because the component Z of the result of the multiplication between the quaternion by $[1,0,0]$ is relatively below the perpendicular of the Z axis. This took a slightly negative value (Figure 4.8c).

By increasing the foot inclination with the fingers toward the ground, the sensor Z component approaches the perpendicularity to the Z axis of the reference axis: the value is close to 0, as shown in the third chart presented in Figure 4.5.

Considering events of PS, where the foot is tilted with the fingers toward the ground, the tracker also tilts the same way, with the LED facing upwards (Figure 4.2). In this case, the value of X_Z becomes even more negative, almost to the point of being aligned inversely with the Z of the global axis, as can be seen in the first graph shown in Figure 4.5.

According to this interpretation of the video and the signals, it can be concluded that identifying the PS event involves identifying the signal valleys.

Contact With the Ground - Initial Contact

From the analysis of Figure 4.6, it can be noted that events of placing the foot on the ground were near the positive peak of the signal. By analyzing the signal more carefully, it can be seen that X_Z increases with dorsiflexion of the ankle, or the movement of the foot with the fingers pointing upwards. In this case the value of X_Z approaches 0, and Z_Z approaches 1 (Figure 4.8a). With this information, it can be concluded that the positive peak can be close to the IC event. In Figure 4.6, it can be observed that, in most cases, IC events were slightly after the positive peaks of the signal. Observing in more detail, it is observed that there was a high relation between a small signal disturbance with higher frequency and the video IC annotation. The disturbance makes sense to occur, being related to the contact with the ground, i.e. the shock absorption of the foot (Figure 4.9). Before contact with the ground, the foot is advancing in the air having no disturbance of greater frequency, until the moment the foot is placed on the ground.

In this way, a healthy person in constant movement (not being at the end of the march), the detection of the IC moment is to detect the disturbance soon after the positive peak of the signal.

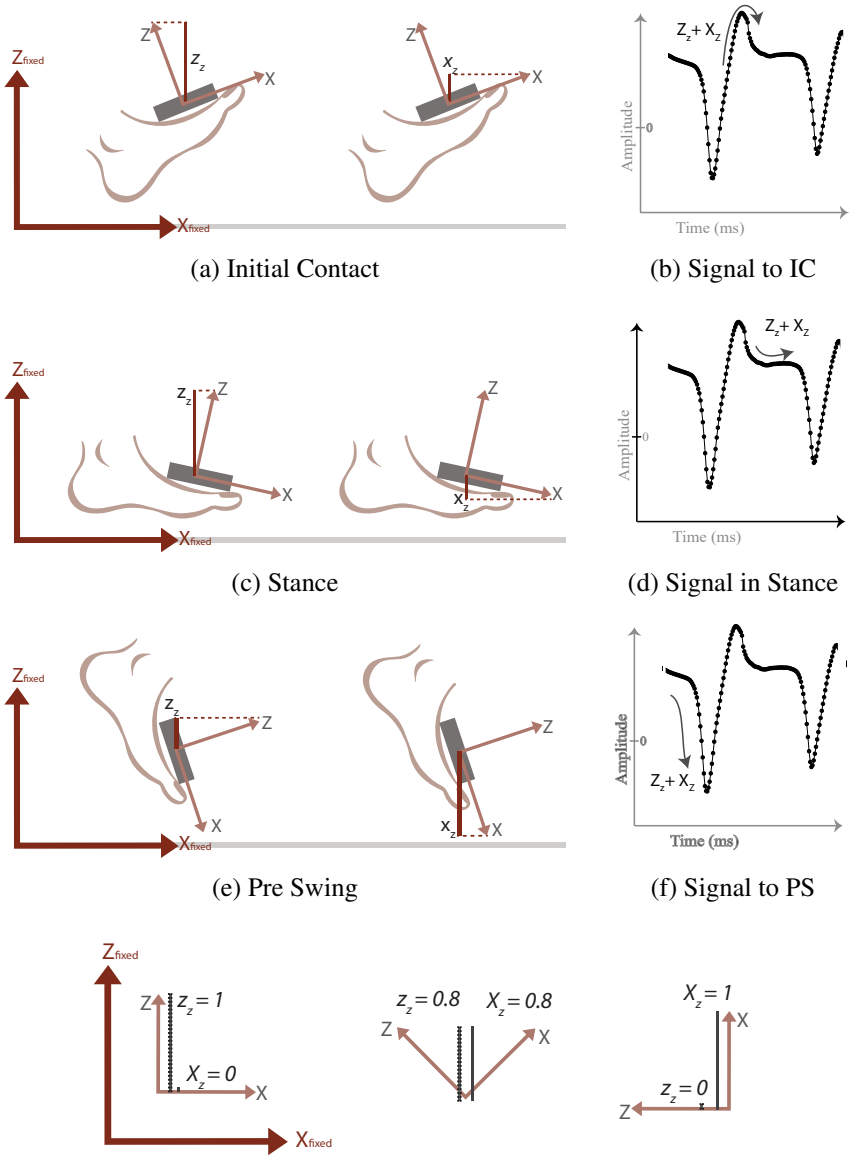

(a) Initial Contact (b) Signal to IC

(c) Stance (d) Signal in Stance

(e) Pre Swing (f) Signal to PS

(g) Signal Z_Z and X_Z representations.

Figure 4.8: Sensors orientation along the three main gait phases. The arrow in (b), (d) and (f) represent the signal moments before the event illustrated in (a), (c) and (e), respectively.

Swing Event

After interpreting the previous events (IC and PS), it can be determined which segments of the signal correspond to the swing. By the definition described in Subsection 2.2.3, the swing is the advancement of the foot in the air, which corresponds to the moment when the foot leaves the floor (PS) and the foot again comes into contact with the floor (IC). In the image 4.6, it can be seen that the signal between the continuous blue vertical lines and the dashed red vertical lines corresponds to swing moments.

After the foot leaves the ground, it rotates in axis approximately centered on the knee till the

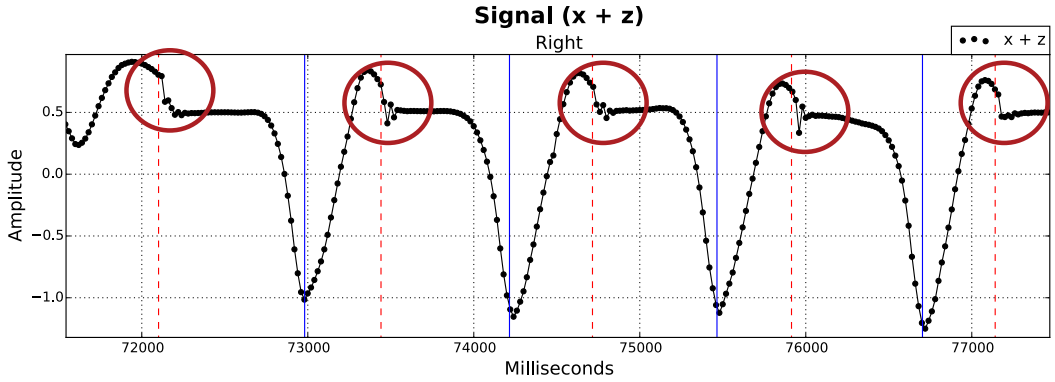

Figure 4.9: Detail of the signal with emphasis of the IC moment with video annotations, characterized by shock absorption, which causes a higher variation in the signal. The vertical red dashed lines is the IC event noted in the video. The red circle is presented just to enhance the region in analysis. The label $X+Y$ refers to the sum of the resulting Z components of the multiplication of the signal with the X and Z fixed frame: $X_Z + Z_Z$.

calcaneous by rotating the sensor from the position shown in Figure 4.8e to the position shown in Figure 4.8a. In this way, it goes from the negative (minimum) value to a positive value that almost reaches the maximum. Thus, it can be concluded that the swing phase is related to the instants between the PS and IC, being a drastic increase in the signal value.

Stance Event

In the stance event, the foot is much of that time perched on the floor in an almost stable form, supporting the total weight of the body. This phase occurs between the IC and PS instant. Observing the sign of Figure 4.6, it is noticed that there is a small platform in which the foot is practically at rest. At this time, the value of Z_Z is close to 1 and the value of X_Z is slightly negative (Figure 4.8c). This results in a value a little above 0 and quite stable. This can be seen in Figure 4.6, where the stance is between the dashed red vertical lines and the continuous blue vertical lines.

Concluding this section, the information in the signal can be interpreted as presented in Figure 4.10.

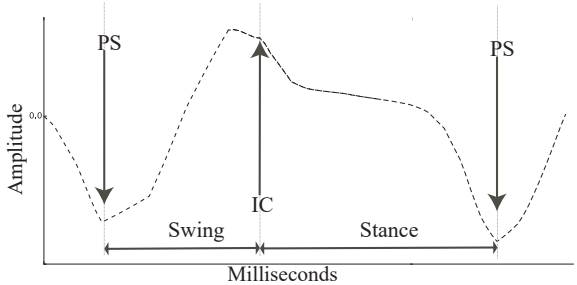

Figure 4.10: Gait Cycle signal with IC and PS events and Swing and Stance phases noted.

4.4 Detection of the Peaks and Valleys

As mentioned in Section 4.3.1, the detection of the IC and PS moments may pass through the detection of peaks and valleys in the signal (Figure 4.6). The detection of these events can start using peak detection algorithms. But, before any processing, it was necessary to verify if was necessary to remove noise from the signal.

4.4.1 Pre Processing

After analyzing the literature, it was verified that there are very few papers that refer to pre processing after obtaining quaternions. It was found that, the processing step was mainly before the Kalman Filter (or similar algorithm) on the signals of each of the sensors: accelerometer, gyroscope and magnetometer, before the fusion algorithm. Since the sensors used in this work already provide the quaternions, and the fusion algorithm includes a pre processing, there was no need to process the signal once again. The signals have almost no noise. On the other hand, by visualizing the walking signal (Figure 4.6), it is observed that the samples are relatively close and in agreement with each other, with little or no observation of outliers.

4.4.2 Peak Detection

This peak detection algorithm was extracted from Github - Peakdetect[4], that is a Python implementation of an algorithm that detects positive and negative peaks in 1D signals[5].

This algorithm takes three input parameters: the number of samples from which to retrieve the maximum or minimum local search, a delta that corresponds to the amplitude in relation to the previous peak, from which it can be considered that the point is a local maximum or minimum, and the signal. From the first two parameters, only local maxima and minima are found throughout the signal, selected according to the defined parameters (Figure 4.11).

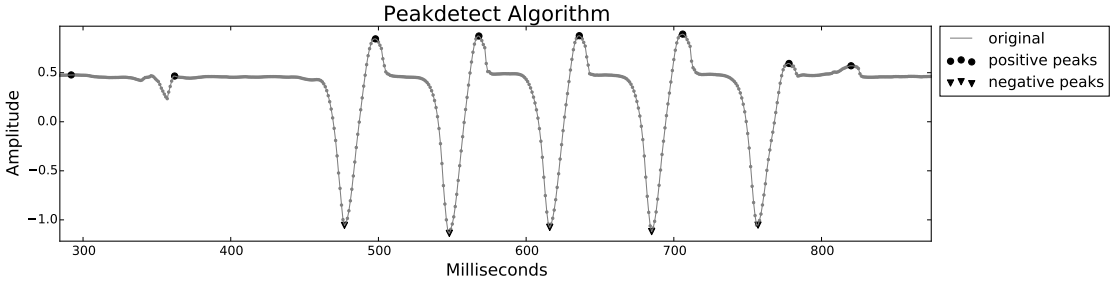

Figure 4.11: Peakdetect algorithm. Detection of peaks and valleys. The result is presented in black, where the circles are the peaks detected and the triangles are the valleys detected. The label *original* refers to the sum of the resulting Z components of the multiplication of the signal with the X and Z fixed frame: $X_Z + Z_Z$.

[4]Peakdetect - GitHub `https://gist.github.com/sixtenbe/1178136` (06/03/2017)
[5]Peakdetect `http://billauer.co.il/peakdet.html` (02/05/2017)

After running this algorithm, it was noted that there are some maximum and minimum locations selected by the algorithm that did not respond to the IC and PS events annotated through the videos. It is also observed that they are mostly on the signal platform which corresponds to the stance phase, characterized by having an amplitude closer to zero. Since the events IC and PS (separately) have approximately the same amplitudes, an adaptive threshold was applied so as to select only the peaks that correspond to the IC and PS separately. After this repair, the peaks detected by the algorithm were closer to the events noted by the video.

4.4.3 Trahanias Algorithm

Due to the limited information on peak detection found in the literature in gait analysis with inertial sensors with quaternions as output, a search was made for peak detection algorithms used in other physiological signals. By visual comparison, the gait signal already presented in some figures in this document, has a certain similarity with the electrocardiogram (ECG) signal. This is because, despite being signals with different frequency ranges, both are periodic and contain peaks and valleys of interest. These two properties are almost enough to bring to the gait analysis algorithms used in ECG analysis in terms of peak detection methods. In this way, the algorithm chosen to be compared with the peakdetect (mentioned in subsection 4.4.2), was the Trahanias Algorithm [Trahanias, 1993]. The Trahanias algorithm was the first ECG method to be implemented in this project. Since the Trahanias algorithm was able to give good results, no further algorithm was implemented.

The Trahanias algorithm begins with a set of morphological operations that allow removing regions of the signal that are not peaks and not valleys, that is, leaving only peaks and valleys of the original signal, while the remaining signal is equalized to zero.

Basic Concepts - Morphological Operations

For the application of the *Trahanias* Algorithm, as already mentioned, it was necessary to collect the morphological operations: erosion and dilation, open and close. All the operations include a structuring element B, that is a symmetric interval around zero.

Erosion is a morphological operation in which the signal f is morphologically subtracted by the structuring element B (Equation 4.3).

$$(f \ominus B)(x) = min\{f(x+x')|x' \in B\} \tag{4.3}$$

Dilate is a morphological operation in which the signal f is morphologically added by the structuring element B (Equation 4.4).

$$(f \oplus B)(x) = max\{f(x+x')|x' \in B\} \tag{4.4}$$

In Figure 4.12c and 4.12d the result of erosion and dilation in a 1D signal with a structuring element B can be observed.

Open is the morphological operation that consists in a erosion operation followed by a dilation operation, obtained with the same structuring element B (Equation 4.5).

$$f \circ B = (f \ominus B) \oplus B \tag{4.5}$$

Close is the morphological operation that is the opposite of the open operation. It begins with the dilate operation and then erosion operation, with the same structuring element B (Equation 4.6).

$$f \bullet B = (f \oplus B) \ominus B \tag{4.6}$$

In Figure 4.12e and 4.12f the result of opening and closing in a 1D signal with a structuring element B can be observed.

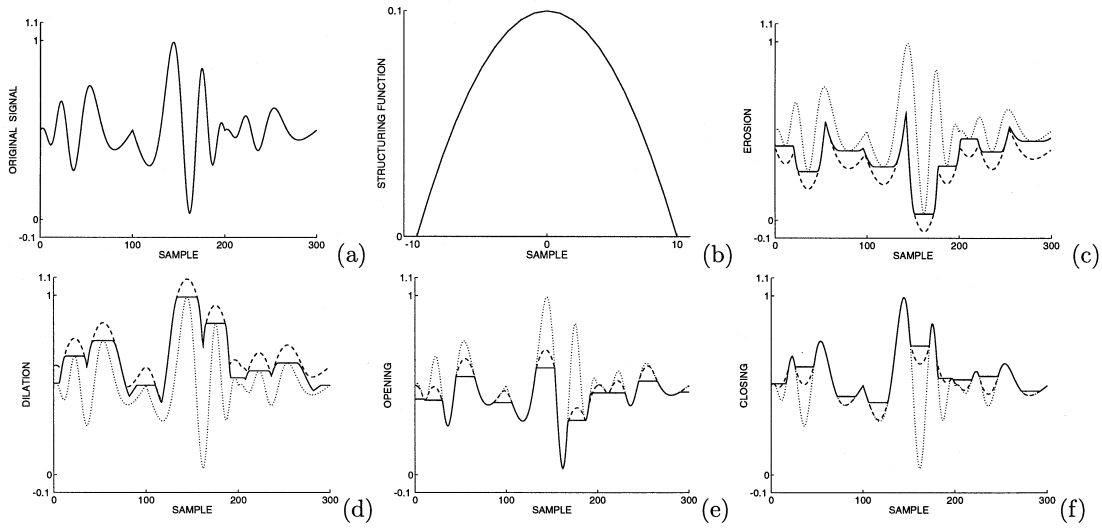

Figure 4.12: Presentation of an example of a signal and structuring element and the result of the described morphological operations [Moragos, 1999]. (a) is the original signal f. (b) is the structuring element g (in this case a parabolic pulse). (c) the dashed line is the result of the erosion, the solid line the result of the flat erosion, and the dotted line is the original signal f. (d) the dashed line is the result of the dilation, the solid line is the result of the flat dilation. (e) the dashed line is open and the solid line is the flat opening. (f) the dashed line is the closing, and the solid line is the flat closing.

Algorithm

With Figure 4.13 it is possible to see the general scheme of the Trahanias algorithm. It begins with a filtering section that consists of the successive application of *Open* and *Close* operations on the signal with a struturing element with small size(similar to the noise size) (Figure 4.13b), followed

by the application of the *peak-value extractor* (PVE) transformation (with a larger structuring element size, close to the peaks and valleys size) (Figure 4.13c) (Equation 4.7),

$$PVE(f) = f - [(f \circ B) \bullet B] \tag{4.7}$$

where f is the input signal and B is the structured element.

The filtering module of the algorithm aims to filter high-frequency peaks and valleys. It eliminates noise without any degradation of the QRS signal (described by the article). In this way, the article suggests that the B is the size equivalent to 3 sample points. As the signal provided by the trackers is already filtered and without apparent noise, this step was ignored.

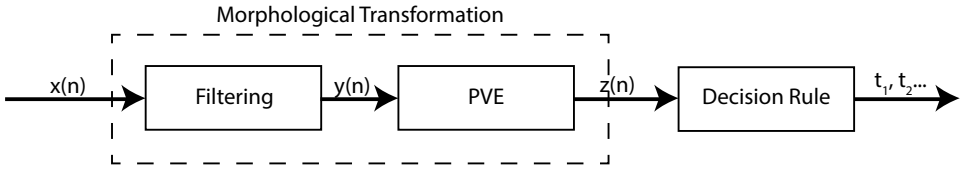

(a) Scheme for the Peaks detection (QRS in the ECG signal).

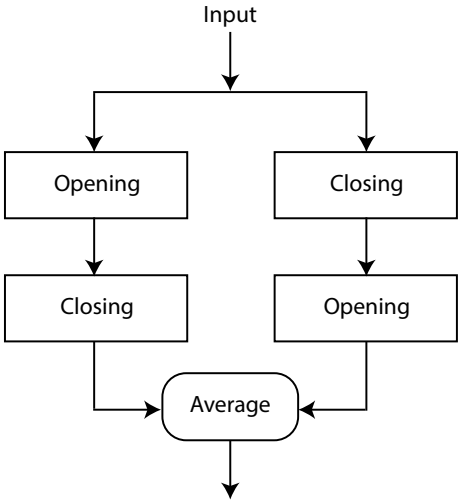

(b) Detailed information of the filtering module.

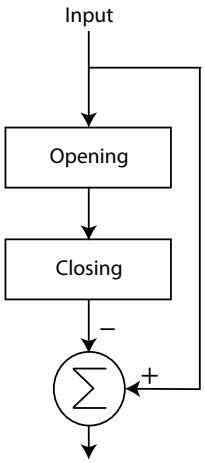

(c) Detailed information of the PVE module.

Figure 4.13: Trahanias Scheme [Trahanias, 1993].

The PVE module allows acquisition of only mountain elements and valleys, making the rest of the signal equal to zero. The successive application of the open and close operations generate peak and valley extraction operations. By subtracting the open of a signal with a structuring element B to the input signal, it generates an output that contains the mountains that do not have the support of B, that is a *top-hat* operation (Equation 4.8).

$$PE(f) = f - (f \circ B) \tag{4.8}$$

Similarly, by subtracting a close of the signal with the structuring element B to the input signal, it generates an output containing the signal valleys, which is a *bottom-hat* operation (Equation 4.9).

$$VE(f) = f - (f \bullet B) \tag{4.9}$$

An example of the result after applying PE and VE functions is presented in Figure 4.14.

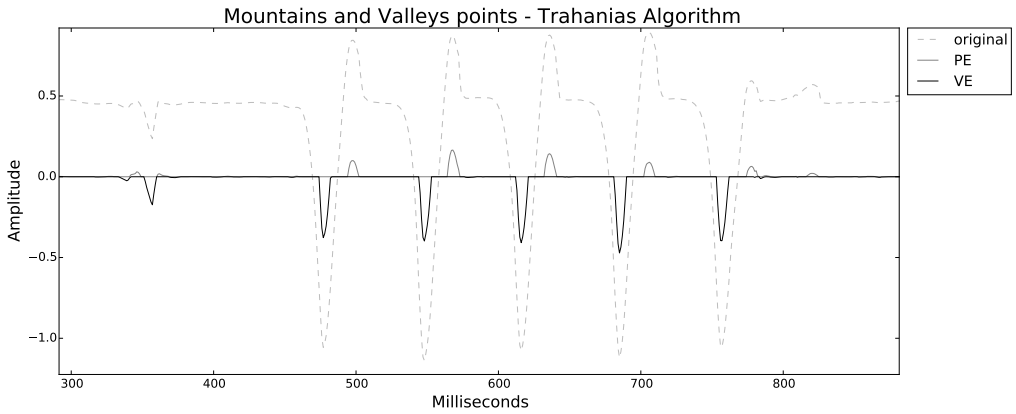

Figure 4.14: Trahanias algorithm: the result of the PE and VE functions. The dashed gray line represents the original signal. The dark gray line is the result of the PE functions, that gives the mountains of the signal and the remaining information is changed to zero. The black line represents the result of the VE function, that gives the valleys of the signal, the remaining information is transformed to zero. The label *original* refers to the sum of the resulting Z components of the multiplication of the signal with the X and Z fixed frame: $X_Z + Z_Z$.

As can be seen from Figure 4.15, the size of the structuring element is determinant to find the peaks and valleys. By analyzing the gait signals, the valleys, associated with the events in which the foot leaves the ground, correspond to generally sharper valleys, whereas, not always, the events of putting the foot on the ground (the positive peaks of the signal) have the same sharpness. For this reason, the L value of the structuring element must be analyzed for the walking signal.

After finding the peaks and valleys of the walking signal, the next step follows to find the maxima and minima of the peaks and valleys, respectively. In order to avoid the noise that still exists, the article suggests the application of an adaptive threshold (Equation 4.10). As they intend to acquire positive and negative peaks, the threshold is applied to the absolute values of the signal. Resulting in positive peaks and negative peaks (Figure 4.16).

$$new\_threshold = (w_a \times previous\_threshold) + (w_b \times previous\_peak\_detected) \tag{4.10}$$

Where the w_a is the weight applied to the previous threshold and w_b is the weight applied to the previous peak detected amplitude.

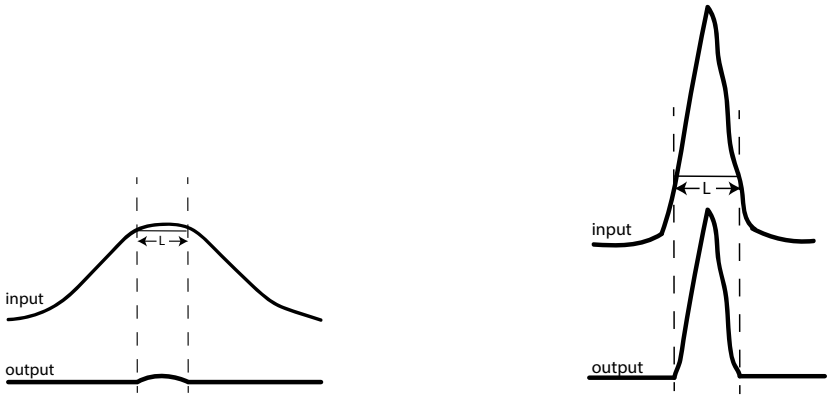

(a) Top-hat with structuring element with size L and a flat peak signal.

(b) Top-hat with structuring element with size L and a sharp peak signal.

Figure 4.15: An example of the structure element size influence in the peaks extraction (Trahanias Algorithm) [Trahanias, 1993]. Applied in two different peaks, the result of the operation (*top-hat*), is shown below each signal. This illustration has the same representation when applied the *bottom-hat*.

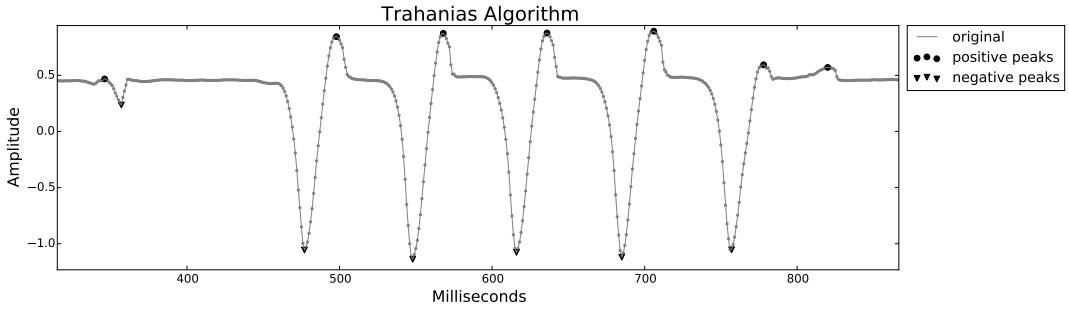

Figure 4.16: Trahanias algorithm. Positive and negative peaks detection.The result is presented in black, where the circles are the positive peaks detected and the triangles are the negative peaks detected. The label *original* refers to the sum of the resulting Z components of the multiplication of the signal with the X and Z fixed frame: $X_Z + Z_Z$.

4.4.4 Detection of the Initial Contact

At the instant of shock absorption, which corresponds to the IC event, the signal acquires a higher frequency component, as shown in Figure 4.9. In this way, a frequency analysis can be performed to identify these moments. The Fourier transform would be an approach for this case, however it lacks information on the location of the components of the various frequencies, and is not enough for the intended application.

The Wavelet Transform parts with the Fourier Transform idea, in which the signal is approximated by the sum of several sine and cosine series. The highest difference in Wavelet Transforms is that it approaches the signal using short lift waves (as shown in Figure 4.17). Each wavelet is characterized by the *compact support* which is the total wavelet wavelength. It represents the ephemerality of the signal (the signal is not finite), and there are different wavelengths, applied at

different frequencies (as will be explained later). Another characteristic of the wavelets is that the area underneath the curve must be zero so that the energy of the wave is equally distributed by the positive and negative component of the wave. This is to control the values of the wavelet result, helping a better understanding without a positive or negative biased value.

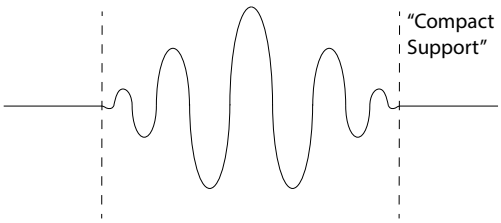

Figure 4.17: An example of a short lift wave used in Wavelet Transform - wavelet, with compact support.

In the Wavelet Transform, there is a convolution between the signal and a wavelet analysis function (Equation 4.11).

$$x(a,b) = \int_{-\infty}^{\infty} x(t)\Psi^*_{a,b}(t)dt \tag{4.11}$$

Where $\Psi^*_{a,b}(t)$ is the wavelet analyzing function. Wavelet Transform results in a two-by-two matrix of coefficients that are identified by their scale and translation.

Translation is about moving the wavelet forward in time while analyzing the entire signal (Figure 4.18a). The scale has an idea close to the scales principles in music, the higher is the pitch of the note, the higher is its frequency and the smaller is its wavelength. The opposite happens with a lower pitch of the notes, the lower the frequency, and the longer the wavelength. For waves with higher frequency, the wavelength is lower, creating a higher resolution in time, because the waves are smaller leading to a better location in time.

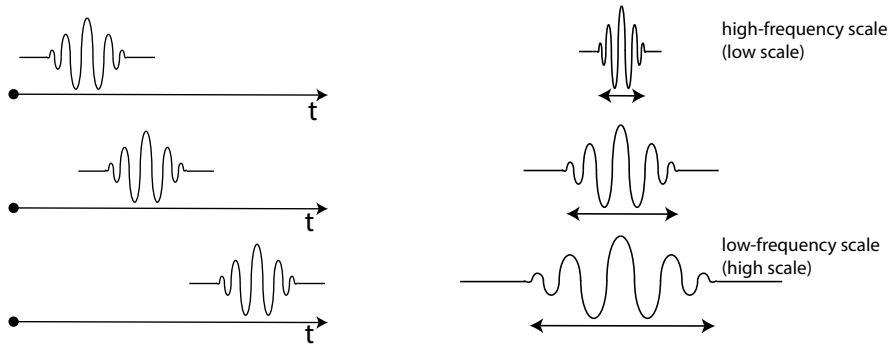

(a) Translation (b) Scale

Figure 4.18: Translation and Scale in Wavelet Transform.

Having a random signal, in time, it takes up the wavelet analyzing the function and multiplies itself by each point in the region of the signal where the translation occurs. After that, the wavelet

analyzing function is scaled and the multiplication process is repeated with this new wavelet by each point of the signal.

Discrete Wavelet Transform (DWT)

The big difference lies in the discretization of the input signal. In this way, high and low pass filters are applied sequentially to the signal and form a filter bank, as shown in Figure 4.19.

The signal is first filtered with a high pass filter and then low pass filtered, obtaining two signals: D1 and A1, respectively.

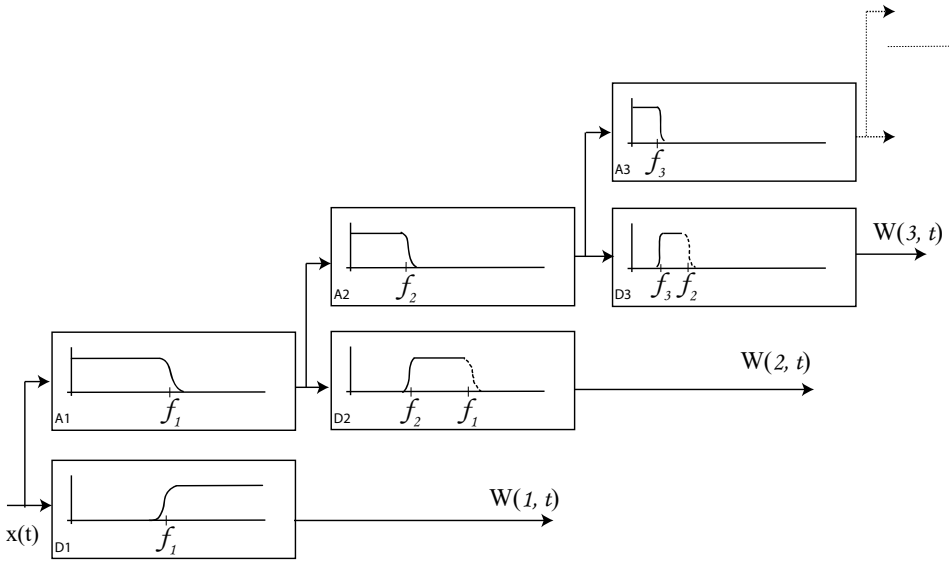

Figure 4.19: Wavelet filter bank [Devasahayam, 2012]

.

These filters have the ability to rebuild the sub-bands as they cancel any aliasing that occurs due to down-sampling. For each new level of decomposition, the low-pass result is down-sampled and this is again applied high and low pass filters, and so on. The number of coefficients in each new level is half the number of coefficients of the previous level, as a result of the dawn sampling. In this way, it is possible to analyze in a more detailed way the signal, particularly the frequency component of the signal at different resolutions, also allowing the signal denoising and signal compression. After this process, Wavelet Transform (translation and multiplication) occurs as mentioned in the previous subsection.

Wavelets Types

Another aspect to take into account regarding the application of Wavelet Transform is the choice of wavelet type. As already mentioned, the wavelet is a wave of short duration that is convoluted with the signal. There are several types and families of wavelets, including those shown in Figure 4.20. The importance of the wavelet format is focused on the correlation with the signal, in order to find the best matching point.

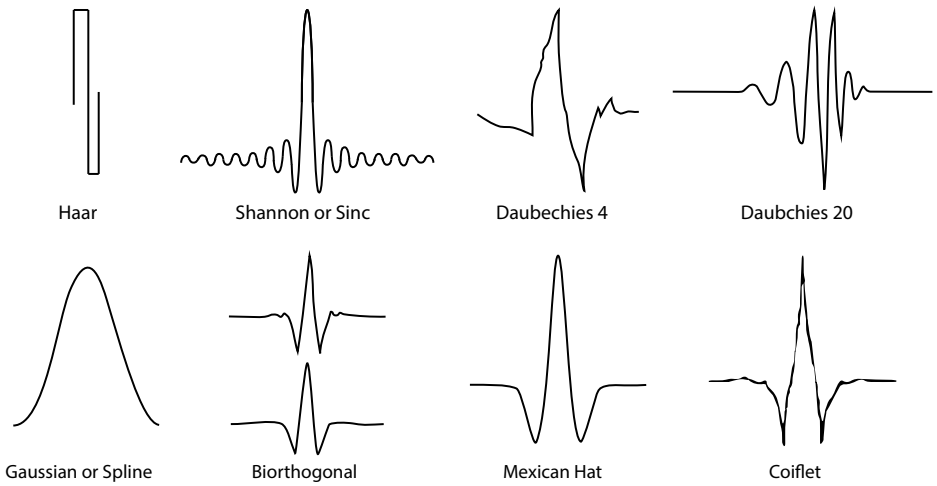

Figure 4.20: Different wavelet types [Al-geelani et al., 2015].

Comparing the different wavelets it is possible to verify that the *Haar* wavelet is very different from the others and there is a wide variety of formats between wavelets (Figure 4.20). In Figure 4.20, not all types of wavelets are represented, it is only used to show the variety of wavelets. Due to the large variety of wavelet families, it is necessary to carry out a study on which is best applied to the gait signals. In this sense, it is necessary to find out the best wavelet to apply to solve the problem.

Concluding this subsection, the choice of the use of the Wavelet Transform applies only to find the contact location of the foot with the ground. This event is related to shock absorption and leads to a higher frequency region in the signal, as shown in Figure 4.9.

4.4.5 Cross-correlation

Throughout the development of the project, many positive and negative peaks that clearly corresponded to noise were detected as IC and PS events by the previously mentioned methods. There is also a need to detect gait, to know at what moments the person was walking. This has a crucial function, for example, to determine when the person stoped walking.

As shown in the figures of the gait signal already displayed in this document (for example Figure 4.16), the gait has a characteristic pattern, which is repeated with each new gait cycle. According to data collected from all individuals, this pattern appears to be fairly similar for all individuals, but the patterns are not exactly the same. This is important for defining gait regions, the time intervals in which the person was walking. Thus, it was decided to define regions where the person was walking with the goal to remove the wrong detection of IC and PS events outside the gait patterns and to detect when the person started and stopped walking.

The first approach implemented was to perform cross-correlation with a model that corresponded to a complete gait cycle, starting with the beginning of the stance and ending at the end

of the stance, as shown in Figure 4.21a. In a second approach, an implementation of two cross-correlations was adopted, in which they differed in the cross-correlation model. The first model corresponds to the start of the gait with the stance (Figure 4.21b) and the second model consisted of starting the swing (Figure 4.21c). But before proceeding with the details of the implementation of cross-correlation, a brief introduction to the theoretical concept follows.

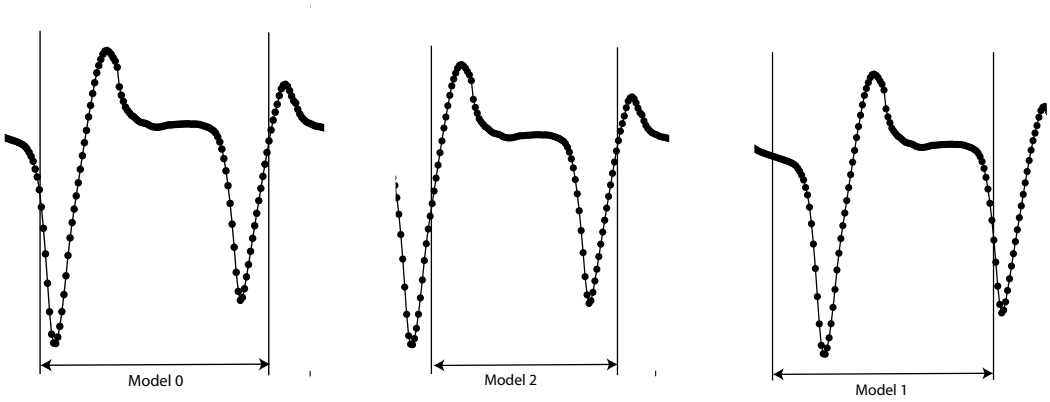

(a) Model Stance Swing (b) Model begin with Stance (c) Model begin with Swing

Figure 4.21: Cross-correlation Models. The model (a) is used in a cross-correlation alone, it includes a large model with stance and swing events. The model (b) is used in cross-correlation parallel with the cross-correlation performed with the model (c).

Cross-correlation Basics

Cross-correlation, in general, allows finding patterns in a 1D signal, which are similar to the chosen model. The model is a segment of a signal that contains a sequence or pattern that it is intended to find. In this way, it is a method that allows finding similarities between the signal and the model, regardless of the location of the pattern in the signal (in the x axis). The mathematical equation that represents the cross-correlation is presented in Equation 4.12.

$$(f * g)[n] \stackrel{\text{def}}{=} \sum_{m=-\infty}^{\infty} f^*[m]g[m+n] \tag{4.12}$$

Where the f is the signal and g is the model with the pattern.

In visual terms, the cross-correlation can be understood as exemplified in Figure 4.22. In the case of the two different signals, a higher value is observed when there is some similarity in the two signs f and g.

As already mentioned, the idea behind cross-correlation, applied in this project, was the detection of patterns related to walking. In this way, with a model with a gait cycle pattern, it was intended to find the moments in which the person was walking. Hypothetically, if the gait signal is the signal presented by the two signals exemplified at the top of Figure 4.23, and considering

[6]Adapted from: Cross-correlation. `https://commons.wikimedia.org/wiki/File:Comparison_convolution_correlation.svg` (19/05/2017)

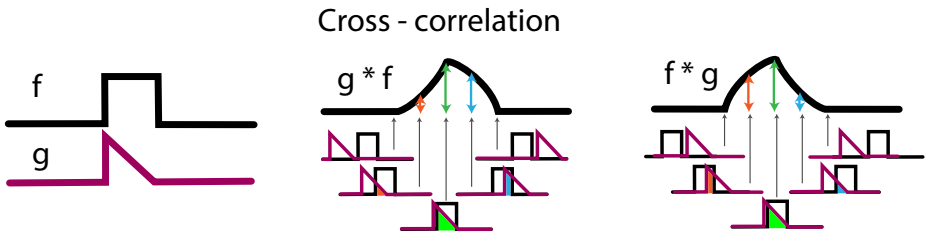

Figure 4.22: Cross-correlation visual application [6].

that each person has a relatively different gait pattern (in this case triangular and quadrangular), the signal obtained after cross-correlation presents peaks in the zones of higher similarity between the signals and is constant and near the null value in areas where there is no similarity. In this case, it is intended to detect moments of gait, ignoring moments in which there is noise (noise with different a pattern than gait), this method seems to have the necessary criteria to segment the region in the time in which the person is walking.

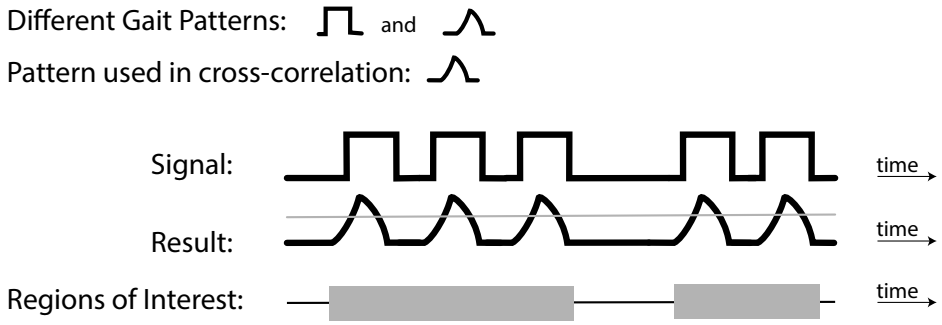

Figure 4.23: Cross-correlation visual application and hypothetical example to gait signal.

At the end of the application of the cross-correlation, it was performed an identification of the places where there was higher correlation, that corresponds to the peaks of the obtained result. To find the most similar points, after finding the local maxima and minima, an adaptive threshold was performed to select the maxima and minima that correspond to the higher correlation between the gait pattern and the signal acquired. The peaks resulting of the adaptive threshold are collected and, at the instant of time to which they belong, is added and subtracted half the value of the gait pattern used as a model in the cross-correlation. The reason is the peak will only occur when the similarity between the model and the signal is reached. Considering a model of gait starting in the stance and ending in the swing, the peak occurs at the end of the stance (in the middle of a gait cycle). At this point, the person already performed the initial contact. If it is not considered the instants previously to the higher similarity, the initial IC is lost.

As it is not intended to lose information, at the moment the maximum similarity occurs, half the duration of the model is subtracted do the point, in order to find what started the cycle. During this process, it is also important to find sequential walking patterns, which correspond when the person is taking several steps in a row. In this sense, it is important to group them by zones of gait,

as can be observed in Figure 4.23 in the bottom of the image, and not gait (region without the gray rectangle).

Cross-correlation With One Model

Two cross-correlation approaches were applied: first consisting of only one gait cycle model (with a full swing and stance phases (Figure 4.21a)) and a second one consisting of the application of two cross-correlations with two different models (one to start with the stance phase and another with the swing phase).

However, there was a disadvantage in applying a fixed model to a variable gait. This is because, when start walking with the right foot, it goes into stance, and the left foot starts to swing. This causes the signals of the two feet to begin at different times of the gait cycle.

When determining the weights of the adaptive threshold, if its value is low, it is possible to detect the start values of a foot that begins with the final phase of the cross-correlation model. However, it is more conducive to recognizing noise as a walking pattern, such as just tilting the foot towards the ground. In the case of increase the threshold weights values, the first event of the foot that begins in the final phase of the model is considered as out of the gait pattern, causing loss of information.

In this sense, it was necessary to find a new strategy that would allow to recover information for beginnings and ends of gait in different phases: beginning in the stance and ending in swing (majority of the right foot of right-handed people) and beginning in swing and ending in the stance (majority for left foot of right-handed people). This strategy would also have to have high noise rejection.

Cross-correlation With Two Models

In order to increase sensitivity for stance gait and swing start, a new cross-correlation approach was implemented. This involved the application of two cross-correlations, with two different gait patterns: one starting in the stance and ending in swing and another beginning in swing and ending in the stance (Figure 4.24).

The result after the application of the cross-correlation with the two models, in separated ways, is presented in Figure 4.25.

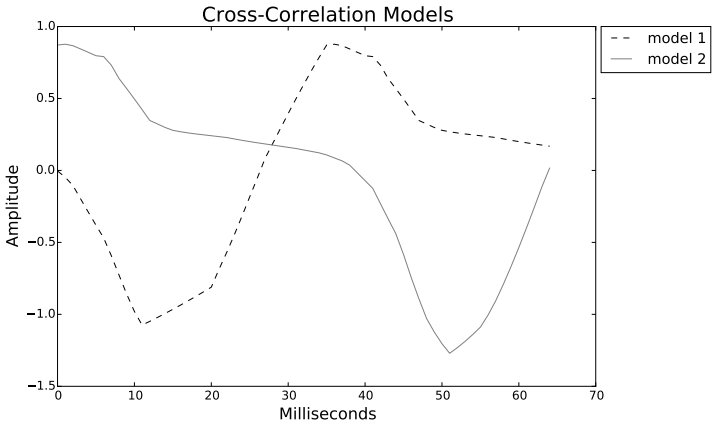

Figure 4.24: Models applied in cross-correlation.

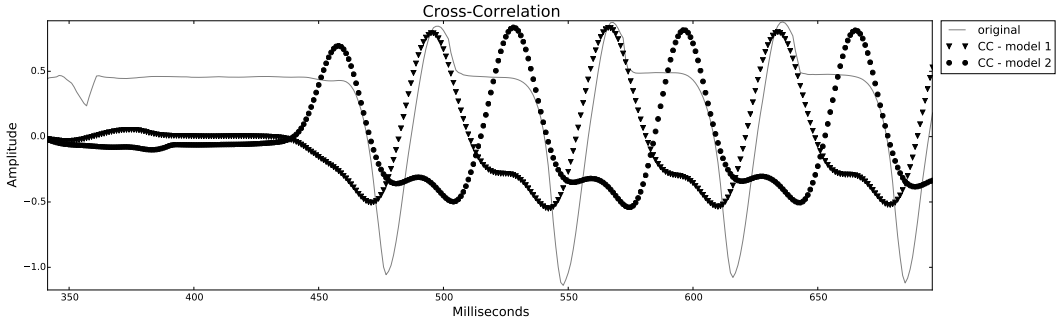

Figure 4.25: Result of the two cross-correlations, with the two models presented in Figure 4.24. The result with model 1 (triangles), that begins with the swing, it was verified that the maximum of the cross-correlation occurred when the cycle was after the beginning of the swing (about a third of the duration of the gait cycle). The result with the model 2 (circles), that starts with stance, had a maximum at the beginning of the march, in which the person had the foot on the ground and started into swing. This allows to find walking instants for when the foot starts on both stance and swing. The label *original* refers to the sum of the resulting Z components of the multiplication of the signal with the X and Z fixed frame: $X_Z + Z_z$.

After locating the gait regions for these two cross-correlations, the peaks and valleys were found for the two lines of processing and were merged. Thus, the relationship between noise and incomplete gait cycles (different from the model for approach one that was verified for coss-correlation with one model), is higher, This enable the separability of regions of the walk, starting with swing or stance, without loss of information.

In conclusion, it is possible to segment the time intervals in which the person walks through cross-correlation, reducing the detection of positive and negative peaks that correspond to noise (outside the moments in which the person is walking).

4.4.6 Project Structure

Combining all the algorithms described above, the project structure can be found in Figure 4.26. This implementation was in static form, which means that it had information of the whole process, and it did not take into consideration the real-time signal acquisition and processing.

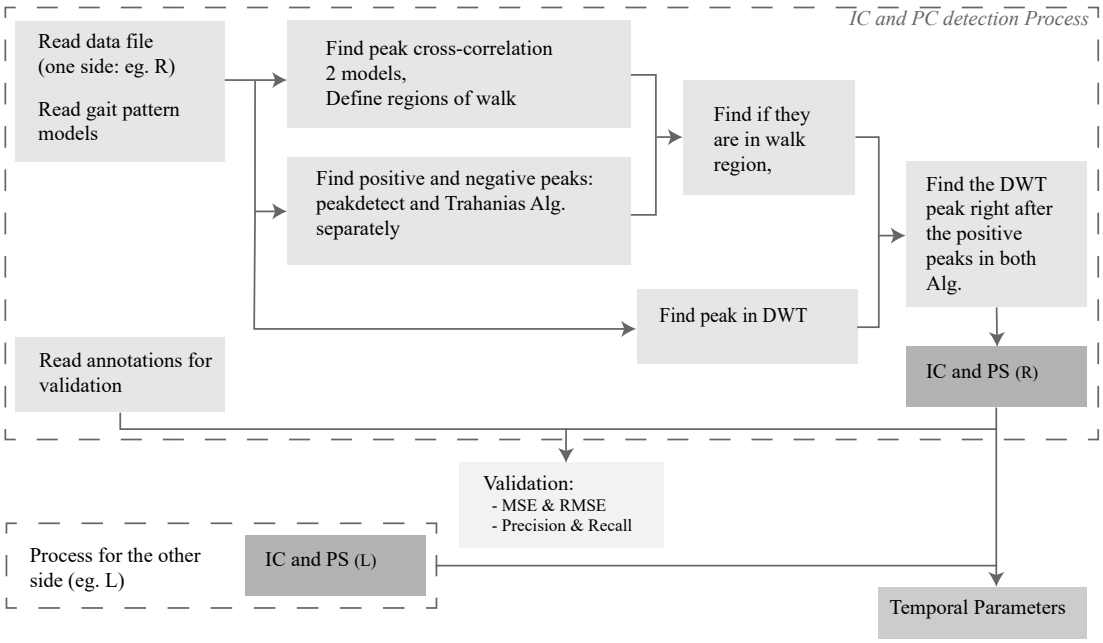

Figure 4.26: Overview of the applied algorithm, related to one side. As an example, supposing that the work-flow presented is related to left side, it is necessary to process, with the same steps, for the right side, in order to have all the information for the temporal parameters calculation. This work-flow is not considering the real-time implementation.

The process started by reading the recorded data file, acquired while a subject walked. The data was manipulated in order to obtain the components X_Z and Z_Z as explained in Subsection 4.3. Then, two gait models were read to be used in cross-correlation step, as indicated in Subsection 4.4.5, and were processed in the same way as the gait signal (sum of component X_Z and Z_Z). The cross-correlation, with the two models, was applied to the gait signal, and the time intervals in which the subject walked were defined, named as gait regions. Peaks and valleys of the gait signal were detected by two separated algorithms, the peakdetect and the Trahanias algorithm. Only the peaks that were within the gait region were taken into account for the next stages of the process, the remaining peaks were discarded as noise. At this stage, the PS events were determined, since they correspond to the negative peaks (for the two algorithms separately). The time instants where there was a higher frequency peak of the signal was determined from the wavelet analysis. The instant (of the high frequenct peak) in the signal that was immediately after the positive peaks determined by peak detection algorithms, was classified as shock absorption. At this point, IC events were determined.

With information on the IC and PS events, the temporal parameters described in Chapter 6 can be implemented. After the events were detected, the validation was performed, which will be described in the following section.

4.5 Validation

The validation of the detection of IC and PS events was performed with three types of annotations: by video (mentioned in Subsection 4.2.1), by manual annotation and by the gold standard annotations (Qualisys[7] system in combination with force platforms).

For each annotation type two validations steps were performed. The first was the error in seconds of the IC and PS event detection (Figure 4.27a). The second was the detection of the event itself on the considered region of interest (Figure 4.27b).

To consider the time error between the annotations and the detection, the Mean Squared Error (MSE) was applied. In this error, only the points (in the notes and the detected ones) that were at a distance smaller than the size of a running cycle were considered, as shown in Figure 4.27a. All the others were compared with the precision and recall metrics, not counting for validation error in seconds. This means, only True Positive (TP) events were used in the MSE calculation. To found events that the algorithm was unable to detect and the ones erroneously considered as of interest, the Precision and Recall metrics were applied, which will be explained below.

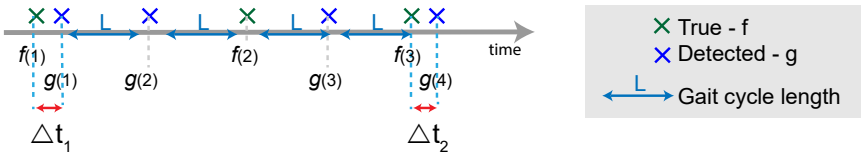

(a) Validation considering the time of each sample of the annotation and the detection through the algorithm.

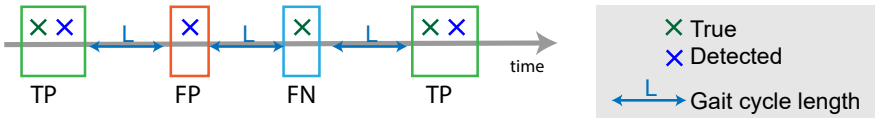

(b) Validation considering each sample of the annotation and the detection through the algorithm.

Figure 4.27: Two algorithm validation approach, considering the error in time (a) and considering the detection or failure of events (b).

[7]Qualisys system: `http://www.qualisys.com/` (20/05/2017)

MSE: It measures the mean square of the deviations or errors between the estimator and what is truly estimated (Equation 4.13).

$$MSE = \frac{1}{n}\sum_{i=1}^{n}(\hat{Y}_i - Y_i)^2 \tag{4.13}$$

Where $\hat{Y}_i$ is the labeled value (annotations) and the Y_i is the predicted value (by the algorithm).

On the other hand, it had to be verified if the algorithm was finding all the events of interest and if noise was being detected as events of interest. In this way, the Precision and Recall metrics were applied.

Precision: It verifies if all the events detected are relevant (or true) (Equantion 4.14).

$$Precision = \frac{TP}{TP+FP} \tag{4.14}$$

Recall: It verifies if all the relevant (or true) events are detected (Equation 4.15)

$$Recall = \frac{TP}{TP+FN} \tag{4.15}$$

TP are events correctly identified by the algorithm as events of interest (that are present in the annotations). False Positives (FP) are events, detected by the algorithm, that are not in the annotations. False Negatives (FN) are events in the annotations that were not detected by the algorithm. It is important to note that the precision value indicates whether all IC and PS events detected by the algorithm are relevant, i.e. if the precision value decreases, the algorithm is detecting noise as events. On the other hand, the recall indicates whether all actual IC and PS events are detected, i.e. if the recall value decreses, it means that the algorithm fails to detect all (true) events annotated.

4.5.1 Validation With Video Annotations and Manual Annotations

The video annotations have already been explained in Subsection 4.2.1. Two problems emerged in the video annotation process: occlusions due to the overlap of the feet in the line of vision of the camera and temporal errors between 20 and 40 milliseconds, even with a video sampling frequency at 100Hz. For this reason, annotations were performed using visual inspection. This annotation, which will be called *manual annotation*, aims to understand the influence of video annotation problems: occlusions and the error of 20 to 40 milliseconds. And try to find the time instants where the occlusions occurred.

Manual annotations were made on the quaternion signal by visually identifying for IC and PS events following the interpretation described in Section 4.2.1. In this way, manual annotations were made on all signals. All negative peaks were marked as PS events, and, to the disturbance detected immediately after the positive peaks was marked as IC events (shock absorption). An example of IC manual annotation event is presented in Figure 4.28, for the remaining events, the process was the same. The points were exactly searched with a cursor that allowed to see the value

of the point sampled by the trackers. However, this annotation may be biased, as it is done directly in the signal manually and visually.

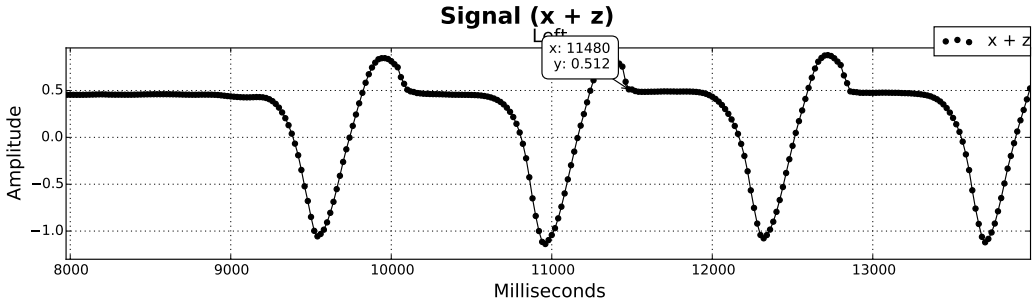

Figure 4.28: Manual annotations process. The label $X+Y$ refers to the sum of the resulting Z components of the multiplication of the signal with the X and Z fixed frame: $X_Z + Z_z$. On the example, the cursor is placed above an IC event.

Validation Process

In order to validate the results of the algorithm with either manual annotations and video annotations, it was necessary consider the following details: when determining the MSE metric, and second when determining the precision and recall. They are described below.

Firstly, it was necessary to consider the points detected as IC and PS that are within a near limit of one walking cycle, as shown in Figure 4.27a by the letter L in that figure. Considering that there was an IC event detected with a time difference margin with less than a gait cycle duration (L) from a IC annotation, the MSE error between these two points was calculated. This allowed a lower biased comparison because it was compared with peaks of IC (and PS) that were with maximum distance of a walking cycle (L). In this way, for each new point detected by each algorithm, it was checked if there was some point in the annotations that was within a limit close to the length of one gait cycle. This is, if there was a point in the annotations within the lower limit (detected point minus half the duration of a gait cycle), and within the upper limit (detected point plus half the duration of a gait cycle). If there was no annotated value corresponding to the detected, it was considered as a FP. So, what happened was, if the error was equal to or higher than the duration of a gait cycle, there was no longer an error and it becomes an FP (considered for the precision and recall metrics). If the there was an annotation for the detected value with a time margin less than half and more than half of a gait cycle time duration, in relation to the instant of the detected point, is a TP. It should be noted that the upper limit value of the MSE will be the time interval corresponding to the duration of a half gait cycle.

Secondly, the detection of FP and FN was done in a similar way, as can be seen in Figure 4.27b. On one hand, to every detected point was verified if there was a point in the notes that have not be considered until that point and was within a margin of less than half the duration of a gait cycle and more than half the duration of a gait cycle. On the other hand, it was verified whether all points of the annotations were used, i.e. check if there was a detection pair for all points scored.

In this way, the first result allows to discover the TP and the FPs and the second result allows not only to validate the TPs but also to discover the FNs. In this way, it was possible to determine Precision and Recall.

4.5.2 Validation With Gold Standard System

The use of this system was aimed at more precise validation and eliminate the problems founded in the validation with video and manual annotations. The systems used to acquire this range of signals were a Qualisys[7] system and a ground forces platforms system (Bertec, USA). The Qualisys system (Qualisys AB, Sweden) composed by twelve retroreflective infrared chambers distributed along the upper perimeter of the laboratory and operates at a sampling frequency of 200 Hz. In Figure 4.29 is presented the LaBioMEP's Qualysis System.

(a) LaBioMEP's room.

(b) LaBioMEP's room, entrance.

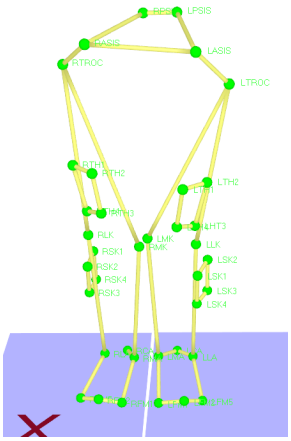

(c) Location of the markers in the lower limbs in Qualisys System signal acquisition.

(d) Markers placed at the lower limb. View from the anterior part. Without the femur and tibia markers. With SWORD Health's sensors system.

Figure 4.29: LABIOMEP camera system Qualysis. It was composed with twelve retroreflective infrared chambers. In (c) the description of the placement of the sensors is presented.

The system was used to track the displacement of maker placed over the joints of the lower limbs according to the Figure 4.29c, in proximal anatomical locations of the segments required for

analysis in their own software. The placement of the SWORD Health's sensors system with the markers of the Qualysis system is shown in Figure 4.29d.

The force platform had five extensiometric platforms (Bertec, USA) and one piezoelectric platform (Kistler, USA), operating at a sampling frequency of 2000 Hz. The platforms setup is presented in Figure 4.30a.

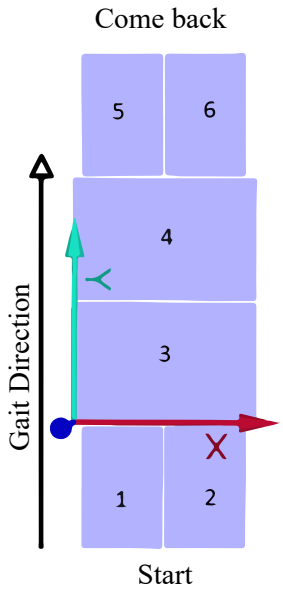

(a) Identification of the five platforms in the force platform system.

(b) LaBioMEP's room, with the force platform system.

Figure 4.30: Force platform system.

The force platform system was in the center of the room where the accuracy of the Qualisys system was higher. This is because in the center there is higher visibility of all the chambers and it is where the calibration of the system is carried out. These two systems were used simultaneously and in synchrony to improve the accuracy of the instants detection of the IC and PS events. As there were no ambiguities in the acquisition of the events instants with the platforms, the data acquired by Qualisys was not necessary for validation.

In the following subsubsection, the data acquisition protocol with this system is presented.

Acquisition protocol

Firstly, it was necessary to synchronize the platform system and Qualisys together with the system under study. This synchronization was done in a very similar way to the one made with the video (Subsection 4.2.1), in which the right tracker was hit with a Qualisys system marker. Thus, the point at which the marker goes back in the trajectory was synchronized with the time when there was a high-frequency movement in the sensor (similar to that shown in Figure 4.3b in Subsection 4.2.1).

The acquired sequence of movements is represented in Figure 4.31.

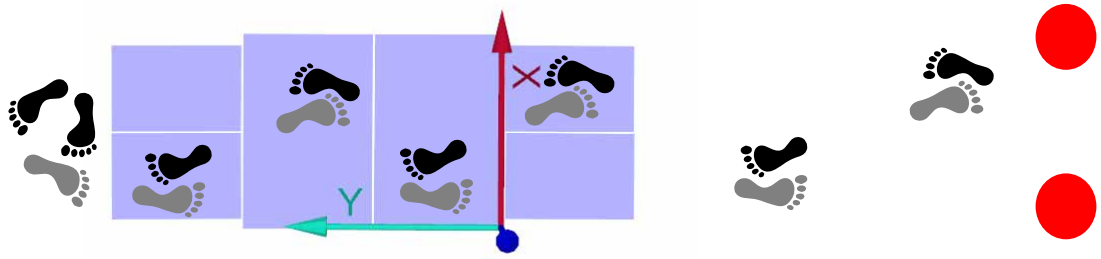

Figure 4.31: Gait trajectory performed in the LaBioMep, in relation to the force platforms and the pins (red cicle) presented in Figure 4.30b.

Ten acquisitions of signals were made, and all of them consisted of the following sequence:

1. Move forward, starting between the red pins,
2. On the force platform, place the feet precisely as indicated in Figure 4.31 in the platforms (black footprints),
3. Rotate at the end of the platform, without stopping,
4. Back, placing the feet on the same platforms as before, according to Figure 4.31 (gray footprints),
5. Stop next to the red pins.

The data acquired was only from one person, who is person no.1 described in Table 4.1, in the beginning of this section.

The annotations were obtained in instants where the pressure stopped being zero to positive, indicating the presence of pressure, in the platforms of force. Since they have a sampling frequency of 2000Hz, the error associated with this measurement is 0.5 ms. In addition, the processing was not very extensive and, from the information provided by LaBioMEP, there is no article associated with the software that processed this data.

Validation Process

The validation with these data was similar to the validation that was made with the annotations of the videos (Subsection 4.5.1). Calculation of the MSE between all the TPs and their respective annotations, and calculation of precision and recall with the remaining points, as well as the detected points that were not true (FP) and the undetected points that were true (FN).

The region of higher precision for the Qualysis system was in the center of the laboratory, where the force platforms are located. In this way, the data annotated was from only these locations - on top of the force platforms.

It was necessary to clean the signal, that is, to remove information of gait in the sensors signal that had no notes, as the case of the trajectory from pins to the platforms, the rotation in the back

return, and from the platform to the pins. After the synchronization, the signal was cleaned as described above, so as to obtain only data related to the time the feet were on the force platforms.

4.6 Summary

Initially, data from five people was acquired in which the signal obtained by the sensors was synchronized and compared with video obtained by a camera. After the interpretation of the signal, it was concluded that the signal negative peaks correspond to the PS events and the disturbance soon after the positive peak corresponds to the events of IC. Between an IC and PS events is the stance phase and between a PS and IC events is the swing phase.

Detection of these two events involves the detection of signal negative peaks and disturbances after the positive peak. Thus, two methods of peak detection (peakdetect and Trahanias algorithm) were implemented, and the Discrete Wavelet Transform was applied to locate the moments of shock absorption (disturbance soon after the positive peak). In relation to these methods, it is still necessary to study some parameters, such as the structuring element of the Trahanias algorithm and the wavelet type in the DWT. To detect gait moments, cross-correlation was also implemented with a gait pattern model, which gives information on whether or not the person is walking.

The validation of the detection of the events IC and PS was made in relation to the error in *ms* in the detection of the peaks and in relation to the hit or failure detection of the peak and valley. The validation was done with annotations obtained by videos, by manual annotations and by a system combined by Qualisys system and LaBioMEP Forces Platforms.

Chapter 5

Temporal Events Results

In this chapter, the results for the detection of IC and PS events are discussed. It was implemented and used two detection algorithms: peakdetect and Trahanias, it was also used three types of annotations based on video, manual and gold standard. In the case of video annotations, a small study was done on the influence of occlusions on the results.

Within these topics (manual, video and gold standard) the following studies were done, among them: study on the best wavelet type to be applied to the acquired data set and the structuring element of the Trahanias algorithm.

5.1 Event Detection With Video and Manual Annotations

As mentioned in Subsection 4.3.1, at the same time the first database was collected a video was recorded for each acquisition to obtain notes on the instants in which the gait IC and PS events occurred. In these videos, occlusions were observed (as mentioned in Subsection 4.3.1), and the notes did not contain information about the location of the occlusions.

After understanding the signal, a manual annotation was also made on it, where the instants relative to each event were recorded directly in the signal, according to Subsection 4.5.1. In this way, a manual analysis was performed, in order to compare the results of the videos and the results of the manual annotations: the number of steps and, in the signals, the number of events found. Thus, in this first validation phase, the influence that occlusions brought to the results is presented.

5.1.1 With and Without Video Occlusions

This study aimed to understand the influence that the occlusions presented in the video annotations brought to the results when comparing the algorithm results with this annotations. Thus, it was a manual comparison between the video and its notes and also the results obtained by the program. It was performed in two of the five signals of the first data set. Since all subjects did a similar gait trajectory in the same place, under similar conditions, this study was not performed for any further signals.

The occlusions, in this study, were obtained from the visualization of the video along with the annotations previously made, in order to verify how many occlusions there were and in which time intervals they occurred. After this verification, all new TP, FP, and FS were selected, taking into account that the occlusions are inserted with the label IC or PS event in a time location closer to the occlusion in the video. The comparison of the precision and recall between both results (with and without occlusions) is shown in Figure 5.1.

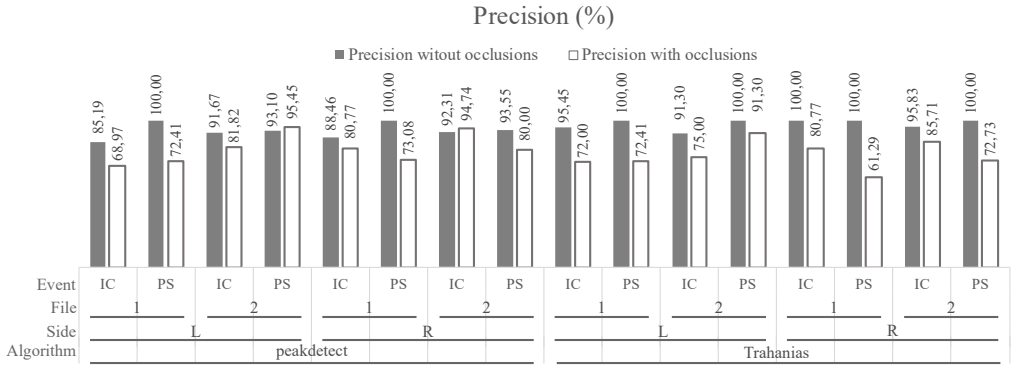

(a) Precision comparison between results obtained with annotations that included notes about the occlusions and notes without occlusions.

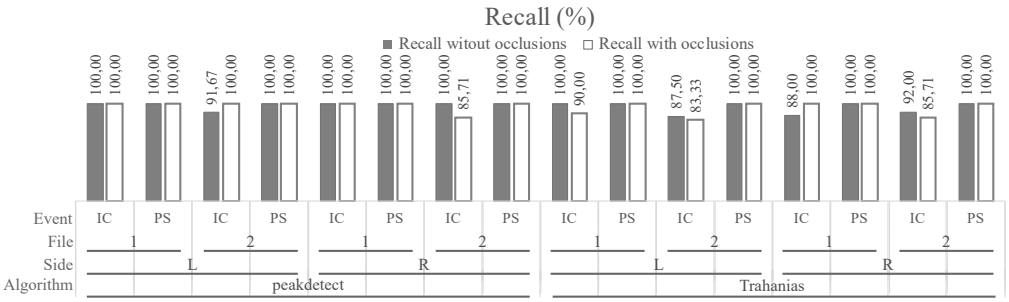

(b) Recall comparison between results obtained with annotations that included notes about the occlusions and notes without occlusions.

Figure 5.1: Precision and recall comparison between results obtained with annotations with notes about occlusions and notes without occlusions. The events are the IC and PS, for both sides (L and R). The algorithms considered in two different branches are the peakdetect and Trahanias algorithm.

The parameters were empirically chosen for both algorithms acording to visually inspection during the execution of the project. However, a more in-depth study of these parameters will be presented later.

According to Figure 5.1a, it can be observed that precision increased when it took into account notes with occlusions. That is, they indicate which locations where there were events that were not noted due to video occlusions, but which occurred. Thus, it means that the FP component of precision decreased when some occlusions were revealed. In this sense, it can be said that the algorithm designed, either with peakdetect or with Trahanias algorithm, detected more true events

than those obtained after the validation with video annotations. This helps to ensure that there was no relationship between occlusions in the video and FP and NF in the algorithm results.

In Figure 5.1b, it is observed that the recall remained relatively constant between the analysis that took into account notes of occlusions and notes without occlusions. In this way, it was possible to perceive whether or not the algorithm failed to detect the events that were hidden. The FN component of the recall remained almost unchanged. This means that whenever the location of an occlusion was revealed, the algorithm was able to detect this occlusion.

In summary, by the increasing precision and recall when the occlusion location were discovered and taken into account, the algorithm (in this case both Trahanias and peakdetect) detected events correctly. In this way, when comparing the results with video annotations, the occlusions should be taken into account. If they did not exist, the results would be better for the precision.

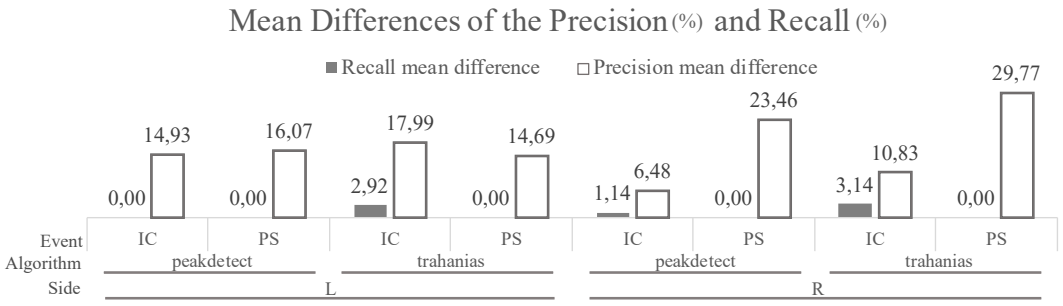

Figure 5.2: Mean difference of the precision and recall obtained by the analysis of two data files. It is divided by events (IC and PC), sides (L and R), and algorithms used (Trahanias and peakdetect). This bar chart is related to the data presented in Figure 5.1.

In Figure 5.2 the mean difference of the precision and recall, presented in Figure 5.1, for both data files, is addressed. Considering the Figure 5.2 it can be observed that the prevalence of occlusions in IC and PS events, was similar for both events (IC and PS). This was also true for both sides, i.e. it did not occurred more on one side more than the other. This means that the occlusions were generally homogeneous for the IC and PS events and for the right and left feet, due to the trajectory made by the subjects. In the analysis of the results with videos, the occlusions should be taken into account, and they were, in general, equally distributed by all events described. It can be said that it was equally distributed because, given that only two data files were used, the observed difference for precision between both sides and between events, is reduced. It is also observed that the recall presents small difference values, as expected from the justification already presented together with Figure 5.1b.

Concluding this first study, considering situation *A* as annotations that took into account hidden events, and situation *B* as annotations that did not take into account the hidden events, in the situation *A* the precision increased and the recall remained substantially constant in relation to situation *B*. That is, in *A*, with more events, these were detected by the algorithm and, thus, the FP detected were less. It also means that in *B* there were events that were not considered, being detected by the algorithm, and then classified as FP, but which were not real negatives. On the other hand,

as the recall remained constant, it means that the algorithm continued to detect the occluded true events (case of situation *A*). Even with the revelation of more events, the algorithm was capable of detect these events. Hence, when the video annotations are used in validation, it must be taken into account that they are annotations with occlusions and, therefore, the precision values may be higher than those presented in the validation results in the following studies. However, even with the problems encountered with video annotations, these annotations were important for the validation of the temporal error of the TPs (in the MSE metric). In addition, they were annotations without any influence on the signals of the sensors, and were not biased.

5.1.2 Study of the Wavelet Type

As already explained in Section 4.4.4, the wavelets were applied in this project in order to find the moments in which the shock absorption occurs. The shock absorption was a high frequency component of the gait signal, already addressed. In this same section it was mentioned that, for the application of wavelets, it was necessary to apply a type or family of wavelets. Considering that there were several moments of foot placement in the ground, for this data set, it was chosen to investigate which type of wavelet gives the best results (for the presented data). In this way, DWT was applied with all wavelet families and the results were compared to both algorithms (peakdetect and Trahanias).

The protocol consisted in, for each type of wavelet, run the whole process (Figure 4.26), to compare the results obtained for events of IC and PS with different wavelets. The families of the wavelets used are all available in pywavelets[1] Given the role of the DWT in this project, a higher influence on the IC events was expected. This is because, as already explained, the DWT was implemented to locate in the gait signal the moments in which shock absorption occurred, which was during the IC event.

In the following paragraphs, an analysis of the results with different wavelets is carried out, taking into account validation of events detected (precision and recall) and validation in milliseconds (MSE).

It is necessary to perceive the behavior of the precision and recall according to the type of wavelet used. In this way, this study focused on the observation of the precision and recall of the detection of PS events for all types of wavelets. The ten best precision results with video annotations are shown in Figure 5.3. The remaining results can be found in the Appendix A with video and manual annotations. It should be noted that the maximum precision value was higher for the Trahanias algorithm than for the peakdetect algorithm, for approximately the same standard deviation. This means that the Trahanias algorithm was able to find less noise as IC events than peakdetect, reducing the FP component of precision. However, considering that this analysis was done with video annotations, it may have failed detection of occlusions that it should have actually detected. In order to verify this, the precision was also observed with manual annotations. The top ten results are shown in Figure 5.4.

[1] PyWavelet. `http://wavelets.pybytes.com/` (06/03/2017)

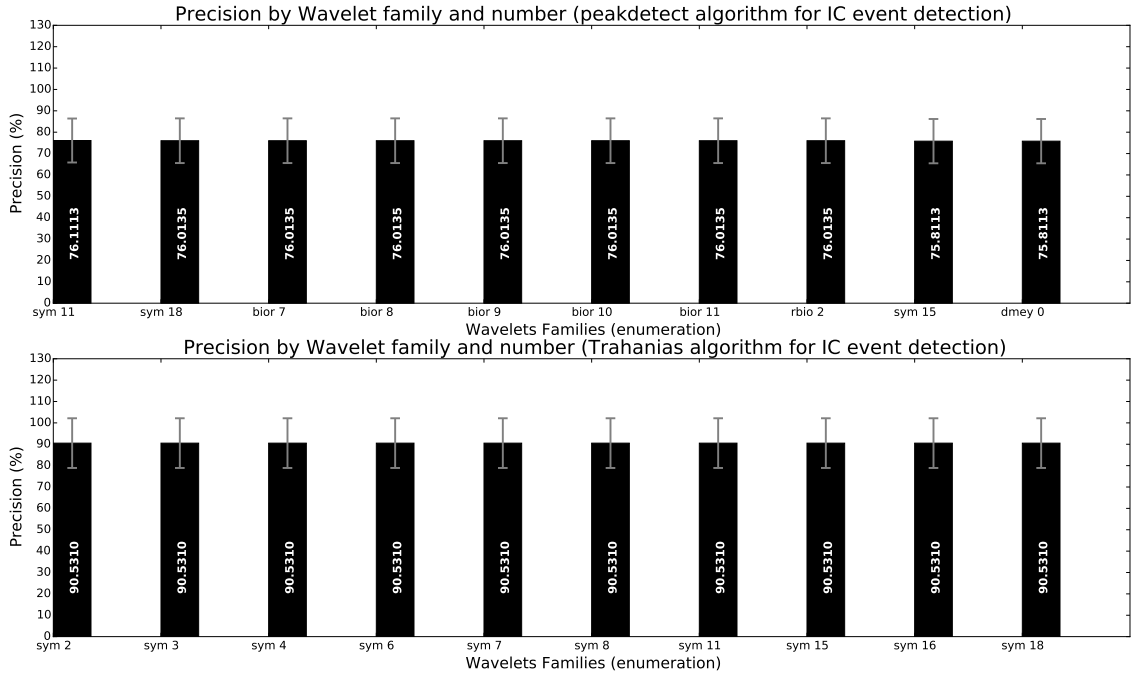

Figure 5.3: Ten best precision results of the application of DWT with different wavelets families on the detection of IC events by peakdetect and Trahanias algorithms, compared with video annotations. The gray bar represents the standard deviation.

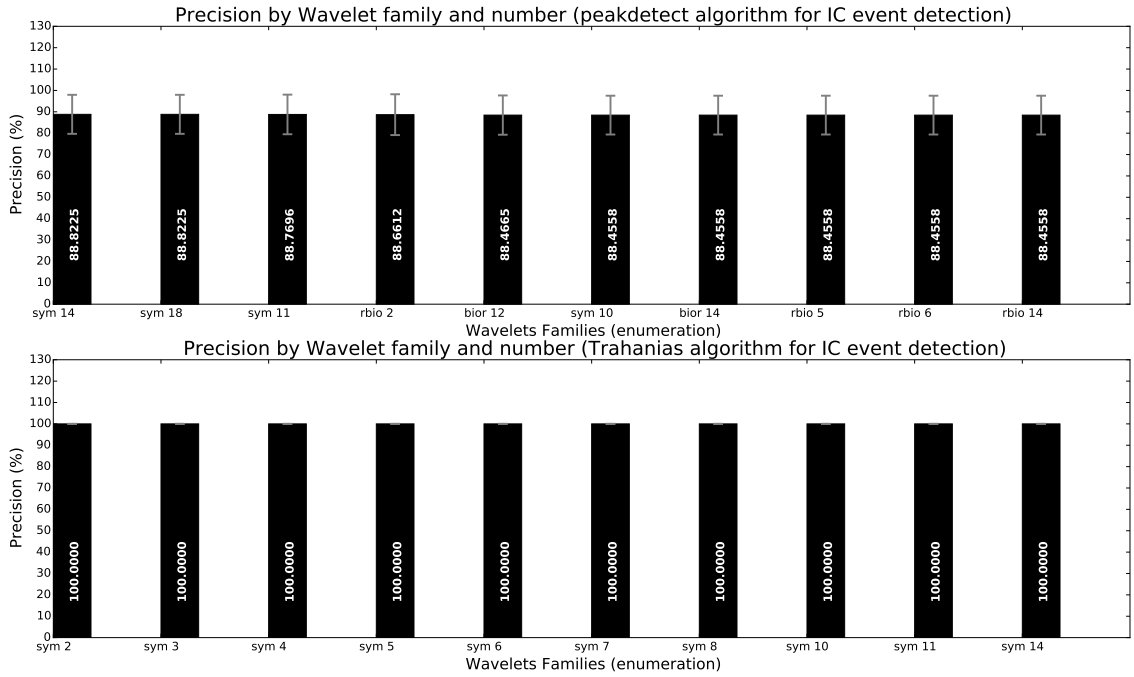

Figure 5.4: Ten best precision results of the application of DWT with different wavelets families on the detection of IC events by peakdetect and Trahanias algorithms, compared with manual annotations. The gray bar represents the standard deviation.

In Figure 5.4, which considered manual annotations for the validation, it is observed that the precision continued to be higher for the Trahanias algorithm. However, it can be verified that the precision continues to have very similar values throughout the different families of wavelets (see Apendix A). The standard deviation for the Trahanias algorithm was practically zero, which means that this precision occurred for all data used in this study.

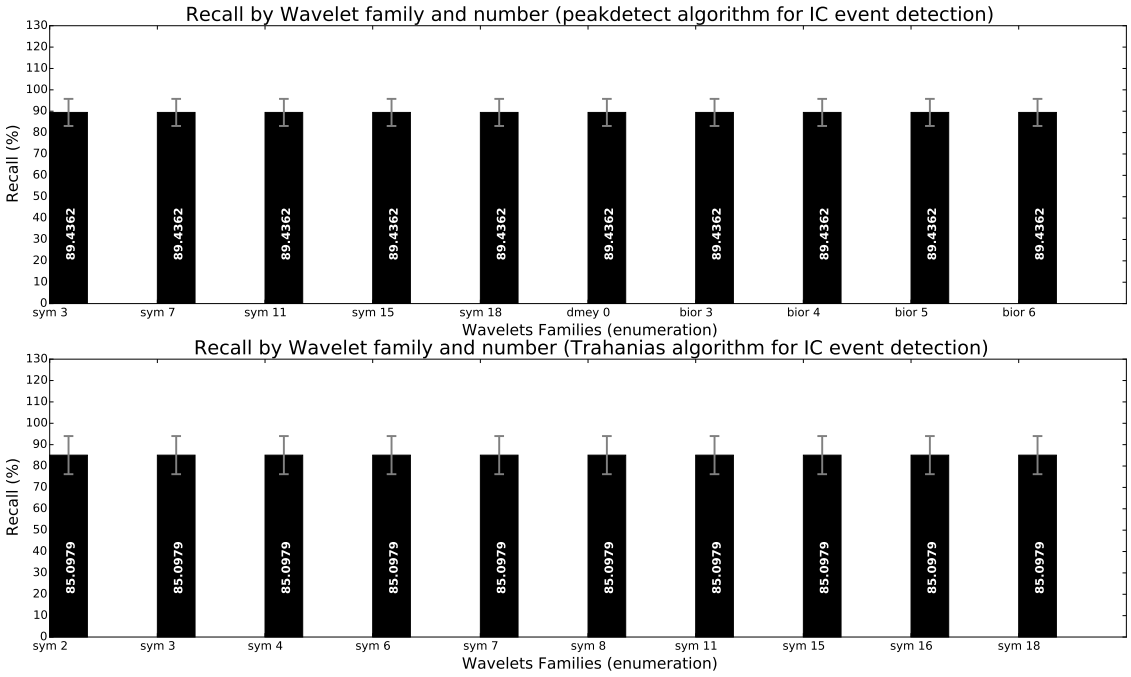

Figure 5.5: Ten best recall results of the application of DWT with different wavelets families on the detection of IC events by peakdetect and Trahanias algorithms, compared with video annotations. The gray bar represents the standard deviation.

In Figure 5.5 the recall results obtained with video annotations for the processes with algorithm Trahanias and peakdetect are shown. It can be observed that in the recall, the peakdetect algorithm behaved better than the Trahanias. This means that the peakdetect algorithm was more sensitive in detecting the positive points, reducing the FN in relation to the Trahanias.

Comparing with manual annotations (Figure 5.6), the recall values decreased by about 1% for the peakdetect algorithm, but for the Trahanias algorithm, it dropped by almost 6%. These values mean that the algorithm was detecting correctly the true events, but failing some of them, i.e. increasing the FN, especially those hidden by the annotations of the videos.

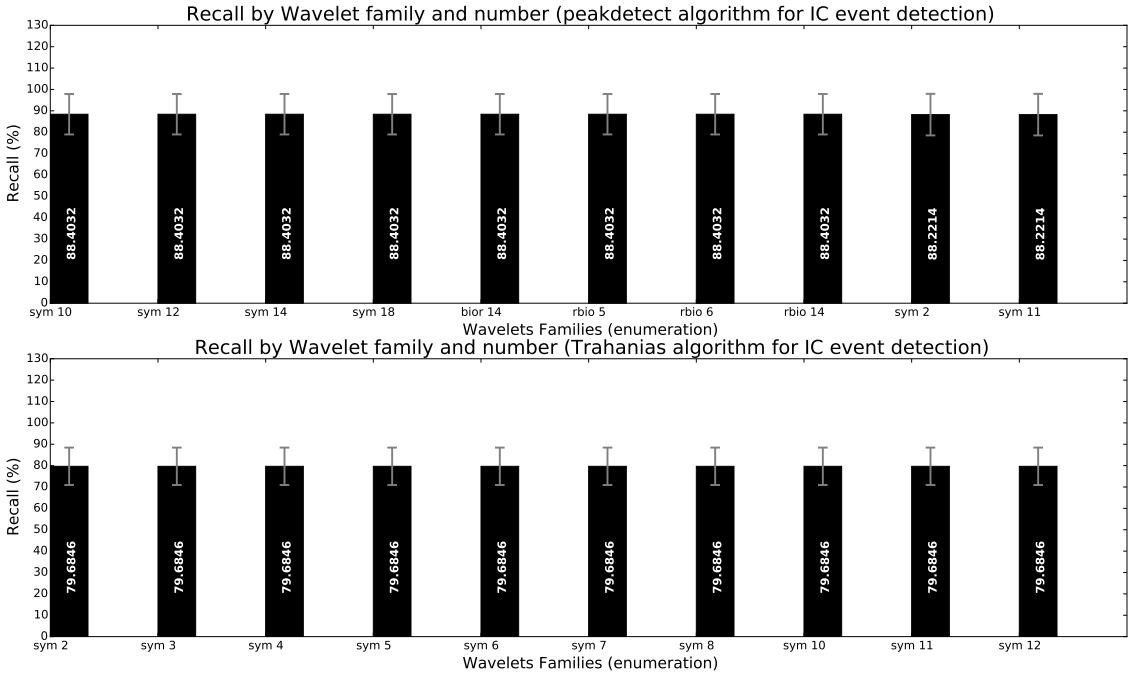

Figure 5.6: Ten best recall results of the application of DWT with different wavelets families on the detection of IC events by peakdetect and Trahanias algorithms, compared with manual annotations. The gray bar represents the standard deviation.

For peakdetect algorithm, the precision and recall were similar. However for the Trahanias algorithm, with manual annotations, the precision reached 100 % for a large set of wavelets types. That is, it detected only relevant (true) events, not detecting noise as events. However, it presented low recall values, about 20 % less than precision. With this, it can be concluded that the Trahanias algorithm was highly specific for event detection, but it was not able to detect all true events, falling some of them. One way improve this is to increase the number of true events detected by the algorithm. Maintaining precision in order to increase the recall. Additional data information can be found in Appendix A.

Then, for all TPs, the event detection error (in milliseconds) was discussed. The events obtained by the algorithm and the events annotated by the video visualization, acquired at the same time as the signals, are compared. In Figure 5.7a are the MSE results of the IC detection by the peakdetect algorithm for the different wavelet families.

It can be observed that the detection of the IC event was not the same for all wavelet types. For Daubechies (db) 10 (corresponds to $db11$ in the bar chart) reaches 138 ms (maximum value) and for Reverse biorthogonal (rbio) 3.1 (corresponds to $rbio7$ in the bar chart) was close to 11 ms (minimum value). The numbering of the wavelets in the graphs is in the order of these in each family and not by the name (and number) that identify them, in order to be simpler. Thus, when $db11$ appears it means that it is 12^{th} wavelet of the Daubechies family (the enumeration starts with number zero), which corresponds to *Doubechie 10*. The standard deviation was slightly the same for all families of approximately 20 to 30 ms.

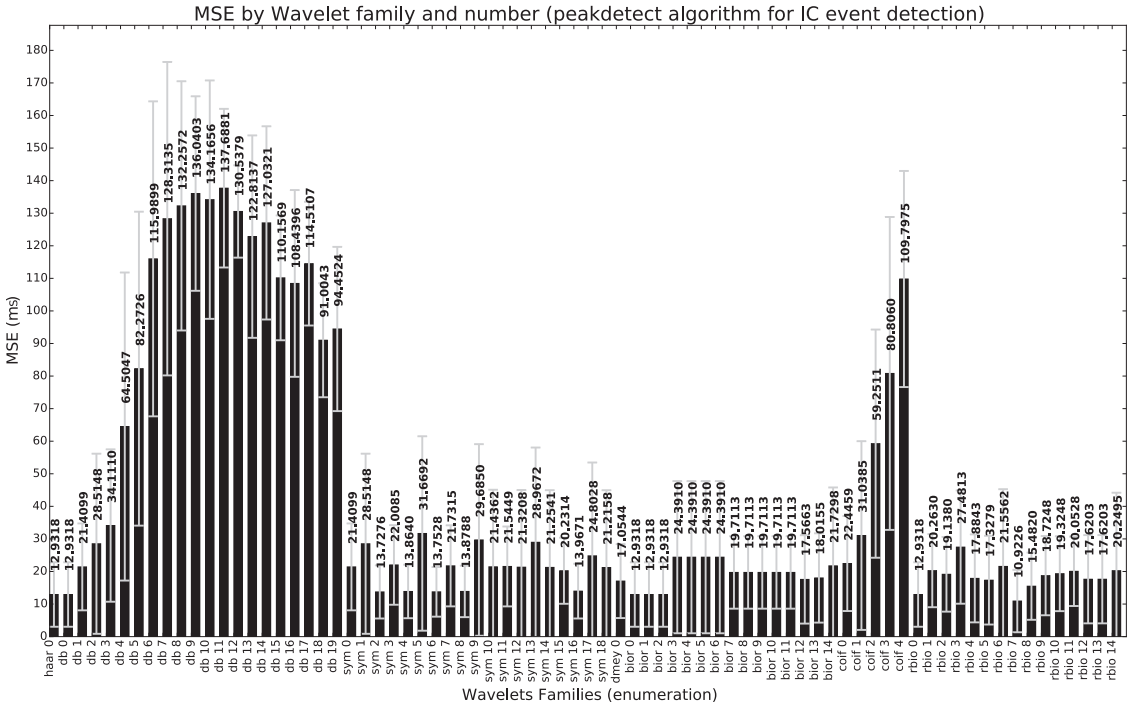

(a) MSE Results of the application of DWT with different wavelets families on the detection of IC events with the peakdetect algorithm.

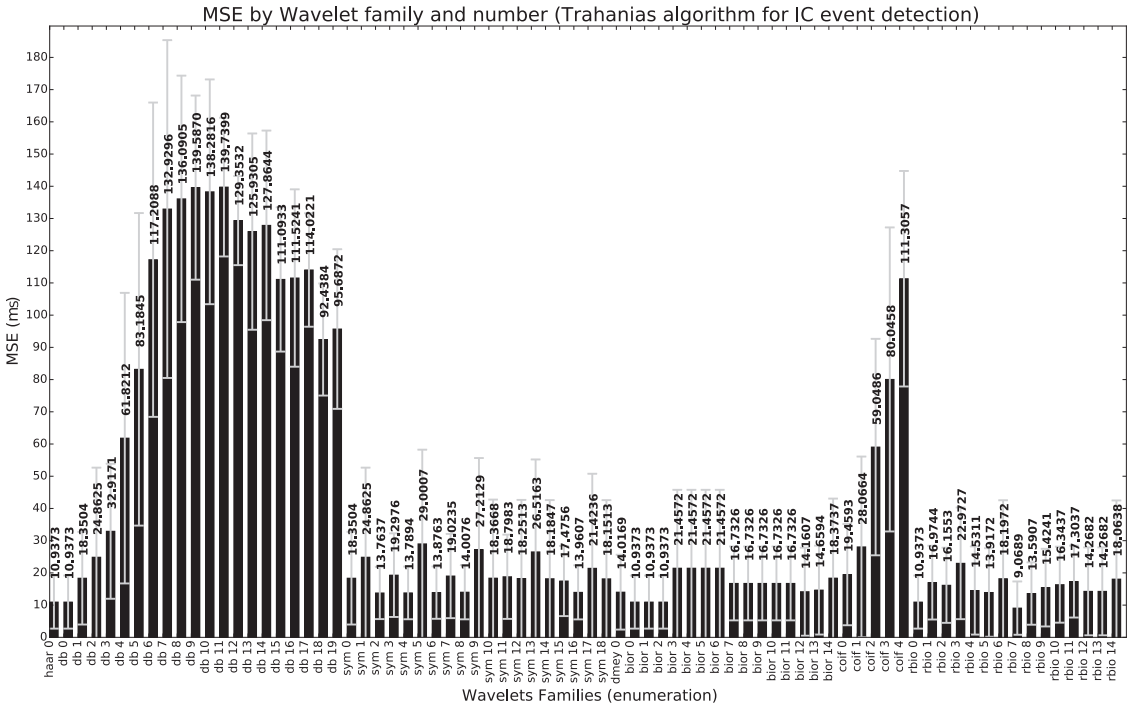

(b) MSE Results of the application of DWT with different wavelets families on the detection of IC events with rthe Trahanias algorithm.

Figure 5.7: MSE Results of the application of DWT with different wavelets families on the detection of IC events with both algorithms applied, compared with video annotations. The gray bar represents the standard deviation.

The determination of the IC events between the wavelet families was heterogeneous, with a standard deviation similar to all of them. Where in some cases, the standard deviation reached the mean value. The best result was achieved with an MSE of approximately 11 ms (Reverse biorthogonal (rbio) 3.1 that is *rbio*7 in the bar chart), and the worst with approximately 140 ms (with the Daubechies (db) 10 that is *db*11 in the bar chart).

In Figure 5.8 the ten best results for each of the algorithms are presented, in this case, the video annotation were also considered for the validation.

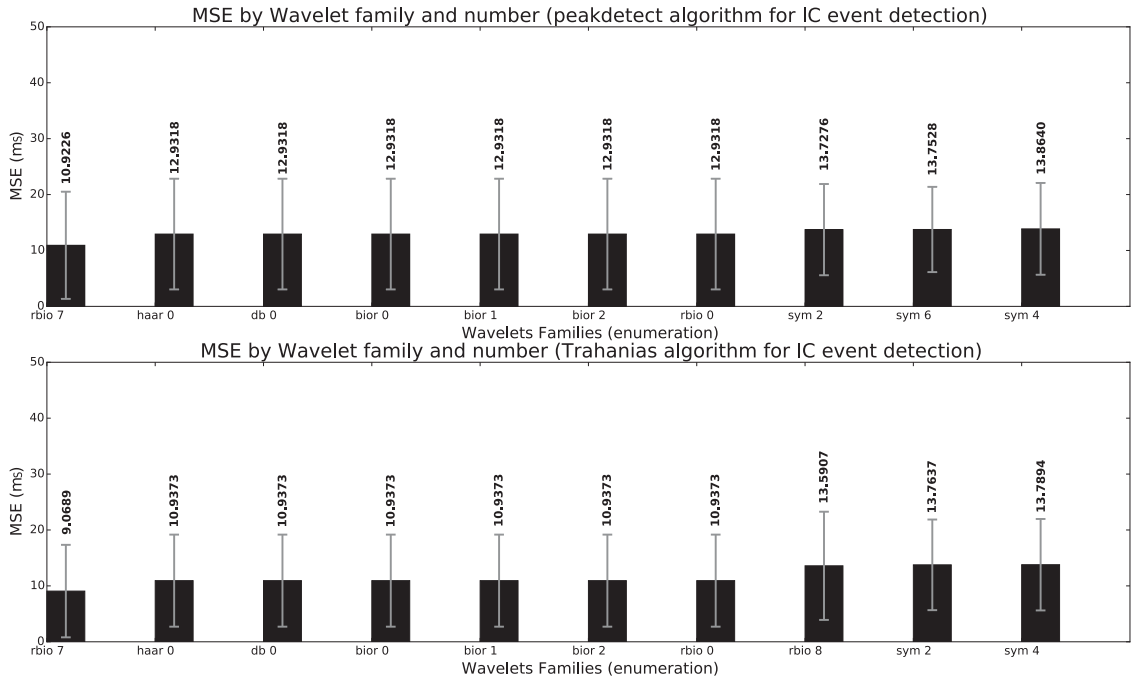

Figure 5.8: Ten best MSE results of the application of DWT with different wavelets families on the detection of IC events by peakdetect and Trahanias algorithms, compared with video annotations. The gray bar represents the standard deviation.

It can be observed that the best result for both algorithms was using the Reverse biorthogonal wavelet (rbio) 3.1 (*rbio*7) and the result was slightly better for the Trahanias algorithm than for the peakdetect. The wavelet are specific according to the shape of the signal component to be found, as explained in Subsection 4.4.4. In addition, it was also possible to observe that the ten best values were very similar among them, there were even several with the same value. However, it must be taken into account that it was a study done with only five subjects. Therefore, the sample is not representative of the entire population.

The annotations used in this study were the annotations of the videos and, as presented in Subsection 4.3.1, there was difficulty in the accuracy of the annotation of the exact moment when the events occurred due to the quality reduction in saving the video (in about 20 to 30 ms). Due to that, this study was also performed on manual annotations (as described in Subsection 4.5.1). In Figure 5.9 the ten best results obtained for both algorithms, now with manual annotations are presented.

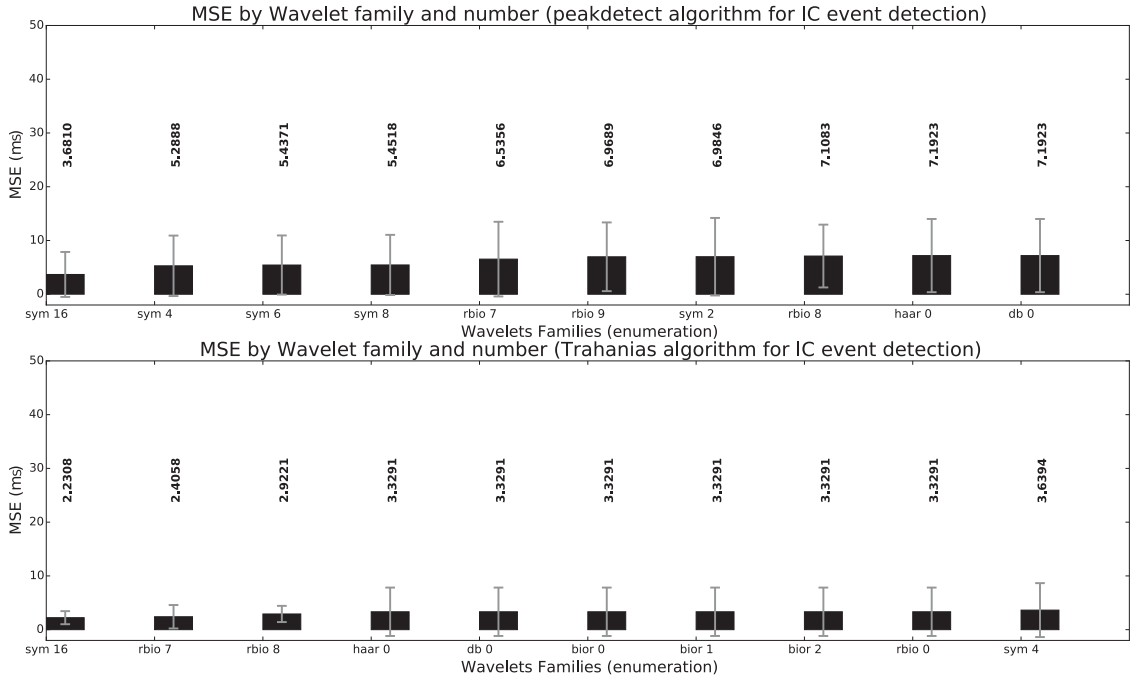

Figure 5.9: Ten best MSE results of the application of DWT with different wavelets families on the detection of IC events by peakdetect and Trahanias algorithms, compared with manual annotations. The gray bar represents the standard deviation.

With the results of manual annotations, it can be observed that lower MSE values were reached, and the best result was not achieved with the best-performing wavelet family for video annotations. However, the differences between the top ten results for both algorithms are close, there were several of them with the same result, and the wavelet that gave better results with video annotations was also one of the top ten for manual annotations in both algorithms. It is recalled that the MSE study only considers TPs, where occlusions of video annotations only reduce the number of samples compared.

The combination of results with precision and recall values is as follows. Despite not being present in the top ten results, the wavelet that presented the best results for MSE validation also presented good results for precision: 75.1676 % for peakdetect with video annotations and 90.5310 % for Trahanias with video annotations. For manual annotations: 86.7763 % for peakdetect and 100.0000 % for Trahanias algorithm. The recall of the wavelet that offers the best MSE result had a recall of 88.7792 % with peakdetect and 85.0979% for Trahanias, with video annotations, and 86.5382% with peakdetect and 79.6846% with Trahanias, with manual annotations.

The next phase of study is focused on increasing the number of true IC events detected by Trahanias algorithm, while continuing to avoid detecting noise as events.

To conclude this section, the wavelet that best results offered, taking into account the balance of temporal error and precision in detecting events, was the Reverse biorthogonal wavelet (rbio) 3.1 (*rbio*7 in bar charts). And it was with this wavelet that the following studies were developed. It is recalled that this parameter is probably not optimal, due to the non-representativeness of the

data.

5.1.3 Study of the Structuring Element (Trahanias Algorithm)

The study that follows focuses on increasing the recall of the Trahanias algorithm, trying to maintain its precision. Recalling the description of this algorithm in Subsection 4.4.3, what may influence the sensitivity of the Trahanias algorithm is the size of the structuring element used in morphological operations. Therefore, in this study, different structural elements with lengths ranging from 2 to 23 (focusing essentially on the odd ones) were applied. The wavelet used was the one with the best result in the previous study (Reverse biorthogonal wavelet (rbio) 3.1 (*rbio*7 in bar charts)), and the results were compared with manual annotations due to the absence of event occlusions. The analysis is divided in the same way as the previous study, focusing initially on precision and recall and then on MSE analysis. It is noted that, at this stage, only the behavior of the Trahanias algorithm was evaluated. The peakdetect algorithm does not depend on the structuring element, so it was not included in this study.

In Figure 5.10 the precision results for detection of IC events and in Figure 5.11 for detection of PS events are presented.

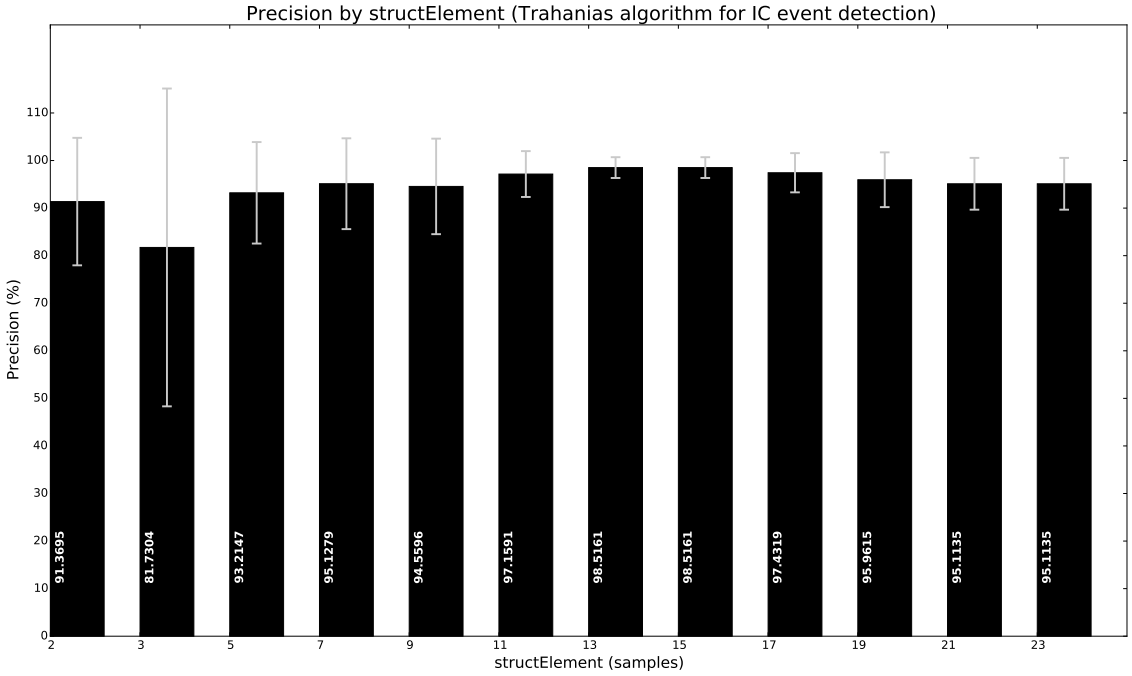

Figure 5.10: Precision results of the application of several structuring elements on the Trahanias algorithm, for the detection of IC events, compared with manual annotations. The gray bar represents the standard deviation.

It can be seen that the precision value tended to increase with increasing the size of the structuring element. However, for the detection of IC events, there was an optimal value for the size of the structuring element, which was about in the central part of the graph shown in Figure 5.10. It

should be noted that these values are different from those shown in Subsection 5.1.2. In this data, the results were with optimized weights of the adaptive threshold. This optimization caused a decrease in precision, aiming to increase the recall. It was a study done with few results in concrete. However, the goal was to optimize the weight of the Thrahanias algorithm's adaptive threshold in order to reduce the precision as minimum as possible, increasing the recall as much as possible. In this case, the precision values were smaller than the 100% presented previously, in about 4%. But the recall increased more than 10 %.

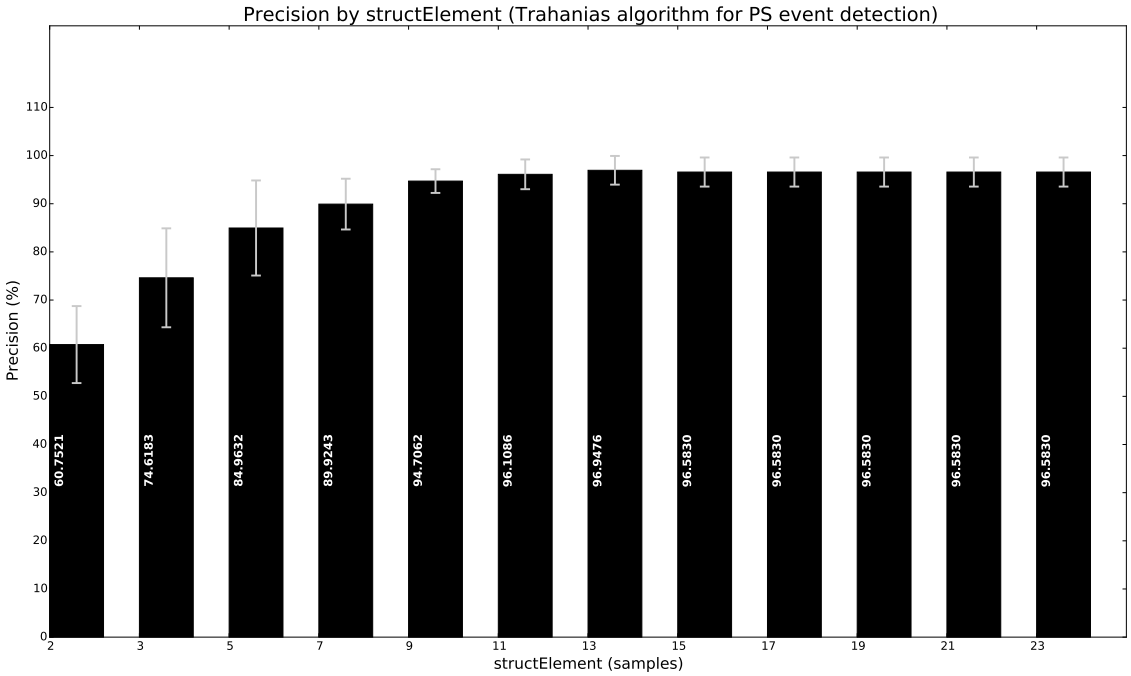

Figure 5.11: Precision results of the application of several structuring elements on the Trahanias algorithm, for the detection of PS events, compared with manual annotations. The gray bar represents the standard deviation.

It can be observed that for small structural elements were where there was a large amount of noise detected as true events, causing the increase of FP (note that this result was with manual annotations). This behavior is in accordance with the algorithm characteristics, that is for both IC and PS event detection. Its justification, based on the description of the algorithm, also has logic, that is, with the application of small structuring elements, more noise was detected as mountains and valleys, causing identification of noisy peaks.

In Figure 5.12 the recall results for detection of IC events and in Figure 5.13 for detection of PS events are presented. The recall values were lower for the detection of both events, and with higher standard deviation for IC event detection. Comparing these results with the recall of about 79% obtained in Subsection 5.1.2, having a structuring element greater than 9 samples was possible to achieve a recall of 88%, being about 10% higher than that presented in the wavelets study.

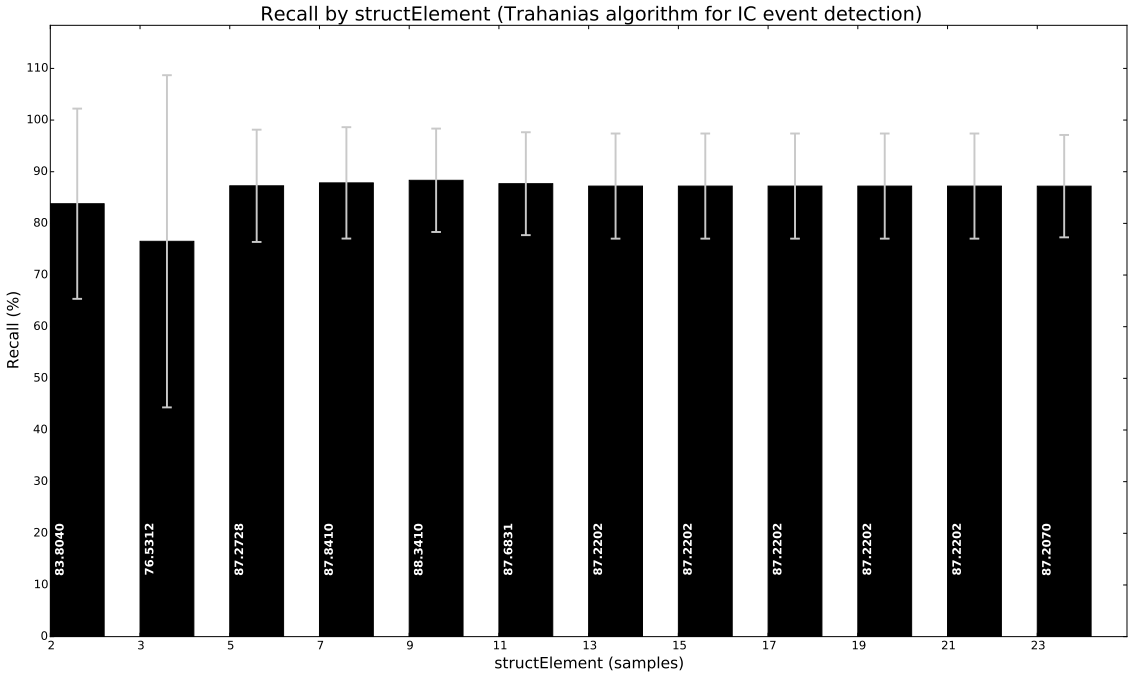

Figure 5.12: Recall results of the application of several structuring elements on the Trahanias algorithm, for the detection of IC events, compared with manual annotations. The gray bar represents the standard deviation.

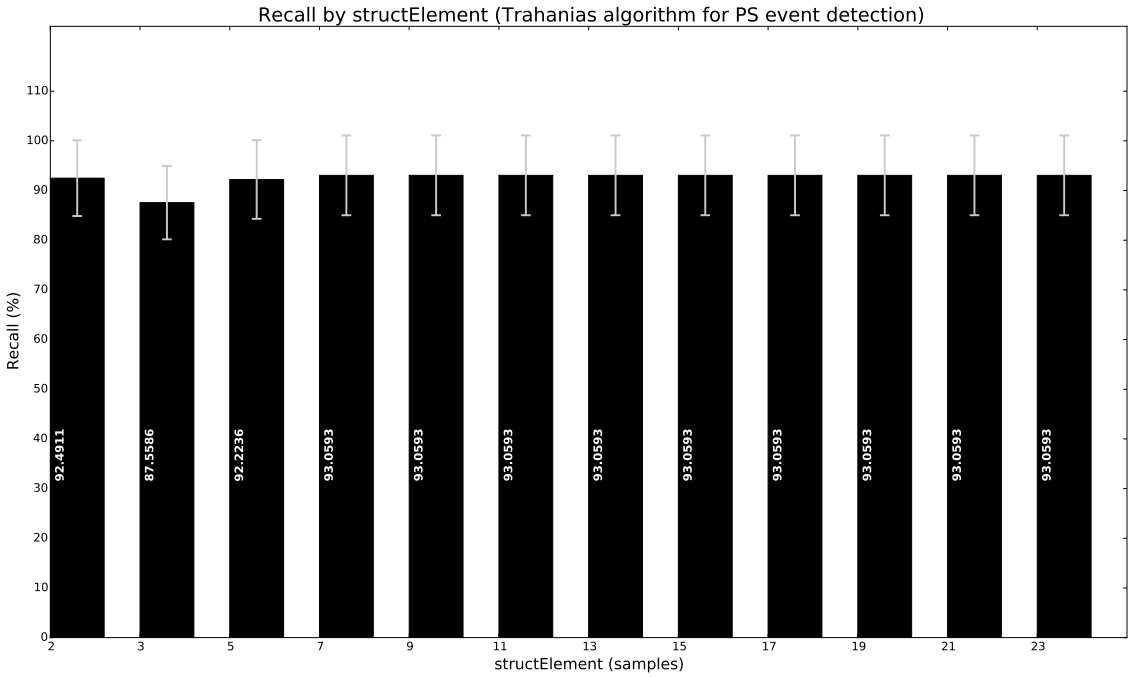

Figure 5.13: Recall results of the application of several structuring elements on the Trahanias algorithm, for the detection of PS events, compared with manual annotations. The gray bar represents the standard deviation.

Combining the results of recall and precision, it can be noted that the best obtained results were for structuring elements with 9 till 23 samples size. However, for structuring elements with more than 15 samples, the precision value for the detection of IC events started to decrease.

In the case of the recall, the smaller the size of the structuring element, the more difficult it was to find mountains in the signal and to find positive events, which causes a decrease in the recall due to the increase in FN. For larger values of structuring element size, there were more mountains to be considered to be potencial events. Another note to take into account in this study was the maximum size of the structuring element to be used, which is 23 samples. Using 23 samples corresponds, in this project, to 23×20 (ms) which results in 460 (ms), that was close to half a second. This was the maximum value used because, from this value, it started to be half-way down the gait cycle. Since, only the components of IC and PS were necessary to be selected, which were a small portion of the time of the walking cycle, a larger structuring element did not have any interest in this study.

In Figure 5.14 the MSE result with manual annotations for the IC events and in Figure 5.15 for the PS events is presented. The idea of using only manual annotations to study the structuring element was related to the presence of occlusions in the video annotations and to understand which was the best structuring element that was able to better detect the higher amount of events.

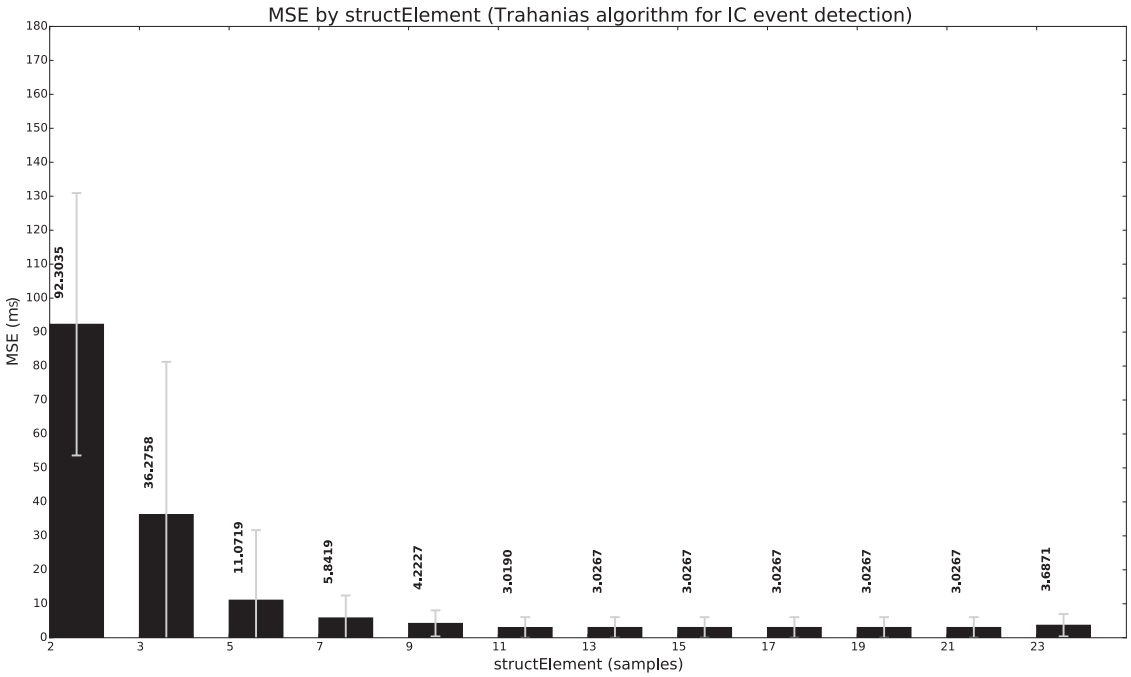

Figure 5.14: MSE results of the application of several structuring elements on the Trahanias algorithm, for the detection of IC events, compared with manual annotations. The gray bar represents the standard deviation.

The structuring element of odd dimension was to allow each sample of the signal to have the same number of points of the structuring element for each side of the sample. Size 2 only serves as the minimum structuring element size, and it is observed in both figures that it was the

one that returned a higher error. Another observation that can be made in both figures (i.e., both for detection of IC and PS events) is that the MSE result would tend to a fixed value while the structuring element was increasing. This means that the increased in the size of the structuring element, from a certain value, no longer influences the temporal detection of the events, always being detected in the same place. This happens for both IC and PS events.

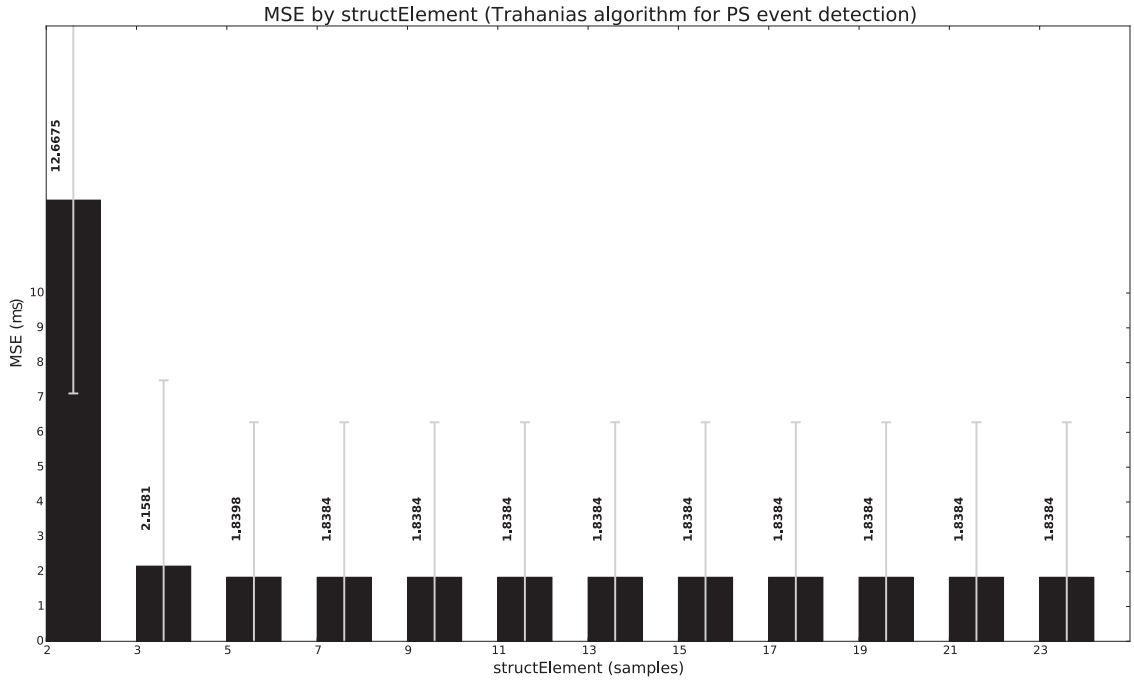

Figure 5.15: MSE results of the application of several structuring elements on the Trahanias algorithm, for the detection of PS events, compared with manual annotations. The gray bar represents the standard deviation.

Concluding this section, based on MSE, precision and recall values, the 9-sample size structuring element was chosen to proceed with the project studies. This structuring element size improves the recall of the Trahanias without greatly impairing the detection of noise as events. It should be noted that these parameters are the most indicated for the data used, not being representative of the population. Much less optimal to be applied to people with gait impairments, without specific studies in these patients. This is because this type of results is always limited with the amount and variability of data used. As already explained, the sample collected is not representative of the healthy population. This data is also not representative of the population with gait abnormalities, which is the population that is intended to be reached as the ultimate goal in rehabilitation.

5.2 IC and PS Events Results With Gold Standard Annotations

In this section, the results of the algorithm developed in relation to the gold standard are presented. The gold standard is described in Subsection 4.5.2. Here a study of the best wavelet family and also the best structuring element of the Trahanias algorithm are discussed.

Using the parameters found in the previous section the results with data and gold standard annotations are found in Table 5.1.

Table 5.1: Result of the performance of the algorithms with the parameters selected in the previous section, in the data with gold standard annotations.

Algorithm	**Metric**	**Event**	**Value**
Trahanias	Precision	IC	93.7500 ± 12.9312 (%)
Trahanias	Precision	PS	99.0000 ± 4.4721 (%)
Trahanias	Recall	IC	64.1667 ± 14.5849 (%)
Trahanias	Recall	PS	100.0000 ± 0.0000 (%)
Trahanias	MSE	IC	35.6150 ± 29.7250 (ms)
Trahanias	MSE	PS	39.6979 ± 30.2979 (ms)
Peakdetect	Precision	IC	95.4157 ± 11.3023 (%)
Peakdetect	Precision	PS	99.0000 ± 4.4721 (%)
Peakdetect	Recall	IC	66.2500 ± 11.3023 (%)
Peakdetect	Recall	PS	100.0000 ± 0.0000 (%)
Peakdetect	MSE	IC	42.9650 ± 53.1813 (ms)
Peakdetect	MSE	PS	39.6979 ± 30.2979 (ms)

With these results, it was possible to conclude that the recall of the detection of IC events considerably dropped (about 20 %) comparing with the previous data. The precision decreased about 3 %. In addition, it can be observed that the temporal error of the IC events highly increased. For example, for the peakdetect algorithm IC detection, the MSE standard deviation was higher than its mean value.

On the other hand, the detection values of the PS event improved compared to previous studies. Thus, it was decided to proceed with a wavelet analysis on the detection of IC events, in order to reduce the MSE error and increase the precision and recall. Also, to study the structuring element of the Trahanias algorithm, in order to improve the results for detection of IC events without impairing the detection of PS events. And with that, understand what might have happened with this decreased IC event detection.

5.2.1 Study of the Wavelet Type

This study started with study of wavelets, as previously presented, for the reason that the data are not representative of the population. In the study of the best wavelet, the process was similar to that presented in Subsection 5.1.2. For all the data collected in the LaBioMEP all the wavelets were applied. The results regarding MSE, precision, and recall are presented and discussed. It is worth to note that, for the study of wavelets, only the comparison of the results of the IC events was important, considering the two algorithms (peakdetect and Trahanias). The data used in the

studies presented in this section was from only one person, 10 round-trip sequences as described in Subsection 4.5.2.

Taking into account the precision and recall values (Figure 5.16 and Figure 5.17 respectively), it can be seen that the precision value was slightly better for the Trahanias algorithm than for the peakdetect. However, the recall was relatively similar. That is, the Trahanias algorithm was able to detect the relevant events correctly while not detecting noise as relevant events, maintaining the same positive detection as the peakdetect algorithm.

Observing now the families of wavelets, it is verified that the values of precision and recall were not similar throughout all the families. In Figures 5.16 and Figure 5.17 are only the ten best results. The remaining results, where the different values of precision and recall by the different wavelet families are, can be found in Apendix A.

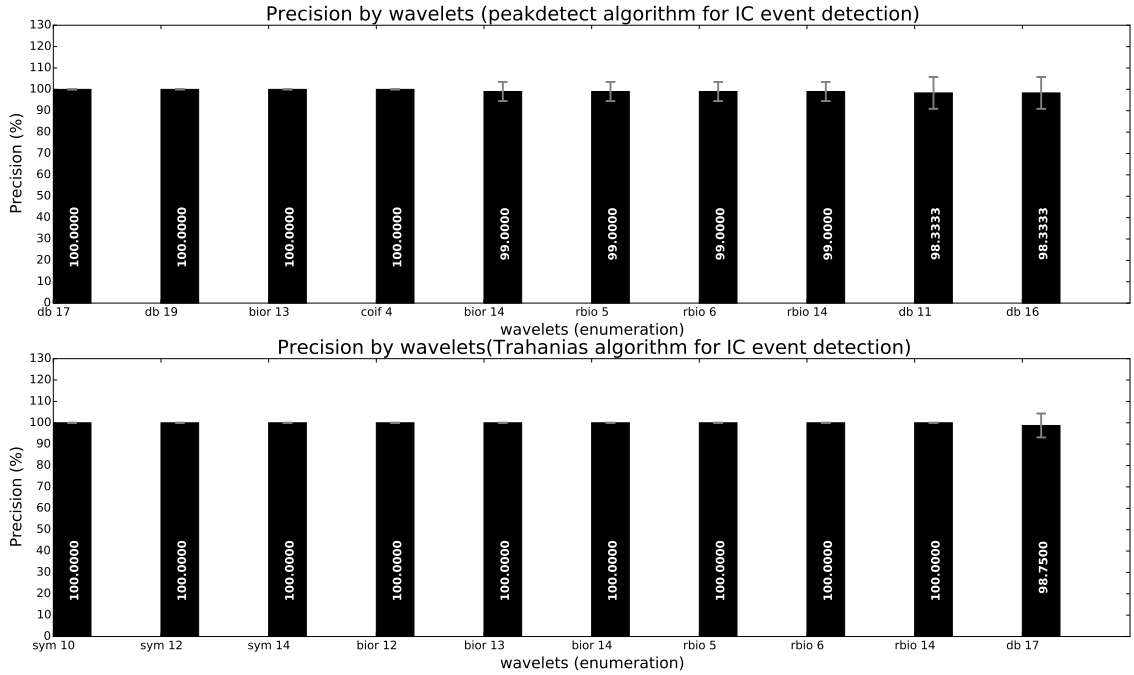

Figure 5.16: Ten best precision results of the application of DWT with different wavelets families on the detection of IC events by peakdetect and Trahanias algorithms, compared with gold standard annotations. The gray bar represents the standard deviation.

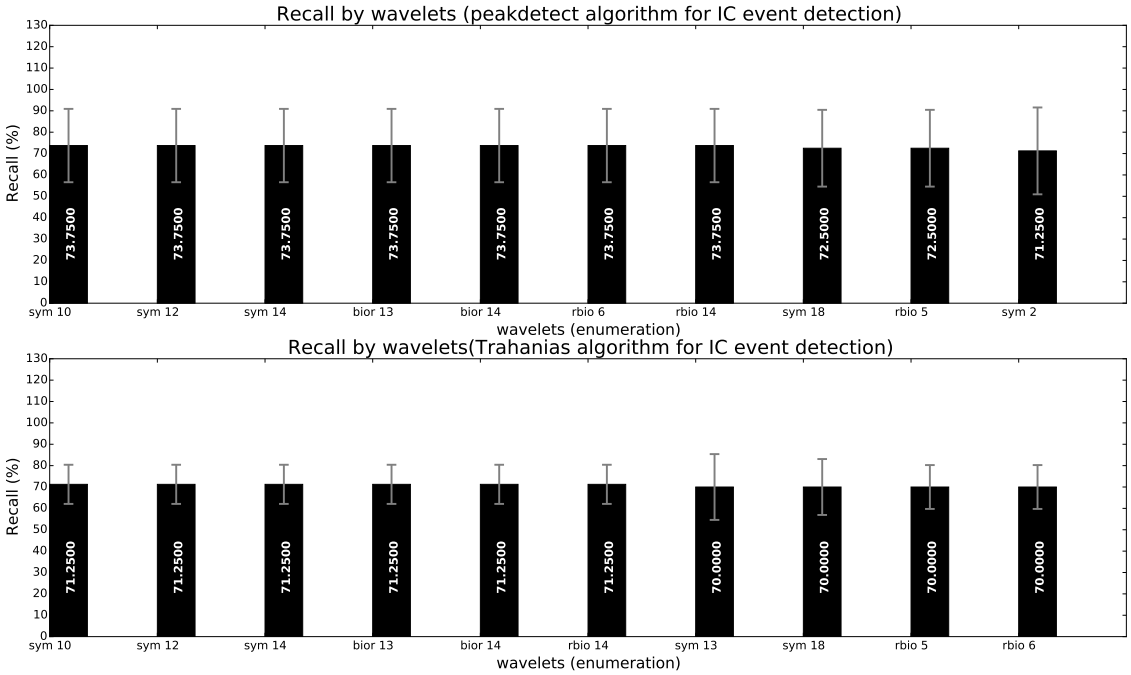

Figure 5.17: Ten best recall results of the application of DWT with different wavelets families on the detection of IC events by peakdetect and Trahanias algorithms, compared with gold standard annotations. The gray bar represents the standard deviation.

On the contrary to the first data set with video and manual annotations, in this study, there was no great similarity between the families regarding precision and recall. It is observed that, for some families, the precision was high, reaching 100 % with small standard deviation for both the Trahanias and peakdetect algorithms, but the recall was lower by about 30 %. This means that under these conditions, the algorithm tended to better detect the positive data by failing some of them.

For the precision results for the peakdetect algorithm, the maximum value obtained was 100 % with the wavelets $db17$, $db19$, $bior13$, and $coeif4$, with a minimum value of about 91.6667 % with the wavelets $bior3$, $bior4$, $bior5$, $bior6$, and $coeif0$. For these values, the standard deviation was similar, having a value close to 30 %. The precision of the Trahanias algorithm had a maximum value of 100 % with the wavelets $sym10$, $sym12$, $sym14$, $bior12$, $bior13$, $bior14$, $rbio5$, $rbio6$, and $rbio14$, and the minimum value of 91.6667 % with the wavelets $bior3$, $bior4$, $bior5$, and $bior6$. With a standard deviation between 20 and 40 %, being higher for lower precision probabilities. For the recall results for the peakdetect algorithm, the maximum value obtained was $73,7500$ %, with the wavelets $sym10$, $sym12$, $sym14$, $bior13$, $bior14$, $rbio6$, $rbio14$, and $rbio14$, while the minimum achieved was about $56,2500$ % with the $db5$ wavelet. In the case of the recall, the standard deviation was around 40 % and was similar for all wavelets. The recall of the Trahanias algorithm had a maximum value of 71.2500 % achieved with the families $sym10$, $sym12$, $sym14$, $bior13$, $bior14$, and $rbio14$, while the minimum value was 52.5000 % with the $db13$ family. In this case, the standard deviation was about 40 %. For more information, supplementary results are

shown in the Appendix A.

After this result, it was tried to perceive the reason for behind this value, analyzing the signals. What was found was that, after turning around to go back to the starting point (towards the red pins), the first IC event was almost always failed by the algorithms. That lowered the recall on detecting IC events. In the return, even before the beginning of the trajectory, it begins with a small step. Thus, it turns out to be a start of march in which the heel attacks slightly ahead to the ground, different from the other steps. This causes that the attack to the ground is less intense, having smaller positive peak in the signal. This kind of behavior had already occurred before, using video annotations. That is, the start and end of the march are situations with most difficult events to be detected because the gait cycle is incomplete. And it also because, it is close to the non-gait region.

In Figure 5.18 the MSE results of the event detection IC with the peakdetect algorithm, comparing with golf standard annotations are presented. In Figure 5.19 the same results are presented but with the Trahanias algorithm. The structuring element used in the Trahanias algorithm was what best results offered in the previous study with video annotations (size of 9 samples).

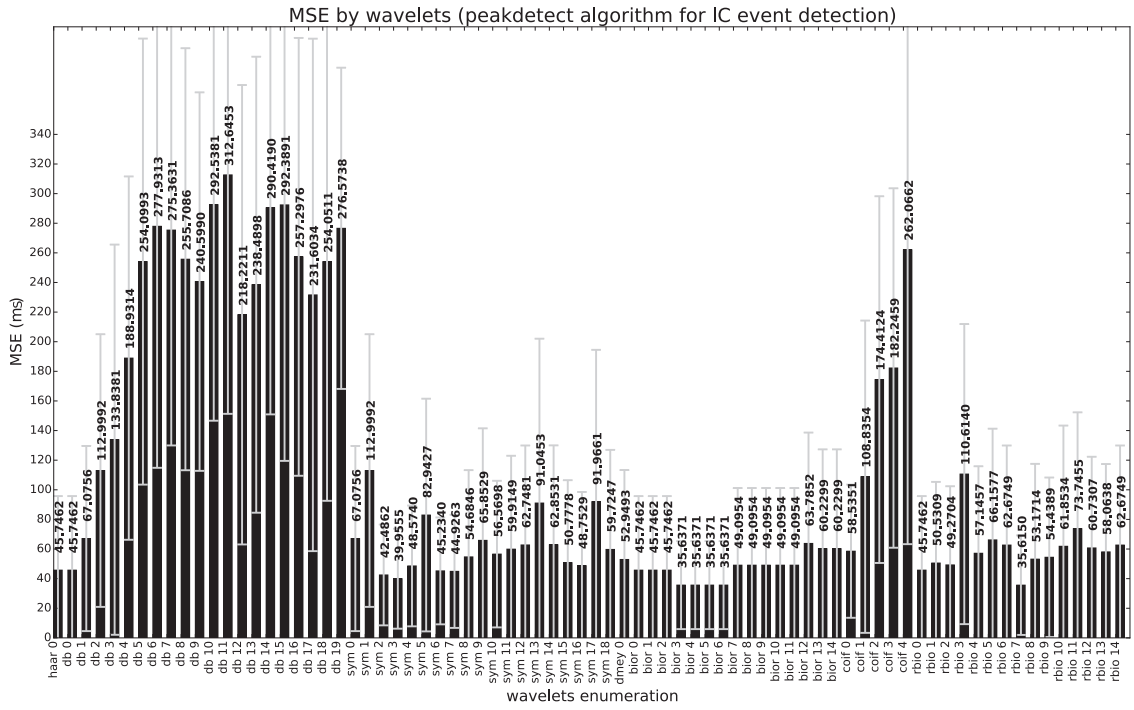

Figure 5.18: MSE Results of the application of DWT with different wavelets families on the detection of IC events with peakdetect algorithm, compared with gold standard annotations. The gray bar represents the standard deviation.

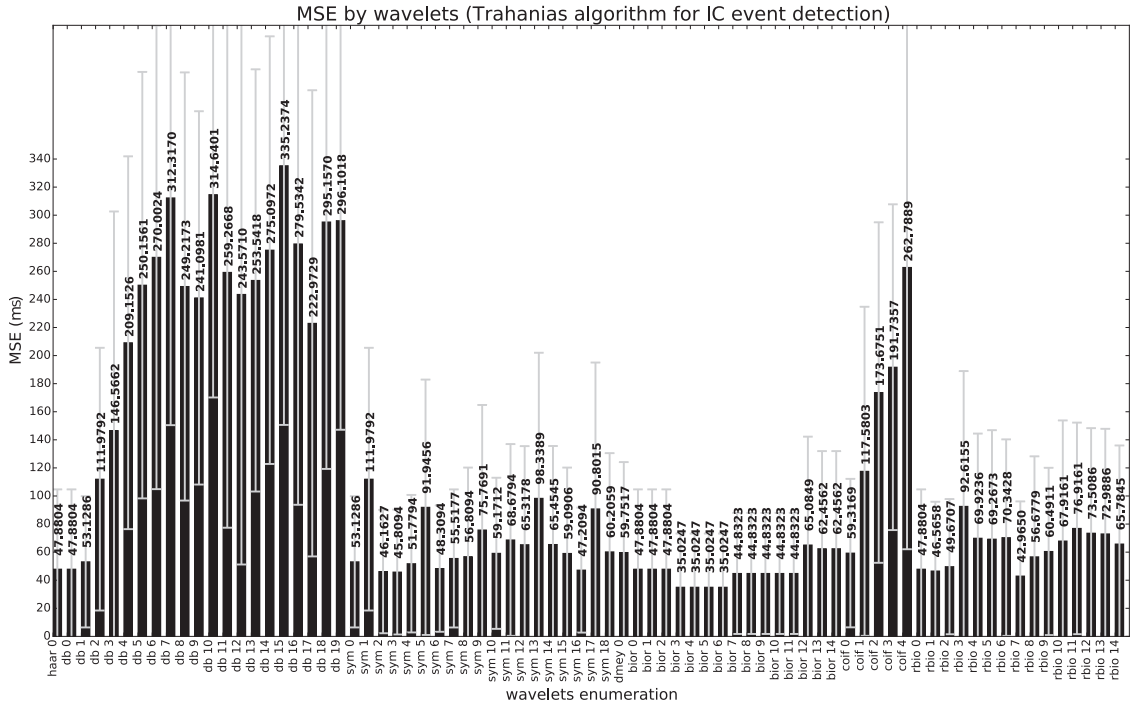

Figure 5.19: MSE Results of the application of DWT with different wavelets families on the detection of IC events with Trahanias algorithm compared with gold standard annotations. The gray bar represents the standard deviation.

It can be noticed that, although the error had increased in value, the behavior of the MSE along the different wavelets was similar to that obtained for video and manual annotations, even though the data was acquired under different conditions. However, the best-performing wavelets for this study were Biorthogonal (bior) 2.2, 2.4, 2.6 and 2.8 (corresponding to *bior*3, 4, 5 and 6 in bar graphs). A very important aspect to note in these data is the standard deviation. Regarding the data presented for video and manual annotations, the standard deviation with standard gold annotations increased considerably, going from 30 ms to more than 130 ms. To understand the reason for this, the signal in parallel with the annotations were analyzed in more detail. which is described below.

By carefully analyzing a figure collected during this acquisition, it can be noted that the events described in Subsection 4.3.1 were not always found in the places identified above. As for example, in Figure 5.20, the events were often detected earlier than expected. Comparing the events marked with a gold standard in a signal, Table 5.2 was obtained, in which it compares places where there was a delay in the annotations. The numbers of the platforms are as shown in Figure 4.30a. It can be observed that the delay was constant between the samples, being only different for the platform 3. It would make sense to conclude that the problem would be of synchronization. However, the right and left sensors were synchronized at the same time. If this were the problem, it would have to happen on both sides. Another aspect to take into account was the behavior of the signal that is within the circles indicated in Figure 5.20. Note that there was a quick change of the signal. This type of behavior is normally associated with signal compensation. One aspect to take

into account was that, during the LaBioMEP acquisition, the tablet and the computer that were connected to the sensors were at a distance of about 8 meters. What may have happened was, using BLE connection this distance is too large. Thus, there was a loss of sensor packets upon reaching the tablet, that caused a delay in the signal. The compensation behaviour is common in this type of systems, however, the algorithm responsible for this event is confidential, it is not possible to analyze in detail or recover the lost data.

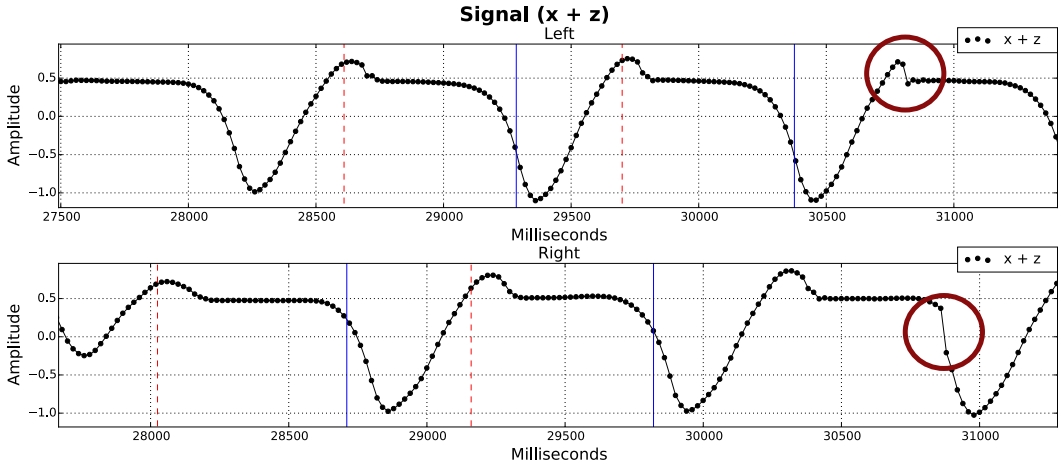

Figure 5.20: Detail of signal where a delay of the signal in relation to the annotations can be observed, and the rapid change of the signal surrounded by the red circle.

Table 5.2: Manual counting of the delay time and the platforms that contained this delay for each side (R and L) of a data file.

Platform	**Side**	**Status**	**Error (sec.)**
2	L	Correct	-
2	R	Before	0.12
3	L	Before	0.18
3	R	Before	0.12
4	L	Correct	-
4	R	Before	0.12
5	L	Correct	-
5	R	Before	0.12

This phenomenon occurred for all data acquired in the laboratory, therefore there was a high error in milliseconds, increasing the mean and standard deviation of the MSE. However, it was verified in most of the data that the events described in Subsection 4.3.1 go according to the one obtained by the gold standard. That is, the negative peaks correspond to the events of PS and the higher variation in frequency after the positive peak corresponds to the shock absorption of the event IC.

The choice of wavelet had to be balanced between precision and recall values. In this study, it was observed that the wavelet with better performance for both recall and precision in the Trahanias algorithm was the *sym*10. In the MSE of this wavelet, it can be verified that its value was not the best, being about 59.1712 ms, however, it was decided to proceed with it for the following

studies of structuring element. It should be noted that the result of the chosen wavelet is not the best result obtained with MSE metric, but according with precision and recall results. This is because the data is compromised due to packet loss. Therefore, it was assumed that the data detected as TP were not compromised by the loss of packets, because the deviation was smaller than the size of a gait cycle.

For the peakdetect algorithm, the *sym*10 wavelet also offered minimally concordant results between precision and recall, compared with the remaining wavelets.

Concluding this analysis, the Symlet wavelet (sym) 12 (*sym*10 in bar graphs) was chosen to proceed with the following studies.

5.2.2 Study of the Structuring Element (Trahanias Algorithm)

In order to find a balance between the precision and the recall of the results obtained with the Trahanias algorithm, in a similar way to that presented in Subsection 5.1.3, the study of the size of the structuring element was implemented. Thus, the goal was to find the most suitable structuring element in order to maintain precision by increasing the recall.

In this study, the wavelet symlet wavelet (sym) 12 (*sym*10 in bar graphs) was used which, as explained in the previous section, seemed to be the wavelet that better results in balancing MSE, precision, and recall. In this study only Trahanias algorithm data is presented, focusing on IC and PS events.

In the precision results shown in Figures 5.21 and Figure 5.22 for detecting IC and PS events, respectively, it can be seen that the standard deviation also decreased with increasing structuring element size, and the mean value increased with increasing of the structuring element. This means that by increasing of the structuring element size, fewer peaks were detected as wrong events, decreasing FPs.

The precision values for IC event detection reach 100 % from the structuring element size 7 samples, and 99 % for PS event detection from the structuring element size 13 samples. Thus, it is now necessary to find a structural element that allows to maintain the precision while increasing the recall.

Recall results are present in Figure 5.23 for IC event detection and in Figure 5.24 for PS event detection. With a precision of about 99 % and a recall of about 100 %, it can be concluded that the algorithm was able to correctly identify the IC and PS events while discarding not relevant events as noise.

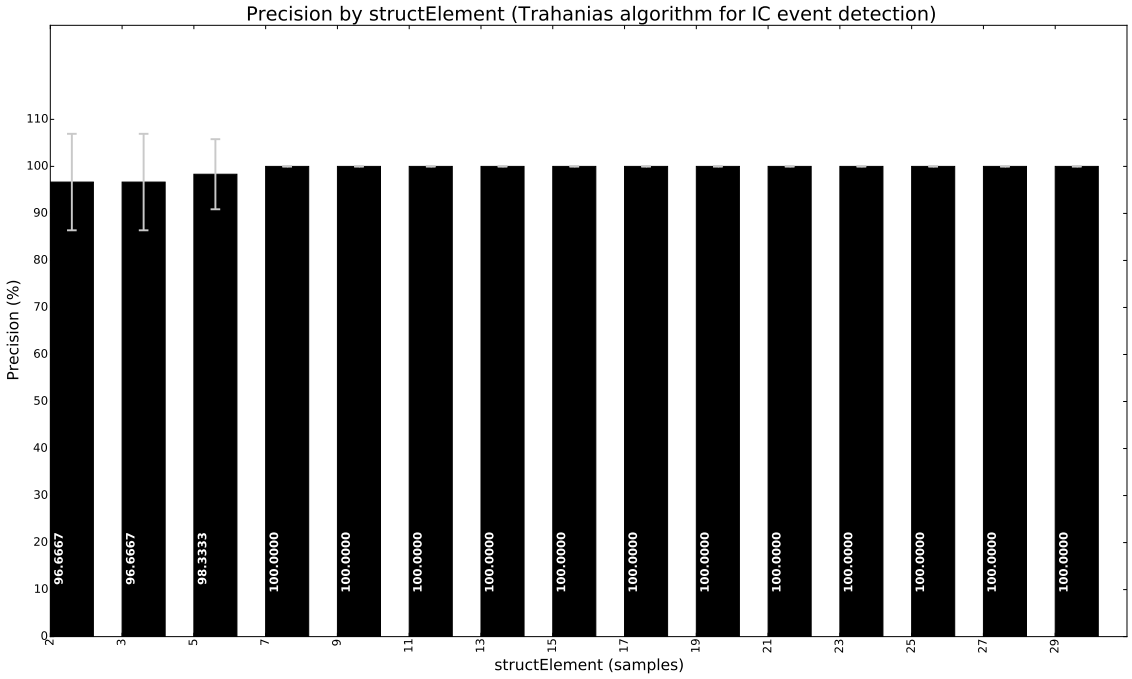

Figure 5.21: Precision results of the application of several structuring elements on the Trahanias algorithm, for the detection of IC events, compared with gold standard annotations. The gray bar represents the standard deviation.

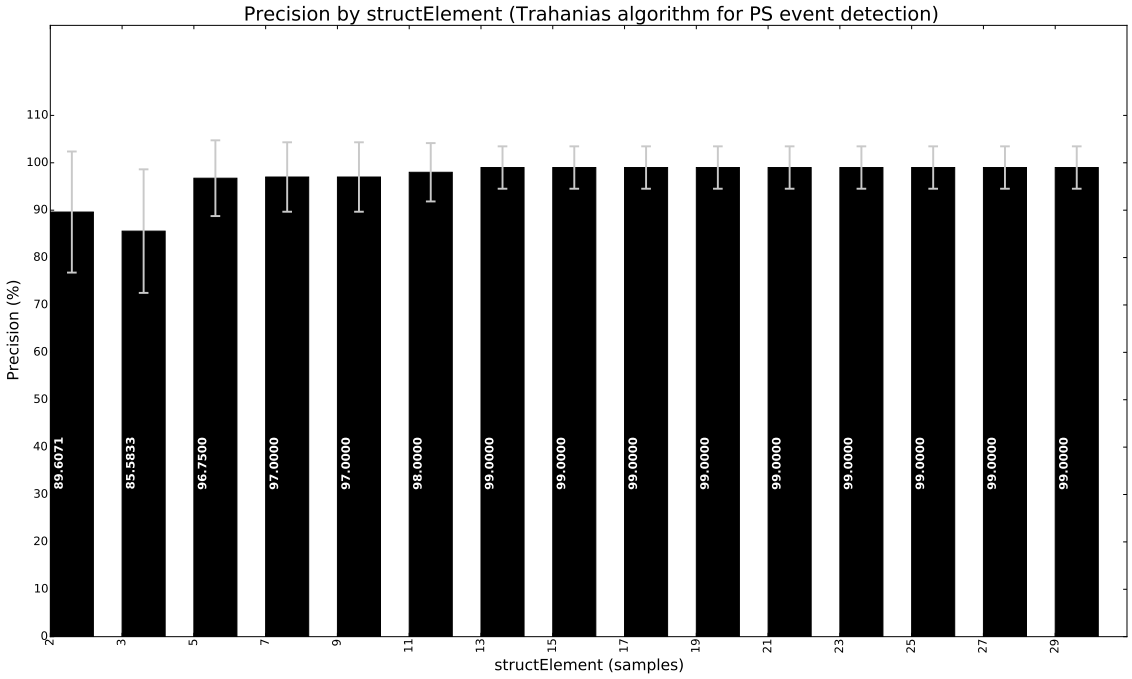

Figure 5.22: Precision results of the application of several structuring elements on the Trahanias algorithm, for the detection of PS events, compared with gold standard annotations. The gray bar represents the standard deviation.

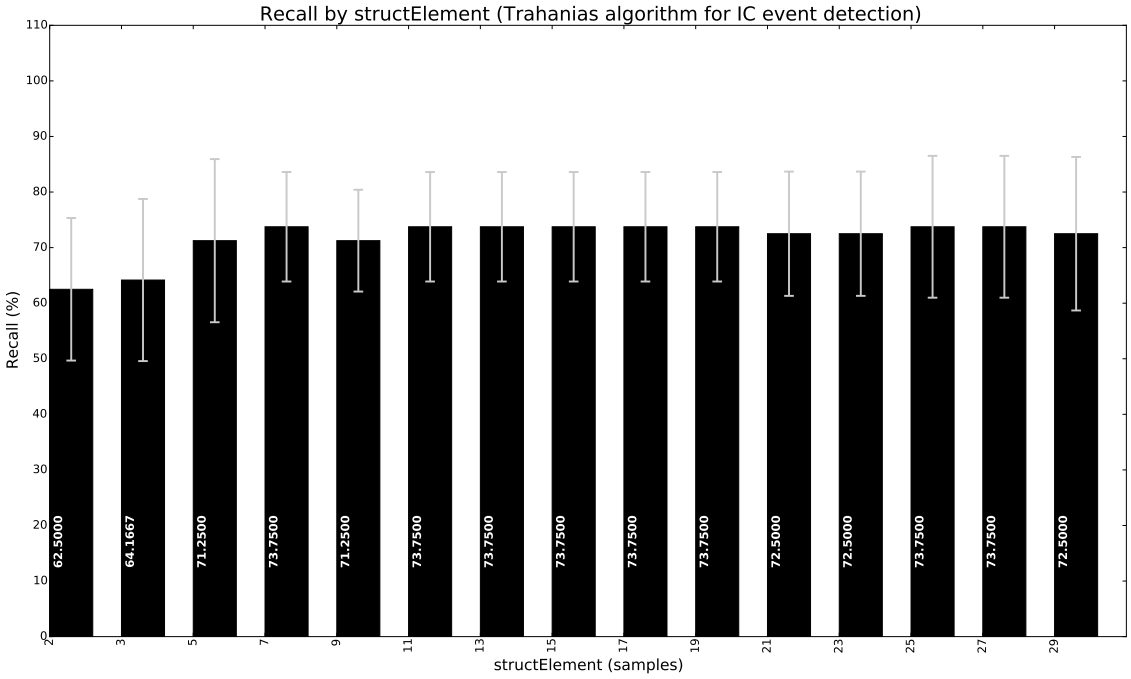

Figure 5.23: Recall results of the application of several structuring elements on the Trahanias algorithm, for the detection of IC events, compared with gold standard annotations. The gray bar represents the standard deviation.

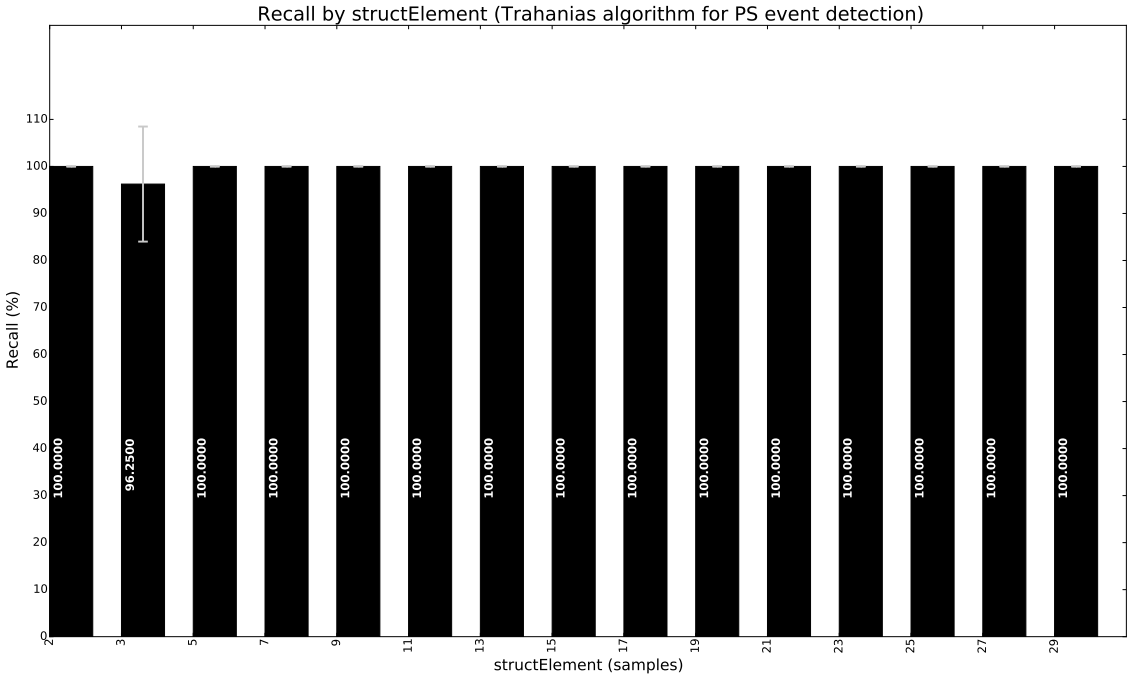

Figure 5.24: Recall results of the application of several structuring elements on the Trahanias algorithm, for the detection of PS events, compared with gold standard annotations. The gray bar represents the standard deviation.

Observing the recall results for detecting IC events, it turns out that the same was no longer the case. The recall was greatly reduced, which leads to the conclusion that the algorithm was failing to detect many positive events, should be more specific in the detection. The reason this has happened is the same as presented in the previous section. That is, the first IC on the return of the trajectory is shorter and closer to the region where the gait inversion occurred. In this sense it resulted in a smaller event (in the signal) than the other events. In addition it was also close to a region that was not walking pattern (region to go around with both feet together). In this way, the algorithm often did not detect this event. It should be noted that this did not happened at the beginning of the trajectory because the annotations start midway through the way of the march. In this way, there was no ambiguity in determining the remaining events.

In Figure 5.25 the MSE result for the IC and in Figure 5.26 PS events, are presented.

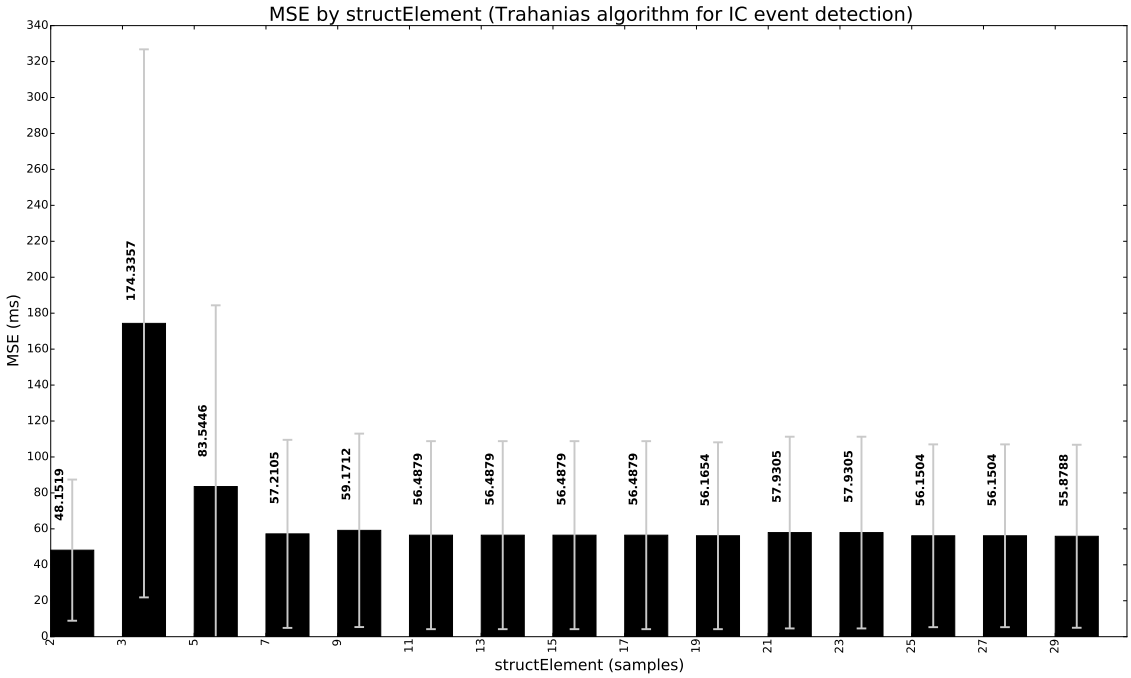

Figure 5.25: MSE results of the application of several structuring elements on the Trahanias algorithm, for the detection of IC events, compared with gold standard annotations. The gray bar represents the standard deviation.

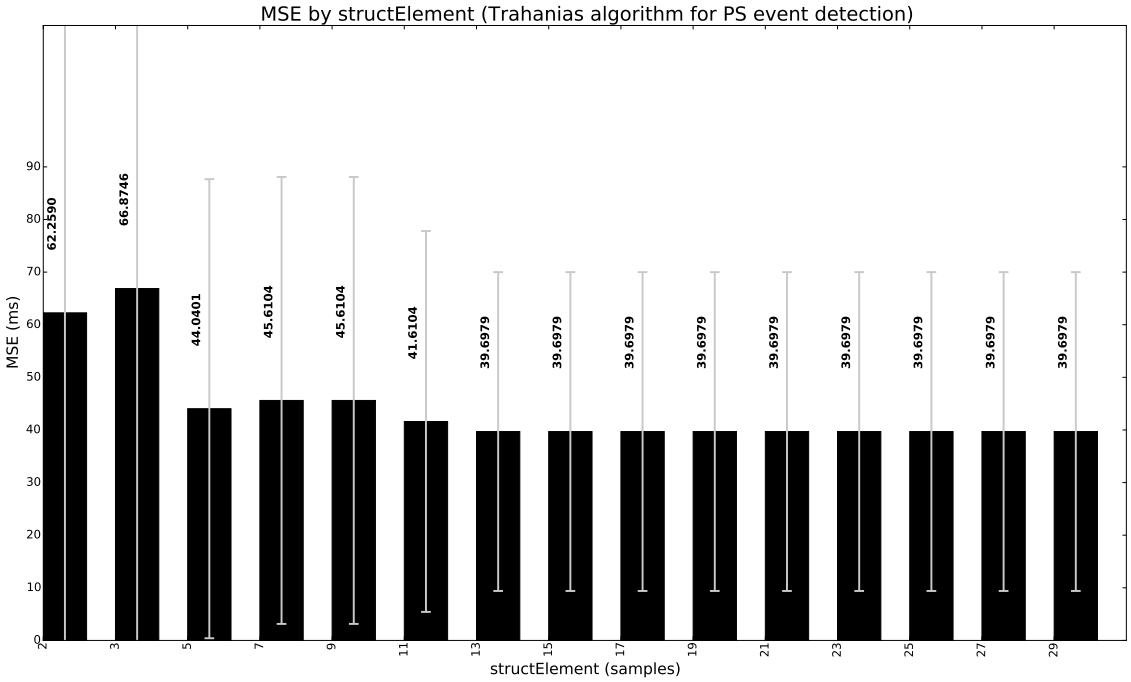

Figure 5.26: MSE results of the application of several structuring elements on the Trahanias algorithm, for the detection of PS events, compared with gold standard annotations. The gray bar represents the standard deviation.

With these two graphs, it is observed that there was a very high standard deviation for both events. The standard deviation reaches the same value as the mean, which gives little confidence about the results. But comparing with the structuring element, it seems that from the size of 13 samples both the mean error and the standard deviation begin to stabilize the MSE error of the IC and PS events.

In conclusion, there is some dependence of the results regarding the size of the structuring element of the Trahanias, however, that from the size of 13 samples this dependence decreased, although in the recall of the detection of the IC event was relatively important. However, the difference was reduced considering the size of the data used.

5.2.3 Event IC and PS Detection Comparison

In this Subsection, the results comparison obtained for detection of the IC and PS event with gold standard annotations are presented.

In Table 5.3 the results for detection of the PS event are presented, for the peakdetect and Trahanias algorithm using the structuring element that gave the best result in the study carried out in Subsection 5.2.2. It has been observed that they present exactly the same values for both algorithms, where the recall was about 100 %. This means that both algorithms behaved well to detect all the true events. On the other hand, it is observed that the MSE was about 40 ms, with a considerable standard deviation for both algorithms, of about 60 ms. The reason why this occurs was already justified in subsection 5.2.1. Recalling, given the distance of the tablet and computer

from the sensors used to acquire the signal, there was loss of information by the BLE connection. What happened was a compensation for loss of information. This compensation was performed by a confidential algorithm, and it was impossible to recover the lost information. On the other hand, the determination of the walking time was made taking into account the number of samples that arrives at the system. As there were packet loss, the frequency was no longer 50Hz, or there was loss of some of the points, not 50Hz continuously. The determination of the walking time was implemented as each sample represents a 20 ms time advancement. With loss of information, the obtained time was a delay of the signal in relation to what was measured. This is the reason why, in many cases, the gold standard annotations were before the event occurred in the sensors. The standard deviation for the value of the MSE metric is almost equal to the mean of this value. This brings little credibility to the value but the error will not be more than 70 ms. However the standard deviation for precision and recall is reduced.

Table 5.3: MSE, precision and recall results comparison obtained for detection of PS event with peakdetect algorithm and Trahanias. The Trahanias algorithm was applied with a structuring element of 13 samples of length, chosen based on the results presented in Subsection 5.2.2.

Metric	**Value Peakdetect**	**Value Trahanias**
MSE	39.6979 ± 30.2979 (ms)	39.6979 ± 30.2979 (ms)
Precision	99.0000 ± 4.4721 (%)	99.0000 ± 4.4721 (%)
Recall	100.0000 ± 0.0000 (%)	100.0000 ± 0.0000 (%)

Considering the detection of the IC event, taking into account both algorithms the results are compared in Table 5.4. Also for detection of the IC event, the algorithms behave similarly. Comparing the MSE, with the Trahanias algorithm it was possible to obtain 0.0819 (ms) better than the peakdetect, however, considering that the data dimension was reduced and the standard deviation for both results was large, these values can be considered roughly equal. By comparing accuracy, the Trachanias algorithm had a better precision than the peakdetect at just over 2 %. Already considering the recall, both had the same result. These results lead to the conclusion that both algorithms played almost the same way on the detection of IC events, and Trahanias were better when selecting only the positive events, and were more likely to detect noise, in relation to peakdetect. The standard deviation values were also high for the MSE metric, but remained lower for precision and recall.

Table 5.4: MSE, precision and recall results comparison obtained for detection of IC event with peakdetect algorithm and Trahanias. The Trahanias algorithm was applied with a structuring element of 13 samples of length, chosen based on the results presented in Subsection 5.2.2. The wavelet used in this comparison was the wavelet *sym*10, chosen in Subsection 5.2.1.

Metric	**Value Peakdetect**	**Value Trahanias**
MSE	56.5698 ± 49.4977 (ms)	56.4879 ± 52.3057 (ms)
Precision	97.7500 ± 6.7041 (%)	100.0000 ± 0.0000 (%)
Recall	73.7500 ± 17.1583 (%)	73.7500 ± 9.8509 (%)

5.3 Summary

Studies were done on data collected with video and manual annotations, as well as with gold standard annotations. Based on the results obtained, the best family wavelets were chosen for the detection of shock absorption in the IC event and also the structuring element of the Trahanias algorithm was analyzed. Finally, the results of both algorithms were compared.

As the final goal was to compare both algorithms, the extensive study was done for the data obtained with video camera and with gold standard data. Although the data set used was not representative, it was concluded that the algorithms behave similarly for healthy walking people.

A lower recall than precision has been found, where for every 4 steps 1 IC was failed. However, it corresponded always to the same step, that was the start of gait after returning back in the trajectory. This has been found in other results, in which the start and end of the march are of greater difficulty in detecting the events, because the cycle is not complete in those zones. And because it is close to non-gait regions.

When choosing an algorithm it is necessary to take into account the precision and recall balance. These metrics are important to understand if what is failing is the low detection of the relevant events or the high detection of noise as events. In this case, precision was high in almost all conditions (IC and PS, peakdetect and Trahanias), which leaded to a good detection of only those events that are true. But some failed as shown by the low recall. During development of an application, it is necessary to study whether it is worth more just to lose true event detection and detect less noise, or to detect more events by finding also more noise.

According to this case study, these metrics were balanced so as not to detect noise and only detect true events. This is because, upon detecting noise, it will influence the time parameters that are calculated with the IC and PS events. Upon detecting fewer true events, the parameter is ignored (because does not make sense in the relation of ICs and PSs), and the next step parameter is calculated. For questions of variability and asymmetry (explained in the following Chapter), it turns out to be more interesting to find only temporal parameters that correspond to reality, even if some fail, such as the beginning and end of the march. If a parameter corresponding to a poor detection is taken into account for the time parameters, the variability and asymmetry are changed, which can cause alarm to the physiotherapist, not corresponding to a problem of the patient, but of the system.

Chapter 6

Temporal Parameters, Real Time Implementation and Pathology Simulation

The gait parameters are the metrics that will give physiotherapists information about the gait of the patient. In this sense, it was important to obtain the metrics that are directly derived from the events of IC and PS.

The real-time implementation plays an important rule when addressing rehabilitation environments. This is crucial in order to guide the patient to perform the exercises correctly. In this project, it was implemented the signal processing in real-time, described at the end of this chapter.

6.1 Temporal Parameters

The temporal parameters can be divided into two classes: those that refer only one foot at a time and those that refer the two feet together. In this sense, those who refer one foot at a time, exist for the left side and the right side. While those that refer both feet there is only one set of results.

6.1.1 With one foot

The temporal parameters obtained through IC and PS event relationships are Stance, Swing and Gait Cycle. More information about these temporal parameters is presented in Subsection 2.3.1. The achievement of each of them was as follows:

> *Stance Time*: time between the PS event and the previous IC event (Equation 6.1). It is the amount of time that the foot is on the ground while walking. It begins with the contact of the calcaneus with the ground and ends with the toes rising from the ground.

$$Stance\,(ms) = PS(t) - IC(t-1) \tag{6.1}$$

Swing Time: time between the IC and the previous PS event (Equation 6.2). It is the amount of time that the foot is on the air, moving forward while walking. It begins with the toes rising from the ground and ends when the calcaneus contacts with the ground.

$$Swing\,(ms) = IC(t) - PS(t-1) \tag{6.2}$$

Gait Cycle Time: time between two successive IC events (Equation 6.3). It is the amount of time that the foot needs to complete a gait cycle: between two successive contacts with the ground.

$$Gait\_Cycle\,(ms) = IC(t) - IC(t-1) \tag{6.3}$$

In equations presented above, the t is referred to the sequence of time instants in which IC and PS events occur. This means that, for each event, it was necessary to search for the previous event of interest that occurred.

The challenges in the implementation of these temporal parameters were to find events IC and PS that belong to the same segment of gait. As for example, in the sequence to begin to walk, to stop and to resume the walking, there was a portion of time in which the person was stopped, not having a moment of gait. This period must delimiter the parameters calculation. That is, the detection restarts when the person starts walking, and ends when the person also ends walking. This was to avoid obtaining very long gait parameters, which correspond to moments in which the person was stopped, easily confused with moments of stance.

One way to avoid this was to use the walking regions defined in Subsection 4.4.5. Thus, whenever the person finishes walking, the walking region ends, and the temporal parameters stop at the same time. This way the temporal parameters can be forced to stop for the instants that the person did not walk.

6.1.2 With both feet

The gait parameter that requires information from both feet is the step time. This parameter can be calculated from both sides (L and R), and the results are merged at the end. It is described as:

Stem Time (L): time between the IC event of the right side and the IC event of the left side (Equation 6.4). It is the amount of time between two successive IC events (in this case starting with the left side), of both feet.

$$Step\,(ms) = IC_R(t) - IC_L(t-1) \tag{6.4}$$

Stem Time (R): time between the IC event of the left side and the IC event of the right side (Equation 6.5). It is the amount of time between two successive IC events (in this case starting with the right side), of both feet.

$$Step\,(ms) = IC_L(t) - IC_R(t-1) \tag{6.5}$$

In the equations above, the t element had the same meaning as described in Subsection 6.1.1. That was the reference to the time instants sequence in which IC and PS events occur.

With this information, it is also possible to count steps. The count of steps has a similar implementation of the determination of the step time, however, it is not necessary to take into account the time factor.

Step Count: it is the number of times that the feet were placed at the ground (Equation 6.6).

$$Steps = \sum_{begin\,walking}^{end\,walking} number\,of\,IC\,events\,that\,occurred \tag{6.6}$$

Also it was considered to use the PS events to count the number of steps, taking into account that they obtained better results to detect these events. However, according to the literature presented in Table 2.3 and Table 2.2, the step is the difference between placing one foot on the floor and then placing the other foot on the floor. This is true for both the step length and time parameters. In order to maintain the same logic of step counting, the same implementation of ICs was performed.

6.1.3 Generic Parameters Applied to Temporal Parameters

There are also two parameters that can be implemented at any gait parameter. In this case they were implemented in temporal parameters. These are variability and asymmetry and are described in Subsection 2.3.1.

Variability: it is the coefficient of variation or standard deviation of any parameter, along the walking period, considering one foot (Equation 6.7). Variability refers to the variation of the temporal parameter, along the gait exercise.

$$Variability = standard\_deviation(Temporal\,Parameter\,with\,one\,foot) \tag{6.7}$$

Asymmetry: it is the coefficient of variation or standard deviation of any set of right and left parameter along the walking period (Equation 6.8). Asymmetry refers to the variation of the temporal parameter determined for right and left side.

$$Asymmetry = standard\_deviation(Temporal\,Parameter\,with\,both\,feet) \tag{6.8}$$

These parameters were applied to each set of gait parameters. For example, considering the stance time, the variability of the stance time was determined by the standard deviation of the stance time values for one side (right, left) separately. The asymmetry was the standard deviation of the stance time values of both the right and left side merged. This type of evaluation allows a more processed feedback of the gait to the physiotherapist, containing information about the regularity and stability of the person's gait.

6.1.4 Conclusions - Temporal Parameters

After implementation, the results were the time intervals of each parameter for each gait cycle. For the parameters that are parts of the gait cycle, such as stance and swing time, it had been verified that its values were less than the running cycle.

However, it should be noted that no validation implementation was done for these parameters because it would be two processes to be evaluated with the same errors made while the detection of IC and PS events (presented in Chapter 5). Since the time parameters already depend on the events IC and PS that were previously validated, it was assumed that the error was propagated to these parameters.

To proceed with the validation of these parameters, it would be necessary to do the same processing on the gold standard annotated data. That is, implement the parameters for the IC and PS events of the annotations. For example, in the case of data obtained with a gold standard, in which there was a loss of packets by the sensors. It would be interesting to evaluate the relevance of packet loss in obtaining temporal parameters. However, it seems not to be very logical if better values were obtained for time intervals of the temporal parameters when the IC and PS event detection error was high. In addition, the process of packet loss is unknown, it is not known what the conditions that cause this event. For a better understanding, it would be necessary more tests that evaluate parameters like, for example, the presence of obstacles in the line between the tablet and sensors, and the distance between the tablet and the sensors.

A conclusion found visually, without a very extensive analysis of the data, was the time interval values of the temporal parameters related to each other. That is, the stance and swing times added gave the correspondent gait cycle time. Stance times were generally 60 % of the gait cycle and the swing times were generally 40 % of the gait cycle time, and are values that agreed with the ones indicated in the literature (in Subsection 2.2.3).

6.2 Real Time Implementation

The real-time implementation of this project is important to verify the viability of the algorithms when acquiring signals in real time, that is, without future information. This is important because in a rehabilitation setting, feedback needs to be provided in real time so that the patient can improve the exercises while doing them, and prevent injuries occurred due to the lack of this type of support.

In a first approach, it was thought of a parallel implementation of the system, in which there were several processes running in sequence and in parallel, as described in Figure 6.1.

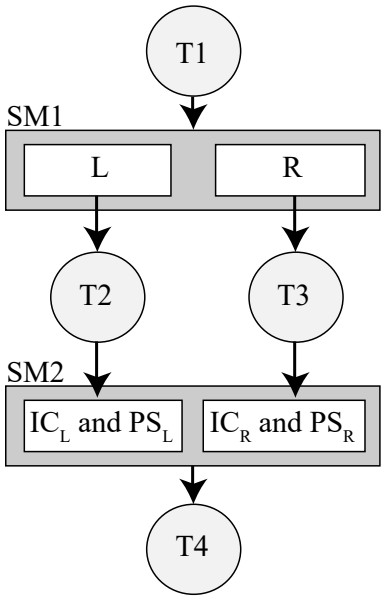

Figure 6.1: Setup of the first approach, considering a parallel implementation to read and process the data in real time. T1, T2, T3 and T4 are threads and SM1 and SM2 are shared memories. The T1 has the function of acquiring the data and place it, separately the right and left side, in the SM1. The T2 and T3 process the signals (left and right respectively and separately) in order to obtain the ICs and PSs on each side. T4 process the ICs and the PSs in order to obtain the temporal parameters.

With this setup, the goal was as follows:

1. *Thread 1 (T1)*: would acquire real-time data and place it in the SM1. This T1 would always collect the data every 20 ms (corresponding to a sampling frequency of 50 Hz). In this sense, this thread would take only this function.

2. *Shared Memory 1 (SM1)*: would stored the acquired data from the sensors, to be picked up by the threads of the next process.

3. *Thread 2 (T2) and Thread 3 (T3)*: each of these two threads would process the data from the sensors on one side: that is, T2 for one side and T3 for the other side. The function would be to obtain the time instants of the IC and PS events occurrence. It would be important to be on different threads because both sides have asynchronous IC and PS events and on

different signals (right side sensor signal and left side sensor signal). This is so that a signal could begin to be processed even though the previous one was not finished, eliminating the processing dependency between the two feet.

4. *Shared Memory 2 (SM2)*: would stored the processed IC and PS values calculated by the two previous threads, to be used by the last thread of the process.

5. *Thread 4 (T4)*: this final thread would aim to join the IC and PS values to obtain the gait parameters. It would be important to be just one and after the previous two threads have finished, so that there were enough data to get the parameters, according to their definitions presented in Section 6.1.

A second approach is the assemble the system only in series, from the real-time acquisition of the signal to the processing of the running parameters. This approach was implemented in order to test the computational capabilities and verify if it was possible without influence the real-time acquisition and processing. This approach consists of: with each new acquisition of data the process runs all from start to finish, i.e., at each $20\,ms$ the following sequence occurs:

1. Acquire one sample from each sensor,

2. Run the process of IC and PS calculation for one of the sides,

3. Run the the same process of IC and PC calculation for the other side,

4. With IC and PS information of both sides, process the temporal parameters.

However, this process was not optimized because with each new sample, there were no new ICs and PCs to be determined and the process runs all the same. On the other hand, it only makes sense to run the 2 and 3 steps for the following two cases: after the person starts walking and after a walking cycle has occurred. In this way, cross-correlation was again used, but in the case, to determine the beginning of the 2 and 3 points (and consequently the 4 point).

6.2.1 Cross-Correlation

Following the concept of cross-correlation, presented in Subsection 4.4.5, its goal in this part was to determine when the person starts walking and determine each new walking cycle that occurs. The importance of finding the instant of the beginning of the gait is crucial for the sencond and third steps of the second approach sequence, previously mentioned. This means that it only makes sense to detect IC and PS events when the person is actually walking. As there are adaptive methods throughout the algorithm, since before the start of the gait there has not yet been any true event, the limit of the adaptive threshold is still low. Thus, the algorithm is likely to consider small variations of noise as events of interest.

The application of cross-correlation in this phase was one of the first things to be processed. It determines if the process advances to steps 2 and 3 if it was at least one right and left side

gait patterns (the processing of the two sides may not occur at the same time). However, since information about a one gait cycle is few for determining temporal parameters (see Subsection 6.1), it was decided to start the second and third steps if the number of gait pattern was equal to two. In this way, when the person starts walking, after four steps (two gait cycles for each foot), begins to have information about temporal parameters. The structure of the real-time implementation is represented by Figure 6.2.

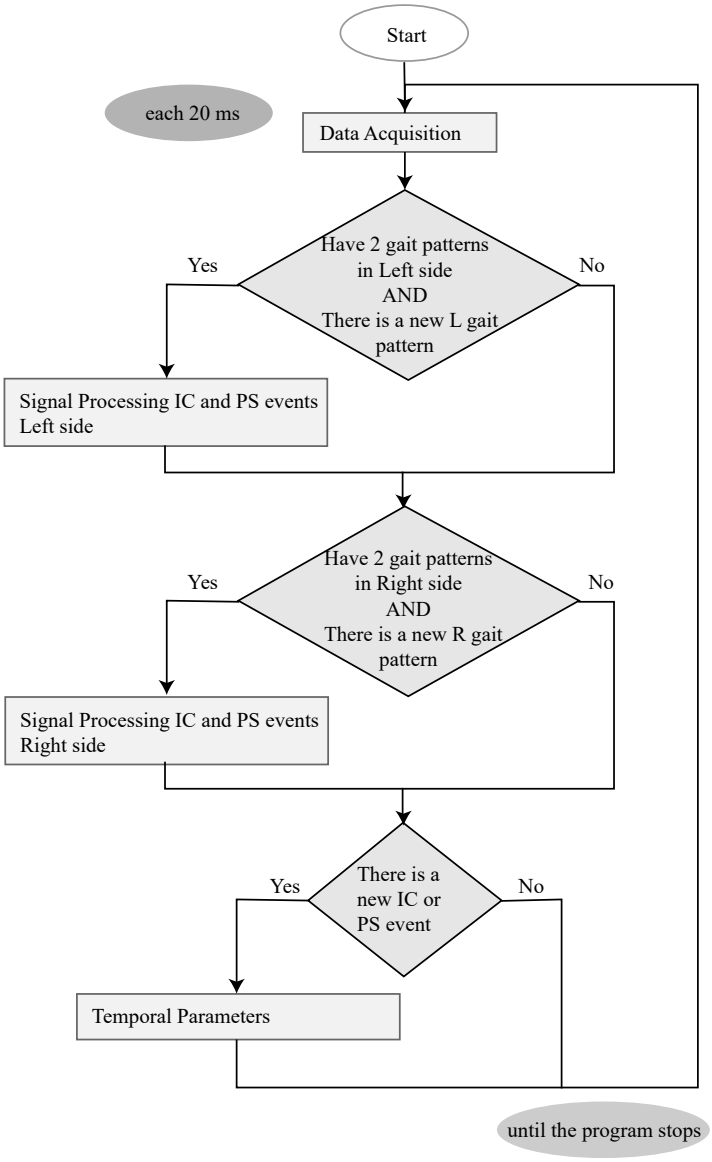

Figure 6.2: Setup of the second approach, considering a series of implementation to read and process the data in real time. Starts with the acquisition of samples and, when there are 2 gait patterns, starts the processing phase, for each side separately. After the first 2 patterns, the processing is done for each new pattern found. The temporal parameters are processed since there are ICs and PSs values and for each new pair of ICs and PSs for both sides.

Following Figure 6.2, the acquisition of signals is done every 20 ms (50 Hz), and for each acquisition, three checks are made:

- If, up to the moment, there are at least two walking patterns for the right and left sensor signals then the IC and PS events are detected,
- If the previous point is verified, it is also checked if there is new gait pattern in relation to the previous iteration (for right and left, it is not necessary to start with the left signal),
- Finally, it is checked if there are IC and PS events already determined sufficient to do the temporal parameters calculation and, for each iteration, if there are new ICs and PSs determined.

To check for new gait patterns, cross-correlation was used as described in Subsection 4.4.5, with only one model, which was close to the model of a complete gait cycle, similar to what is presented in Figure 4.25. Thus, after application of cross-correlation, it was checked whether there was a maximum in the zone of highest correlation of the model with the signal. The number of maxima in the cross-correlation was related to the number of walking patterns in the signal. In this way, before processing the signal information to obtain the ICs and the PCs, it was known if another cycle of the operation has occurred.

With this last approach, it was not necessary to run all of the processing blocks (rectangles in Figure 6.2) every 20 ms. They ran only when the person takes a new step, not stopping the analysis with each new step - the real-time analysis. The first approach, with the shared memories and thread, despite being a more efficient approach considering the problem (with a processot with two or more cores), was not necessary for the sampling frequency used and for the computer capabilities. This means that the system performs well in a series approach, without delay of the feedback provided.

6.2.2 Results - Real Time

The performance of this implementation was not compared to another system, neither video nor force platforms. In this way the results were only comparative between the system and the steps done while testing.

Comparing the output of the system while it was done, it was verified that it identified well all the IC events. This was noted by the correct count of steps that was performed. That is, the system was able to correctly count the steps.

However, it was not the only task implemented. All time parameters implemented in the static component were implemented for real time. However they were not validated.

6.3 Simulation of gait of people with stroke and Parkinson's diseases

After collecting the signal in a natural healthy gait format, some signals of simulation of certain pathologies such as Parkinson's disease and Stroke were also collected. The simulations were based on explanatory videos published by Stanford University[1]. In addition, the videos recorded at the same time as the acquisition of these signs were validated by a physiotherapist and a neurologist MD, clinical director of the company. From the validation of both results they affirm that there is a good similarity between the simulation made and the typical behavior of patients with these two pathologies.

These data were collected in order to understand the similarity of gait signal between Parkinson disease patiensts', stroke survivors and healthy subjects. The abnormal gait of Parkinson's disease is characterized by slightly forward posture, leaning to the ground, with the arms also forward, slightly shaking. The steps are usually small, the patient rarely starts with the heel but with the foot in one whole. The feet are slightly apart to help maintain stability. These were the main aspects taken into account in the simulation of the abnormal gait of Parkinson's disease.

The signal obtained with a simulation of Parkinson's symptoms is shown in Figure 6.3, where it can be seen that the frequency is much higher and the signal amplitude is lower. However, it can be observed that there is a gait pattern similar to that described in Figure 4.10, with peaks indicative of IC, valleys indicative of PS, horizontal platforms indicative of stance phase and also the sharp rise indicative of the swing phase.

[1]Stanford Medicine 25 - Gait Abnormalities `https://stanfordmedicine25.stanford.edu/the25/gait.html` (visited on 28.03.2017)

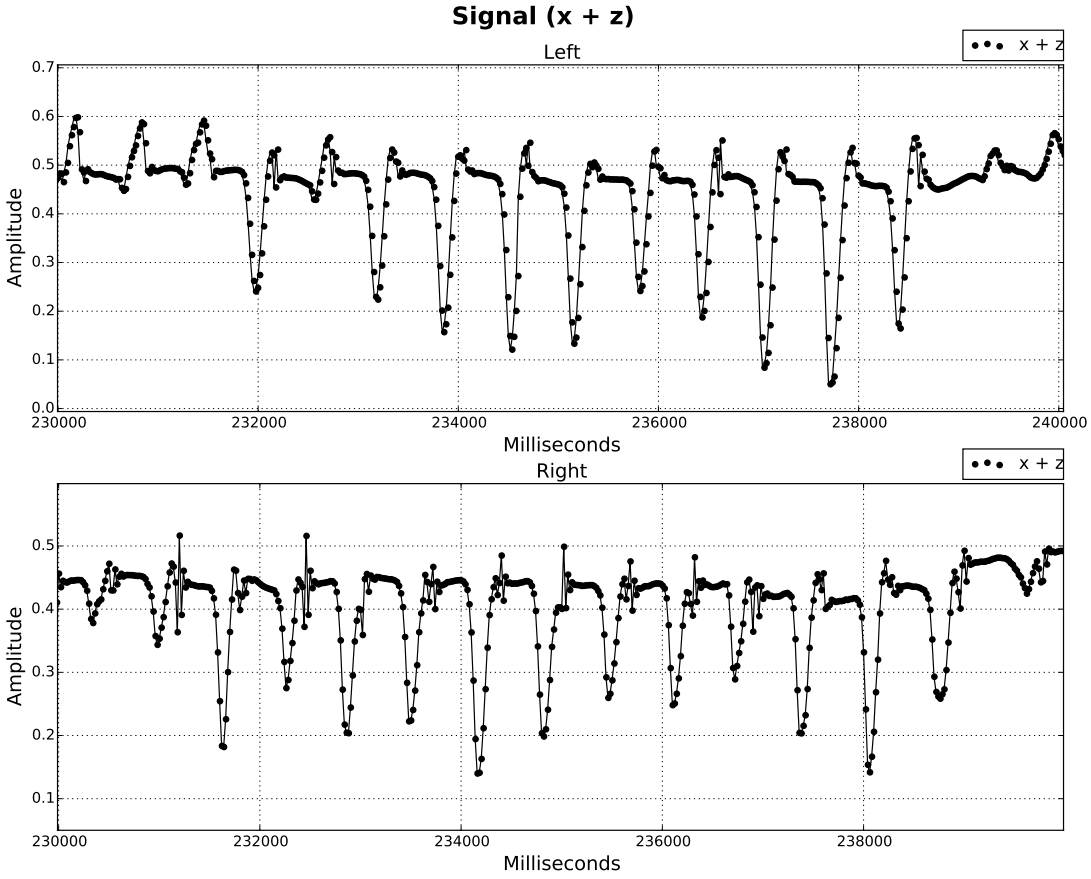

Figure 6.3: Signal resulting from Parkinson disease gait simulation.

Taking into account the differences it is expected that the algorithm would have to be adjusted to detect the events of IC and PS in Parkinson's disease patients. This conclusion is important insofar as this project is incumbent on the rehabilitation goal. People with Parkinson's disease need gait rehabilitation, requiring a system capable of measuring their gait parameters.

Abnormal gait of stroke survivors on the affected side undergoes a circular gait, practically without knee flexion or ankle dorsiflexion. It is a slightly slow gait in which the patient seeks not to lose his balance.

Analyzing now the simulation of a person with stroke with the most affected right side (Figure 6.4), it can be observed that in the resulting signals it is possible to find gait patterns with IC peaks and PS valleys, stance platforms and accentuated rises of the swing. The simulated side with the greatest injury (after stroke) was the right side and in Figure 6.4 and is the less regular side.

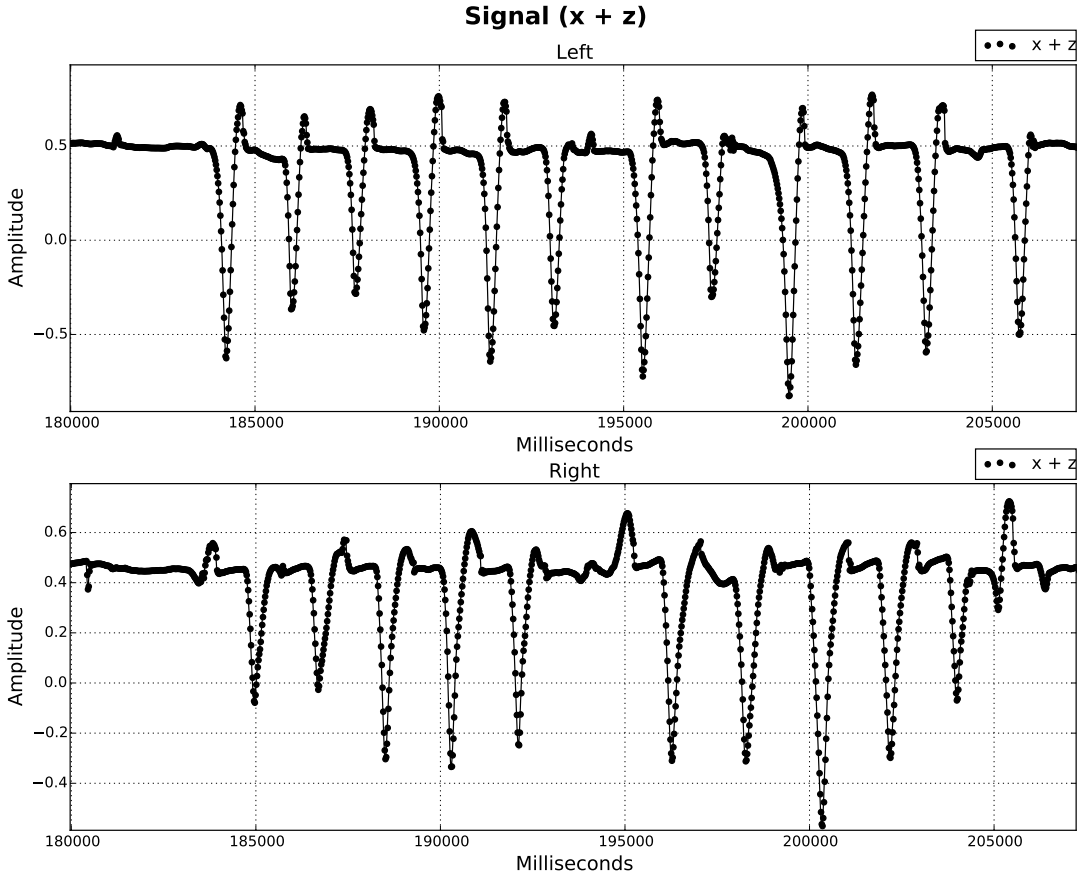

Figure 6.4: Signal resulting from stroke survivor gait simulation.

The left side was maintained at a gait close to normal, and it can be seen from Figure 6.3 that the signal corresponding to the left side was with a regular pattern close to the signal of Figure 4.10.

In this way, can be concluded that there is an approximation between simulated signs of people with Parkinson's and stroke survivors, and it is possible to obtain an algorithm close to that developed for normal people to determine temporal parameters.

6.3.1 Simulation Results and Conclusion

A test was performed in which the algorithm was run on both simulated signals. For the simulation of parkinson's disease the result of Figure 6.5 was obtained and for the simulation of stroke survivor the result of Figure 6.6 was obtained.

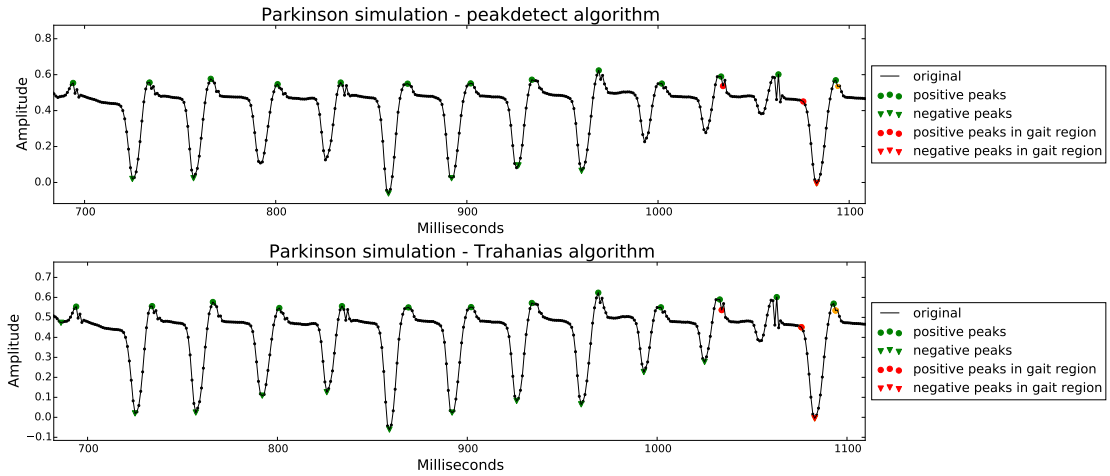

Figure 6.5: Behavior of algorithm on typical gait simulation data of person with Parkinson's disease. Triangular and round green dots are the result of detection of algorithm points. The triangular and round points in red are the points that result from selection in gait regions, obtained by selection after cross-correlation with healthy gait pattern. With both algorithms implemented.

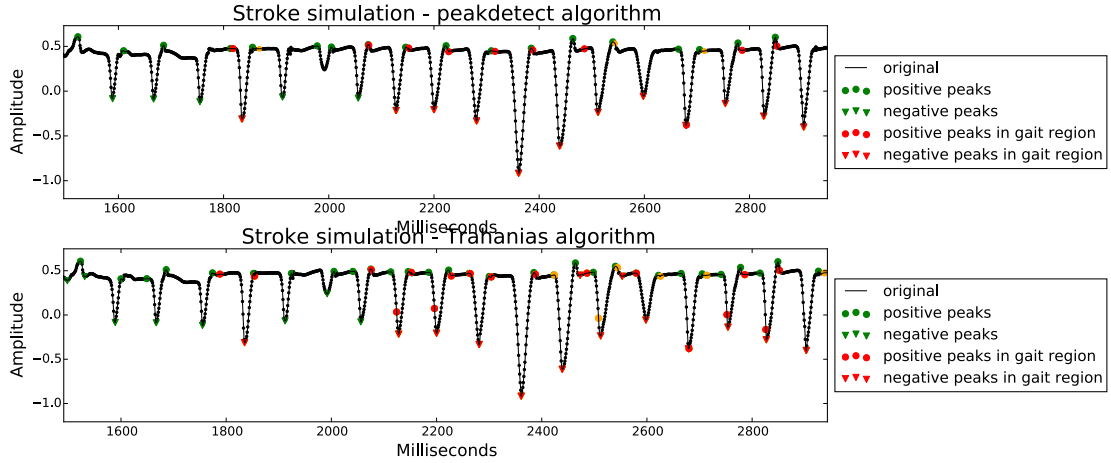

Figure 6.6: Behavior of algorithm on typical gait simulation data of a stroke survivor, in the impaired foot. Triangular and round green dots are the result of detection of algorithm points. The triangular and round points in red are the points that result from selection in gait regions, obtained by selection after cross-correlation with healthy gait pattern. The triangular and round orange dots are the result after cross-correlation with one of the two healthy gait models (see Figure 4.24). With both algorithms implemented.

Analyzing the case of simulation of gait typical of a Parkinson disease patient, it is verified that the Trahanias algorithm detected better the negative points (PS) than the peakdetect. However, in none of them was detected peaks as part of the normal walking pattern. This is because, in the cross-correlation method, two healthy gait models were used. As the walking pattern of a person with Parkinson's disease is shorter, with less amplitude and higher frequency, the correlation with a normal gait pattern is lower. In this way, although the peaks were detected, it was not considered gait.

One solution to this case would be to use a more typical gait pattern of a person with Parkinson's disease to detect when he is walking. Using the Trahanias algorithm as the method for the events detection. However, it will be necessary to acquire gait data from people with Parkinson's disease, in order to validate these assumptions.

Analyzing the behavior of the algorithm on the affected foot signal after stroke, it is verified that there were more peaks detected in red, that is, they were considered as gait region. However, there were some failures in the detection of all points, and especially in the detection of IC events. In this result, it seems that both algorithms could detect the PS events, although in some cases it was considered outside the gait region. But IC events have a larger error. However, it seems that the peakdetect algorithm had a better behavior to detect than the Trachanias algorithm. To better analyze these results it would be important to use actual stroke survivors data.

6.4 Summary

Throughout this chapter the implementation of the temporal parameters with information of the IC and PS events was approached. Although the results were not compared with ground truth information, the relationship between the phases follows the one found in the literature. Then, the real-time implementation approaches were explained. The results obtained were not compared with ground truth, but at least the function of counting steps was correct, as counted and tested in real time.

Finally, the possibility that the algorithm works in pathological marches such as Parkinson and Stroke was discussed. It turns out that, as it was not working well, some suggestions for change are proposed, in particular the gait model used in cross-correlation step, and the detection of peaks.

Chapter 7

Conclusion

7.1 Conclusion

The gait rehabilitation is still a task that highly depends on the continuous evaluation by physiotherapeutic specialists. It is based on subjective criteria and there are few metrics for assessing patients' progress. Although, there are already some video-based solutions and force platforms that offer precise parameters, they are expensive and complex to transport to the patients' home. An alternative and promising solution is the use of inertial sensors to collect gait parameters. Thus, in this dissertation the implementation of gait analysis with inertial sensors was proposed. A starting point for the gait analysis is to obtain the IC and PS events, which mark the moment when the foot is placed on the ground and when it leaves the ground, respectively. From these two events, a series of temporal parameters can be calculated, such as stance, swing and gait cycle times.

We have reached the conclusion that it was possible to obtain the IC and PS events from the orientation of the foot while walking. The values obtained were for the PS event detection a precision of about 99% and a recall of 100%, with a MSE error about 0.0397 seconds (compared with a gold standard system), with both algorithms used. For the IC event detection a precision of 100 % (with Trahanias algorithm), and a recall of 73.75 % (with both algorithms), with a MSE error about 0.0565 seconds (compared with a gold standard system).

It was also possible to determine temporal gait parameters that can be used to understand the gait of patients, such as stance, swing, gait cycle and step times. Although the values of the temporal parameters have not been extensibly tested, through the analysis of the results it was possible to observe similarity with the literature in terms of the percentage of time used in each gait phase in the gait cycle.

One problem that was not yet addressed concerns the choice of the parameter values used in the algorithms. They were tuned for the data set but if other data set is used the parameters have, probably to be tuned again. Since in this study only five healthy people were considered, these parameters are most likely to need to be adjusted. This is because the sample used is not representative of the population, nor is it representative of the patients that need gait rehabilitation.

Regarding the implementation in real time, although it was not tested in terms of temporal parameters, it was verified in a real-time step count that it corresponded to the steps made. That is, it counted the steps correctly as subject walked.

7.2 Future Work

As future work, it would be interesting to repeat the validation with a gold standard, with the tablet closer to the sensors. This would remove the packet loss influence from the results.

It is also suggested to do data set with more people from a healthy and pathological gait. This would be crucial to increase the variability of the sample, in order to increase its representativeness in the population. It would also be interesting to test and adapt the algorithm to people with pathology, who will be the focus of gait rehabilitation.

It is suggested the search for the parameter values limits so as to separate between the healthy and the unhealthy. This step can help to complete the feedback given to the patient, helping to understand if the patient is walking in a way that is close to normal or not. Thus, it would be important to yield real-time feedback to the patient.

After validating the algorithm with gait impaired patients such as with Parkinson's Diseases and Stroke survivors, it would be interesting to study their evolution over time, noting if the system helps them to improve gait.

It is also suggested that other types of gait parameters, such as spatial and kinematic, be implemented. These parameters can help find other walking problems such as balance, knee flexions hip rotations and position of the ankle when placed on the ground. These are usually compensatory attitudes of the patient with difficulty in walking. In this way, more gait parameters would be important to offer a better analysis and greater amount of feedback to the patient.

Appendix A

Supplementary Results

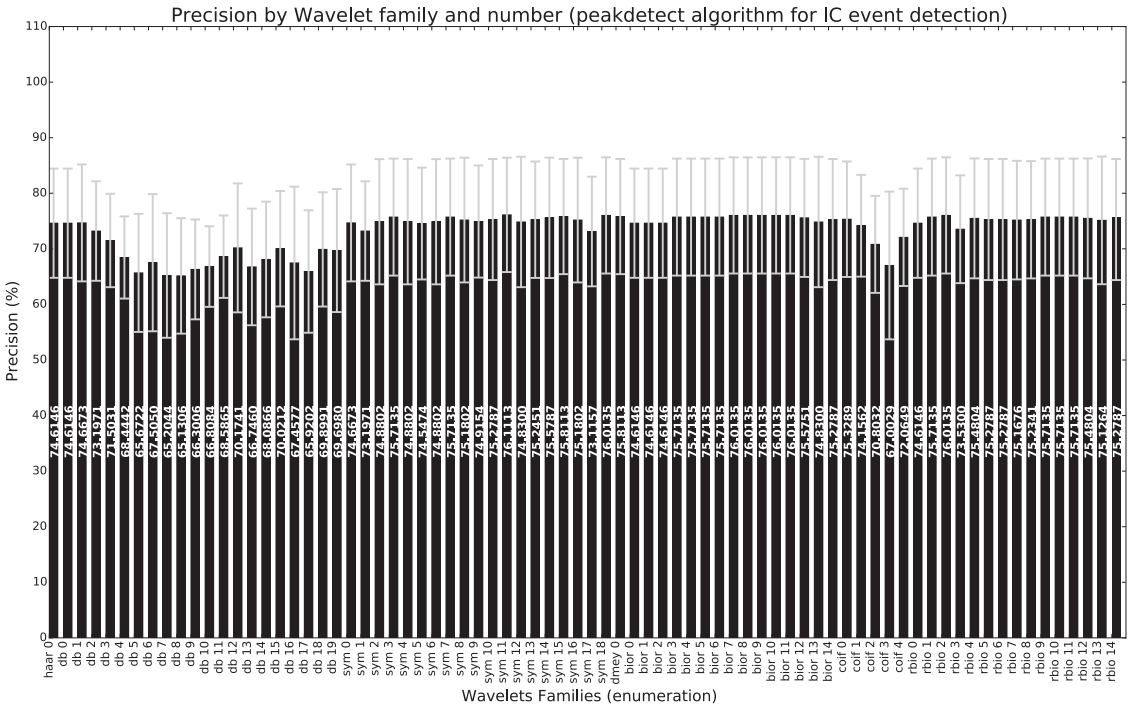

Figure A.1: Precision results of the application of DWT with different wavelets families on the detection of IC events by peakdetect algorithms, compared with video annotations. The gray bar represents the standard deviation.

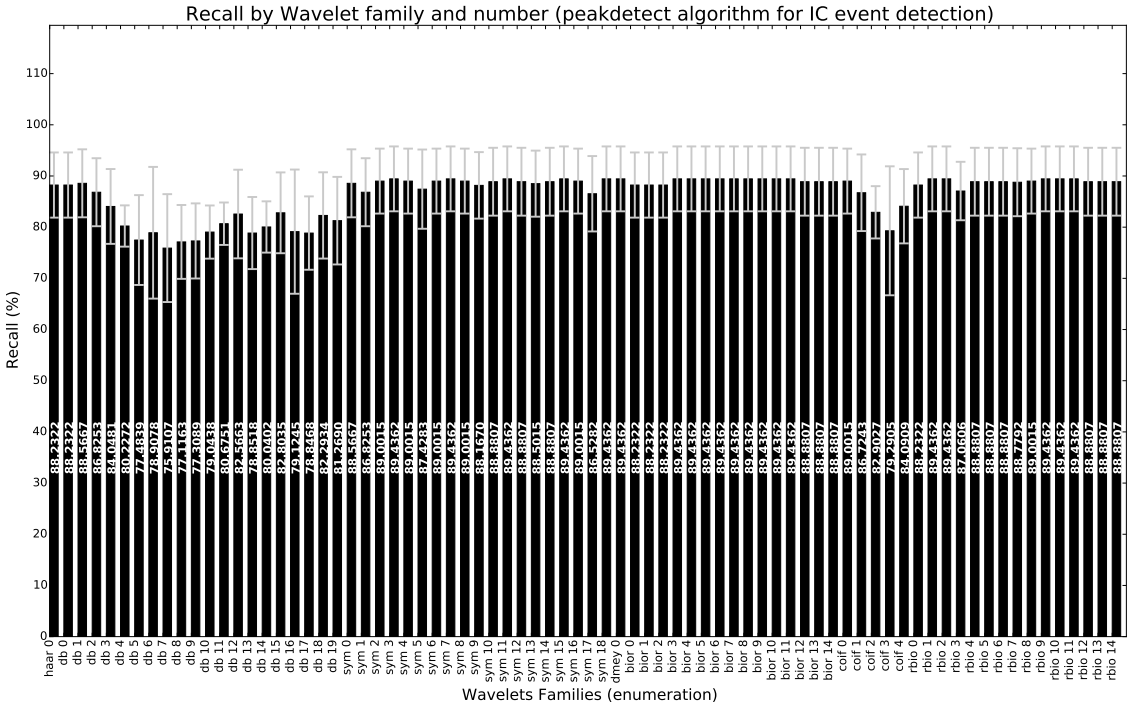

Figure A.2: Recall results of the application of DWT with different wavelets families on the detection of IC events by peakdetect algorithms, compared with video annotations. The gray bar represents the standard deviation.

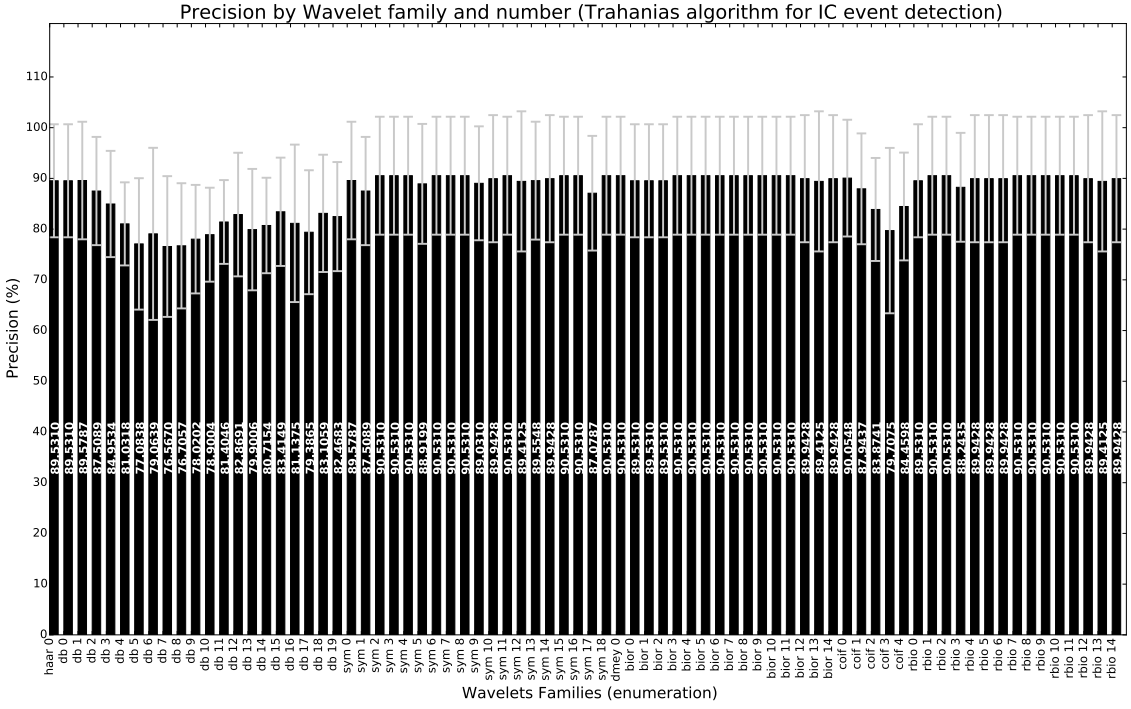

Figure A.3: Precision results of the application of DWT with different wavelets families on the detection of IC events by Trahanias algorithms, compared with video annotations. The gray bar represents the standard deviation.

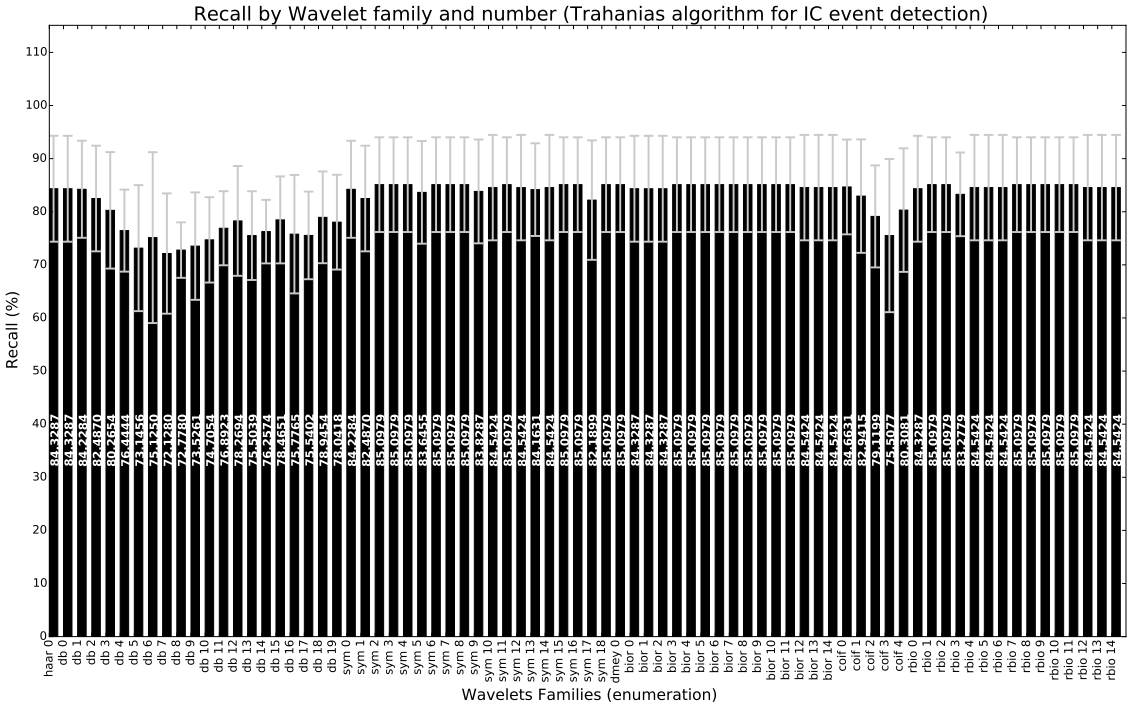

Figure A.4: Recall results of the application of DWT with different wavelets families on the detection of IC events by Trahanias algorithms, compared with video annotations. The gray bar represents the standard deviation.

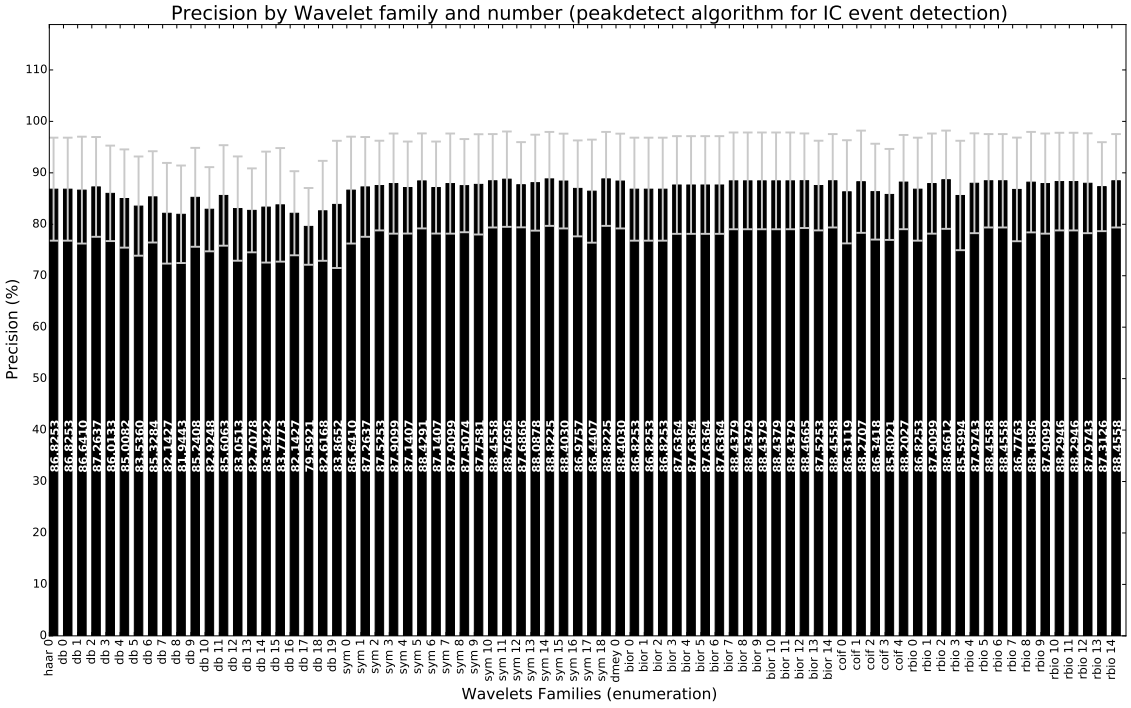

Figure A.5: Precision results of the application of DWT with different wavelets families on the detection of IC events by peakdetect algorithms, compared with manual annotations. The gray bar represents the standard deviation.

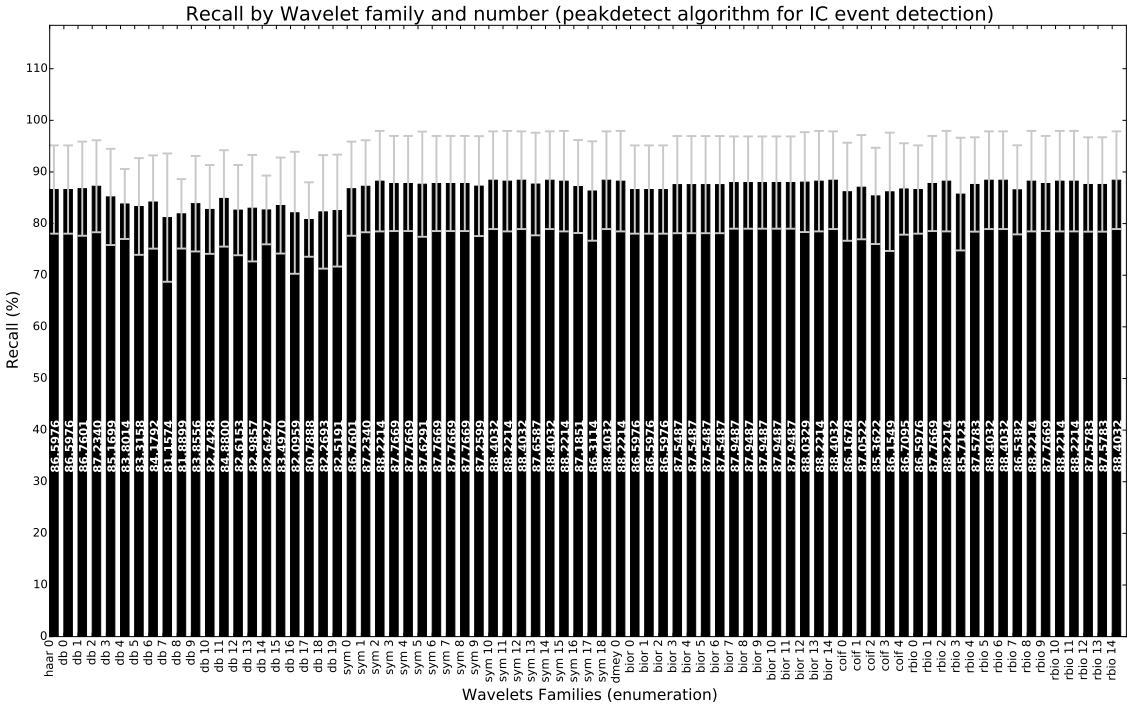

Figure A.6: Recall results of the application of DWT with different wavelets families on the detection of IC events by peakdetect algorithms, compared with manual annotations. The gray bar represents the standard deviation.

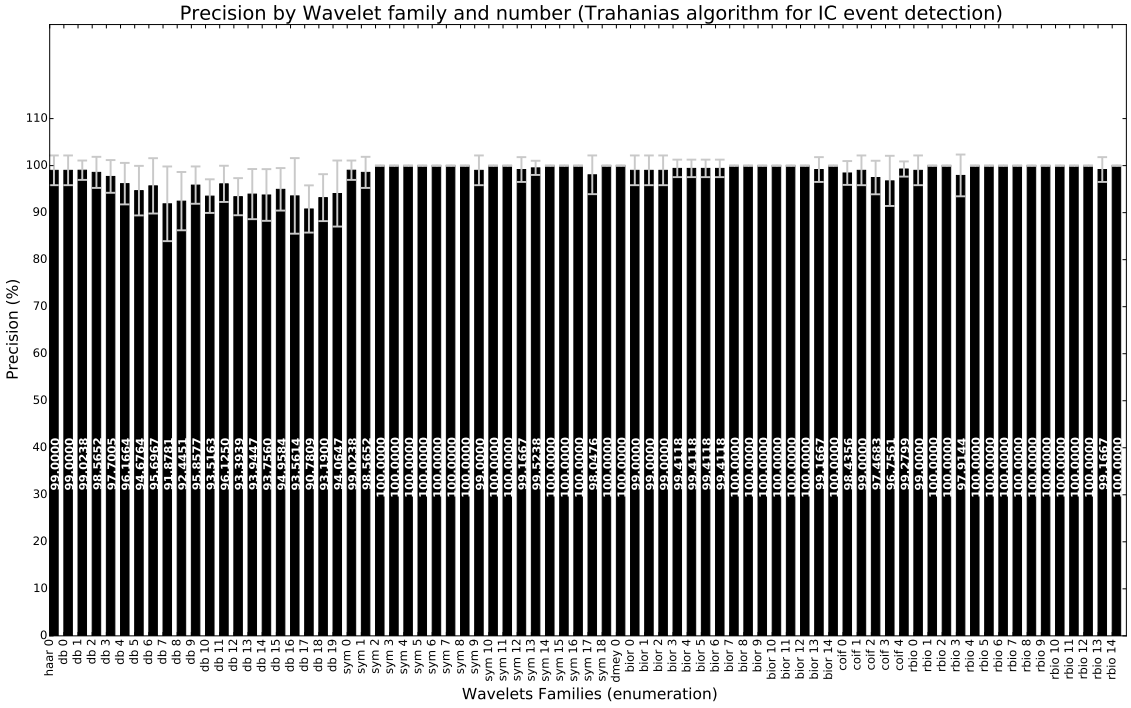

Figure A.7: Precision results of the application of DWT with different wavelets families on the detection of IC events by Trahanias algorithms, compared with manual annotations. The gray bar represents the standard deviation.

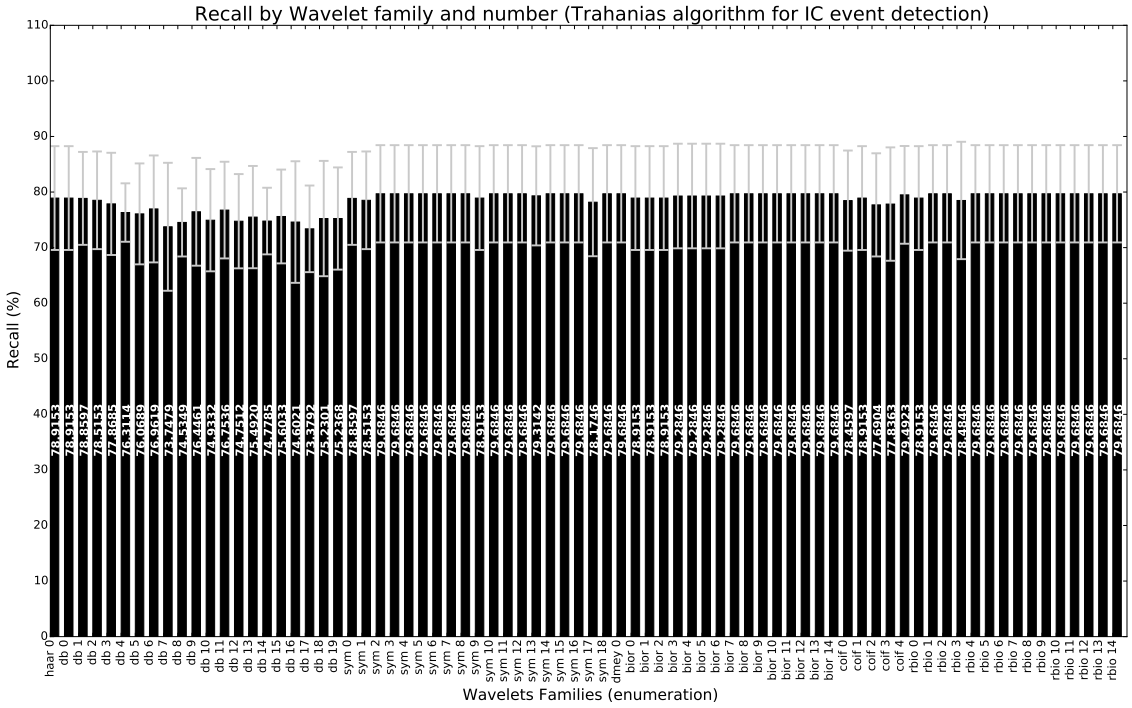

Figure A.8: Recall results of the application of DWT with different wavelets families on the detection of IC events by Trahanias algorithms, compared with manual annotations. The gray bar represents the standard deviation.

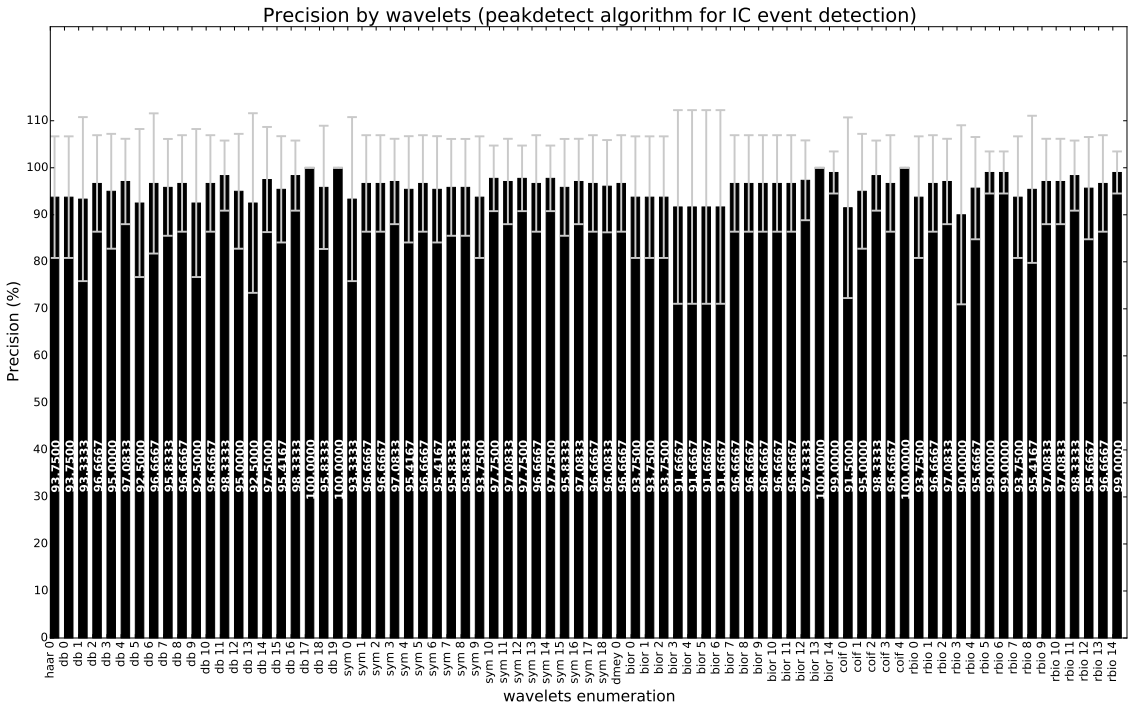

Figure A.9: Precision results of the application of DWT with different wavelets families on the detection of IC events by peakdetect algorithms, compared with gold standard annotations.

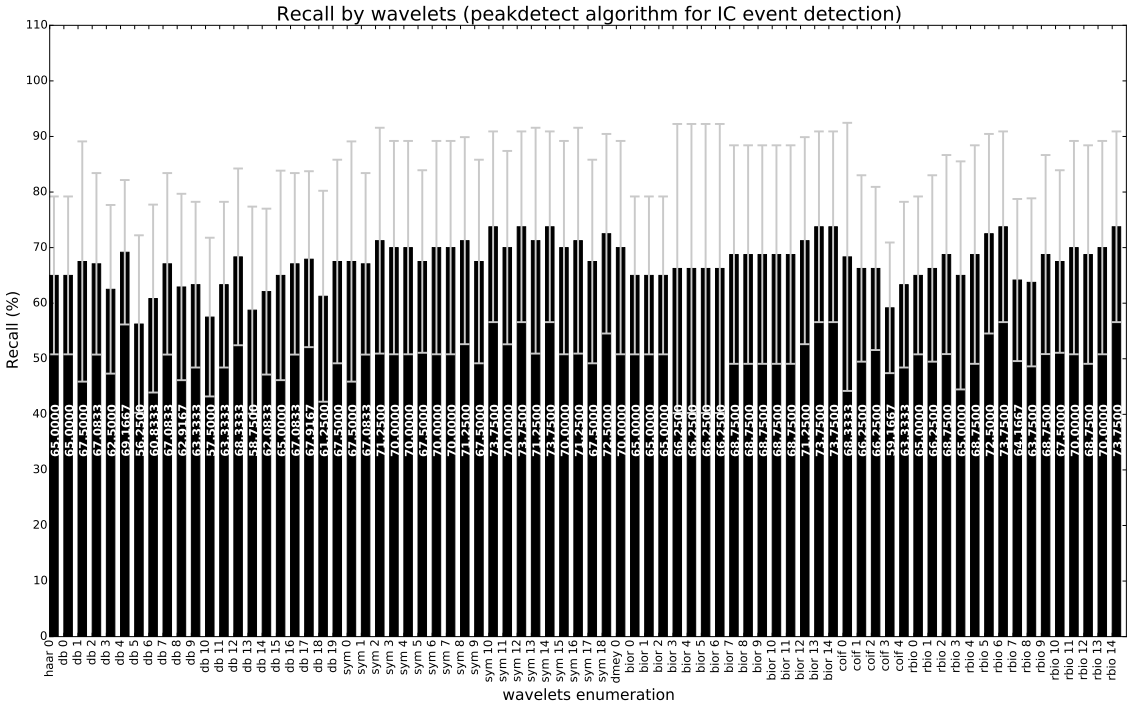

Figure A.10: Recall results of the application of DWT with different wavelets families on the detection of IC events by peakdetect algorithms, compared with gold standard annotations.

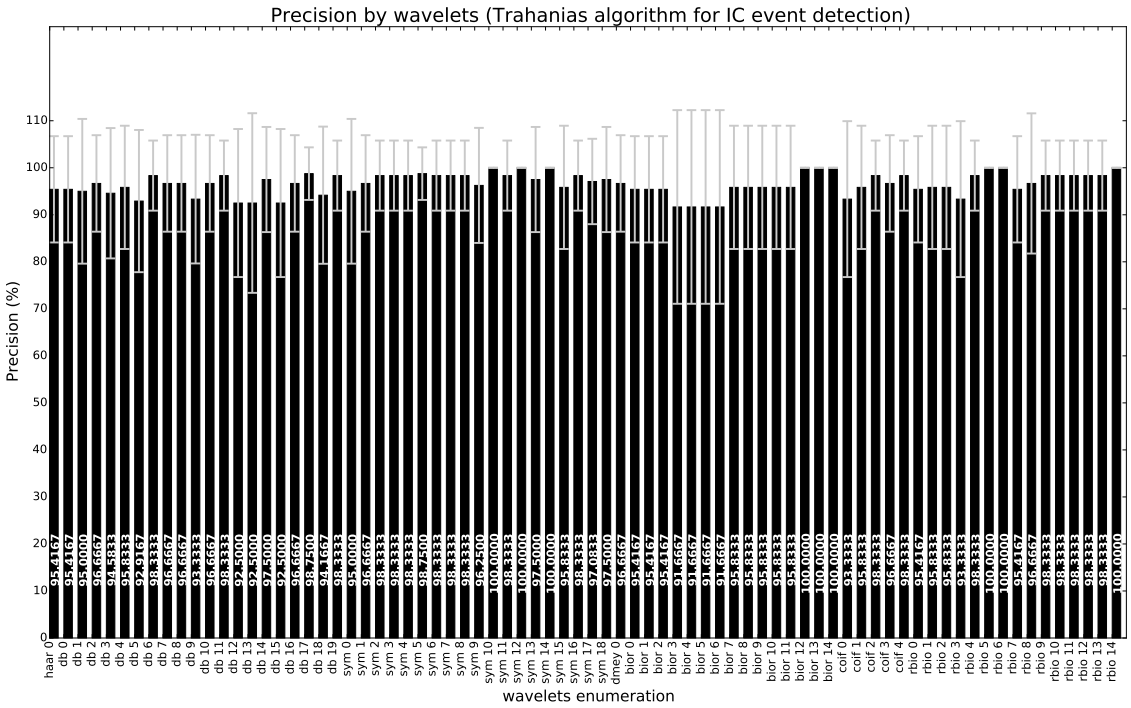

Figure A.11: Precision results of the application of DWT with different wavelets families on the detection of IC events by Trahanias algorithms, compared with gold standard annotations.

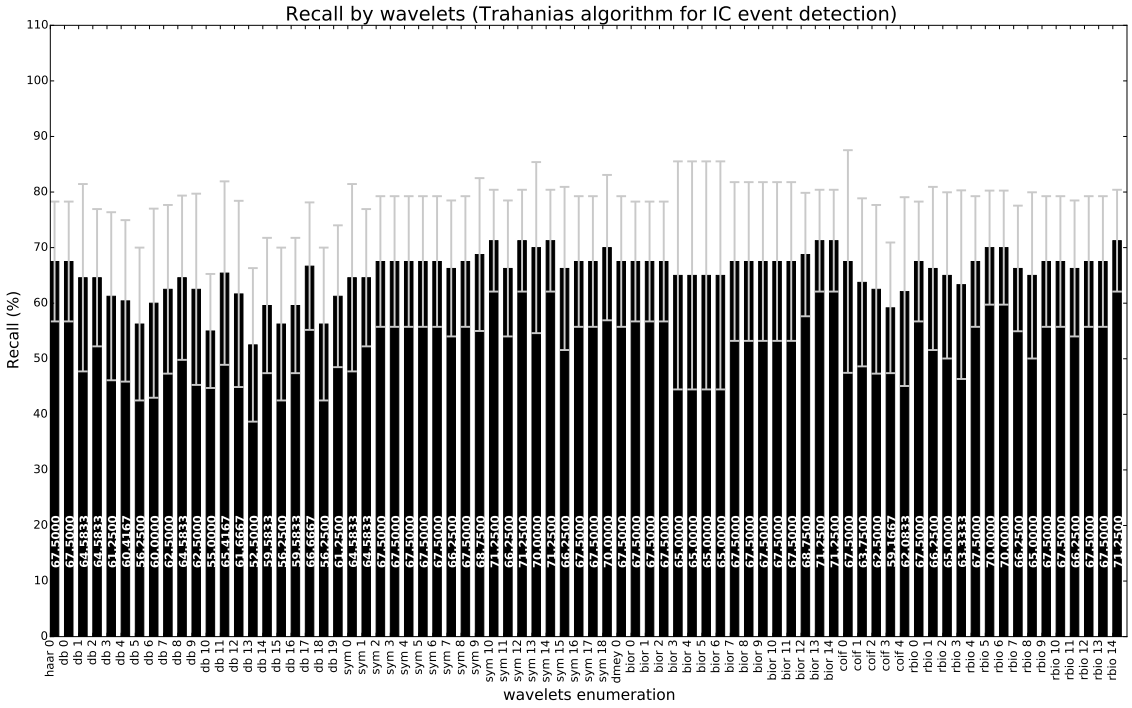

Figure A.12: Recall results of the application of DWT with different wavelets families on the detection of IC events by Trahanias algorithms, compared with gold standard annotations.

References

[PNI,] SENtral® M&M Motion & Measurement Modules. Technical Report 1020129 revG, PNI Sensor Corporation.

[xse, 2015a] (2015a). MVN User Manual: User Guide MVN, MVN BIOMECH MVN link, MVN Awinda. Technical Report Document MV0319P, Revision N, Xsens Technologies B.V.

[xse, 2015b] (2015b). Preliminary Data sheet: Xsens MTwTM Bluetooth Wireless moton tracker. Technical report, Xsens Technologies B.V., Pantheon 6a P.O. Box 559 7500 AN Enschede The Netherlands.

[Fai, 2015] (2015). XKF3 - Low-Power, Optimal Estimation of 3d Orientation using Inertial and Magnetic Sensing. Technical Report Rev. 1.1, FairChild Semiconductor Corporation.

[Ahmadi et al., 2015] Ahmadi, A., Richter, C., O'Connor, N. E., and Moran, K. (2015). Automatic detection, extraction and analysis of unrestrained gait using a wearable sensor system.

[Al-geelani et al., 2015] Al-geelani, N. A., Piah, M. A. M., and Bashir, N. (2015). A review on hybrid wavelet regrouping particle swarm optimization neural networks for characterization of partial discharge acoustic signals. *Renewable and Sustainable Energy Reviews*, 45:20–35.

[Al-Zahrani et al., 2008] Al-Zahrani, K. S., , and Bakheit, M. O. (2008). A historical review of gait analysis. *Neurosci (Riyadh)*, 13(2):105–108.

[Alfuth, 2017] Alfuth, M. (2017). Textured and stimulating insoles for balance and gait impairments in patients with multiple sclerosis and parkinson's disease: A systematic review and meta-analysis. *Gait & Posture*, 51:132–141.

[Aminian et al., 2002] Aminian, K., Najafi, B., Büla, C., Leyvraz, P.-F., and Robert, P. (2002). Spatio-temporal parameters of gait measured by an ambulatory system using miniature gyroscopes. *Journal of biomechanics*, 35(5):689–699.

[Aminian et al., 2004] Aminian, K., Trevisan, C., Najafi, B., Dejnabadi, H., Frigo, C., Pavan, E., Telonio, A., Cerati, F., Marinoni, E., Robert, P., et al. (2004). Evaluation of an ambulatory system for gait analysis in hip osteoarthritis and after total hip replacement. *Gait & posture*, 20(1):102–107.

[Baker, 2006] Baker, R. (2006). Gait analysis methods in rehabilitation. *Journal of NeuroEngineering and Rehabilitation*, 3(1):1.

[Baker, 2007] Baker, R. (2007). The history of gait analysis before the advent of modern computers. *Gait & posture*, 26(3):331–342.

[Baum and Rothschild, 1981] Baum, H. M. and Rothschild, B. B. (1981). The incidence and prevalence of reported multiple sclerosis. *Annals of neurology*, 10(5):420–428.

[Bell et al., 2011] Bell, D. R., Guskiewicz, K. M., Clark, M. A., and Padua, D. A. (2011). Systematic review of the balance error scoring system. *Sports Health: A multidisciplinary approach*, 3(3):287–295.

[Bergamini et al., 2014] Bergamini, E., Ligorio, G., Summa, A., Vannozzi, G., Cappozzo, A., and Sabatini, A. M. (2014). Estimating orientation using magnetic and inertial sensors and different sensor fusion approaches: accuracy assessment in manual and locomotion tasks. *Sensors*, 14(10):18625–18649.

[Bots et al., 1996] Bots, M. L., Looman, S. J., Koudstaal, P. J., Hofman, A., Hoes, A. W., and Grobbee, D. E. (1996). Prevalence of stroke in the general population the rotterdam study. *Stroke*, 27(9):1499–1501.

[Casamassima et al., 2014] Casamassima, F., Ferrari, A., Milosevic, B., Ginis, P., Farella, E., and Rocchi, L. (2014). A wearable system for gait training in subjects with parkinson's disease. *Sensors*, 14(4):6229–6246.

[Chen, 2011] Chen, B.-r. (2011). Legsys: wireless gait evaluation system using wearable sensors. In *Proceedings of the 2nd Conference on Wireless Health*, page 20. ACM.

[Chen et al., 2016] Chen, L., Chen, J., Peng, Q., Chen, J., Zou, Y., and Liu, G. (2016). Effect of sling exercise training on balance in patients with stroke: A meta-analysis. *PloS one*, 11(10):e0163351.

[Cloete and Scheffer, 2008] Cloete, T. and Scheffer, C. (2008). Benchmarking of a full-body inertial motion capture system for clinical gait analysis. In *Engineering in Medicine and Biology Society, 2008. EMBS 2008. 30th Annual International Conference of the IEEE*, pages 4579–4582. IEEE.

[Cloete and Scheffer, 2010] Cloete, T. and Scheffer, C. (2010). Repeatability of an off-the-shelf, full body inertial motion capture system during clinical gait analysis. In *Engineering in Medicine and Biology Society (EMBC), 2010 Annual International Conference of the IEEE*, pages 5125–5128. IEEE.

[Comber et al., 2016] Comber, L., Galvin, R., and Coote, S. (2016). Gait deficits in people with multiple sclerosis: A systematic review and meta-analysis. *Gait & Posture*.

[Cummings and Melton, 2002] Cummings, S. R. and Melton, L. J. (2002). Epidemiology and outcomes of osteoporotic fractures. *The Lancet*, 359(9319):1761–1767.

[Dam et al., 1998] Dam, E. B., Koch, M., and Lillholm, M. (1998). *Quaternions, interpolation and animation*. Datalogisk Institut, Københavns Universitet.

[Devasahayam, 2012] Devasahayam, S. R. (2012). *Signals and systems in biomedical engineering: signal processing and physiological systems modeling*. Springer Science & Business Media.

[Duncan et al., 2011] Duncan, R. P., Leddy, A. L., and Earhart, G. M. (2011). Five times sit-to-stand test performance in parkinson's disease. *Archives of physical medicine and rehabilitation*, 92(9):1431–1436.

[Elmenreich, 2002] Elmenreich, W. (2002). Sensor fusion in time-triggered systems.

[Eng and Tang, 2007] Eng, J. J. and Tang, P.-F. (2007). Gait training strategies to optimize walking ability in people with stroke: a synthesis of the evidence. *Expert review of neurotherapeutics*, 7(10):1417–1436.

[Evans and Arvind, 2014] Evans, R. L. and Arvind, D. (2014). Detection of gait phases using orient specks for mobile clinical gait analysis. In *Wearable and Implantable Body Sensor Networks (BSN), 2014 11th International Conference on*, pages 149–154. IEEE.

[Felson et al., 2000] Felson, D. T., Lawrence, R. C., Dieppe, P. A., Hirsch, R., Helmick, C. G., Jordan, J. M., Kington, R. S., Lane, N. E., Nevitt, M. C., Zhang, Y., et al. (2000). Osteoarthritis: new insights. part 1: the disease and its risk factors. *Annals of internal medicine*, 133(8):635–646.

[González et al., 2010] González, R. C., López, A. M., Rodriguez-Uría, J., Álvarez, D., and Alvarez, J. C. (2010). Real-time gait event detection for normal subjects from lower trunk accelerations. *Gait & posture*, 31(3):322–325.

[Gordon R. Kelley, 2015] Gordon R. Kelley, M. (2015). Parkinson's disease incidence & prevalence.

[Hamdi et al., 2014] Hamdi, M. M., Awad, M. I., Abdelhameed, M. M., and Tolbah, F. A. (2014). Lower limb motion tracking using imu sensor network. In *Biomedical Engineering Conference (CIBEC), 2014 Cairo International*, pages 28–33. IEEE.

[Horak et al., 2015] Horak, F., King, L., and Mancini, M. (2015). Role of body-worn movement monitor technology for balance and gait rehabilitation. *Physical therapy*, 95(3):461–470.

[Horak and Mancini, 2013] Horak, F. B. and Mancini, M. (2013). Objective biomarkers of balance and gait for parkinson's disease using body-worn sensors. *Movement Disorders*, 28(11):1544–1551.

[Jasiewicz et al., 2006] Jasiewicz, J. M., Allum, J. H., Middleton, J. W., Barriskill, A., Condie, P., Purcell, B., and Li, R. C. T. (2006). Gait event detection using linear accelerometers or angular velocity transducers in able-bodied and spinal-cord injured individuals. *Gait & posture*, 24(4):502–509.

[Kalman, 1960] Kalman, R. E. (1960). A new approach to linear filtering and prediction problems. *Transactions of the ASME–Journal of Basic Engineering*, 82(Series D):35–45.

[Kotiadis et al., 2010] Kotiadis, D., Hermens, H., and Veltink, P. (2010). Inertial gait phase detection for control of a drop foot stimulator: Inertial sensing for gait phase detection. *Medical engineering & physics*, 32(4):287–297.

[Kraan et al., 2016] Kraan, C., Tan, A., and Cornish, K. (2016). The developmental dynamics of gait maturation with a focus on spatiotemporal measures. *Gait & Posture*.

[Liu et al., 2009] Liu, T., Inoue, Y., and Shibata, K. (2009). Development of a wearable sensor system for quantitative gait analysis. *Measurement*, 42(7):978–988.

[Madgwick, 2010] Madgwick, S. O. (2010). An efficient orientation filter for inertial and inertial/magnetic sensor arrays. *Report x-io and University of Bristol (UK)*.

[Mariani et al., 2012] Mariani, B., Rochat, S., Büla, C. J., and Aminian, K. (2012). Heel and toe clearance estimation for gait analysis using wireless inertial sensors. *IEEE Transactions on Biomedical Engineering*, 59(11):3162–3168.

[Martori et al., 2013] Martori, A. L., Carey, S. L., Lura, D. J., and Dubey, R. V. (2013). Knee angle analysis using a wearable motion analysis system for detection and rehabilitation of mild traumatic brain injury. In *ASME 2013 Summer Bioengineering Conference*, pages V01AT20A032–V01AT20A032. American Society of Mechanical Engineers.

[Meng et al., 2013a] Meng, X., Yu, H., and Tham, M. P. (2013a). Gait phase detection in able-bodied subjects and dementia patients. In *Engineering in Medicine and Biology Society (EMBC), 2013 35th Annual International Conference of the IEEE*, pages 4907–4910. IEEE.

[Meng et al., 2013b] Meng, X., Zhang, Z.-Q., Wu, J.-K., and Wong, W.-C. (2013b). Hierarchical information fusion for global displacement estimation in microsensor motion capture. *IEEE Transactions on Biomedical Engineering*, 60(7):2052–2063.

[Moragos, 1999] Moragos, P. (1999). Morphological signal and image processing. *CRC Press LLC*.

[Muro-de-la Herran et al., 2014] Muro-de-la Herran, A., Garcia-Zapirain, B., and Mendez-Zorrilla, A. (2014). Gait analysis methods: an overview of wearable and non-wearable systems, highlighting clinical applications. *Sensors*, 14(2):3362–3394.

[Murray et al., 1964] Murray, M. P., Drought, A. B., and Kory, R. C. (1964). Walking patterns of normal men. *J Bone Joint Surg Am*, 46(2):335–360.

[Najafi et al., 2009] Najafi, B., Helbostad, J. L., Moe-Nilssen, R., Zijlstra, W., and Aminian, K. (2009). Does walking strategy in older people change as a function of walking distance? *Gait & posture*, 29(2):261–266.

[Najafi et al., 2011] Najafi, B., Khan, T., and Wrobel, J. (2011). Laboratory in a box: wearable sensors and its advantages for gait analysis. In *2011 Annual International Conference of the IEEE Engineering in Medicine and Biology Society*, pages 6507–6510. IEEE.

[Perry and Burnfield, 1992] Perry, J. and Burnfield, J. M. (1992). *Gait Analysis: Normal and Pathological Function*. Slack Thorofare, NJ, FIRST Edition edition.

[Pohl and Mehrholz, 2006] Pohl, M. and Mehrholz, J. (2006). Immediate effects of an individually designed functional ankle-foot orthosis on stance and gait in hemiparetic patients. *Clinical Rehabilitation*, 20(4):324–330.

[Qiu et al., 2014] Qiu, S., Yang, Y., Hou, J., Ji, R., Hu, H., and Wang, Z. (2014). Ambulatory estimation of 3d walking trajectory and knee joint angle using marg sensors. In *Innovative Computing Technology (INTECH), 2014 Fourth International Conference on*, pages 191–196. IEEE.

[Ren et al., 2016] Ren, P., Karahan, E., Chen, C., Luo, R., Geng, Y., Bayard, J. F. B., L, M., Bringas, Y., Dezhong, Kendrick, K. M., and Valdes-Sosa, P. A. (2016). Gait influence diagrams in parkinson's disease. *IEEE Transactions on Neural Systems and Rehabilitation Engineering*.

[Roetenberg et al., 2009] Roetenberg, D., Luinge, H., and Slycke, P. (2009). Xsens mvn: full 6dof human motion tracking using miniature inertial sensors. *Xsens Motion Technologies BV, Tech. Rep*.

[Rueterbories et al., 2014] Rueterbories, J., Spaich, E. G., and Andersen, O. K. (2014). Gait event detection for use in fes rehabilitation by radial and tangential foot accelerations. *Medical engineering & physics*, 36(4):502–508.

[Sabatini, 2005] Sabatini, A. M. (2005). Quaternion-based strap-down integration method for applications of inertial sensing to gait analysis. *Medical and Biological Engineering and Computing*, 43(1):94–101.

[Salzman, 2010] Salzman, B. (2010). Gait and balance disorders in older adults. *Am Fam Physician*, 82(1):61–68.

[Seel et al., 2013] Seel, T., Schäperkötter, S., Valtin, M., Werner, C., and Schauer, T. (2013). Design and control of an adaptive peroneal stimulator with inertial sensor-based gait phase detection. In *Proceedings of the 18th Annual International FES Society Conference, San Sebastian, Spain*, pages 6–8.

[Simoes, 2011] Simoes, M. A. (2011). Feasibility of wearable sensors to determine gait parameters.

[Sousa-Uva and Dias, 2014] Sousa-Uva, M. and Dias, C. M. (2014). Prevalência de acidente vascular cerebral na população portuguesa: dados da amostra ecos 2013.

[Spain et al., 2012] Spain, R., George, R. S., Salarian, A., Mancini, M., Wagner, J., Horak, F., and Bourdette, D. (2012). Body-worn motion sensors detect balance and gait deficits in people with multiple sclerosis who have normal walking speed. *Gait & posture*, 35(4):573–578.

[Su et al., 2014] Su, X., Tong, H., and Ji, P. (2014). Activity recognition with smartphone sensors. *Tsinghua Science and Technology*, 19(3):235–249.

[Sutherland, 2002] Sutherland, D. H. (2002). The evolution of clinical gait analysis: Part ii kinematics. *Gait & posture*, 16(2):159–179.

[Tadano et al., 2016] Tadano, S., Takeda, R., Sasaki, K., Fujisawa, T., and Tohyama, H. (2016). Gait characterization for osteoarthritis patients using wearable gait sensors (h-gait systems). *Journal of biomechanics*, 49(5):684–690.

[Tao et al., 2012] Tao, W., Liu, T., Zheng, R., and Feng, H. (2012). Gait analysis using wearable sensors. *Sensors*, 12(2):2255–2283.

[Tereso et al., 2014] Tereso, A., Martins, M., Santos, C., da Silva, M. V., Gonçalves, L., and Rocha, L. (2014). Detection of gait events and assessment of fall risk using accelerometers in assisted gait. In *Informatics in Control, Automation and Robotics (ICINCO), 2014 11th International Conference on*, volume 1, pages 788–793. IEEE.

[Trahanias, 1993] Trahanias, P. (1993). An approach to qrs complex detection using mathematical morphology. *IEEE Transactions on Biomedical Engineering*, 40(2):201–205.

[Uchitomi et al., 2016] Uchitomi, H., ichiro Ogawa, K., Orimo, S., Wada, Y., and Miyake, Y. (2016). Effect of interpersonal interaction on festinating gait rehabilitation in patients with parkinson's disease. *PloS one*, 11(6):e0155540.

[United Nations and Affairs, 2009] United Nations, D. o. E. and Affairs, S. (2009). *World population ageing 2009*, volume 295. United Nations Publications.

[van Meulen et al., 2016] van Meulen, F. B., Weenk, D., van Asseldonk, E. H., Schepers, H. M., Veltink, P. H., and Buurke, J. H. (2016). Analysis of balance during functional walking in stroke survivors. *PloS one*, 11(11):e0166789.

[Whittle, 1996] Whittle, M. W. (1996). Clinical gait analysis: A review. *Human Movement Science*, 15(3):369–387.

[Williams et al., 2015] Williams, B., Allen, B., True, H., Fell, N., Levine, D., and Sartipi, M. (2015). A real-time, mobile timed up and go system. In *Wearable and Implantable Body Sensor Networks (BSN), 2015 IEEE 12th International Conference on*, pages 1–6. IEEE.

[Wrisley and Whitney, 2004] Wrisley, D. M. and Whitney, S. L. (2004). The effect of foot position on the modified clinical test of sensory interaction and balance. *Archives of physical medicine and rehabilitation*, 85(2):335–338.

[Yamamoto et al., 2015] Yamamoto, T., Smith, C. E., Suzuki, Y., Kiyono, K., Tanahashi, T., Sakoda, S., Morasso, P., and Nomura, T. (2015). Universal and individual characteristics of postural sway during quiet standing in healthy young adults. *Physiological reports*, 3(3):e12329.

[Yang et al., 2012] Yang, M., Zheng, H., Wang, H., McClean, S., and Newell, D. (2012). igait: an interactive accelerometer based gait analysis system. *Computer methods and programs in biomedicine*, 108(2):715–723.

[Yang et al., 2013] Yang, S., Zhang, J.-T., Novak, A. C., Brouwer, B., and Li, Q. (2013). Estimation of spatio-temporal parameters for post-stroke hemiparetic gait using inertial sensors. *Gait & posture*, 37(3):354–358.

[Young, 2010] Young, A. D. (2010). Wireless realtime motion tracking system using localised orientation estimation.

[Yuwono et al., 2014] Yuwono, M., Su, S. W., Guo, Y., Moulton, B. D., and Nguyen, H. T. (2014). Unsupervised nonparametric method for gait analysis using a waist-worn inertial sensor. *Applied Soft Computing*, 14:72–80.

[Zampolini et al., 2007] Zampolini, M., Todeschini, E., Bernabeu, G. M., Hermens, H., Ilsbroukx, S., Macellari, V., Magni, R., Rogante, M., Scattareggia, M. S., Vollenbroek, M., et al. (2007). Tele-rehabilitation: present and future. *Annali dell'Istituto superiore di sanità*, 44(2):125–134.

[Zatsiorsky, 2002] Zatsiorsky, V. M. (2002). *Kinetics of human motion*. Human Kinetics.

[Zhang et al., 2012] Zhang, B., Jiang, S., Wei, D., Marschollek, M., and Zhang, W. (2012). State of the art in gait analysis using wearable sensors for healthcare applications. In *Computer and Information Science (ICIS), 2012 IEEE/ACIS 11th International Conference on*, pages 213–218. IEEE.

[Zhao et al., 2014] Zhao, W., Espy, D. D., Reinthal, M. A., and Feng, H. (2014). A feasibility study of using a single kinect sensor for rehabilitation exercises monitoring: A rule based approach. In *Computational Intelligence in Healthcare and e-health (CICARE), 2014 IEEE Symposium on*, pages 1–8. IEEE.

[Zhou and Hu, 2004] Zhou, H. and Hu, H. (2004). A survey-human movement tracking and stroke rehabilitation. *University of Essex, Colchester United Kingdom*.